LKB1 AND AMPK NEGATIVELY REGULATE THE WARBURG EFFECT IN CANCER

Brandon Faubert

Physiology Department
McGill University
Montreal, Quebec, Canada

April, 2015

This thesis is submitted to the Faculty of Graduate Studies and Research in partial fulfillment of the requirements of the degree of Doctor of Philosophy

ABSTRACT

Many of the common mutations in cancer affect key metabolic signaling pathways. These mutations promote altered cellular metabolism (Hanahan and Weinberg, 2011). This change in metabolism, termed the "Warburg Effect" describes the phenomenon where many cancer cells preferentially use aerobic glycolysis for energy production, despite an adequate oxygen supply. This change in metabolism supplies both the necessary energy and biosynthetic intermediates for proliferation, and confers a selective growth advantage for cancer cells. AMP-activated protein kinase (AMPK) is an evolutionarily conserved central regulator of cellular metabolism and energy homeostasis. Under conditions of energetic stress, AMPK is activated by its upstream kinase LKB1, and initiates a number of biological pathways aimed at preserving cellular energy levels. In addition, AMPK is situated in a signaling cascade of tumour suppressors, its specific role in cancer remains controversial. The work in this thesis characterizes the energy sensing LKB1-AMPK pathway in regulating tumor metabolism. Specifically, the role of AMPK in suppressing MYC-driven tumourigenesis, as well as its negative regulation of the Warburg effect is examined. We further address the previously unidentified role of LKB1 loss in cancer metabolism. In both studies, these metabolic phenotypes were driven by the normoxic stabilization of HIF1α. Mechanistically, we demonstrate that this stabilization is due to chronically elevated levels of mitochondrial ROS in the absence of AMPK. We conclude that LKB1 and AMPK negatively regulate the Warburg effect in cancer.

RÉSUMÉ

Parmi les mutations qui sont fréquemment présentes dans les cancers, un grand nombre affecte des voies clés de la signalisation métabolique, ce qui provoque généralement une altération du métabolisme cellulaire (Hanahan and Weinberg, 2011). Cette modification du métabolisme, appelée « l'effet Warburg », correspond à un phénomène au cours duquel de nombreuses cellules cancéreuses utilisent de manière préférentielle la glycolyse aérobie afin de produire de l'énergie, et ce malgré un approvisionnement suffisant en oxygène. Ce phénomène permet de fournir l'énergie et les intermédiaires biosynthétiques nécessaires à la prolifération, conférant ainsi un avantage de croissance sélectif aux cellules cancéreuses. La kinase activée par l'AMP (AMPK) est une protéine conservée au cours de l'évolution et qui détient un rôle central dans la régulation du métabolisme cellulaire et l'homéostasie énergétique. LKB1 est la kinase présente en amont d'AMPK et l'active en réponse à des conditions de stress énergétique. Etant donné qu'AMPK se situe aussi dans la cascade de signalisation des suppresseurs de tumeurs, le rôle précis qu'il joue dans le cancer reste controversé. Le travail présenté dans cette thèse caractérise le rôle de la voie de signalisation, LKB1/AMPK dans la régulation du métabolisme cancéreux. Plus précisément, les rôles de la protéine AMPK dans la répression de la tumorigénèse initiée par MYC et de l'effet Warburg sont examinés plus en détails. Nous abordons aussi les conséquences de la perte de LKB1 sur le métabolisme cancéreux, mécanisme qui n'était pas connu au départ. Au cours de ces deux études, les phénotypes métaboliques observés résultent de la stabilisation de HIF-1α dans des conditions de normoxie. Nous démontrons que les mécanismes de cette stabilisation impliquent une augmentation chronique des niveaux de dérivés réactifs de l'oxygène provenant de la mitochondrie en réponse à l'absence d'AMPK. Finalement, nous concluons que les protéines LKB1 et AMPK régulent de manière négative l'effet Warburg au cours du cancer.

PREFACE

The work described in this thesis has been published as follows:

Chapters 1 and 5: Several sections in the introduction and discussion were published in a review.

Faubert B, Vincent EE, Poffenberger M, Jones RG. (2014). The AMP-activated protein kinase (AMPK) and cancer: many faces of a metabolic regulator. *Cancer Letters*. 356(2) 165-170.

Chapter 2: **Faubert B**, Boily G, Izreig S, Griss T, Samborska B, Dong Z, Dupuy F, Chambers C, Fuerth BJ, Viollet B, Mamer OA, Avizonis D, DeBerardinis RJ, Siegel PM, Jones RG. (2013). AMPK is a negative regulator of the Warburg Effect and suppresses tumor growth *in vivo*. *Cell Metabolism*. 17(1):113-24.

Chapter 3: **Faubert B**, Vincent EE, Griss T, Svenson R, Mamer OA, Avizonis D, Shaw RJ, Jones RG. (2014). Loss of the tumor suppressor LKB1 promotes metabolic reprogramming of cancer cells via HIF-1α. *PNAS*. 111(7):2554-9.

Chapter 4: **Faubert B**, Ma E, Andrzejewski S, St. Pierre J, Jones RG. (2015). Regulation of mitochondrial ROS through an AMPK-dependent metabolic circuit. (Manuscript in preparation).

CONTRIBUTION OF AUTHORS

Chapters 1 and 5: The work presented in chapters 1 and 5 was helpfully reviewed and edited by Mark Verway, Fanny Dupuy, Said Izreig, Takla Griss, Eric Ma, Dr. Emma Vincent and Dr. Russell Jones.

Chapter 2: The work presented in Chapter 2 has been realized with the collaboration of co-authors. In this work I created the mouse embryonic fibroblast (MEF) cell lines, as well as characterized their metabolism via enzymatic assays, GC-MS and the Seahorse BioAnalyzer. I identified the signaling cascades involved via western blot and qPCR. Dr. Gino Boily and Said Izreig performed the *in vivo* experiments, including tracking tumour onset, derivation of tumor cell lines, and analysis of tumours via western blotting. Tumour lines were metabolically characterized by Said and Gino, as well as NMR analysis by Dr. Daina Avizonis. Takla Griss created the H1299 cell line, as well as performed qPCR analysis. Zhifeng Dong and Fanny Dupuy performed IHC analysis on extracted tumours. Chris Chambers performed initial mass isotopomer labeling experiments. Ben Fuerth provided guidance and technical assistance in development of the project. Dr. Benoit Viollet provided AMPK-null MEFs. Dr. Orval Mamer provided technical expertise and teaching of the GC-MS. Dr. Ralph Deberardinis gave expert analysis and insight into the project, including experimental design and critical feedback. Dr. Peter Siegal provided critical feedback on the preparation of the manuscript. Dr. Russell Jones supervised the work, designed experiments, and prepared the manuscript. I prepared the figures under the supervision of Dr. Russell Jones, and contributed in critical feedback of the manuscript.

Chapter 3: The work performed in this chapter was performed with the following contributions from co-authors. I created the MEF cell lines (LKB1 wild type and knockout), characterized the metabolic phenotype of the MEFs and cancer cell lines. Furthermore, I performed apoptosis assays, as well immunoblot analysis of the signaling pathways involved. Dr. Emma Vincent performed soft agar assays and growth assays of the cancer cell lines. Takla Griss created and metabolically analyzed the H1299 cell line. Bozena Samborska provided samples of siRNA-mediated knockdown of LKB1 in various cell lines. Said Izreig provided western blots confirming the established signaling pathway, and helped track xenograft tumor growth in nude mice. Dr. Orval Mamer and Dr. Daina Avizonis provided expertise and materials for GC-MS analysis. Dr. Rueben Shaw provided the a549 cancer cell line featuring LKB1 re-expression created by Dr. David Shackelford and used by Robert Svensson. Dr. Russell Jones designed experiments, supervised and edited the manuscript. I created the figures and wrote the first draft of the paper under the guidance of Dr. Russell Jones.

Chapter 4: The work performed in this chapter was performed with the following contributions from co-authors. I created the MEF cell lines (expressing RISP shRNA) and performed the metabolic and FACS assays, as well as immunoblotting and qPCR. Eric Ma created the mitochondrial specific ROS scavenger Mito-CP, and performed qPCR. Takla Griss created the H1299 cell line expressing AMPK shRNA. Sylvia Andrzejewski performed mitochondrial isolations and respiration assays of the mitochondrial complexes. Dr. St. Pierre provided valuable insight and technical expertise. Dr. Russell Jones and I designed experiments, wrote and edited the manuscript.

TABLE OF CONTENTS

Chapter 1: Literature Review

List of Figures

Chapter 1

Chapter 2

Chapter 3

List of Tables

Chapter 2

LIST OF ABBREVIATIONS

4E-BP1	4E binding protein 1
ACC	Acetyl-CoA Carboxylase
ADP	Adenosine diphosphate
AICAR	5-amino-1-β-D-ribofuranosyl-imidazole-4-carboxamide
ANOVA	Analysis of Variance
AMP	Adenosine monophosphate
AMPK	AMP-activated Kinase
ASC	Ascorbate
ATP	Adenosine Tri-phosphate
CaMKK	Calcium/calmodulin-dependent protein kinase kinase 2
CBS	cystathionine beta synthase
CPT-1	Carnitine palmitoyl transferase I
CO_2	Carbon Dioxide
DMEM	Dulbecco's Modified Eagle Medium
DMSO	Dimethyl sulfoxide
DNA	Deoxyribonucleic Acid
FAS	Fatty Acid Synthase
FBS	Fetal Bovine Serum
FOXO	Forkhead Box O3
HIF-1α	Hypoxia-inducible factor 1α
LDH-A	Lactate Dehydrogenase
LKB1	Liver Kinase B1
NAD^+	Nicotinamide adenine dinucleotide
NSCLC	Non-small cell lung carcinoma

mTOR	mammalian target of rapamycin
PBS	phosphate buffered saline
PFK	phosphofructokinase
PGC-1α	Peroxisome proliferator-activated receptor gamma coactivator 1a.
Pi	Phosphate
PI	Propidium Iodide
PTEN	Phosphatase and tensin homolog
ROS	Reactive Oxygen Species
RPMI	Roswell Park Memorial Institute Medium
SDS-PAGE	Sodium Dodecyl Sulfate Poly-Acrylamide Gel Electrophoresis
siRNA	Small Interfering Ribonucleic Acid
TCA	Tricarboxylic acid cycle

ACKNOWLEDGEMENTS

This thesis would not have been possible without the help and support of many.

My mother Brenda Faubert.

My supervisory committee, Dr. John White, Dr. Alvin Shrier, Dr. Arnim Pause.

My non-official committee, Dr. Julie St. Pierre, Dr. Rick Roy, Dr. Nichol Beauchemin, Dr. Daina Avizonis, Dr. Orval Mamer, Dr. John Orlowski, Dr. Connie Krawczyk.

Present and past members of the Jones lab. In particular, Dr. Gino Boily, Takla Griss, Said Izreig, Eric Ma, Kim Wong, Ben Fuerth, Joelle Behkazi, Fanny Dupuy, Julianna Blagih, Dr. Maya Poffenberger and Dr. Emma Vincent.

My Oncometabolism team co-workers, Dmitri Khadri, Dr. Marie-Claude Gingras, Cathy Dufour, Luc Choniere, Dr. Gaelle Bridon, Shawn McGuirk, Sylvia Andrzejewski, Dr. Simon-Pierre Gravel.

My friend, collaborator and coworker, Mark Verway.

My supervisor Dr. Russell Jones.

OBJECTIVES AND RATIONALE

The field of cancer metabolism has seen renewed interest since the seminal discoveries of Dr. Otto Warburg in the 1920s. Dr. Warburg discovered that cancer cells preferentially produce higher amounts of lactate than non-tumour tissue, regardless of oxygen concentration. Further development upon Otto's work went largely stagnant for decades. It is now appreciated that an estimated 70% of all cancer cells display this increased glycolysis. One consequence of an increased growth rate is that cancer cells require more energy and demand more resources than normal cells. To meet these new requirements, cancer cells must undergo fundamental changes in energy metabolism and nutrient uptake or else they risk apoptosis. These fundamental changes may confer a selective growth advantage, allowing tumours to maintain cellular bioenergetics while proliferating under sub-optimal conditions. Identifying the key molecular mechanisms that drive cancer metabolism will help elucidate the benefits of this altered metabolism for growing tumours.

In 2010, a project was initiated in the Jones lab at McGill to explore an established signaling cascade that was hypothesized to be involved in cancer metabolism. The LKB1-AMPK axis had long been defined as an energetic checkpoint. Activation of this pathway by metabolic stress initiates a series of processes that decrease energy utilization and increase catabolic activity to restore energy balance. Despite this clear role in the regulation of cellular energetics, the metabolic effects of this pathway had not been explored in cancer. As such, the objective of this thesis is to characterize the role of AMPK in cancer metabolism.

In Chapter 2, we studied the role of AMPK in negatively regulating metabolism in cancer cells, and its ability to inhibit tumour growth *in vivo*. To do so, we generated an Eμ-myc-driven murine lymphoma model. We bred these mice to have wild-type, heterozygous loss, or

homozygous loss of the alpha1 allele of AMPK, the only catalytic unit expressed in B cells. We observed enhanced tumour onset in the absence of AMPK, as well characterized the metabolic changes induced by AMPK loss. Importantly, we found that HIF-1α was responsible the enhanced glycolytic metabolism in the absence of AMPK.

The role of AMPK loss in promoting tumour growth prompted us to examine LKB1, the upstream kinase of AMPK. LKB1 had previously been characterized as a tumour suppressor in Peutz-Jeghers patients, and its loss has been observed in a variety of tumour types, including KRAS-driven lung cancer. However, the role of LKB1 in modulating cancer metabolism had yet to be fully elucidated. In Chapter 3, we observed that loss of LKB1 resulted in the metabolic reprogramming of cancer cells. These results included increased glycolysis and glutaminolysis, biosynthesis and survival under nutrient stress, each of which were mediated by HIF-1α.

In Chapter 4 we explore the mechanism leading to the normoxic stabilization of HIF1α in the absence of AMPK. Here we observed that increased mitochondrial ROS in the absence of AMPK led to the stabilization of HIF-1α. In this work we identified a novel role of AMPK response to physiological levels of ROS. We characterize the ability of AMPK to increase antioxidant responses, as well as determine the mechanism of HIF1α stabilization in the absence of AMPK.

The overall objective of this project was aimed at better understanding the role of the LKB1-AMPK pathway in cancer metabolism. We have helped identify and characterize the metabolic changes induced by LKB1 or AMPK loss, and what effects these have on tumour growth.

Chapter 1

LKB1 and AMPK negatively regulate the Warburg effect in cancer: A literature review

1.1 Introduction of Cancer

Cancer is a disease characterized by deregulated cell growth. This disease arises through genetic alterations such as mutation, loss of function, amplification, and gene re-arrangement (Hanahan, 2000). Genes involved in the development of cancer are generally described as being *oncogenes,* which contribute to and drive the processes of transformation and cancer growth, or *tumour suppressors,* which protect a cell from the cancer forming process. Multiple mutations are necessary for the development of cancer, which ultimately result in a growth advantage in mutated cells. Cancerous cells can arise from diverse tissues of origin and often display variability in their genetic lesions (Hanahan, 2000). For instance, even histologically identical cancers of the same tissue of origin can have different oncogene and tumour suppressor combinations driving its deregulated growth. It is estimated that there are thousands of mutations that may contribute to cancer development (Loeb et al., 2003). Cancer can therefore be considered a group of different diseases that are unified by a series of characteristics or 'hallmarks', which are governed by a dozen core signaling pathways and processes. These hallmarks of cancer originally consisted of six biological capabilities including: sustained proliferative signaling, evading growth suppression, evading apoptosis, replicative immortality, angiogenesis, and invasion/metastasis (Hanahan, 2000).

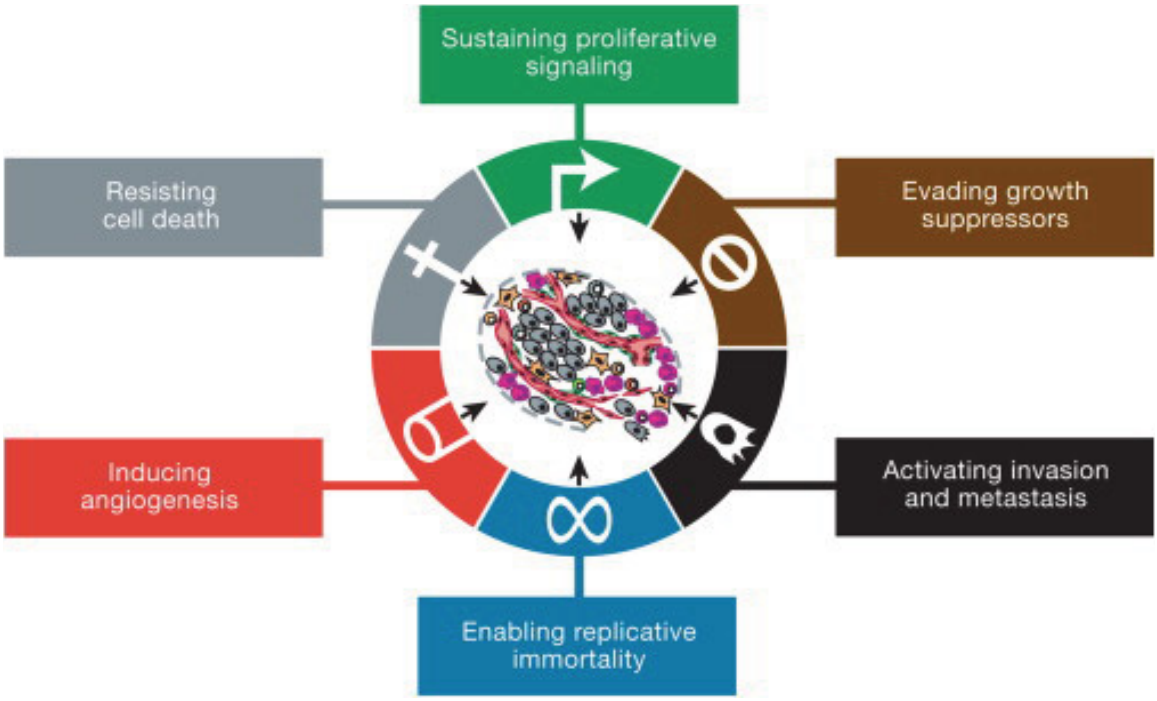

Figure 1.1: The original hallmarks of cancer. Displayed are factors and acquired attributes that characterize the cancer phenotype. Adapted from (Hanahan and Weinberg, 2011).

In recent years, new cancer hallmarks have emerged, including the deregulation of cellular energetics (Hanahan and Weinberg, 2011). It is now understood that many of the commonly mutated oncogenes and tumour suppressors that promote cancer growth are also integrally involved in pathways of biosynthesis, proliferation, and metabolism (Cairns et al., 2011; Vander Heiden et al., 2009). The initial discovery of altered metabolism in cancer occurred nearly 90 years ago. In 1925 Dr. Otto Warburg demonstrated that cancer cells did not metabolize glucose in the same manner as did fully differentiated non-cancerous cells (Warburg, 1956). Specifically under conditions of normoxia, cancer cells converted about 85% of glucose to lactate, despite the presence of adequate oxygen (Vander Heiden et al., 2009). Warburg's seminal finding of altered metabolism in cancer has since sparked interest in both basic science and clinical application. Now termed "The Warburg Effect", this preferential use of glucose by

tumours is utilized as a diagnostic marker of cancer. The positron-emitting glucose analogue ^{18}Fluoro-Deoxyglucose (FDG) can accumulate in tumours as the missing oxygen on the second carbon renders it incapable of being metabolized (Wick et al., 1957). As glucose uptake in tumours far exceeds the majority of non-diseased tissues, the tumour mass can be differentiated from the non-cancerous surrounding tissue when measured by positron emission tomography (PET). This type of measurement has been used extensively as a means of measuring tumour size, response to treatment, staging, and other clinical aspects of cancer (Blodgett et al., 2007). Despite the robust nature of this phenotype, the underlying molecular mechanisms that drive this altered metabolism are still being defined.

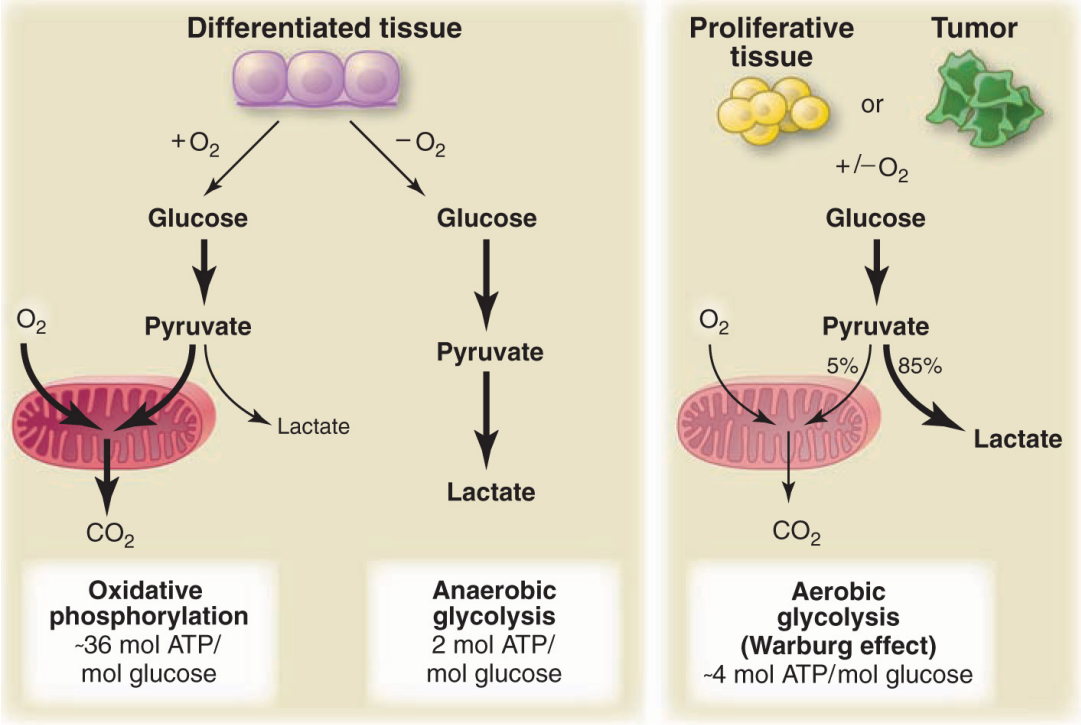

Figure 1.2: The Warburg effect. In non-proliferative, non-tumour tissue, the majority of glucose enters the mitochondria. In tumour cells the majority of glucose in the tumour is

converted to lactate and exported out of the cell regardless of oxygen concentration. Adapted from (Vander Heiden et al., 2009)

Cancer cells must acquire the requisite energy and biosynthetic intermediates to support uncontrolled growth. They must also adapt their metabolism under conditions of energetic stress, where growth rates may outstrip nutrient supply (Jones and Thompson, 2009). There is an emphasis on understanding the underlying signaling pathways that promote this altered metabolism, the biological advantages of this type of metabolism, and importantly, if these changes reveal therapeutic vulnerabilities in cancer. Before identifying the altered metabolic processes in cancer cells, it is important to understand healthy metabolic systems.

1.2 Metabolism

Metabolism can be defined as the chemical processes occurring within a living cell or organism that are necessary for the maintenance of life. This simple definition encompasses thousands of reactions and metabolites, which can be separated into three main processes (Berg, 2012). *Anabolism* refers to the synthesis of simple molecules into complex macromolecules, such as the formation of carbohydrates from simple sugars, proteins from amino acids, and fatty acids from acetyl-CoA molecules (Voet, 2011). Under pro-growth conditions anabolic processes allow for the creation of the necessary macromolecules for cellular growth and proliferation. *Catabolism* refers to the degradation of larger molecules into simpler components in order to release and create energy (Voet, 2011). Molecules such as glucose (catabolized by glycolysis) and fatty acids (catabolized by β-oxidation) create the precursors and molecules necessary to fuel ATP generation (Voet, 2011). The *elimination and recycling of waste products* allows cells to maintain normal functions. For example, high levels of ammonia (derived from transformation of

glutamine to glutamate) can be lethal to cells and organisms. Ammonia is converted to a less toxic metabolite (urea) which can be safely tolerated and removed as waste (Voet, 2011). The survival and function of all living cells are dependent upon the dynamic regulation of metabolism, energetic processes and waste management. The state of cell growth is directly correlated with the state of metabolism. In a quiescent state, there exists a balance between anabolic and catabolic metabolism, namely matching energy generation and consumption to ensure cell survival (Vander Heiden et al., 2009). In a state of growth and proliferation, this balance is shifted towards anabolic processes, as parental cells must effectively double their lipids, nucleotides and DNA content to create two healthy daughter cells. Growth and proliferation must be exquisitely matched to the energetic level of the cell, in order to prevent growth under nutrient limiting conditions, which could ultimately lead to cell death.

1.2.1 Cellular Energy.

The main energetic molecule of a cell is adenosine triphosphate (ATP). ATP is utilized as a cofactor in cellular processes, donating the necessary energy for enzymatic reactions. The energy of ATP is derived from its phosphoanhydride bonds, which when hydrolyzed release 7.3kCAL (ADP + Pi), or 10.9kCAL (AMP + PPi) as energy (Berg, 2012). ATP formation occurs by a series of complex processes. The process begins with the breakdown of macromolecules such as sugar, protein and fats into glucose, amino acids and glycerol/fatty acids. These nutrients can be further metabolized through distinct metabolic pathways, including glycolysis and oxidative phosphorylation in order to generate ATP (Berg, 2012). The amount of ATP is tightly regulated in cells, as the proper maintenance of ATP levels is necessary for cell viability (Izyumov et al., 2004). The breakdown of ATP produces inorganic phosphate (Pi) and ADP,

which is then catalyzed in pairs by adenylate kinase to form AMP and ATP. The action of adenylate kinase maintains relatively constant ATP levels while increasing AMP concentration, which acts as an intracellular signal to restore energy balance (Hardie, 2007). The dynamic changes of the adenylate ratios within a cell (AMP:ADP:ATP), are influenced by a variety of metabolic processes, several of which will be discussed in the following sections.

1.2.2 Glycolysis.

One of the most important substrates on the whole body and cellular level is glucose. Absorbed into the blood during digestion, glucose is ubiquitously used a fuel source (Lunt and Vander Heiden, 2011). The enzymatic breakdown of glucose to pyruvate features a series of reactions that can be divided into 2 phases: the preparatory phase, which consumes energy to process glucose and the pay-off phase, where further enzymatic-processing results in ATP generation. In the preparatory phase, glucose enters the cell via a glucose transporter where it is subsequently phosphorylated by hexokinase to form glucose-6-phosphate (G6P) (Voet, 2011), which prevents glucose from exiting the cell. G6P is isomerized into fructose-6-phosphate (F6P) by glucose phosphate isomerase. A second ATP is consumed as F6P is phosphorylated by phosphofructokinase to create fructose 1,6 bisphosphate, before the eventual conversion into molecules of glyceraldehyde 3-phosphate (GAP) and dihydroxyacetone phosphate (DHAP) by aldolase (Voet, 2011). These two molecules can be interconverted by the action of triose phosphate isomerase (Voet, 2011). Further processing of the GAP is termed the 'pay-off' phase, as 4 ATP and 4 NADH are produced before the molecules have been completely converted to pyruvate. Conversion of GAP to 1,3 bisphosphoglycerate (1,3 BPG) by the enzyme glyceraldehyde 3-phosphate dehydrogenase generates one NADH per molecule. Two ATP are

generated by the conversion of 1,3BPG to 3-phosphoglycerate (3PG) by phosphoglycerate kinase. The phosphate group of 3PG is moved to the second carbon by the enzyme phosphoglycerate mutase to form 2-phosphoglycerate (Voet, 2011). Enolase then converts 2-phosphoglycerate into phosphoenolpyruvate, which is converted to pyruvate by pyruvate kinase, generating two ATP in the process (Voet, 2011). Pyruvate can have several metabolic fates. Pyruvate can be further reduced to lactate by lactate dehydrogenase, and then subsequently secreted from the cytoplasm into the extracellular space by monocarboxylate transporters (MCT) (Halestrap and Price, 1999). In the presence of adequate oxygen, pyruvate can enter the mitochondria as acetyl-CoA (via pyruvate dehydrogenase) or as oxaloacetate (via pyruvate carboxylase), and promotes oxidative phosphorylation via the tricarboxylic acid cycle (TCA).

The high levels of lactate production from glycolysis may also benefit a growing tumour. There is evidence that the lactate produced in hypoxic sections of a heterogeneous tumour can be used by adjacent cells as a fuel for OXPHOS (Sonveaux et al., 2008). Secondly, the excretion of lactate in the surrounding tumour microenvironment causes a local acidification, which can promote the degradation of the extracellular matrix, thereby enhancing metastatic potential (Gatenby and Gillies, 2008; Parks et al., 2011).

The bioenergetic and biosynthetic demands of cancer cells are significant. Cancer cells must generate biomass (lipids, proteins, nucleic acids) in addition to ATP in order to divide. Though glycolysis can provide sufficient amounts of ATP necessary for the energetic requirements, some glucose must be diverted to the biosynthesis of macromolecular precursors such as acetyl-CoA for fatty acids, glycolytic intermediates for amino acids, and ribose for nucleotides. Therefore, enhanced glycolysis in tumour cells serves a variety of growth-promoting purposes as well as energy production (Lunt and Vander Heiden, 2011).

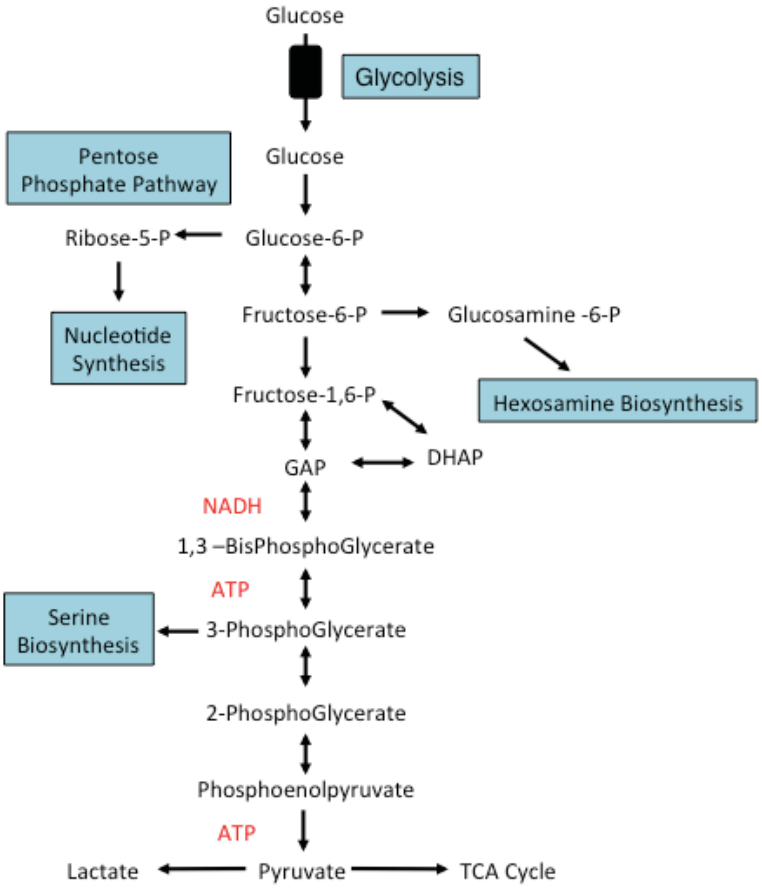

Figure 1.3: Schematic of the enzymatic breakdown of glucose. Production of reducing equivalents or ATP is shown in red. Ancillary metabolic pathways from glycolysis are shown in blue.

1.2.3 Ancillary Pathways from Glycolysis.

Pentose Phosphate Pathway. In addition to generating energy for cellular processes, glycolytic intermediates can be re-directed to provide the key carbon precursors necessary for the synthesis of various macromolecules. The enzyme G-6-P dehydrogenase converts the glucose-6-phosphate produced in glycolysis to 6-P-gluconolactone, committing this molecule to the pentose phosphate pathway (Voet, 2011). This anabolic pathway generates two molecules of NADPH, as

well as 5-carbon sugars such as ribose. Like glycolysis, the pentose phosphate pathway consists of two main phases: the oxidative phase that produces NADPH, and the non-oxidative synthesis of the 5-carbon sugars (Voet, 2011). The NADPH generated from this process is important for several processes, including the maintenance of ROS scavenging molecules such as glutathione (Jeon et al., 2012; Winkler et al., 1986). NADPH is a critical antioxidant that promotes cancer cell survival during metabolic stress, as it helps cancer cells manage oxidative stress while still achieving anabolic needs. Cells lacking the ability to increase NADPH levels were more prone to oxidative damage-induced cell death when faced with stresses such as glucose limitation or 2-Deoxyglucose treatment (Jeon et al., 2012).

Serine biosynthesis. 3-phosphoglycerate (3PG) can similarly be re-directed from glycolysis for use in other biosynthetic processes. The enzyme 3-phosphoglycerate dehydrogenase (PHGDH) commits 3-PG into the serine biosynthesis pathway. Serine and glycine provide precursors for the synthesis of proteins, nucleic acids, and lipids that are crucial to cancer cell growth (Locasale et al., 2011). This pathway also produces important intermediates in the folate pool, which feeds purine and pyrimidine biosynthesis (Locasale et al., 2011). Folate drives the methionine cycle, which recently has been shown to be a possible driver of oncogenesis, as increased PHGDH expression predisposed cells to transformation, and contributed to cancer cell proliferation (Locasale et al., 2011).

Hexosamine biosynthesis. Intermediates from glycolysis can also be shunted into the hexosamine biosynthesis pathway (HBP). The biosynthesis of hexosamine occurs as fructose-6-phosphate (Fruc-6-P) is removed from glycolysis by fructose-6-phosphate-amidotransferase (GFAT), and forms glucosamine-6-P (GlucN-6-P) (Voet, 2011). GlucN-6-P is subsequently acetylated and isomerized to UDP-N-acetylglucosamine (UDP-GlucNAc), which acts as the

parent molecule for conversion into specific amino sugars (Voet, 2011). Of particular interest of hexosamines in cancer is O-linked β-N-acetylglucosamine (O-GlcNAc), which acts as a post-translational modification of intracellular proteins by binding serine or threonine residues (Torres and Hart, 1984). O-GlcNAc binding occurs via the activity of O-GlcNAc tranferase (OGT), which converts UDP-GlcNAc to O-GlcNAc bound to serine or threonine (Voet, 2011). O-GlcNAcase (OGA) can reverse this binding. O-GlcNAc modification can promote several key drivers of cancer metabolism by affecting their stability, activity, or localization, thereby allowing for increased cell survival and metabolism. In example, O-GlcNAc can inhibit α-ketoglutarate from participating in the PHD-mediated regulation of HIF-1α (Ferrer et al., 2014), as well as promote c-MYC stabilization in human prostate cancers (Itkonen et al., 2013).

Taken together, the simple breakdown of glucose primes the cells for energy production (pyruvate entry into the mitochondria) and generates the necessary precursors for biosynthesis. Additionally, the pentose phosphate, hexosamine and serine biosynthesis pathways provide important intermediates and supply biosynthetic pathways to promote cell growth. Taken together, these processes highlight the overall importance of glucose uptake and conversion to its glycolytic intermediates in proliferating cancer cells.

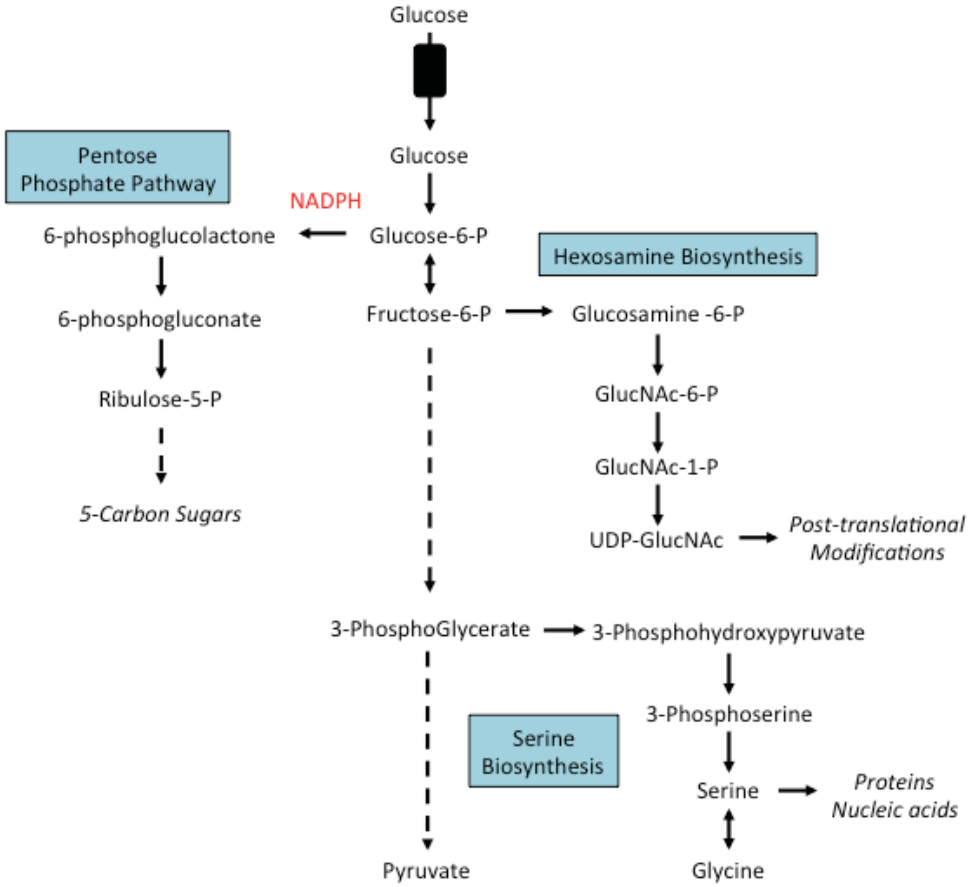

Figure 1.4: Ancillary pathways from glycolysis. Several glycolytic intermediates can be shunted off to other essential metabolites and processes, such as amino acids, redox homeostasis, and post-translational modifications.

1.2.4 Glutaminolysis.

Glutamine is a five-carbon amino acid containing 2 amine groups. It is the most abundant amino acid in humans as well as the second most consumed nutrient in cell culture (Bergstrom et al., 1974; Jain et al., 2012). Glutamine plays a role in various physiological functions, including acting as a source of cellular energy and protein synthesis (DeBerardinis et al., 2007) and

ammonia transport (Weiner and Hamm, 2007). Glutamine is converted to glutamate via glutaminase (Voet, 2011). Glutamate can then be converted to α-ketoglutarate (α-KG) by one of several processes. Glutamate dehydrogenase directly converts glutamate to α-KG (Voet, 2011). Alternatively, the enzyme glutamate pyruvate transferase combines glutamate and pyruvate to form alanine and (α-KG) (Voet, 2011). Or, glutamate oxaloacetate transaminase reacts with glutamate and oxaloacetate to form α-KG and aspartate (Voet, 2011). Glutamine is also used in a wide array of metabolic processes by tumour cells. The importance of glutamine to tumour metabolism is also highlighted by oncogenic mutations such as MYC, which promotes a transcriptional program to increase glutamine uptake and glutaminolysis (Wise et al., 2008a; Yuneva et al., 2007). It has been demonstrated that the ability of tumours to metabolize glutamine directly correlates with tumour growth (Knox et al., 1969; Lobo et al., 2000). Glutamine can be utilized as an anaplerotic substrate to fuel the TCA cycle, contributing to both oxidative phosphorylation as well as lipid synthesis (DeBerardinis et al., 2007). Importantly, glutamine can also be used in the management of oxidative stress as it can fuel glutathione synthesis (Jin et al., 2015).

Reductive Carboxylation. Several groups observed a unique glutamine flow through the TCA cycle in cancer cells (Metallo et al., 2012; Mullen et al., 2012; Wise et al., 2011). Canonical glutamine entry into the TCA cycle involves the conversion to glutamate and α-ketoglutarate, before continuing to succinate (Voet, 2011). In cancer cells that feature mitochondrial dysfunction (Mullen et al., 2012) or under conditions of hypoxia (Metallo et al., 2012), α-ketoglutarate was shown to undergo reductive carboxylation to isocitrate and citrate, where it is then exported for fatty acid synthesis. In short, cancer cells were able to adapt to a high glucose-to-lactate flux by utilizing reductive processes to drive glutamine to fuel fatty acid synthesis.

1.2.5 TCA Cycle.

The pyruvate generated from glycolysis can also fuel the tricarboxylic acid cycle (TCA) cycle. The TCA cycle produces NADH and $FADH_2$, which act as electron donors in the electron transport chain (Voet, 2011). These factors are produced as byproducts of a series of reactions that were first identified in 1937 by Hans Krebs (Krebs and Johnson, 1937). The initiation of the TCA cycle begins with pyruvate entry into the mitochondria by the MTC transporter. Pyruvate is converted to acetyl-CoA by pyruvate dehydrogenase and forms citrate via combination with oxaloacetate by citrate synthase (Voet, 2011). Citrate is an important metabolic node as it can be exported from the mitochondria, to be metabolized back to acetyl-CoA, where it can be used for fatty acid synthesis, or for protein/histone acetylation (Hatzivassiliou et al., 2005). Conversion of citrate to isocitrate by aconitase commits the molecule to the TCA cycle, where it undergoes a series of oxidation and decarboxylation reactions (Voet, 2011). First isocitrate is decarboxylated by isocitrate dehydrogenase to form α-ketoglutarate, which is further decarboxylated to form succinyl-CoA (Berg, 2012). Both reactions result in the production of NADH. Succinyl-CoA is next metabolized to succinate, where it is dehydrogenated to fumarate, by succinate dehydrogenase (complex II of the electron transport chain) (Berg, 2012). Fumarate is hydrated by fumarate hydratase to create malate. Malate re-forms oxaloacetate through the action of malic enzyme that results in NADH production (Berg, 2012). These series of reactions are depicted in Figure 1.5. Glucose-derived pyruvate is not the only source of fuel for the TCA cycle. *Anaplerosis* is the act of replenishing TCA cycle intermediates that have been extracted for biosynthesis. Enzymes such as pyruvate carboxylase, which converts pyruvate directly to oxaloacetate to be used for citrate synthesis, and the conversion of glutamine to glutamate can be used to replenish the pools of α-ketoglutarate in the TCA cycle (DeBerardinis et al., 2007).

Similar to glycolysis, TCA metabolites are used for anabolic processes to sustain cell proliferation (Lunt and Vander Heiden, 2011). In addition to the previously described roles of citrate, several non-essential amino acids necessary for nucleotide and protein synthesis can be derived from TCA intermediates (Voet, 2011).

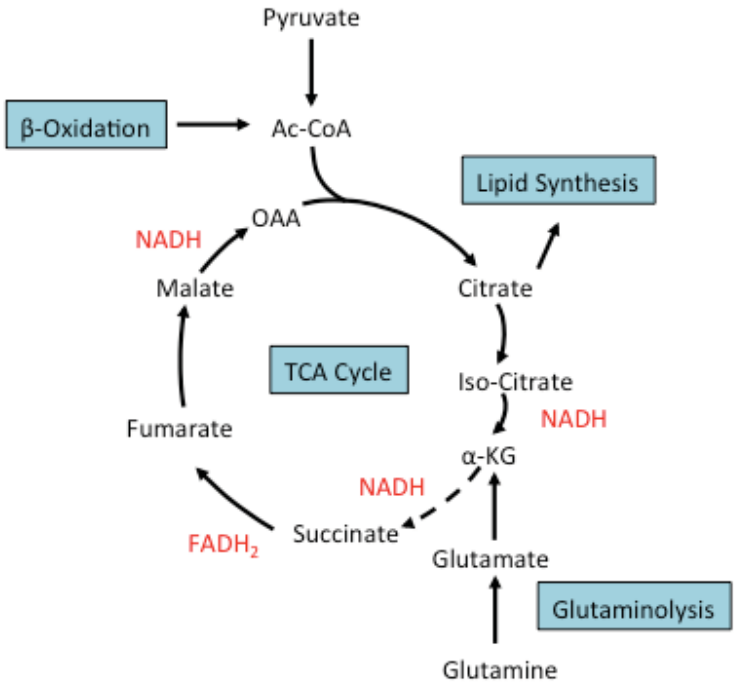

Figure 1.5: Schematic of the TCA cycle. Production of reducing equivalents or ATP is shown in red. Contributing metabolic pathways are shown in blue.

Alterations of TCA cycle activity in cancer. The role of the TCA cycle as an energetic and biosynthetic hub makes it an important node in cancer metabolism. There is evidence that several of the TCA cycle enzymes are mutated or inhibited in cancer, although the effects and importance of these changes can be of differing significance based on the tumour type (Gaude

and Frezza, 2014; Sullivan and Chandel, 2014). The strongest and most consistent phenotypes are associated with mutations or losses of isocitrate dehydrogenase, fumarate dehydrogenase, and succinate dehydrogenase (Ashrafian et al., 2010; Yan et al., 2009).

IDH. Novel mutations of the isocitrate dehydrogenase (IDH) genes have been observed in leukemia and glioma (Yan et al., 2009). Importantly, these mutated IDH enzymes produced an enantiomer of α-ketoglutarate, the (R)-hydroxyglutarate (Ye et al., 2013). This metabolite has not been observed in great quantities in non-mutated metabolic processes and therefore may be used as a cancer biomarker (Guo et al., 2011; Pope et al., 2012). Recent literature suggests that accumulation of 2-HG acts as an oncometabolite, by competitively inhibiting enzymes and processes that rely on α-ketoglutarate as a cofactor, including HIF-1α-mediated angiogenesis or Jumonji-mediated histone modifications (Dang et al., 2009; Lu et al., 2012). Similarly it has been reported that these mutations may predispose tumours to various forms of oxidative stress due to the depletion of antioxidants (Kil et al., 2007; Lee et al., 2004).

SDH/FH. Inactivating mutations of SDH have been linked to various cancer types including paraganglioma (Baysal et al., 2000), renal carcinoma (Ricketts et al., 2008) and breast cancer (Kim et al., 2013). SDH appears to behave as a classical tumour suppressor, as the mutated allele is inherited in heterozygous fashion, while the wild type is lost (Gimm et al., 2000). The phenotype of SDH loss is driven by hypoxia inducible factor (HIF-1α, see Section 1.9). High levels of succinate inhibit the α-ketoglutarate-dependent enzymes that regulate HIF-1α degradation (Selak et al., 2005). Similar processes are observed with the loss of fumarate hydratase. FH loss leads to the stabilization of HIF-1α, as high fumarate levels also competitively inhibit the prolyl hydroxylase reaction that regulates HIF (Isaacs et al., 2005). Given the recent

nature of these discoveries, it stands to reason that other enzymes in the TCA may yet prove instrumental to tumour growth in various models.

1.2.6 Beta-Oxidation.

One of the most potent energy producing processes in the cell is the oxidation of fatty acids. The catabolism of fatty acids involves the generation of acetyl-CoA, as well as $FADH_2$ and NADH. The oxidation of a fatty acid (i.e., palmitate) will result in 7 NADH, 7 $FADH_2$ and 8 acetyl-CoA, which can result in a net gain of 129 ATP molecules (Voet, 2011). The acetyl-CoA generated fuels numerous processes, including the TCA cycle as well as protein and histone acetylation. The rate-limiting step of these reactions is the transfer of fatty acids into the mitochondria (Berg, 2012). In the cytosol, the carnitinepalmitoyl transferase 1 (CPT1) combines acetyl-coA and carnitine to form acyl-carnitine (Berg, 2012). This molecule passes through the outer mitochondrial membrane, where it is transported into the mitochondrial matrix by a translocase (Berg, 2012). Upon entry into the matrix, the molecule is broken down into its constituents, acyl-coA and carnitine by CPT2 (Berg, 2012). In the mitochondrial matrix, the fatty acid is then broken down in a series of dehydrogenation and hydrogenation reactions, which systematically generate two carbon units from the fatty acid chain, until the entire fatty acid has been oxidized (Berg, 2012). Acyl-CoA dehydrogenase catalyzes the first dehydration reaction, forming 2,3 enoyl-CoA from Acyl-CoA and creating $FADH_2$ in the process (Berg, 2012). The resulting fatty acid is hydrated by enoyl-CoA hydratase, forming 3-hydroxyacyl-CoA, before being acted on by β-hydroxyacyl-CoA dehydrogenase and creating NADH (Voet, 2011). The resultant molecule, 3-ketoacyl-CoA is removed from the fatty acid chain by Acyl-CoA acetyltransferase (Voet, 2011). The newly formed NADH and $FADH_2$ can then be used in the

electron transport chain for ATP generation. Increased β-oxidation can occur in tumours undergoing metabolic stress as a means to promote cell survival (Sanchez-Macedo et al., 2013; Zaugg et al., 2011).

1.2.7 Electron Transport Chain.

A main function of the TCA cycle is the production of reducing equivalents that are utilized by the electron transport chain (ETC). The ETC consists of a series of five protein complexes, Complex I-IV and ATP synthase, which are embedded in the mitochondrial membrane (Voet, 2011). The donation of electrons from NADH and $FADH_2$ drives a series of redox reactions to create a proton gradient in the intermembrane space. The proton motive force drives ATP synthase and provides the energy to create ATP from ADP and phosphate ions (Pi) (Mitchell, 1961; Rich and Marechal, 2010).

Complex I (NADH dehydrogenase). Upon entry into complex I, NADH dehydrogenase removes the proton from NADH to form NAD^+, H^+ and $2e^-$ (Voet, 2011). The proton is pumped out into the intermembrane space, while the electrons from NADH are transferred in a series of reactions from flavin mononucleotide, to a Fe-S cluster, to coenzyme Q (Voet, 2011). Coenzyme Q acts as a carrier molecule to transfer electrons to Complex III (Voet, 2011).

Complex II (succinate dehydrogenase). Complex II is unique in the electron transport chain as it is a direct link with the TCA cycle. The conversion of succinate to fumarate by succinate dehydrogenase results in the formation of $FADH_2$ (Voet, 2011). Electrons from $FADH_2$ are similarly transferred to coenzyme Q, but no protons are pumped into the intermembrane space (Voet, 2011). The product fumarate is further metabolized to malate and oxaloacetate in the

continuation of the TCA cycle. Complex II can also accept the $FADH_2$ generated from β-oxidation, via glycerol-3-phosphate dehydrogenase (Voet, 2011).

Complex III (coenzyme Q-cytochrome c reductase). This complex contains cytochrome b, cytochrome c, and the rieske iron-sulfur protein (Voet, 2011). Termed the Q-cycle, this complex transfers electrons from coenzyme Q (originating from either complex I or II) to cytochrome c, resulting in the pumping of 4 protons into the intermembrane space (Voet, 2011).

Complex IV (cytochrome c oxidase). Complex IV acts as the terminal complex of the chain. This complex removes the electrons from the cytochrome c and transfers them to molecular oxygen to form water (Voet, 2011). During this process, four protons flow into the intermembrane space. The result is the production of a proton gradient that can be utilized by ATP synthase (Voet, 2011). ATP synthase consists of two main units, F_o and F_1. The F_o subunit acts as an ion channel that allows for proton flux back into the mitochondrial matrix (Voet, 2011). This flux releases energy that the F_1 complex uses to combine ADP and Pi to create ATP (Voet, 2011).

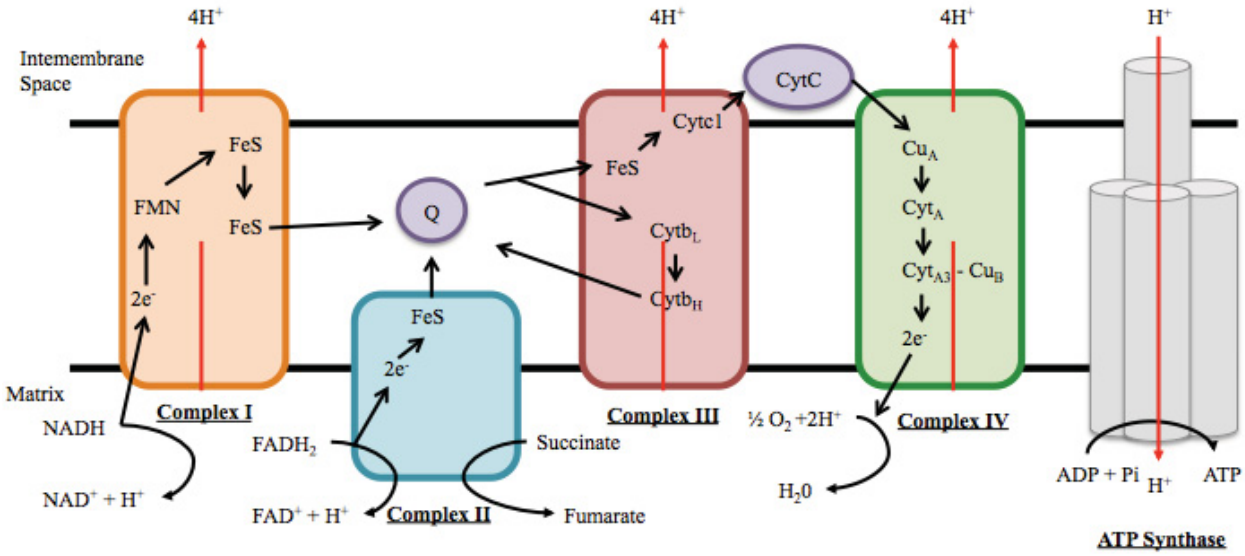

Figure 1.6: Schematic of the electron transfer and proton movement in the electron transport chain. Proton flux through the various complexes is shown in red.

Complex I mutations are the most common electron transport chain mutation in cancer (Chatterjee et al., 2006). Mutations in CI alter both cellular energetics and redox homeostasis. This enhancement of ROS has been shown to increase ROS-dependent metastatic processes in lung and breast cancer cells (Chatterjee et al., 2006; Ishikawa et al., 2008). However, the degree of mutation and dysfunction correlates with tumorigenic potential. Cancer cells with a severe CI deficiency were strongly inhibited in growth and survival as compared to those with mildly mutated CI. In addition, complex I activity was essential for cell survival under metabolic stress in certain cancers (Iommarini et al., 2014).

1.3 Reactive Oxygen Species.

Metabolism and redox status are intertwined processes, as the mitochondrial electron transport system is the major site for generation of reactive oxygen species in the cell (Aon et al., 2010; Cortassa et al., 2014). During respiration, superoxide (O_2^-) is produced by the incomplete reduction of O_2 at the flavin mononucleotide site of complex I and the Q cycle of complex III (Brand, 2010; Murphy, 2009). O_2^- is dismutated to H_2O_2 by superoxide dismutase 1 (SOD1) in the cytosol (Bordo et al., 1994), or by $Mn2^+$-dependent superoxide dismutase (SOD2) in the mitochondrial matrix (Oberley and Oberley, 1988). H_2O_2 can be further reduced to water by catalase, glutathione peroxidase (GRX) or peroxiredoxin (PRX) (Holmstrom and Finkel, 2014). The balance of the reduced state vs. the oxidized state of a biochemical system is referred to as redox status. This status is a result of the production rate of reactive oxygen species and the relative capacity of the antioxidant system to neutralize ROS production (Holmstrom and Finkel, 2014). This redox balance reciprocally acts on metabolism. Many metabolic processes can be affected by the redox state as the enzymes can either be reduced or oxidized to promote or inhibit function (Yang et al., 2014). To maintain normal function the enzyme must be reduced or oxidized back to its original state. Therefore, proper maintenance of redox balance is necessary for cell function.

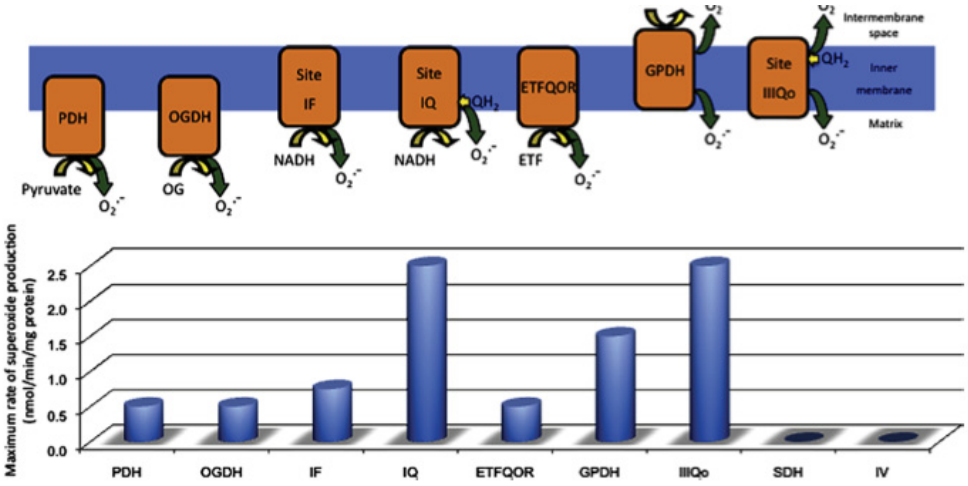

Figure 1.7: ROS topology and production. Direction and amount of ROS production throughout the electron transport chain. The major sites of ROS production are complex I and III. Complex III is the major driver of ROS production directed outside of the mitochondria. Figure from (Brand, 2010).

1.3.1 ROS-dependent signaling.

There is increasing appreciation for the role of ROS as a signaling molecule. The stability and membrane diffusion capability of H_2O_2 allows for the H_2O_2-induced oxidation of cysteine residues of nearby proteins, including key signaling pathway molecules (Yang et al., 2014). This protein oxidation generally results in a disulfide (S-S) bond, which can be reversed by GRX and TRX (Reczek and Chandel, 2014). Growth factor-receptor binding can cause increase intracellular ROS. This increase in ROS can inhibit the protein phosphatases that regulate growth factor receptors, allowing for the enhancement of the growth signal (Yang et al., 2014). This effect can be negated through redox reactions within the cell, as attenuation of ROS levels and reactivates the phosphatase activity. As such, pro-growth effects can be correlated with increased ROS levels. Therefore, ROS-induced signaling can play a significant, non-damaging role in cellular processes including metabolism and growth.

1.3.2 Antioxidants.

Proper maintenance of ROS is necessary to ensure cell viability and health. Aberrant levels of ROS can be damaging to a variety of cell organelles (Cross et al., 1987). In order to maintain ROS levels in a healthy range, a host of enzymes act to convert highly reactive/damaging species of ROS into less reactive forms, including the SOD enzymes converting superoxide to H_2O_2. High levels of H_2O_2 can be dangerous depending on the location of their production as they cause Fenton reactions with Fe^{2+} or Cu^{+} to form hydroxyl radicals (Dizdaroglu and Jaruga, 2012). These hydroxyl radicals are highly reactive and will irreversibly damage any macromolecule in the vicinity. To prevent this, H_2O_2 production is often restricted to compartments with antioxidants that convert H_2O_2 to water. Antioxidants such as glutathione peroxidase (GPX), peroxiredoxins (PRX) are spatially regulated (Cox et al., 2010; Murphy, 2012). GPX and PRX are found in a variety of locations including the cytosol, mitochondria and endoplasmic reticulum (Wood et al., 2003).

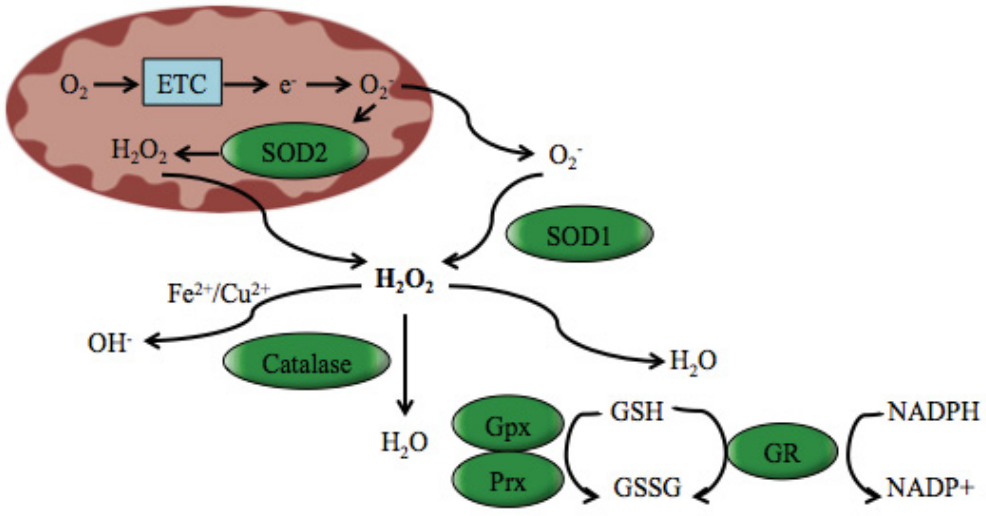

Figure 1.8: Fates of mitochondrial-produced ROS. Antioxidant proteins are shown in green.

1.4 Techniques for Measuring Metabolism.

1.4.1 Seahorse XF Analyzer.

Recent methods and techniques have expanded upon the classical biochemical assays for measuring reaction rates of metabolic processes. These new methods have included fluorometric assays that react with the resultant products or cofactors from an enzymatic reaction. One of the widely used applications of this technology is the Seahorse XF analyzer. When cells are actively exporting lactate, a release of protons into the extracellular space also occurs, resulting in a concomitant acidification of the media. Changes in oxygen consumption by the cells can be measured via fluorophores that react with oxygen (Gerencser et al., 2009). The XF analyzer combines these reactions to a fluorometric probe. Cells are incubated in a buffer-free media, and a measuring cartridge is held 200 microns above the cells. Changes in proton release/media acidification (a proxy measurement of lactate production) and oxygen consumption are transmitted to the Seahorse machine, allowing for real-time measurement of both processes (Gerencser et al., 2009). This technology is coupled with drug-injection ports, which can introduce drugs that affect mitochondrial reactions, allowing for the investigation of various mitochondrial processes, as well as the immediate metabolic response to a variety of drugs. Though problems such as gas exchange may occur in the plate-based system that must be taken into account (compared to the closed chamber of a Clark electrode), the high-throughput capability of the plate-based system remains an attractive option (Gerencser et al., 2009).

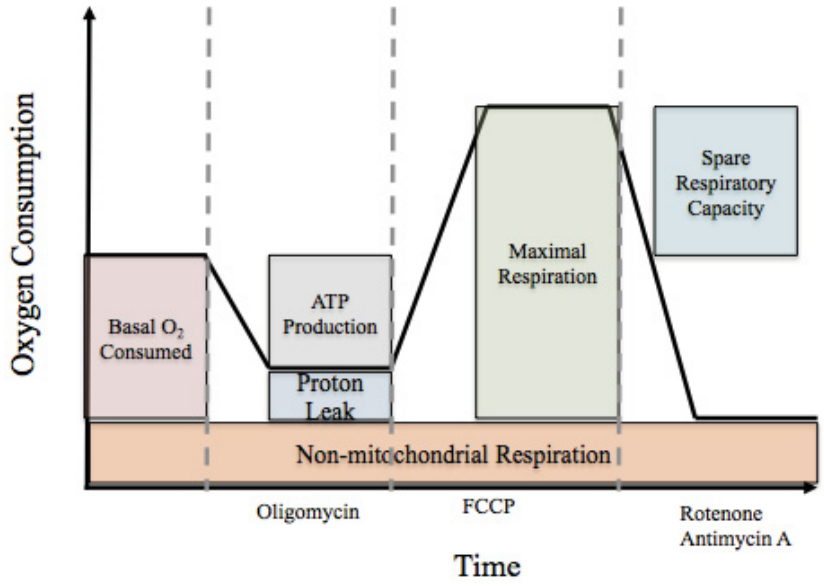

Figure 1.9: Diagram of mitochondrial evaluation by the Seahorse XF Analyzer. States of mitochondrial respiration can be analyzed by the addition of various drugs, including oligomycin (ATP synthase inhibitor), FCCP (protononophore/uncoupler) and the combination of rotenone and antimycin, A which inhibit complex I and complex III respectively.

There are several applications of this technology in the study of cancer metabolism. High throughput analysis of basal levels in glycolytic and oxidative metabolism, as well as metabolic responses to therapeutic drugs are a large advantage in comparison to classical single enzyme assays (Gerencser et al., 2009). This technology can be used to explore other metabolic, oxygen consuming pathways such as β-oxidation, though the addition of free fatty acids with and without the drug etoxomir to block fatty acid oxidation.

1.4.2 Gas chromatography Mass spectrometry.

One of the techniques currently used in the field of cancer metabolism is using gas chromatography/mass-spectrometry (GC-MS) to quantify relative metabolite levels. The GC-MS

uses inert gas to push samples though a heated capillary column. This first stage resolves molecules based on their retention time in the column (Gordon and Frigerio, 1972). Upon entry to the mass spectrometer, the molecules undergo electron ionization by electrons emitted from a filament. The molecules are then fragmented into various pieces with specific mass to charge ratios (Gordon and Frigerio, 1972). The time of elution of the molecule from the column, the mass spectra of the fragmented pieces, and the specific mass to charge ratios allow for the specific identification of a wide various of molecules (Gordon and Frigerio, 1972).

1.4.3 Mass Isotopomer Labeling.

When a GC-MS is used for metabolic analysis, it is able to quantify metabolite abundance. However, this quantification is not necessarily informative of enzymatic flow, carbon transfer, or dynamic processes. In order to elucidate these aspects of metabolism the GC-MS technology can be used in the identification of mass isotopomers. These experiments take advantage of heavy-labeled nutrients that are metabolized to produce heavy-labeled products. These heavy-labeled products can be differentiated from the natural pool of metabolites, allowing for determination of metabolite flux in cells (Inbar and Lapidot, 1987; Mullen et al., 2012). For instance, a typical experiment may use a glucose molecule in which each of the natural ^{12}C carbons has been replaced with non-radioactive, heavy-labeled ^{13}C carbons. Growing cells are then cultured in a medium where entire pool of ^{12}C-glucose has been replaced with ^{13}C-glucose. As glucose is enzymatically processed the ^{13}C-carbons are transferred to other metabolites. Upon measuring these metabolites on GC-MS, the extra weight of the ^{13}C vs. ^{12}C carbon units allows for the unique identification of the carbon fate of the labeled nutrient. Taken together, the breakdown and flow from these ^{13}C carbon units can be traced by GC-MS, allowing for very

specific measurement of metabolic flow (Inbar and Lapidot, 1987; Kalderon et al., 1988; Mullen et al., 2012).

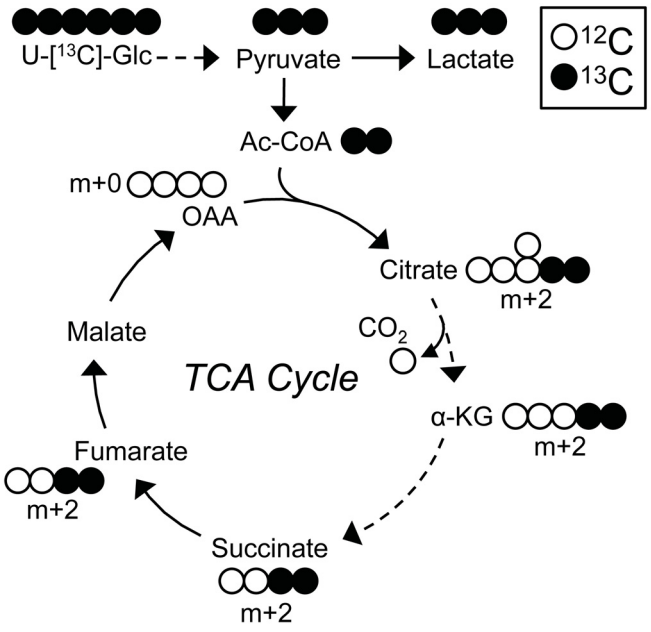

Figure 1.10 Mass isotopomer (MI) distribution in the TCA cycle. Representative diagram of MI labeling of glucose breakdown to lactate and the TCA cycle. Closed circles indicate ^{13}C carbons. The transfer of heavy-labeled carbons from the glucose input to downstream metabolites can be measured and quantified by GC-MS.

1.5 Mediators of Oncometabolism.

The prevailing metabolic change in tumours is the Warburg effect, which has primarily been utilized diagnostically with ^{18}FDG-PET scans. Several attempts have been made to target this enhanced glucose uptake therapeutically, but this has not yielded satisfactory results. Enhanced glucose uptake is a pro-growth metabolic phenotype shared with normal physiological function, such as in proliferating cells within the immune system (Chang et al., 2013). Therefore

unless cancer-specific targeting of these glycolysis-promoting enzymes can occur, targeting metabolism could produce the same toxicity observed by current chemotherapeutic methods. Elucidating and understanding the distinct molecular mechanisms that drive glucose uptake in tumours compared to normal physiological cells must occur in order to advance the therapeutic benefits of targeting cancer metabolism. Several of these mutated oncometabolic pathways are listed below.

1.5.1 PI3K-AKT

The PI3K pathway is one of the most commonly altered signaling pathways in human cancers, and regulates pro-growth signals as well as metabolism (Engelman et al., 2006; Thorpe et al., 2015). Activation of this pathway can occur at several steps, such as by loss of the tumour suppressor PTEN, activating mutations of PI3K, or activation of the cell receptors (Thorpe et al., 2015). One of the main effectors downstream of PI3K is AKT. Activation of AKT increases the expression and membrane translocation of glycolytic enzymes (Elstrom et al., 2004; Plas and Thompson, 2005), and stimulates activity of the mammalian target of rapamycin, by inhibiting its negative regulator TSC2 (Inoki et al., 2002). In short, the PI3K-AKT signaling pathway engages a wide variety of cancer-promoting processes, including cell survival, growth and proliferation, and metabolism (Cairns et al., 2011).

1.5.2 Mammalian Target of Rapamycin (mTOR).

mTOR exists as two distinct, large protein complexes, mTORC1 and mTORC2. mTOR is regulated principally by the heterodimeric tuberous sclerosis complex (TSC1/2) (Inoki et al., 2002). This complex acts as a GTPase activating protein, which negatively regulates the GTPase

Rheb, which is required for mTORC activation (Garami et al., 2003). mTORC1 functions as a key metabolic checkpoint, as it integrates nutrients and growth signals into pro-growth programs (Guertin and Sabatini, 2007). Under conditions of low energy, mTOR is negatively regulated by the AMP-activated protein kinase (AMPK), through inhibition of Raptor and activation of the negative regulator TSC2 (Gwinn et al., 2008). mTOR reacts to favourable levels of inputs such as oxygen, amino acids, growth factors and energy levels by increasing macromolecular biosynthesis, promoting cells cycle progression and increasing growth and metabolism (Laplante and Sabatini, 2009). Specifically, mTORC1 controls the translation of many cell growth regulators, including HIF-1α and MYC, which in turn promote angiogenesis, glucose and glutamine metabolism, and cell growth (Guertin and Sabatini, 2007; Laplante and Sabatini, 2009).

1.5.3 p53.

Referred to as the 'Guardian of the Genome', p53 is the most widely mutated tumour suppressor in cancer. A well-characterized transcription factor, p53 is known for its functions in the DNA damage response and apoptosis, as well as engaging anti-proliferative pathways by activating or repressing key effector genes (Zilfou and Lowe, 2009). With regard to metabolism p53 has been shown to enact a cell cycle checkpoint under conditions of metabolic stress (Jones et al., 2005). p53 is also involved in the modulation of autophagy (the process of degrading/recycling cellular components), as it activates the damage related autophagy modulator (DRAM) (Crighton et al., 2006). There are also varied effects on glycolysis and the pentose phosphate pathway. p53 directly binds and inactivates glucose-6-phosphate dehydrogenase, thereby preventing flux into the pentose phosphate pathway (Jiang et al., 2011). p53 also

promotes oxidative phosphorylation by activating the expression of SCO2, which assembles the cytochrome c oxidase complex and helps regulate mitochondrial respiration (Matoba et al., 2006).

1.5.4 MYC.

MYC is a pleiotropic transcription factor that regulates a variety of processes including cell cycle progression, apoptosis, and metabolism (Dang, 1999, 2010). The N-terminal domain of MYC mediates transcriptional activation via direct contact with the basal transcription machinery (Hateboer et al., 1993). MYC activation has been shown to be a potent inducer of glutamine metabolism by increasing the transcription of glutamine transporters, and similarly, MYC over-expression was found to sensitize cancer cells to glutamine deprivation (Wise et al., 2008b). Anapleurotic flux of glutamine into the TCA cycle was observed to be essential in these cells (Wise et al., 2008a). MYC can also promote glycolytic activity by directly activating the transcription of glycolytic genes, such as LDHA and HKII (Kim et al., 2007; Shim et al., 1997).

1.5.5 HIF-1α.

Cellular adaptation to O_2 deprivation (hypoxia) is a physiological response during normal development as well as pathogenic conditions. The main response to these conditions is the stabilization of the transcription factor hypoxia-inducible factor 1 (HIF-1), which drives global responses to hypoxic gene expression (Semenza, 2004). HIF1 is a heterodimer, combining HIF-1α or HIF-2α with HIF-1β. Dimerization causes the translocation of the dimer into the nucleus to initiate the transcriptional activity. HIF-1α drives both angiogenesis and glucose uptake as a means of responding to energetic stress (Gordan and Simon, 2007). By transcriptionally increasing GLUT1 (increasing glucose uptake), aldolase (increasing glucose processing), LDHA

(increased export of glucose waste products) and PDHK1 (directing pyruvate away from the mitochondria), HIF-1α metabolically alters cells away from oxidative phosphorylation and increases glycolysis (Semenza et al., 1994). The increased glycolysis acts as an emergency energy mechanism until oxygen can be re-supplied. In addition, HIF-1α increases the transcription of vascular endothelial growth factor (VEGF) to re-vascularize an area with blood supply and oxygen. As tumor cells proliferate, they outgrow the local blood supply, creating regions of hypoxia. In response, the cancer cells adapt to limited oxygen supply by via HIF1 (Keith et al., 2012). HIF-1α remains an attractive therapeutic target as its expression is tied with metabolism, growth, metastasis, and radiation resistance (Moeller et al., 2005).

HIF-1α is continuously transcribed, and translated in an mTORC1-dependent fashion (Shackelford et al., 2009; Thomas et al., 2006). Under normoxic conditions, the prolyl hydroxylase enzyme uses oxygen and α-ketoglutarate to add hydroxyl groups onto HIF-1α at Pro-402 and Pro-564 (Ivan et al., 2001). This reaction converts Fe^{2+} to Fe^{3+}, which is reduced by ascorbate, producing CO_2 and succinate (Figure 1.5). The hydroxylated prolines are recognized by the VHL complex, which acts as an E3 ubiquitin ligase that modifies HIF and commits it to proteosomal degradation (Hon et al., 2002). The activity of HIF can also be inhibited by the asparagine hydroxylase factor inhibiting HIF (FIH), which hydroxylates HIF at asparagine 803, thereby preventing transactivation (Mahon et al., 2001). Under hypoxic conditions, low O_2 levels inhibit the activity of PHD, allowing HIF-1α to escape degradation and accumulate to bind to HIF-1β, which then translocate to the nucleus and promotes O_2-regulated gene expression (Semenza, 2007). HIF-1α can also be stabilized in the presence of oxygen. Loss of the VHL tumour suppressor can result in aberrant HIF-1α signaling (Cockman et al., 2000; Maxwell et al., 1999). Recent evidence has shown that in renal cell carcinomas featuring loss of the TCA cycle

enzymes succinate dehydrogenase (Selak et al., 2005) or fumarate dehydrogenase (Isaacs et al., 2005), cause stabilization of HIF-1α through inhibition of PHD activity. Increased levels of reactive oxygen species allow for the stabilization of HIF-1α, putatively through inhibition of the PHD reaction as well. There has been considerable debate if HIF-1α stabilization can be induced through aberrant levels of reactive oxygen species, though the majority of evidence indicates that ROS stabilizes HIF-1α (Bell et al., 2007; Brunelle et al., 2005b; Simon, 2006).

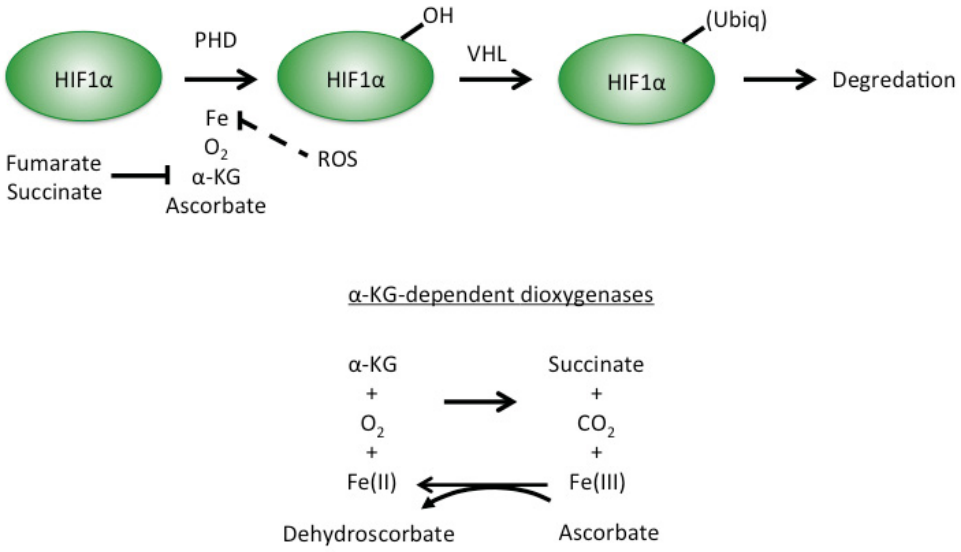

Figure 1.11. **HIF-1α regulation and factors that can cause degradation.** HIF-1α protein is regulated by post-translational modifications, including prolyl hydroxylation by PHD. Factors that promote or inhibit this reaction, such as fumarate, succinate, and ROS are shown.

1.6 AMPK: Coupling Energy and Growth

All living cells must be able to couple nutrient availability to growth and proliferation. In order to survive metabolic stress or nutrient withdrawal, cells must be able to engage alternative metabolic pathways to maintain energetic balance. Failure to adapt to changing nutrient levels can result in cell death. One of the major regulators of adaptation to metabolic stress is the AMP-activated protein kinase (AMPK). AMPK is a serine/threonine kinase that acts as a cellular energy rheostat. AMPK acts as a buffer against various stresses that result in energy depletion, including nutrient depletion, heat shock, hypoxia, and exercise. AMPK responds to this change in energy level by shifting metabolism towards energy generation, while concomitantly inhibiting processes that result in energy expenditure (Hardie et al., 2012). AMPK acts as a guardian of cellular energy levels.

1.6.1 History of AMPK.

AMPK is an evolutionarily conserved energy sensor. AMPK is a heterotrimer comprised of α, β, and γ subunits. There exist 2 α, 2 β, and 3 γ subunits, with varying expression levels of the different isoforms in different tissues. The genes for these subunits are well conserved evolutionarily, as they are found in most eukaryotes including yeast, fungi, plants and animals (Hardie, 2007; Hardie et al., 1998). The discovery of AMPK occurred in increments during the 1970's and 1980's, and involved a number of labs in a variety of disciplines. Specifically, work in mammalian and yeast models combined to elucidate the composition, function and evolutionary conservation of AMPK. In 1973 two groups working on HMG-CoA reductase (Beg et al., 1973) and Acetyl-CoA carboxylase (ACC) (Carlson and Kim, 1973) respectively, discovered that isolation of their protein could be inhibited by phosphorylation. It was later

reported that this inactivation of ACC was stimulated by AMP (Yeh et al., 1980) and was also later shown in HMG-CoA (Ferrer et al., 1985). With both ACC and HMC-CoA being substrates of a kinase requiring AMP, the enzyme responsible for these phosphorylation's was renamed AMP-activated protein kinase. However the functional and physiological relevance of AMPK in mammalian systems had yet to be defined.

In *Saccharomyces cerevisiae*, the sucrose non-fermenting-1 (SNF1) gene was discovered by a screen for mutations that caused failure to grow on non-fermentable carbon sources (Carlson et al., 1981), and was later found to encode for a protein kinase (Celenza and Carlson, 1986). For budding yeast, glucose is the preferred carbon source. When glucose is available, the genes for gluconeogenesis, respiration, and peroxisome biogenesis are repressed. Stimulation of these genes is critical for survival when glucose is lacking, and is mediated by SNF1 (Simon et al., 1992; Thompson-Jaeger et al., 1991). In 1994 it was discovered that SNF1 is the orthologue of AMPK, when the mammalian subunits were sequenced (Mitchelhill et al., 1994; Woods et al., 1994). The conservation of AMPK between species, and the combined biochemical and genetic approaches to study of this enzyme by various groups converged to identify AMPK. The overlapping functions of AMPK in various systems began to elucidate the role of AMPK as an energetic regulator in cells.

Several non-mammalian models in addition to *S. cerevisiae* have proven important in further elucidating the role(s) of AMPK. *Caenorhabditis elegans* is a free-living nematode that feeds on bacteria. The generation times are 3-4 days, and a single hermaphrodite and produce about 200 progeny (Beale, 2008). *C. elegans* is a metazoan which has been used as a genetic model to dissect AMPK signaling and physiological effects, as all three AMPK subunits are highly conserved in this worm (Beale, 2008). Using *C. elegans* as a model, AMPK has been

shown to regulate life span, nutritional control and cell proliferation (Apfeld et al., 2004; Curtis et al., 2006; Narbonne and Roy, 2009).

1.6.2 Biochemistry of AMPK.

One unique feature of AMPK is its regulation by adenylate levels in the cell (Hardie et al., 2011). Mammalian AMPK γ has 4 cystathionine-beta-synthase (CBS) adenosine phosphate binding sites (Bateman, 1997). All adenylate molecules (ATP, ADP, AMP) compete for binding in CBS1 and CBS3, whereas AMP constantly occupies CBS4, regardless of nucleotide concentration (Hardie, 2011b). AMPK activation can occur by AMP or ADP binding, implying AMPK is regulated by adenylate energy charge rather than solely by levels of AMP (Xiao et al., 2007; Xiao et al., 2011). Binding of AMP to the gamma subunit can promote phosphorylation of T172 in its activation loop (T loop), and allosterically increase AMPK activity. This binding initiates an assembly cascade to facilitate phosphorylation. AMP-binding directly triggers a signaling loop for AMPK activation, promoting AMPK interaction with the scaffolding protein AXIN and LKB1. This resulting complex facilitates phosphorylation of AMPK by LKB1 (Zhang et al., 2013). Recent work has further characterized the activation process of AMPK. AMP binding and phosphorylation of AMPK by its upstream kinases causes a partial protection against the activity of phosphatases. Use of the direct pharmacological activator A-769662 promotes binding between of the CBM domain of the beta subunit to the kinase domain (Sanders et al., 2007), though an endogenous metabolite or factor that causes this effect has yet to be elucidated. This conformational change results in an active AMPK that his highly protected from phosphatases (Xiao et al., 2013). In addition to conformational changes, post-translational modifications have been shown to alter AMPK activity. AMPK can be myristoylated on the β1-

subunit, as well as phosphorylated at Ser108 residue, which is required for AMPK localization and activity (Oakhill et al., 2010). An inhibitory phosphorylation mark on Ser485 (α1) or Ser491 (α2) has been demonstrated by several kinases including AKT (Valentine et al., 2014), and p70 S6K (Dagon et al., 2012). Inactive AMPK can be bound to glycogen via the glycogen-binding domain on the β subunits. Furthermore, phosphorylation of T148 in response to glucose withdrawal, allowing for changes in cellular localization (Oligschlaeger et al., 2015).

1.6.3 Kinase Activation of AMPK

STK11 encodes the liver kinase B1 (LKB1), a serine/threonine kinase that plays multifaceted roles in cell proliferation, polarity, metabolism, and survival (Alessi et al., 2006). The liver kinase B1 (LKB1) functions as a master regulator of growth and metabolism in cells. LKB1 was identified as a tumour suppressor, as mutation or loss of this gene is responsible for causing Peutz-Jeghers Syndrome (Hemminki et al., 1998). Furthermore, LKB1 is frequently mutated in sporadic human non-small cell carcinomas and cervical cancers (Ji et al., 2007). AMPK is a downstream effector of LKB1 and carries out many of the key tumour suppressor functions of LKB1. However, AMPK can be phosphorylated by additional kinases (i.e. CAMKKβ), and therefore may act independently of LKB1, even in LKB1-null tumours. Conversely, LKB1 phosphorylates a number of AMPK-related kinases in addition to AMPKα1 and α2 (Lizcano et al., 2004). Thus, many of the phenotypes of LKB1-deficient tumors may not result from disrupted AMPK signaling. LKB1 acts to co-ordinate a series of signaling pathways through phosphorylation of multiple downstream targets. When in complex with STRAD and the scaffolding protein MO25, LKB1 phosphorylates 12 downstream kinases, termed the AMPK-related kinases (AMPKRKs). LKB1 phosphorylates the T-loop of most of the members of this

subfamily to activate these kinases (Lizcano et al., 2004). Recent evidence indicates that LKB1 contributes to maintenance of genomic stability, homeostasis of stem cells, and other processes that are independent of AMPK. NuAK1/2, and SIK1-3 have also been linked to tumor formation and metastasis, indicating that AMPK may not be the only putative effector of the tumor suppressor role of LKB1 (Cheng et al., 2009; Liu et al., 2012). Similarly LKB1 mediates cell polarity through the microtubule affinity-regulating kinases (MARKs) (independently of AMPK) and loss of this signaling has been shown to promote melanoma invasion (Chan et al., 2014). In *C. elegans* (Guo and Kemphues, 1995) and *D. melanogaster* (Martin and St Johnston, 2003) genetic models, the earliest identified roles of LKB1 were in mediating cell polarity. Taken together, although AMPK and LKB1 are closely linked, they display distinct differences in signaling that may account for divergent roles relating to tumourigenesis.

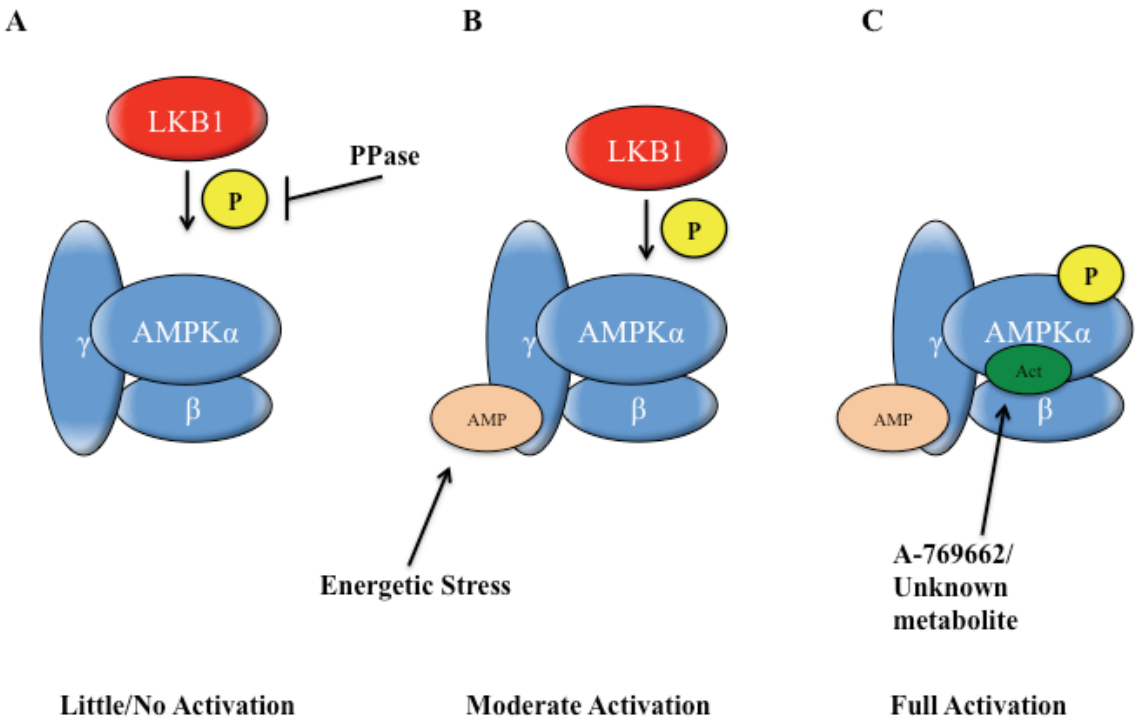

Figure 1.12. **Biochemical activation of AMPK.** A) Phosphatases act to remove the phosphate from AMPK-activated kinases under energetically favourable conditions. B) Energetic stress increases AMP levels, which bind to AMPK and partially prevent the action of phosphatases. C) Binding of A-769662 to the β1 subunit induces a further conformational change that fully protects AMPK from phosphatases.

1.6.4 AMPK activation by reactive oxygen species

There is increasing interest in the ability of ROS to stimulate AMPK activity. ROS has been identified as an activator of AMPK, which appears to act independent of LKB1 (Emerling et al., 2009; Mungai et al., 2011). Cells completely lacking mitochondria, and thus unable to produce high levels of ROS, failed to activate AMPK, but could be rescued with exogenous H_2O_2 (Emerling et al., 2009). It has also been demonstrated that Cys299 was at least partly responsible

for the H_2O_2-induced activation of AMPK (Zmijewski et al., 2010). Activation of AMPK by ROS may be tissue or context-dependent, as oxidation of AMPK Cys130 and Cys174 in cardiac cells resulted in decreased activity by interfering with the interaction between AMPK and LKB1 (Shao et al., 2014). These studies have also shown ROS-induced AMPK activation under physiological and pathological conditions may possibly be independent of changes in AMP/ATP levels (Emerling et al., 2009; Zmijewski et al., 2010), though this is still contested (Auciello et al., 2014).

1.6.5 Pharmacological Activation of AMPK.

Several pharmacologic agents have been used to activate AMPK. Most prevalent among these is the use of metformin as a first-line therapy for type II diabetes (Ferrannini, 2014). Metformin is a biguanide that acts as an inhibitor of complex I of the electron transport chain. Inhibition of OXPHOS promotes an increase in intracellular ADP and AMP, leading to indirect AMPK activation (Zhou et al., 2001). The major effect of metformin action has been to lower blood glucose levels in patients by blocking gluconeogenesis (Madiraju et al., 2014). Similar to metformin is phenformin, a more potent biguanide. Phenformin acts via the same mechanism as metformin, but features a higher affinity and transport activity as well as longer half-life duration. Due to these potent effects, phenformin was removed from clinical use in the treatment of diabetes for lactic acidosis toxicity (Pernicova and Korbonits, 2014). Other AMPK agonists include the AMP mimetic AICAR, and the synthetic activator A-769662. AICAR is transported into the cell via adenosine transporters, is subsequently metabolized into ZMP, which can bind the γ-subunit in place of AMP (Corton et al., 1995). A-769662 is a direct AMPK activator, capable of promoting AMPK activity independently of adenylate levels by binding to the β1 subunit (Cool et al., 2006). A-769662 requires auto-phosphorylation of Ser108 of the β subunit

(Scott et al., 2014). The role of AMPK in the observed effects of these activators has recently been called into question, as the observed metabolic effects of several of these activators may not actually require AMPK (Vincent et al., 2014). Further study with direct, AMPK-specific activators such as A-769662 and others in development will help to elucidate these discrepancies.

1.6.6 Metabolic Control by AMPK

For cancer cells to survive metabolic stress or conditions of nutrient withdrawal, they must be able to engage alternative metabolic pathways to maintain energetic balance. As mentioned, AMPK responds to changes in energy levels regulating both biosynthetic and energy-consuming processes (Hardie, 2011b). Cells with a functional LKB1-AMPK pathway can survive metabolic stress, whereas cells lacking LKB1 or AMPK undergo programmed cell death, suggesting LKB1-AMPK signaling is critical for maintaining energetic homeostasis (Bungard et al., 2010; Godlewski et al., 2010; Inoki et al., 2003; Kato et al., 2002; Shaw et al., 2004b). One way AMPK promotes energy homeostasis is through the direct regulation of metabolic enzymes by phosphorylation. AMPK inhibits fatty acid synthesis and stimulates lipid oxidation through the phosphorylation and inactivation of ACC1 (Davies et al., 1990) and ACC2 (Merrill et al., 1997), respectively. AMPK activation can also further stimulate lipid oxidation by increasing carnitinepalmitoyl transferase 1c (CPT1c) Increased expression of this protein enhances β-oxidation and increases cell survival under conditions of metabolic stress (Sanchez-Macedo et al., 2013; Zaugg et al., 2011). AMPK also regulates autophagy, a catabolic process important for the maintenance of cellular energy and cell survival in starved cells (Lum et al., 2005). AMPK-dependent phosphorylation of the ULK kinases directly induces autophagy in starved cells, resulting in the removal of damaged mitochondria through specific activation of mitophagy

(Egan et al., 2011; Kim et al., 2011). ULK kinases in turn can negatively regulate AMPK signaling through phosphorylation of AMPK subunits (Loffler et al., 2011). In situations of chronic nutrient starvation, AMPK can elicit changes in transcription through a number of mechanisms including phosphorylation of the transcriptional co-activator PGC-1α (Jager et al., 2007), the transcription factor FOXO3 (Greer et al., 2007), or the core histone H2B (Bungard et al., 2010).

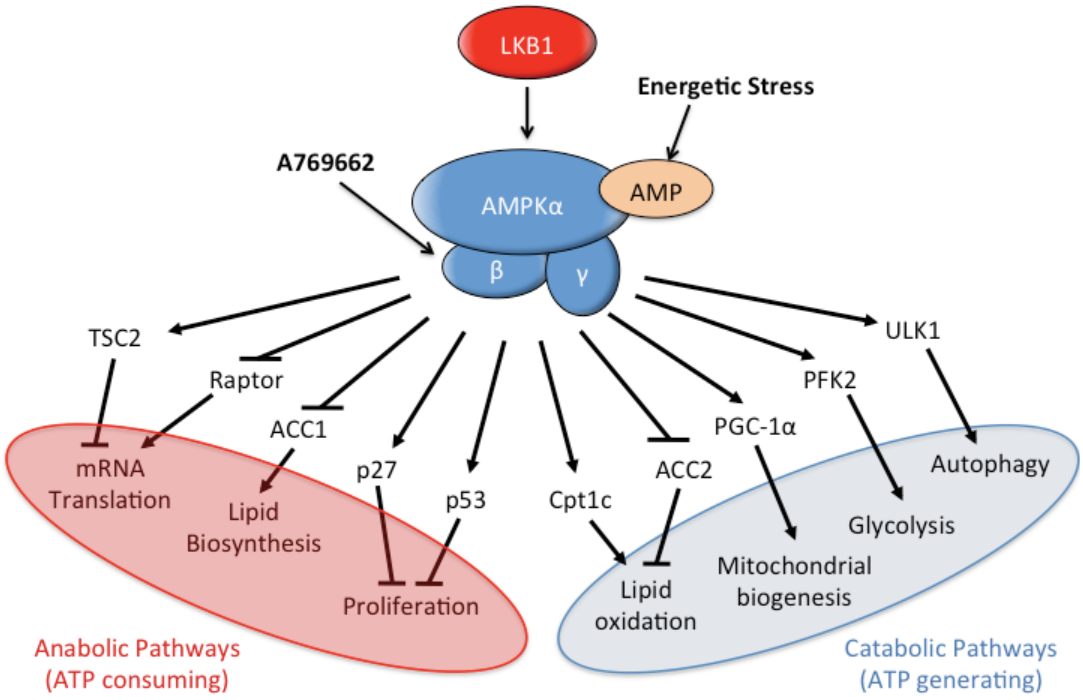

Figure 1.13 Phosphorylation targets of AMPK-mediated metabolic control. Activation of AMPK by energetic stress or A-769662 acts to decrease a variety of anabolic pathways, and increase ATP-generating catabolic pathways.

1.7 AMPK in Cancer

From a signal transduction perspective, AMPK is situated at the center of a tumor suppressor network known to regulate cell growth and proliferation in response to stress. AMPK is regulated by phosphorylation by the tumor suppressor LKB1 (Hawley et al., 2003; Shaw et al., 2004a); likewise, the tumor suppressors TSC2 (Inoki et al., 2003) and p53 (Jones et al., 2005) are downstream targets of AMPK activity. AMPK can also initiate cell cycle arrest through stabilization of p53 (Imamura et al., 2001; Jones et al., 2005) and the cyclin dependent kinase (CDK) inhibitors $p21^{WAF1}$ and $p27^{CIP1}$ (Liang et al., 2007). The proximity of AMPK to these established tumor suppressors and inhibition of cell growth implicate AMPK as a potential tumor suppressor. However, data from the Cancer Genome Atlas (TCGA) sequencing efforts indicate that mutations in AMPK subunits are relatively rare in cancer. Moreover, retaining AMPK activity and the ability to adapt to metabolic stress may function to promote tumor survival and growth. The role of AMPK in cancer remains incompletely defined.

1.7.1 Genomic disruption of AMPK.

AMPK is rarely somatically mutated in human cancer and there is no evidence for a germline cancer predisposition syndrome involving AMPK subunits (Liang and Mills, 2013). This may be due in part to redundancy in AMPK isoform expression. Humans harbor two genes for the α catalytic subunit (*PRKAA1*, *PRKAA2*), two β subunit genes (*PRKAB1, PRKAB2*) and three γ subunit genes (*PRKAG1, PRKAG2, PRKAG3*), and expression of these subunits varies between tissue types. Screening for AMPK mutations in a subset of TCGA datasets indicate that AMPK is mutated at low frequency in most tumor types (Cancer Genome Atlas, 2012a, b; Cancer Genome Atlas Research, 2012), although the functional impact of these mutations has not been fully characterized. Expression levels of AMPKα subunits also vary between cancer

subsets. AMPK loss alone is insufficient to initiate transformation of mouse embryonic fibroblasts (MEFs) (Laderoute et al., 2006), and spontaneous tumor formation in AMPKα-deficient mice has not yet been demonstrated, suggesting that AMPK loss is itself insufficient to drive tumourigenesis.

1.7.2 AMPK Isoform Specificity.

To date, the differential expression of AMPK subunits in cancer has not been extensively investigated. However, there is some evidence that isoform-specific changes of AMPK subunits may occur. Phoenix *et al.* recently observed that AMPKα2-null, but not AMPKα1-null, MEFs display increased susceptibility to H-RasV12 transformation *in vitro* and tumor development as xenografts *in vivo* (Phoenix et al., 2012). In primary breast cancer tissues, α2 mRNA levels can be suppressed by oncogenic PI3K signaling, with no observable effects on α1 subunit expression (Fox et al., 2013). Similarly, forced expression of AMPK-β1 has been shown to inhibit tumor cell growth (Li et al., 2003). These data suggest AMPK isoforms may differentially contribute to tumor cell growth and proliferation. Conditional animal models will help elucidate the role of individual AMPKα subunits in tumor development and progression.

1.7.3 Other pathways of AMPK regulation.

Mechanisms of AMPK regulation independent of genomic alterations may also affect its activity in cancer. One such possible mechanism is AMPK regulation by microRNAs (miRNAs). The miRNA miR-451 was recently linked to control of LKB1-AMPK signaling within the context of glioma. Expression of miR-451 was shown to decrease in response to low cellular glucose levels, leading to modulation of LKB1/AMPK signaling in response to metabolic stress

(Godlewski et al., 2010). miR-451 targets expression of the LKB1 component MO25. Loss of miR-451 expression under low glucose levels promotes the stabilization of MO25 levels, leading to enhanced LKB1 expression and LKB1-dependent AMPK activation. miR-148b has been linked to suppression of AMPKα1 expression, and its expression correlates with poor prognosis in pancreatic cancer (Zhao et al., 2013). Many miRNAs can function as drivers of tumor growth, and it is tempting to speculate that miRNAs that target LKB1-AMPK signaling may promote dynamic transcriptional/translational regulation of this energy-sensitive pathway independent of genomic alterations.

Phosphatases and scaffold proteins for LKB1 and AMPK kinase complexes may also serve as regulators of AMPK kinase activity. For example, the phosphatase α-SNAP was identified as a negative regulator of AMPK activity (Wang and Brautigan, 2013). Cells deficient for α-SNAP expression display constitutive AMPK activation in the absence of energetic stress. Similarly, the tumor suppressor folliculin (FLCN) and its interacting proteins FNIP1 and FNIP2 have been identified as AMPK binding proteins (Baba et al., 2006; Preston et al., 2011). Loss of FLCN promotes constitutive AMPK activation regardless of cellular AMP levels, suggesting that FLCN is a negative regulator of AMPK activity (Yan et al., 2014). Additional work will need to be performed to assess the impact of these AMPK regulators on tumor progression using established cancer models.

1.7.4 Evidence for the role of AMPK in cancer.

Decreasing AMPK activity in Cancer. Several studies have demonstrated that loss of AMPK activity can cooperate with oncogenes to promote tumor progression. One demonstration of AMPK inhibition in cancer is the suppression of LKB1 function by mutated B-RAF (V600E)

in melanoma. Mutant B-RAF V600E promotes ERK and RSK-dependent phosphorylation of LKB1 in melanoma cells, resulting in AMPK inhibition (Zheng et al., 2009). Reversing this block in LKB1 signaling leads to the suppression of B-RAF V600E-mediated transformation (Zheng et al., 2009). Recently it has been shown that AMPK can also signal back to B-RAF to attenuate MEK-ERK signaling (Shen et al., 2013). Inhibition of AMPK has also been observed in a PTEN-deficient model of thyroid cancer (Antico Arciuch et al., 2013) and NSCLC cells expressing the mitochondrial HSP90 chaperone TRAP-1 (Caino et al., 2013). Finally, transformation by certain oncogenes, notably EN and H-RasV12, can promote defects in cellular responses to nutrient deprivation, which is characterized by decreased phospho-AMPK levels (Leprivier et al., 2013). The ability to uncouple energy sensing by AMPK may prove beneficial as a means to avoid growth inhibition (Caino et al., 2013) in newly transformed cells. Taken together, it is evident that irreversible loss of AMPK increases the risk of losing metabolic plasticity as well as the ability to adapt to stressful growth conditions.

Increasing AMPK activity in Cancer. Tumour cells grown under chronic nutrient-restricted conditions develop resistance to metabolic stress in part by selecting for increased AMPK activity (Leprivier et al., 2013). It remains to be determined whether increased AMPK activity is selected for during tumour progression, such as in metastatic or drug-resistant tumour populations. Survival in the context of stress such as hypoxia and nutrient deprivation makes AMPK activity advantageous to cancer cells. AMPK is activated in cells in response to a broad range of stresses (Bungard et al., 2010; Frigo et al., 2011; Park et al., 2009), and can provide cells with the metabolic flexibility to survive periods of stress. This flexibility includes engaging non-glucose sources of energy, such as β-oxidation. By inhibition of ACC1/2, AMPK acts to increase fatty acid catabolism. Specifically, AMPK activity is necessary to increase levels of carnitine

palmitoyltransferase 1C (CPT1c), a transporter of fatty acids into the mitochondria (Zaugg et al., 2011). Enhanced levels of CPT1c resulted in increased transport of fatty acids, allowing for enhanced β-oxidation under both basal and energetic-stress conditions. Inhibition of CPT1c sensitized cells to energetic stresses such as glucose withdrawal, hypoxia and xenograft tumour growth (Sanchez-Macedo et al., 2013).

1.8 Conclusions.

AMPK lies situated in a signaling node of tumor suppressors, including p53 and LKB1. The activities of AMPK appear to be both tumour promoting (increased catabolic activity to restore energy levels in stressed conditions) and tumour inhibiting (inhibiting anabolism and cell growth/cell cycle to help restore energy balance). It appears as though AMPK is primed to play a role in cancer metabolism, though this role has yet to be elucidated.

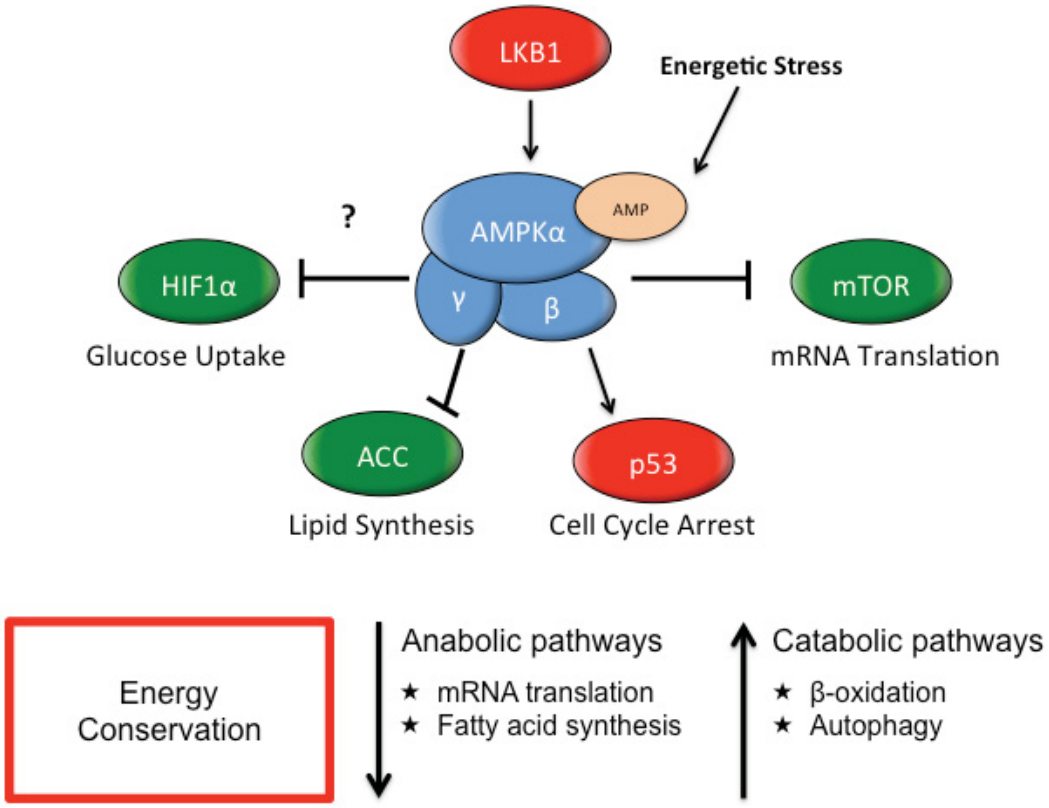

Figure 1.14: **Tumour suppressor vs tumour promoter functions of AMPK.** The effects of AMPK can be broadly grouped into two classes: inhibition of anabolic function, and promoting catabolic pathways in order to restore energy balance.

Thesis Hypothesis and Objectives:

"**AMP-activated protein kinase is a cellular energy sensor that regulates metabolic homeostasis. It is situated in a network of tumour suppressor genes, but its role in cancer remains undefined."**

Specific Objectives:

i) To examine the role of AMPK in cancer metabolism.

ii) To identify the putative tumour suppressive role of AMPK

iii) To examine the contribution of LKB1 loss to cancer metabolism

iv) To elucidate the mechanism of normoxically stabilized HIF-1α in AMPK-null cells.

Preface to Chapter 2

During transformation, cancer cells lose their natural brakes on cell proliferation. One consequence of this increased growth is the requirement for more energy and more resources than normal cells. To meet this new demand for energy, cancer cells undergo fundamental changes in their pathways of energy metabolism and nutrient uptake. One hallmark of many cancers is the preferential use of glucose for energy production, a phenomenon known as the Warburg effect. This change to glycolytic metabolism may confer a selective growth advantage to cancer cells, allowing them to proliferate when under sub-optimal growth conditions.

Many of the common genes mutated in cancer cells can also influence metabolic pathways. For example, the tumor suppressor p53 initiates cell cycle arrest and apoptosis in response to cellular stress, but can also regulate the metabolic processes of glycolysis, lipid oxidation, and autophagy (Buzzai et al., 2007). These observations have led us to hypothesize that oncogene and tumor suppressor pathways are intricately linked with metabolic regulation in cancer (Vogelstein and Kinzler, 2004). However, our understanding of how oncogene and tumor suppressor networks regulate metabolism remains poor.

The AMP-activated protein kinase (AMPK) is a central regulator of cellular metabolism and energy homeostasis, and functions to preserve cellular energy levels (Hardie, 2003). Our laboratory has previously found that AMPK couples cellular energy levels to the control of cell division, by activating a p53-dependent metabolic cell cycle checkpoint when cellular energy levels are low, and can stimulate ATP production through lipid oxidation and autophagy (Buzzai et al., 2007) (Jones et al., 2005). *We hypothesize that AMPK is a central regulator of cellular bioenergetics and stress adaptation, and that the regulation of its activity may affect cancer cell metabolism.*

Chapter 2

Role of AMPK in cancer metabolism and tumour suppression

(Published as)

AMPK is a negative regulator of the Warburg Effect and suppresses tumor growth *in vivo*

Brandon Faubert[1,2], Gino Boily[1,2,*], Said Izreig[1,2,*], Takla Griss[1,2], Bozena Samborska[1,2], Zhifeng Dong[1], Fanny Dupuy[1,3], Christopher Chambers[4], Benjamin J. Fuerth[1,2], Benoit Viollet[5,6,7], Orval A. Mamer[1,8], Daina Avizonis[1,8], Ralph J. DeBerardinis[4,9,10], Peter M. Siegel[1,3,11], and Russell G. Jones[1,2].

[1]Goodman Cancer Research Centre, McGill University, Montreal, QC, H3A 1A3, Canada; [2]Department of Physiology, McGill University, Montreal, QC, H3G 1Y6, Canada; [3]Department of Biochemistry, McGill University, Montreal, QC, H3G 1Y6, Canada; [4]Children's Medical Center Research Institute, University of Texas – Southwestern Medical Center at Dallas, Dallas, Texas, 75390, USA; [5]Inserm, U1016, Institut Cochin, Paris, France; [6]CNRS, UMR 8104, Paris, France; [7]Université Paris Descartes, Sorbonne Paris Cité, Paris, France; [8]Metabolomics Core Facility, McGill University, Montreal, QC, H3A 1A3, Canada; [9]McDermott Center for Human Growth and Development, University of Texas – Southwestern Medical Center at Dallas, Dallas, Texas 75390, USA; [10]Harold C. Simmons Comprehensive Cancer Center, University of Texas – Southwestern Medical Center at Dallas, Dallas, Texas, 75235, USA; [11]Department of Medicine, McGill University, Montreal, QC, H3G 1Y6, Canada.

Corresponding author: Russell G. Jones, Goodman Cancer Research Centre, Department of Physiology, McGill University, 3655 Promenade Sir William Osler, Room 705, Montreal, Quebec, H3G 1Y6, CANADA. Email: russell.jones@mcgill.ca, Phone: (514) 398-3336, Fax: (514) 398-6769.

*These authors contributed equally to this work.

Summary

AMPK is a metabolic sensor that helps maintain cellular energy homeostasis. Despite evidence linking AMPK with tumor suppressor functions, the role of AMPK in tumorigenesis and tumor metabolism is unknown. Here we show that AMPK negatively regulates aerobic glycolysis (the Warburg effect) in cancer cells, and suppresses tumor growth *in vivo*. Genetic ablation of the α1 catalytic subunit of AMPK accelerates Myc-induced lymphomagenesis. Inactivation of AMPKα in both transformed and non-transformed cells promotes a metabolic shift to aerobic glycolysis, increased allocation of glucose carbon into lipids, and biomass accumulation. These metabolic effects require normoxic stabilization of the hypoxia-inducible factor-1α (HIF-1α), as silencing HIF-1α reverses the shift to aerobic glycolysis and the biosynthetic and proliferative advantages conferred by reduced AMPKα signaling. Together our findings suggest that AMPK activity opposes tumor development, and its loss fosters tumor progression in part by regulating cellular metabolic pathways that support cell growth and proliferation.

Highlights

- Loss of AMPKα1 cooperates with the Myc oncogene to accelerate lymphomagenesis
- AMPKα dysfunction enhances aerobic glycolysis (Warburg effect)
- Inhibiting HIF-1α reverses the metabolic effects of AMPKα loss
- HIF-1α mediates the growth advantage of tumors with reduced AMPK signaling

Introduction

Genetic lesions that drive cancer progression affect key biological control points including cell cycle entry, DNA damage checkpoints, and apoptosis. However, the initiation of uncontrolled proliferation also presents a significant bioenergetic challenge to cancer cells; they must generate enough energy and acquire or synthesize biomolecules at a sufficient rate to meet the demands of proliferation. It is now appreciated that many of the predominant mutations observed in cancer also control tumor cell metabolism (Levine and Puzio-Kuter, 2010), suggesting that oncogene and tumor suppressor networks influence metabolism as part of their mode of action. One of the primary metabolic changes observed in proliferating cells is increased catabolic glucose metabolism. Many tumor cells adopt a metabolic phenotype characterized by high rates of glucose uptake and lactate production regardless of oxygen concentration, a phenomenon commonly referred to as the "Warburg Effect" (Vander Heiden et al., 2009). While the energetic yield per molecule of glucose is much lower for aerobic glycolysis compared to oxidative phosphorylation (OXPHOS), the metabolic shift towards the Warburg effect appears to confer both bioenergetic and biosynthetic advantages to proliferating cells by promoting increased non-oxidative ATP production and generating metabolic intermediates from glucose that are important for cell growth (DeBerardinis et al., 2008a).

Appreciation of the generality of the Warburg effect in cancer has stimulated the broader concept that a "metabolic transformation" accompanies tumorigenesis (Jones and Thompson, 2009). However, the metabolic control points and signal transduction pathways that regulate the Warburg Effect during tumorigenesis and their importance to tumor progression *in vivo* remain poorly defined. The AMP-activated protein kinase (AMPK) is a highly conserved Ser/Thr protein kinase complex that plays a central role in the regulation of cellular energy homeostasis. AMPK

is activated in response to declining fuel supply, and functions in the decision to allocate nutrients towards catabolic/energy-producing or anabolic/growth-promoting metabolic pathways (Hardie, 2011a). From a metabolic standpoint, AMPK promotes ATP conservation under conditions of metabolic stress by activating pathways of catabolic metabolism such as autophagy (Egan et al., 2011; Kim et al., 2011) and inhibiting anabolic processes including lipid biosynthesis (Davies et al., 1990), TORC1-dependent protein biosynthesis (Gwinn et al., 2008; Inoki et al., 2003), and cell proliferation (Imamura et al., 2001; Jones et al., 2005). AMPK activity has been recently linked to stress resistance and survival in tumor cells (Jeon et al., 2012; Liu et al., 2012).

Due to its involvement in cellular stress resistance, AMPK has been linked to the regulation of tumorigenesis (Shackelford and Shaw, 2009). The upstream AMPK-activating kinase LKB1 is a tumor suppressor gene inactivated in patients with Peutz-Jegher's syndrome (Alessi et al., 2006), a condition that predisposes patients to gastrointestinal polyps and malignant tumors (Giardiello et al., 1987; Hearle et al., 2006b). Cells lacking LKB1 display defective energy-dependent AMPK activation (Hawley et al., 2003; Shaw et al., 2004b). Additional evidence supporting a tumor suppressor function for AMPK is derived from experiments with the glucose-lowering drug metformin, which acts in part by activating AMPK (Zhou et al., 2001). Treatment of animals harboring tumor xenografts or naturally arising lymphomas with metformin can delay tumor progression (Buzzai et al., 2007; Huang et al., 2008). However, to date the role of AMPK in tumorigenesis and tumor metabolism has remained unclear.

In this work we demonstrate that loss of AMPK signaling cooperates with Myc to accelerate tumorigenesis. Moreover, silencing AMPKα in both transformed and non-transformed cells results in a switch to aerobic glycolysis (Warburg effect) in the absence of energetic crisis. This metabolic shift is characterized by increased glucose uptake, redirection of carbon flow

towards lactate, increased flux of glycolytic intermediates towards lipid biosynthesis, and an increase in net biomass (size). Induction of this metabolic shift is dependent on HIF-1α, as silencing of HIF-1α by shRNA ablates the effects of AMPKα loss on aerobic glycolysis, biosynthesis, and tumor growth *in vivo*. Our findings indicate that AMPK is a metabolic sensor essential for the coordination of metabolic activities that support cell growth and proliferation in cancer cells, and that disruption of AMPK signaling promotes metabolic reprogramming of cancer cells to drive the Warburg effect and influence tumor development and progression *in vivo*.

Results

Loss of AMPKα1 accelerates Myc-driven lymphomagenesis

AMPK lies downstream (Hawley et al., 2003; Shaw et al., 2004b) and upstream (Inoki et al., 2003) of known tumor suppressors (LKB1 and TSC2, respectively), but its role in tumorigenesis has remained unclear. To address this question we generated Eμ-Myc transgenic mice (Adams et al., 1985) harboring a mutation in the gene that encodes AMPKα1 (*prkaa1*), which is the sole catalytic subunit expressed in B lymphocytes (Fig. S1A). Latency to tumor development was monitored by palpation, and both tumor-free survival and overall lifespan were monitored. Compared to Eμ-Myc control mice, Eμ-Myc animals lacking AMPKα1 displayed accelerated lymphomagenesis with a median tumor onset of 7 weeks (Fig. 1A) and a maximum overall survival rate of 20 weeks (Fig. S1B). Eμ-Myc mice heterozygous for AMPKα1 displayed an intermediate phenotype, with a median tumor onset of 10 weeks (Fig. 1A). Lymph node tumors isolated from Eμ-Myc/$\alpha 1^{+/+}$ and Eμ-Myc/$\alpha 1^{-/-}$ mice displayed prominent B220/CD45R staining, indicating that tumors arising in these animals were of B cell origin (Fig. S1C);

however, all AMPKα1-deficient $B220^+$ lymphomas examined lacked surface immunoglobulin (sIg) expression, suggesting that these tumors were pre-B cell tumors, rather than mature B cell tumors (Fig. S1C).

To assess whether the accelerated tumor onset observed in Eμ-Myc/$\alpha 1^{-/-}$ animals was due to a cell intrinsic effect of AMPKα1-deficiency in B cells, we generated chimeric mice using Eμ-Myc/$\alpha 1^{+/+}$ or Eμ-Myc/$\alpha 1^{-/-}$ hematopoietic stem cells (HSCs) to reconstitute lethally-irradiated wild-type mice (C57BL/6 background). All animals reconstituted with Eμ-Myc/$\alpha 1^{-/-}$ HSCs developed palpable lymphomas within 9 weeks of reconstitution, while only 20% of animals receiving Eμ-Myc/$\alpha 1^{+/+}$ HSCs developed tumors 12 weeks post reconstitution (Fig. 1B). These data establish that specific loss of AMPKα1 in B cells can promote accelerated Myc-driven lymphomagenesis.

While lymph node tumors from both genotypes looked histologically similar by H&E staining (Fig. S1D), Eμ-Myc/$\alpha 1^{-/-}$ lymphomas displayed increased proliferation marker Ki-67 staining *in situ* (Fig. 1C). Immunohistochemical (IHC) analysis revealed no major differences in tumor vascularization (measured by CD31 staining) or apoptosis (IHC for cleaved caspase-3) between AMPKα1-deficient and control Eμ-Myc tumors (Fig. S1E). We next silenced AMPKα1 in primary Eμ-Myc lymphoma cells using shRNA (Fig. S1F), and measured the impact of AMPKα1 levels on cell proliferation using an *in vitro* competition assay. Primary Eμ-Myc lymphoma cells were transduced with retroviral vectors co-expressing GFP and control or AMPKα1-specific shRNAs, and the percentage of GFP^+ cells remaining after six days of culture was determined by flow cytometry. AMPKα1 shRNA-expressing cells displayed a competitive growth advantage *in vitro* over cells expressing control shRNA (Fig. 1D).

Activation of AMPK promotes cell survival in response to metabolic stress (Bungard et al., 2010; Buzzai et al., 2007; Jeon et al., 2012). To determine whether loss of AMPK renders Eμ-Myc tumors sensitive to metabolic stress, Eμ-Myc lymphoma cells expressing control or AMPKα1 shRNAs were treated with the glycolytic inhibitor 2-deoxyglucose (2-DG) and cell viability measured after 24 hours. AMPKα1 shRNA-expressing lymphomas displayed normal viability under standard growth conditions but increased cell death in the presence of 2-DG (Fig. 1E). Together these data suggest that loss of AMPKα1 can enhance tumor development driven by oncogenic Myc *in vivo*, but is required to maintain tumor cell viability.

We next explored putative altered signaling events in AMPKα1-deficient lymphomas by IHC analysis of tumor sections. AMPKα, phospho-AMPKα and phospho-ACC (pACC) expression in tumor-bearing lymph nodes confirmed a complete loss of AMPK signaling in Eμ-Myc/$\alpha 1^{-/-}$ tumors (Fig. S1G). Similar to that observed in $Lkb1^{+/-}$ tissues (Shackelford et al., 2009; Shaw et al., 2004a), tumor tissue from Eμ-Myc/$\alpha 1^{-/-}$ mice displayed increased staining for S6 and 4E-BP1 phosphorylation (Fig. 1F), suggesting an increase in basal TORC1 signaling in AMPKα-null lymphomas *in vivo*. Similar data were observed via immunoblotting of primary lymphoma cells isolated immediately *ex vivo* from tumor-bearing lymph nodes. Both TORC1 and AMPK activity (as determined by ACC phosphorylation) were elevated in Eμ-Myc lymphoma cells compared to normal B cells (Fig. 1G). When comparing Eμ-Myc/$\alpha 1^{+/+}$ and Eμ-Myc/$\alpha 1^{-/-}$ lymphomas directly, pACC levels were ablated in $\alpha 1^{-/-}$ tumors, while TORC1 activity was increased in $\alpha 1^{-/-}$ tumors with some variability in levels of both S6 and 4E-BP1 phosphorylation between $\alpha 1^{-/-}$ tumor samples (Fig. 1G).

Loss of AMPKα signaling enhances the Warburg effect in cancer cells

AMPK sits at a central node in the regulation of catabolic and anabolic metabolism (Hardie et al., 2012). To address the role of AMPK in regulating the metabolism of lymphoma cells we conducted a targeted metabolomic analysis of Eμ-Myc lymphoma cells using NMR spectrometry. Employing a stringent statistical cutoff ($p<0.01$) and metabolites displaying a 2-fold change in abundance, we identified 13 metabolites showing differential abundance in shAMPKα1 lymphoma cells (Fig. 2A). By these criteria glucose was the only metabolite significantly decreased in shAMPKα1 lymphoma cells, while lactate displayed the greatest increase (Fig. 2A). Lymphomas expressing AMPKα1 shRNA displayed an elevated extracellular acidification rate (ECAR, Fig. 2B), an index of lactate production (Wu et al., 2007), but displayed no significant difference in their oxygen consumption rate (OCR, Figs. 2C and S2A). AMPKα1 shRNA-expressing Eμ-Myc lymphoma cells also displayed increased glucose consumption (Fig. 2D) and lactate production (Fig. 2E) relative to control lymphoma cells, a metabolic signature consistent with the Warburg effect.

To assess whether reducing AMPK activity is sufficient to enhance the Warburg effect in cancer cells we silenced AMPK in two independent cell lines, H1299 (non-small cell lung carcinoma) and HCT116 (colon carcinoma). Expression of shRNAs targeting both the α1 and α2 subunits of AMPK reduced total AMPKα protein expression in these cell lines (Fig. 2F-G), and AMPKα silencing promoted a significant increase in the basal ECAR of both H1299 (Fig. 2H) and HCT116 cells (Fig. 2I). Lactate production was also elevated in H1299 and HCT116 cells expressing AMPKα shRNA (Fig. S2B-C). Taken together with our observations using AMPKα1 shRNA-expressing Eμ-Myc lymphoma cells, these data suggest that downregulation of AMPK signaling is sufficient to enhance the Warburg effect in transformed cells.

Loss of AMPK signaling promotes increased ATP levels and anabolic metabolism

Given the increased metabolic demands of cell proliferation, we hypothesized that an intact AMPK signaling pathway may function to coordinate metabolism and biosynthesis in actively dividing cells. To address this we generated non-transformed mouse embryonic fibroblasts (MEFs) deficient for AMPKα. Using MEFs deficient for *prkaa1* and harboring a conditional mutation for *prkaa2* (denoted hereafter as $\alpha 1^{-/-}$, $a2^{fl/fl}$), we generated paired isogenic cell lines that possess or completely lack AMPK catalytic activity depending on expression of Cre recombinase (Fig. S3A). MEFs lacking AMPKα (Cre+) displayed increased glucose consumption (Fig. S3B), lactate production (Fig. S3C), and ECAR (Fig. 3A) relative to control (Cre-) cells. We next traced the metabolic fate of ^{13}C-glucose in these cells, and found that AMPKα-deficient cells displayed a progressive increase in the m+3 isotopologue of lactate ($^{13}C_3$-lactate) derived from glucose over time (Fig. 3B), corresponding to a 6-fold increase in the glucose-to-lactate conversion rate.

One possibility for the increased ECAR in cells lacking AMPK activity could be a compensatory response to low cellular energy triggered by AMPK loss. To address this we measured the adenylate energy charge in unstressed, actively growing MEFs by HPLC. Remarkably, cellular ATP levels were elevated in AMPKα-deficient MEFs relative to controls (Fig. 3C). In contrast, the AMP:ATP ratio was not significantly affected by the loss of AMPK activity in proliferating cells (Fig. 3D), suggesting no significant change in basal cellular energy charge when AMPKα is absent.

The metabolic shift to the Warburg effect facilitates the redirection of glucose-derived carbon towards biosynthetic pathways to generate biomass (Vander Heiden et al., 2009),

including extrusion of glucose-derived citrate from the citric acid cycle (CAC) for lipid biosynthesis (Hatzivassiliou et al., 2005). Consistent with this, total citrate levels were elevated in AMPKα-deficient cells relative to control cells as determined by gas chromatography-mass spectrometry (GC-MS) (Fig. 3E). We next measured glucose-dependent lipid biosynthesis by culturing MEFs with D-[6-^{14}C]-glucose, and found that AMPKα-deficient cells displayed increased ^{14}C-labelling in lipids (Fig. 3F). Decreased ACC phosphorylation in AMPKα-null cells is predicted to contribute to lipid synthesis, but may also decrease fatty acid oxidation. Baseline palmitate oxidation remained low in proliferating cells grown under full glucose conditions regardless of AMPK expression (Fig. 3G). However, cells expressing AMPKα shRNA displayed a reduced ability to oxidize lipid upon complete removal of glucose (Fig. 3G), suggesting that AMPK is required to trigger catabolic lipid metabolism specifically under nutrient poor conditions.

Consistent with shunting of glucose-derived carbon towards biosynthesis in proliferating cells, AMPKα-null MEFs displayed a 20% increase in median cell size as determined by forward scatter (FSC) using flow cytometry (Fig. 3H). TORC1 is a central regulator of cell size (Laplante and Sabatini, 2009), and AMPK can negatively regulate TORC1 activity under energy stress (Inoki et al., 2003; Shaw et al., 2004a). Consistent with this, the AMPK agonist AICAR suppressed TORC1 activity (as determined by reduced pS6 and p4E-BP levels) only in cells with wild type AMPKα (Fig. S3D). Notably, growth factor-dependent TORC1 activity in cells was similar regardless of AMPKα status (Fig. S3E), suggesting the existence of TORC1-independent pathways of biomass regulation in AMPKα-deficient cells.

Loss of AMPKα promotes a glycolytic signature and increased HIF-1α expression

We next investigated potential mechanisms governing the glycolytic phenotype associated with AMPKα-deficient cells. We first used quantitative PCR (qPCR) to examine the relative levels of mRNA transcripts encoding for proteins involved in glycolytic regulation. AMPKα-null MEFs displayed a glycolytic gene signature marked by increased mRNA expression of Aldolase A (*aldoa*), Lactate dehydrogenase A (*ldha*), and pyruvate dehydrogenase kinase 1 (*pdk1*) (Figs. 4A and S4A), a pattern of gene expression also displayed by shAMPKα1 lymphoma cells (Fig. S4B). Elevated Aldolase, LDHA and PDK1 protein levels were also detected in AMPKα-deficient MEFs (Fig. 4B) and shAMPKα1 lymphoma cells (Fig. 4C).

PDK1 curbs pyruvate flux to Acetyl-CoA and entry into the TCA cycle by antagonizing the action of the pyruvate dehydrogenase (PDH) complex (Kim et al., 2006; Papandreou et al., 2006). Thus, elevated PDK1 levels observed in AMPKα-deficient cells may be predicted to affect glucose flux to citrate. To measure this we cultured control or AMPKα-null MEFs in medium containing uniformly labeled [^{13}C]-glucose and measured ^{13}C enrichment in citrate by gas chromatography-mass spectrometry (GC-MS). Glucose-derived pyruvate is converted to Ac-CoA by PDH. Subsequent condensation of [1,2-^{13}C]-Ac-CoA with oxaloacetate (OAA) yields citrate with 2 additional mass units (m+2), while an additional turn through the TCA cycle produces citrate (m+4). We observed modest increases in levels of unlabeled citrate in AMPKα-null MEFs relative to control cells, as well as reduced citrate(m+4) labeling from [^{13}C]-glucose (Fig. S4C). ^{13}C enrichment in citrate was similar between control and AMPKα-null MEFs when [^{13}C]-glutamine was used as carbon source (Fig. S4D).

Several of the enzymes elevated in AMPKα-deficient cells are known targets of the transcription factor HIF-1α, one of the central regulators of glycolysis induced by hypoxia (Keith

et al., 2012; Semenza, 2011a). We observed elevated HIF-1α protein levels under normoxia following acute AMPKα deletion in our isogenic cell lines (Fig. 4D), consistent with previous work demonstrating elevated HIF-1α protein expression in cells with chronic depletion of AMPKα (Shackelford et al., 2009). Moreover, shRNA-mediated knockdown of AMPKα1 in Eμ-Myc lymphomas (Fig. 4E) or HCT116 cells (Fig. 4F) promoted normoxic HIF-1α protein stabilization. Levels of *hif1a* mRNA were unchanged in AMPKα-null MEFs relative to controls (Fig. 4G), suggesting that reducing AMPK activity is sufficient to increase HIF-1α protein levels in cancer cells under normoxic conditions independent of mRNA levels.

TORC1 signaling has been linked to control of HIF-1α expression through differential regulation of its translation (Choo et al., 2008). To examine the contribution of TORC1 signaling to HIF-1α stabilization in AMPKα-deficient cells, we silenced the TORC1 binding partner Raptor using siRNA. Treatment with Raptor siRNA significantly reduced *hif1a* mRNA levels in both control and AMPKα-deficient MEFs, with the latter demonstrating a large drop in *hif1a* mRNA expression upon Raptor depletion (Fig. 4H). Moreover, transient knockdown of Raptor in AMPKα-deficient MEFs reduced HIF-1α protein levels (Fig. 4I), and reduced the expression of the HIF-1α targets *aldoa* (Fig. S4E) and *ldha* (Fig. S4F).

AMPKα-dependent effects on glycolysis are mediated by HIF-1α

To determine the contribution of HIF-1α to the glycolytic phenotype observed in AMPKα-null cells, we stably silenced HIF-1α in control (Cre-) or AMPKα-deficient (Cre+) MEFs using RNAi. Expression of HIF-1α shRNA ablated HIF-1α protein expression in AMPKα-deficient MEFs under normoxia (Fig. 5A), and blocked $CoCl_2$-dependent induction of HIF-1α protein in

both AMPKα-deficient and control cells (Fig. S5A). Expression of HIF-1α shRNA reduced *pdk1* mRNA in AMPKα-null cells to control levels, demonstrating that expression of this shRNA could block HIF-1α-dependent transcription (Fig. 5B). We next determined whether silencing HIF-1α could reverse the Warburg effect triggered by loss of AMPKα activity. While HIF-1α shRNA had little effect on the ECAR of control cells, silencing HIF-1α in AMPKα-deficient cells lowered the ECAR below control levels (Fig. 5C). GC-MS analysis revealed dramatic reductions in intracellular pyruvate and lactate in AMPKα-deficient cells expressing HIF-1α shRNA relative to control shRNA (Fig. 5D). Moreover, silencing HIF-1α ablated the enhanced levels of glucose consumption (Fig. 5E) and lactate production (Fig. 5F) displayed by AMPKα-deficient cells. Similar reductions in glucose consumption and lactate production were observed in AMPKα-deficient MEFs transfected with HIF-1α siRNA (Fig. S5B-D). Silencing Raptor in AMPKα-deficient MEFs, which partially reduced HIF-1α protein levels (Fig. 4I), led to slight reductions in lactate production (Fig. S5E) and ECAR (Fig. S5F).

HIF-1α drives increased biosynthesis in AMPKα-null cells

Next we determined the impact of HIF-1α expression on cellular biosynthesis and proliferation induced by AMPKα loss. Silencing HIF-1α reduced intracellular citrate in AMPKα-deficient cells by approximately 70% (Fig. 6A), restoring citrate levels to that observed in control cells. Moreover, suppression of HIF-1α dramatically reduced glucose-dependent lipogenesis in AMPKα-deficient MEFs (Fig. 6B). Suppression of HIF-1α had little effect on glucose-dependent lipogenesis in control cells (Fig. 6B), consistent with the fact that HIF-1α protein is maintained at low levels in these cells under normoxia.

Given that aberrant HIF-1α expression drives both enhanced glycolysis and glucose-derived lipogenesis, we reasoned that the increased size of AMPKα-deficient cells may be attributed to HIF-1α-dependent changes in anabolic metabolism. While loss of AMPKα promotes increased cell size, silencing HIF-1α restored the size of AMPKα-deficient MEFs to that of control cells (Fig. 6C). Notably, rapamycin treatment also reduced the size of AMPKα-deficient MEFs (Fig. S6A). However, this treatment also reduced *hif1a* mRNA levels in cells regardless of AMPKα expression (Fig. S6B), suggesting rapamycin may exert its effects in part through regulation of HIF-1α mRNA. Finally, suppression of HIF-1α signaling in AMPKα-deficient cells reduced their overall rate of proliferation (Fig. 6D). Collectively the data suggest that AMPK negatively regulates the metabolic (Warburg effect) and biosynthetic programs of proliferating cells through the inhibition of HIF-1α function.

HIF-1α is required for the progression of AMPKα1-deficient lymphomas

Our earlier results (Fig. 2) indicate that reduced AMPK signaling synergizes with Myc to promote the Warburg effect in lymphoma. To determine the contribution of HIF-1α to the glycolytic phenotype of Eμ-Myc lymphoma cells we stably expressed HIF-1α-specific shRNAs in Eμ-Myc lymphoma cells with silenced AMPKα1. Silencing HIF-1α in AMPKα1 shRNA-expressing cells reduced HIF-1α protein expression to control levels (Fig. 7A). Protein levels of the HIF-1α targets Aldolase and LDHA expression also decreased when HIF-1α was silenced in AMPKα1 shRNA-expressing lymphomas (Fig. 7A). We next examined metabolic activity in these lymphomas. Expression of AMPKα1 shRNA increased cellular ECAR as expected, while silencing HIF-1α reduced this enhanced ECAR response by 60% (Fig. 7B). Finally, lymphoma

cells expressing both AMPKα1 and HIF-1α shRNA showed decreased proliferation relative to cells expressing AMPKα1 shRNA alone (Fig. 7C).

We next tested the requirement for HIF-1α for tumor progression *in vivo*. Primary control or AMPKα-deficient Eμ-Myc lymphoma cells were transduced with retroviral vectors expressing GFP and either control or HIF-1α shRNAs, and the percentage of GFP^+ lymphoma cells (expressing the shRNA of interest) was determined by flow cytometry prior to transplantation into recipient mice and following lymphoma formation (Fig. 7D). Expression of control shRNA did not dramatically alter the fraction of GFP^+ Eμ-Myc lymphoma cells regardless of genotype (Fig. 7E,F). Interestingly, silencing HIF-1α in Eμ-Myc lymphomas promoted a general increase in the number of GFP^+ tumor cells, although this did not reach statistical significance (Fig. 7F). However, lymphoma cells expressing HIF-1α shRNA were selectively depleted in AMPKα-null tumors (Fig. 7E,F). Collectively these data suggest that loss of AMPK signaling promotes a metabolic and growth advantage in lymphoma cells, and that HIF-1α is required for the growth of AMPKα1-null tumors *in vivo*.

Discussion

AMPK is a cellular energy sensor that coordinates metabolic activities in many tissues. Under conditions of energetic stress, AMPK activation suppresses cell growth and proliferation, leading to speculation that AMPK may function as part of a tumor suppressor pathway (Hardie, 2011a; Shackelford and Shaw, 2009). Here we provide the first genetic evidence that AMPKα displays tumor suppressor activity *in vivo*. Loss of AMPK signaling cooperates with oncogenic Myc to enhance tumorigenesis in a mouse model of lymphomagenesis, suggesting that AMPK may function as a tumor suppressor (Fig. 1). Moreover, we demonstrate that AMPK is a negative

regulator of both aerobic glycolysis and cellular biosynthesis in cancer cells. Cells deficient for the catalytic alpha subunit(s) of AMPK display increased aerobic glycolysis marked by increased lactate production from glucose (Figs. 2 and 3), and downregulation of AMPK activity is sufficient to induce the Warburg Effect in cancer cells (Fig. 2). We find that HIF-1α is a key mediator of AMPK-dependent effects on cellular metabolism. Reducing AMPKα levels in cells leads to increased HIF-1α protein levels under normoxia in both transformed and non-transformed cells (Fig. 4), and HIF-1α is required to drive both the Warburg effect and the growth of AMPKα1-deficient lymphomas *in vivo* (Fig. 5-7). The results presented here suggest that the downregulation of AMPK activity eliminates a key metabolic checkpoint that normally antagonizes anabolic pro-growth cellular metabolism. Thus, AMPK may act in cancer cells as a metabolic gatekeeper that functions to establish metabolic checkpoints that limit cell division, and its loss of function can enhance both tumorigenesis and tumor progression.

All cells must manage their energetic resources to survive. We and others have established that AMPK is the central mediator of a metabolic cell cycle checkpoint activated in response to nutrient limitation in mammalian cells (Gwinn et al., 2008; Inoki et al., 2003; Jones et al., 2005). However, programs of ATP production and macromolecular synthesis must also be coordinated in proliferating cells to ensure proper cell division. The data presented here suggest that AMPK functions to regulate metabolic homeostasis in proliferating cells in the absence of acute energetic stress. Isogenic MEFs or cancer cells lacking AMPKα activity display a metabolic shift towards aerobic glycolysis, thus allowing cancer cells to engage aerobic glycolysis for ATP production and divert glucose-derived CAC intermediates towards lipid biosynthesis to support increased cell growth. AMPK may also influence lipid biosynthesis through regulation of ACC and other lipogenic enzymes, possibly through its effects on SREBP-

1 (Li et al., 2011). Thus, defective AMPKα signaling promotes the re-wiring of metabolic pathways to favor cell growth pathways.

Interestingly our data provide evidence that AMPKα-deficient tumors display increased activation of the TORC1 targets S6 and 4E-BP1, suggesting that AMPK, as opposed to other AMPK-related kinases, may be the key TORC1 regulator downstream of LKB1 in tumors. Consistent with past work (Inoki et al., 2003; Liu et al., 2006; Shaw et al., 2004a), we find that AMPK functions to downregulate TORC1 activity specifically under conditions of energetic stress, when it is desirable to suppress ATP-consuming processes such as mRNA translation. This may provide a metabolic advantage to proliferating cells, where the loss of AMPK signaling promotes increased ATP production and resource accumulation without affecting the mitogenic properties of TORC1. By concurrently silencing AMPK while maintaining TORC1 signaling, cells may effectively bypass endogenous brakes on cellular metabolism, supporting increased tumor cell growth and proliferation.

Our work here establishes HIF-1α as a key mediator of the metabolic transformation triggered by reduced AMPKα activity in cancer cells. We show that downregulation of AMPK signaling is sufficient to induce normoxic HIF-1α stabilization and enhance the Warburg effect. TORC1 activity appears to contribute in part to this process, as silencing the mTORC1 binding partner Raptor reduces levels of *hif1a* mRNA in AMPKα-deficient cells. However, silencing Raptor moderately reduces HIF-1α protein levels and has a minimal effect on the glycolytic phenotype of AMPKα-deficient cells, suggesting that AMPK may regulate HIF-1α-dependent Warburg metabolism through additional mechanisms. Interestingly, TORC1 inhibition reduces *hif1a* mRNA and reduces glycolysis in cell regardless of AMPK expression, suggesting that TORC1 may function on a more global level as a positive regulator of glycolysis beyond specific

effects on HIF-1α expression (Duvel et al., 2010). Given that TORC1 signaling is elevated in AMPKα1-deficient lymphomas, this may have implications for tumor metabolism *in vivo*. HIF-1α mRNA levels are unaffected by AMPK expression; thus, AMPK may affect normoxic HIF-1α protein expression either through decreased protein turnover or differential translation of HIF-1α mRNA (Choo et al., 2008). Overall we propose that AMPK functions to coordinate glycolytic and oxidative metabolism in proliferating cells by restricting HIF-1α function.

One consequence of AMPK loss in cells is enhanced flux of glucose-derived carbon to citrate for lipid biosynthesis, promoting biomass accumulation and increased cell size. This may appear counterintuitive, as HIF-1α-dependent upregulation of PDK1 under hypoxia is proposed to direct glucose-derived carbon away from the CAC (Kim et al., 2006; Papandreou et al., 2006). However, glucose-to-citrate flux is not blocked in AMPKα-null cells despite elevated PDK1 levels. Rather, the reduced levels of citrate (m+4) in AMPKα-null cells may result from increased use of glucose-derived citrate (m+2) for lipid biosynthesis. Reducing AMPK levels significantly decreases ACC1 inhibition in both tumor cells and tumor tissue, which would permit maximal activity of ACC1 for lipid biosynthesis. Thus, AMPK may regulate lipid biosynthesis and biomass accumulation on multiple levels: substrate availability (HIF-1α-dependent glucose-derived citrate) and ACC activity.

We propose that AMPK may function as a metabolic tumor suppressor, limiting the growth of cancer cells by regulating key bioenergetic and biosynthetic pathways required to support unchecked proliferation. Thus, selection against AMPK activity may represent an important regulatory step for tumor initiation and progression, allowing tumor cells to gain a metabolic growth advantage. Reduced AMPK activity has been detected in primary human breast cancer (Hadad et al., 2009), and reduced expression of *prkaa2*, the gene that encodes for

AMPKα2, has been linked to human breast, ovarian, and gastric cancer (Hallstrom et al., 2008; Kim et al., 2012). It is also well documented that LKB1-deficiency (Shackelford and Shaw, 2009) or genetic events that target LKB1 activity (Godlewski et al., 2010; Zheng et al., 2009) lead to reduced AMPK signaling in tumor cells. Thus, there may be several routes by which AMPK function is suppressed in tumors to provide a selective metabolic growth advantage.

While selection for loss of AMPK function may favor the Warburg effect in tumor cells, it may also eliminate metabolic checkpoints essential for cellular adaptation to stress. AMPK normally plays a protective role to block cell growth in response to poor nutrient conditions, and as such its loss or suppression during tumorigenesis may sensitize tumor cells to apoptosis under hypoxic or nutrient depleted environments (Svensson and Shaw, 2012). Consistent with this, silencing AMPKα1 in Eμ-Myc lymphomas conferred sensitivity to apoptosis induced by the glycolytic inhibitor 2-DG. The increased levels of ACC phosphorylation observed in Eμ-Myc tumors (Fig. 1) infer that lymphomas experience metabolic stress and AMPK activation *in vivo*. Thus, while ablation of AMPK signaling may enhance tumorigenesis, inhibition of this central energy-sensing pathway may offer unique a therapeutic window for the treatment of tumors with metabolic inhibitors. Our data provide a mechanistic rationale in support of the use of AMPK agonists such as metformin for cancer therapy (Buzzai et al., 2007; Evans et al., 2005), as the efficacy of these agents against tumor growth may lie in their ability to engage AMPK-dependent metabolic checkpoints to restrict anabolic growth. Understanding the reprogramming of cellular metabolic networks by AMPK in cancer may aid in the development of novel approaches for cancer therapy.

Experimental Procedures

Cell Lines, DNA Constructs, and Cell Culture

Primary mouse embryonic fibroblasts (MEFs) deficient for *prkaa1* ($\alpha 1^{-/-}$) and conditional for *prkaa2* ($\alpha 2^{fl/fl}$) were generated by timed mating as previously described (Jones et al., 2005), and immortalized with SV40 Large T Antigen. HCT116 cells were obtained from ATCC. Primary Eμ-Myc lymphoma cells were provided by Jerry Pelletier (Robert et al., 2009). DNA plasmids MiCD8t, pKD-HIF-1αhp, and LMP-based shRNAs against mouse and human AMPK$\alpha 1$ and $\alpha 2$ have been described previously (Bungard et al., 2010; Jones et al., 2005; Lum et al., 2007). AMPKα-deficient MEFs were generated by transducing $\alpha 1^{-/-}, \alpha 2^{fl/fl}$ MEFs with Cre-expressing retrovirus to delete α2-floxed alleles. For siRNA transfections, cells were subjected to two rounds of reverse transfection with pooled siRNAs against HIF-1α (Dharmacon) using Lipofectamine RNAimax (Hatzivassiliou et al., 2005). AMPK activity was assessed in cell lines following stimulation with AICAR (1 mM, Toronto Research Chemicals) or metformin (5 mM, Sigma) for 1 hour. To induce HIF-1α protein expression, cells were treated with $CoCl_2$ (100μM) for 1 hour. For mass isotopomer analysis, cells were incubated in glucose- or glutamine-free medium containing 10% dialyzed FBS and either uniformly labeled [^{13}C]-glucose or [^{13}C]-glutamine, respectively (Cambridge Isotope Laboratories).

Mice

Mice deficient for AMPKα1 (Mayer et al., 2008), floxed for AMPKα2 (Jorgensen et al., 2004), and Eμ-Myc transgenic mice (Adams et al., 1985) have been described previously. Eμ-Myc/$\alpha 1^{-/-}$ mice (and littermate controls) were generated by breeding AMPKα1-deficient and Eμ-Myc

transgenic mouse strains. Mice were bred and maintained under specific pathogen-free conditions at McGill University under approved protocols.

Determination of Cell Proliferation, Competition Assays, and Cell Size

Cell proliferation curves for all cell lines was determined by cell counting using trypan blue exclusion, and a TC10 Automated Cell Counter (BioRad). For *in vitro* competition assays, primary Eμ-Myc lymphoma cells were transduced with retroviral vectors co-expressing GFP and AMPKα1-specific shRNA or control shRNA, and the percentage of GFP-positive cells remaining after six days of culture was determined by flow cytometry. Cell size of viable cells was quantified as the mean fluorescence intensity for FSC using flow cytometry. All flow cytometry was conducted using BD FACSCalibur (BD Biosciences) or Gallios (Beckman Coulter) flow cytometers and analyzed with FlowJo software (Tree Star).

Immunoblotting

Cells were lysed in modified CHAPS buffer (10mM Tris-HCl, 1mM $MgCl_2$, 1mM EGTA, 0.5mM CHAPS, 10% glycerol, 5mM NaF) or AMPK lysis buffer (MacIver et al., 2011) supplemented with protease and phosphatase inhibitors (Roche), DTT (1 μg/ml), and benzamidine (1 μg/ml). Cleared lysates were resolved by SDS-PAGE, transferred to nitrocellulose, and incubated with primary antibodies. Primary antibodies to AMPK (pT172-specific and total), AMPKα2, ACC (pS79 and total), p70 S6-kinase (pT389-specific and total), S6 ribosomal protein (pS235/236-specific and total), 4E-BP1 (pT37/46-specific and total), LDHA, PDK1, Aldolase, and actin were obtained from Cell Signaling Technology. Anti-HIF-1α antibodies were from Cayman Biomedical.

Quantitative Real-Time PCR

Total mRNA was isolated from cells using Trizol and cDNA was synthesized from 100ng of total RNA using the Superscript VILO cDNA Synthesis Kit (Invitrogen). Quantitative PCR was performed using SYBR Green qPCR SuperMix (Invitrogen) and an Mx3005 qPCR machine (Agilent Technologies) using primers against *aldoA, ldha, pdk1, hif1a,* and *actin.* All samples were normalized to β-actin mRNA levels. Primer sequences are listed in Table S1.

Metabolic Assays

Respirometry (oxygen consumption rate, OCR) and the extracellular acidification rate (ECAR) of cells were measured using an XF24 Extracellular Flux Analyzer (Seahorse Bioscience). In brief, cells were plated at $5x10^4$/well in 625μl non-buffered DMEM containing 25mM glucose and 2mM glutamine. Cells were incubated in a CO_2-free incubator at 37°C for 1 hr to allow for temperature and pH equilibration prior to loading into the XF24 apparatus. XF assays consisted of sequential mix (3 min), pause (3 min), and measurement (5 min) cycles, allowing for determination of OCR/ECAR every 10 minutes.

Glucose consumption and lactate production were determined using enzymatic assays described previously (Buzzai et al., 2007). Glucose-derived lipid biosynthesis was determined by culturing cells in medium containing ^{14}C-glucose for 3 days, and extracted lipids using a 1:1:1 Water/Methanol/Chloroform extraction procedure (Mullen et al., 2012). Following extraction, the organic layer was isolated, dried via N_2 stream, re-suspended in methanol, and incorporated radioactivity measured using a MicroBeta Liquid Scintillation Counter (Perkin Elmer).

Analysis of Metabolites by NMR and GC-MS

Metabolites from tissue culture cells were extracted as described previously (Xu et al., 2011b). Briefly, cells (2 – 5 x 10^6/10 cm dish) were washed three times with ice cold 0.9% saline solution. Cells were lysed using ice-cold 80% methanol followed by sonication (Diagenode Bioruptor), and extracts dried by vacuum centrifugation. For NMR analysis, cell extracts were re-suspended in 220 mL ^2H_2O containing 0.2mM 4,4-dimethyl-4-silapentane-1-sulfonic acid (DSS), 0.1mM difluorotrimethylsilanylphosphonic acid (DFTMP), and 0.01 mM sodium azide. NMR data collection was performed at the Québec/Eastern Canada High Field NMR Facility on a 500 MHz Inova NMR system (Agilent Technologies) equipped with an HCN cryogenically cooled probe operating at 25 K. Metabolite chemical shift assignments were confirmed by total correlation spectroscopy, and targeted metabolites profiled using a 500 MHz metabolite library from Chenomx.

For GC-MS analysis, dried samples were re-suspended in 30 μL anhydrous pyridine and added to GC-MS autoinjector vials containing 70 μL N-(*tert*-butyldimethylsilyl)-N-methyltrifluoroacetamide (MTBSTFA) derivatization reagent. The samples were incubated at 70^{o}C for 1 hr, following which aliquots of 1 μL were injected for analysis. GC-MS data were collected on an Agilent 5975C series GC/MSD system (Agilent Technologies) operating in election ionization mode (70 eV) and selected ion monitoring. Quantified metabolites were normalized relative to protein content (μg).

Statistical Analysis

Statistics were determined using paired Student's t test, ANOVA, or Log-rank (Mantel-Cox) test using Prism software (GraphPad). Data are calculated as the mean ± SEM unless otherwise

indicated. Statistical significance is represented in figures by: *, $p<0.05$; **, $p<0.01$; ***, $p<0.001$; ****, $p<0.0001$.

Acknowledgements

We would like to thank Connie Krawczyk, Arnim Pause, Jerry Pelletier, Francis Robert, David Shackelford, and Leah Donnelly for technical and administrative help. We are also grateful to Kimberly Wong, Alon Morantz, Valerie Laurin, and Luciana Tonelli for animal expertise. We acknowledge salary support from Canadian Institutes of Health Research (CIHR) (to B.F. and R.G.J.), the Fonds de recherche du Québec – Santé (FRQS) (to G.B. and P.M.S.), the McGill Integrated Cancer Research Training Program (MICRTP) (to B.F, G.B, and T.G.), and the Research Institute of the McGill University Health Centre (RI-MUHC) (to F.D.). R.J.D. was supported by National Institutes of Health Grant R01CA157996. This work was supported by grants to R.G.J. from the CIHR (MOP-93799), Canadian Cancer Society (700586), and Terry Fox Research Foundation (TEF-116128).

Figures:

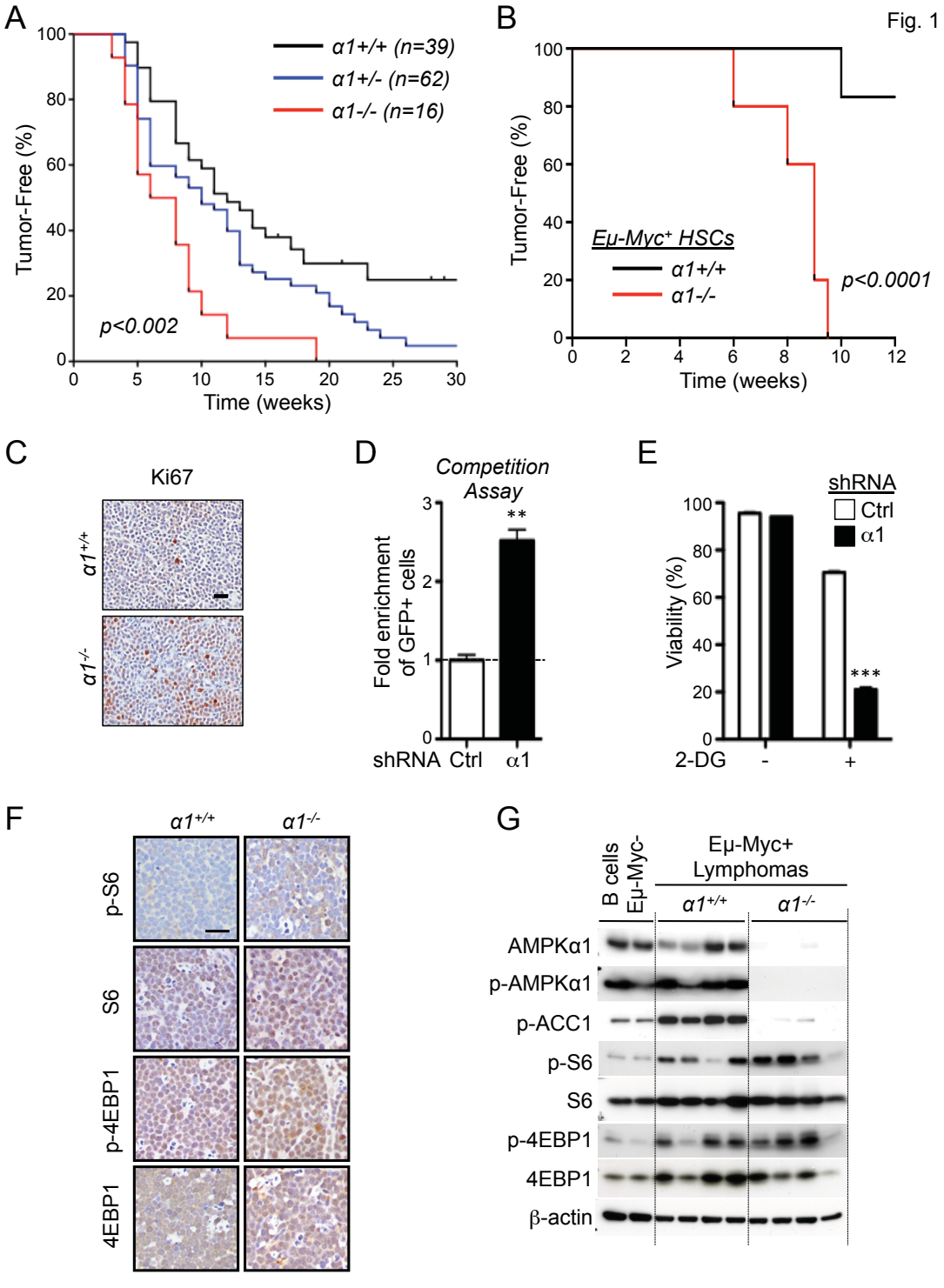
A
Tumor-Free (%)
Time (weeks)
α1+/+ (n=39)
α1+/- (n=62)
α1-/- (n=16)
p<0.002
B
Tumor-Free (%)
Time (weeks)
Eμ-Myc+ HSCs
α1+/+
α1-/-
p<0.0001
Fig. 1
C
Ki67
α1+/+
α1-/-
D
Competition Assay
Fold enrichment of GFP+ cells
shRNA Ctrl α1
**
E
shRNA
Ctrl
α1
Viability (%)
2-DG
***
F
α1+/+
α1-/-
p-S6
S6
p-4EBP1
4EBP1
G
B cells Eμ-Myc-
Eμ-Myc+ Lymphomas
α1+/+
α1-/-
AMPKα1
p-AMPKα1
p-ACC1
p-S6
S6
p-4EBP1
4EBP1
β-actin

Figure 1. AMPKα1 cooperates with Myc to promote lymphomagenesis. A) Kaplan-Meier curves showing latency to tumor development in Eμ-Myc transgenic mice deficient ($\alpha 1^{-/-}$, red), heterozygous ($\alpha 1^{+/-}$, blue) or wild-type ($\alpha 1^{+/+}$, black) for AMPKα1. B) Kaplan-Meier curves showing latency to tumor development in chimeric mice reconstituted with Eμ-Myc/$\alpha^{+/+}$ ($\alpha 1^{+/+}$, black) or Eμ-Myc/$\alpha 1^{-/-}$ ($\alpha 1^{-/-}$, red) HSCs (n=5 per group). C) Representative histological sections of Eμ-Myc/$\alpha^{+/+}$ and Eμ-Myc/$\alpha 1^{-/-}$ lymphomas stained for the proliferation marker Ki-67. D) Competition assay of Eμ-Myc lymphoma cells expressing GFP and control (Ctrl) or AMPKα1-specific (α1) shRNAs. Data are expressed as the fold enrichment in GFP^+ to GFP^- cells after 6 days of growth. E) Viability of control (Ctrl) or AMPKα1 shRNA-expressing Eμ-Myc lymphomas cells after 24h treatment with 2-deoxyglucose (2-DG, 15 mM). F) Immunohistochemical analysis of representative Eμ-Myc/$\alpha^{+/+}$ and Eμ-Myc/$\alpha 1^{-/-}$ lymphomas stained with antibodies to detect TORC1 activity (total and phospho-ribosomal S6 (pS6, S240/244), or total and phospho-4EBP1 (p4EBP1, S37/46)). G) Immunoblot analysis of primary Eμ-Myc/$\alpha^{+/+}$ or Eμ-Myc/$\alpha 1^{-/-}$ lymphomas. Whole cell lysates prepared from sorted primary lymphoma cells were analyzed by immunoblot using the indicated antibodies. Each lane represents an independent tumor. Lysates from non-transformed B cells isolated from Eμ-Myc-negative mice are shown. **, $p<0.01$; ***, $p<0.001$.

Fig. 2

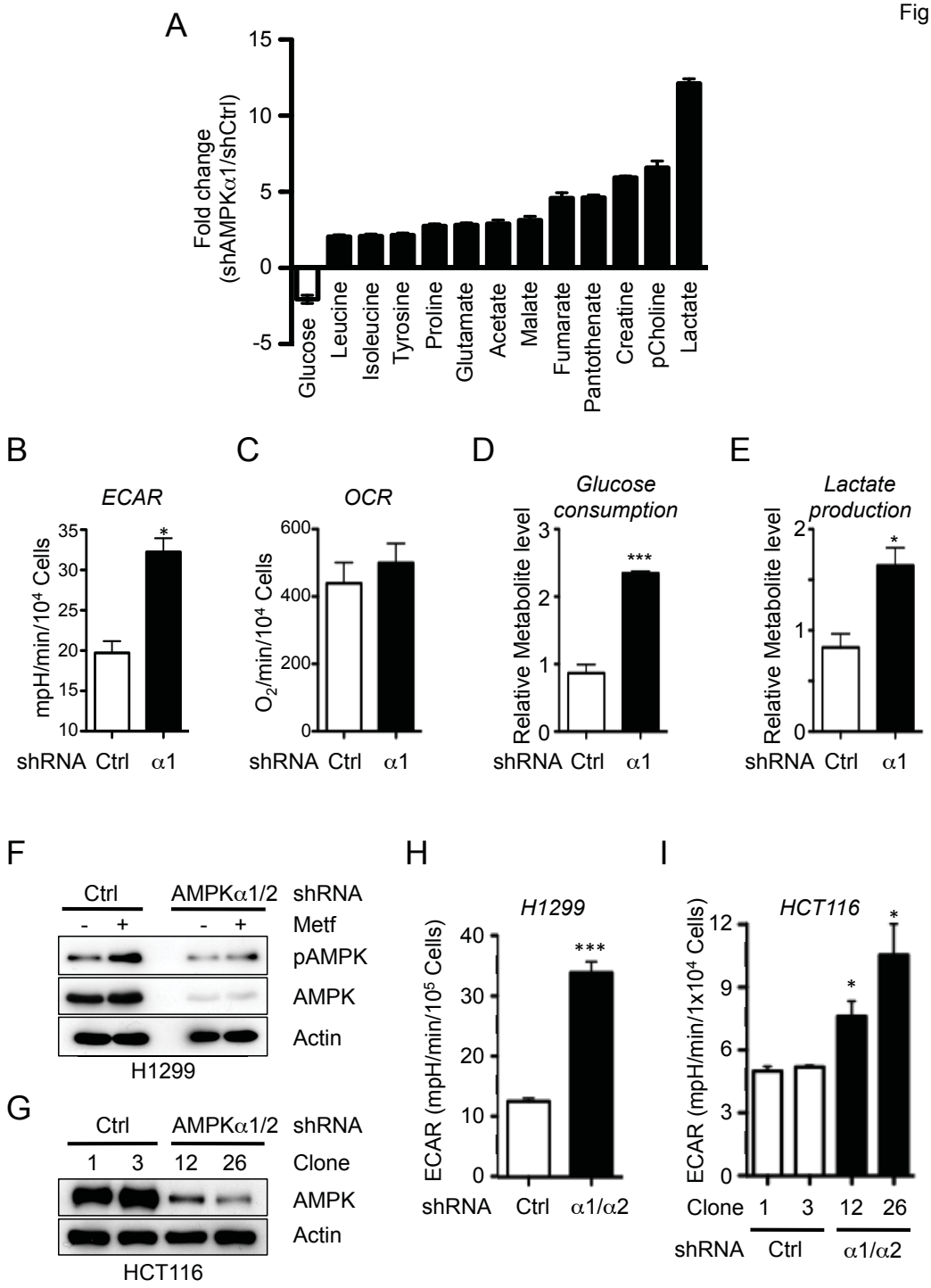
A
Fold change (shAMPKα1/shCtrl)
15
10
5
0
-5
Glucose
Leucine
Isoleucine
Tyrosine
Proline
Glutamate
Acetate
Malate
Fumarate
Pantothenate
Creatine
pCholine
Lactate
B
ECAR
mpH/min/10⁴ Cells
35
30
25
20
15
10
*
shRNA Ctrl α1
C
OCR
O2/min/10⁴ Cells
600
400
200
0
shRNA Ctrl α1
D
Glucose consumption
Relative Metabolite level
3
2
1
0
***
shRNA Ctrl α1
E
Lactate production
Relative Metabolite level
2
1
0
*
shRNA Ctrl α1
F
Ctrl
AMPKα1/2
shRNA
- + - +
Metf
pAMPK
AMPK
Actin
H1299
G
Ctrl
AMPKα1/2
shRNA
1 3 12 26
Clone
AMPK
Actin
HCT116
H
H1299
ECAR (mpH/min/10⁵ Cells)
40
30
20
10
0
***
shRNA Ctrl α1/α2
I
HCT116
ECAR (mpH/min/1x10⁴ Cells)
12
9
6
3
0
*
*
Clone 1 3 12 26
shRNA Ctrl α1/α2

Figure 2. Loss of AMPK signaling enhances the Warburg Effect in cancer cells. A) NMR metabolite profile of AMPKα-deficient lymphomas. Data are expressed as relative metabolite levels for shAMPKα1- versus shCtrl-expressing cells (*p<0.01*) for samples in quintuplicate. Open bars, decreased metabolites; closed bars, increased metabolites. B-C) Extracellular acidification rate (ECAR) (B) and oxygen consumption rate (OCR, C) for proliferating shControl (Ctrl) or shAMPKα1 (α1) Eμ-Myc lymphoma cells. Data represent the mean ± SEM for quadruplicate samples. D-E) Glucose consumption (D) and lactate production (E) of shControl (Ctrl) or shAMPKα1 (α1) Eμ-Myc lymphoma cells grown as in (B-C). (F) Immunoblot of AMPKα T172 phosphorylation and total AMPKα levels in H1299 cell clones expressing control (shCtrl) or AMPKα1/α2-specific shRNAs following treatment with Metformin (5 mM, 1 hour). G) Knockdown of AMPKα1 and α2 in HCT116 cells. (H-I) ECAR of H1299 (H) or HCT116 (I) cell clones expressing control (shCtrl) or AMPKα-specific (α1/α2) shRNAs grown under standard conditions. *, *p<0.05*; ***, *p<0.001*.

Fig. 3

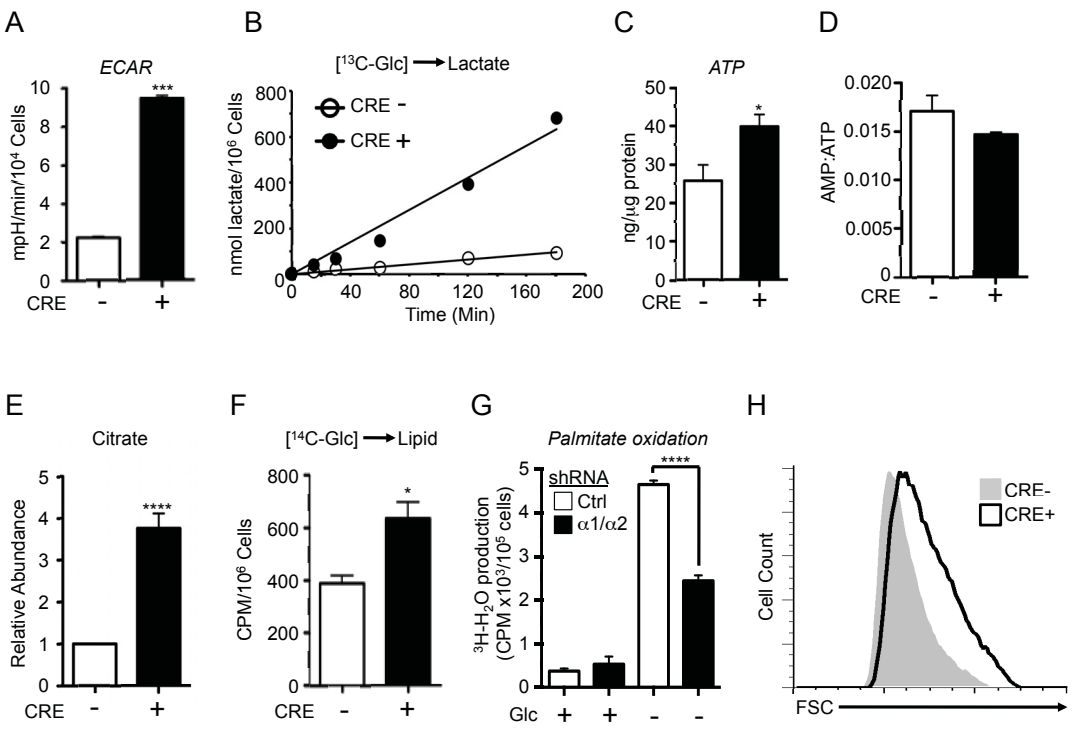
A
ECAR
mpH/min/10^4 Cells
CRE - +
B
[13C-Glc] → Lactate
CRE -
CRE +
nmol lactate/10^6 Cells
Time (Min)
C
ATP
ng/μg protein
CRE - +
D
AMP:ATP
CRE - +
E
Citrate
Relative Abundance
CRE - +
F
[14C-Glc] → Lipid
CPM/10^6 Cells
CRE - +
G
Palmitate oxidation
shRNA
Ctrl
α1/α2
3H-H2O production (CPM x10^3/10^5 cells)
Glc + + - -
H
CRE-
CRE+
Cell Count
FSC

Figure 3. Loss of AMPK signaling promotes increased biosynthesis. A) ECAR of control (Cre-, open bar) or AMPKα-null (Cre+, closed bar) MEFs cultured under standard growth conditions. Values shown are the mean ± SEM for samples in quadruplicate. B) Glucose-to-lactate conversion in control (Cre-) or AMPKα-deficient (Cre+) MEFs. Cells were cultured with medium containing uniformly labeled ^{13}C-glucose, and enrichment of ^{13}C-lactate (m+3) in the extracellular medium was measured at the indicated time points. C) ATP content of control (Cre-) or AMPKα-null (Cre+) MEFs as measured by HPLC. D) AMP:ATP ratios for cells in (C). E) Intracellular citrate levels of control (Cre-) or AMPKα-null (Cre+) MEFs as determined by GC-MS. F) Glucose-derived lipid biosynthesis in control (Cre-) or AMPKα-null (Cre+) MEFs. Cells were incubated with uniformly labeled ^{14}C-glucose for 72 hours, and radioactive counts in extracted lipids measured. G) Palmitate oxidation by MEFs expressing control (Ctrl) or AMPKα1/α2 shRNAs. MEFs were grown in the presence (+) or absence (-) of glucose for 24 hours, followed by culture with [9,10-^{3}H]-palmitic acid and 200 μM etomoxir. Tritiated water produced from palmitate oxidation was measured. H) Forward scatter (FSC) of control (Cre-, grey histogram) or AMPKα-deficient (Cre+, open histogram) MEFs. *, $p<0.05$; ***, $p<0.001$; ****, $p<0.0001$.

Fig. 4

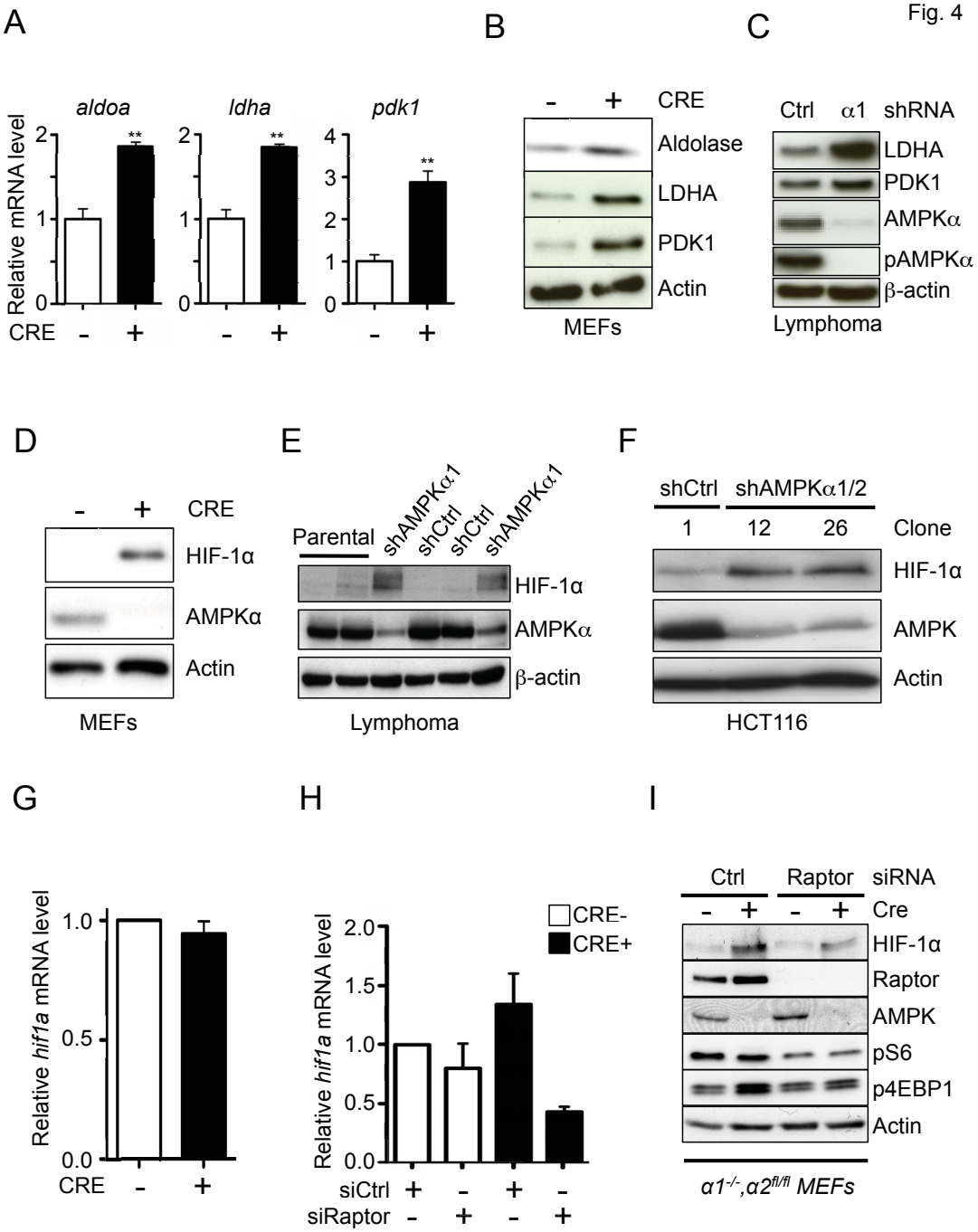
A
aldoa
ldha
pdk1
Relative mRNA level
CRE
B
CRE
Aldolase
LDHA
PDK1
Actin
MEFs
C
Ctrl
α1
shRNA
LDHA
PDK1
AMPKα
pAMPKα
β-actin
Lymphoma
D
CRE
HIF-1α
AMPKα
Actin
MEFs
E
Parental
shAMPKα1
shCtrl
shCtrl
shAMPKα1
HIF-1α
AMPKα
β-actin
Lymphoma
F
shCtrl
shAMPKα1/2
1
12
26
Clone
HIF-1α
AMPK
Actin
HCT116
G
Relative hif1a mRNA level
CRE
H
CRE-
CRE+
Relative hif1a mRNA level
siCtrl
siRaptor
I
Ctrl
Raptor
siRNA
Cre
HIF-1α
Raptor
AMPK
pS6
p4EBP1
Actin
α1-/-,α2fl/fl MEFs

Figure 4. Loss of AMPK promotes a glycolytic signature and increased HIF-1α expression. A) Relative expression of *aldoa*, *ldha*, and *pdk1* mRNA in control (Cre-, open bar) or AMPKα-null (Cre+, closed bar) MEFs as determined by qPCR. Transcript levels were determined relative to *actin* mRNA levels, and normalized relative to control (Cre-) cells. B-C) Immunoblot analysis of Aldolase, LDHA, and PDK1 protein levels in whole cell lysates from control (Cre-) and AMPKα-null (Cre+) MEFs (B) or shControl (Ctrl) and shAMPKα1 (α1)-expressing Eμ-Myc lymphoma cells (C). D-F) Immunoblot of HIF-1α protein levels in whole cell lysates from control (Cre-) and AMPKα-null (Cre+) MEFs (D), shControl (shCtrl) and shAMPKα1-expressing Eμ-Myc lymphoma cells (E), or HCT116 cell clones expressing control (shCtrl) or AMPKα-specific (shAMPKα1/2) shRNAs (F). All cells were grown under 20% O_2. G) Relative *hif1a* mRNA expression in control (Cre-) or AMPKα-null (Cre+) MEFs as determined by qPCR. H-I) Expression of *hif-1α* mRNA (H) and protein levels (I) for control (Cre-) or AMPKα-null (Cre+) MEFs transfected with siRNAs targeting Raptor. Protein lysates were also analyzed for pS6 and p4EBP levels by immunoblot. Raptor, AMPKα, and actin levels are shown as controls. **, $p<0.01$.

Fig. 5

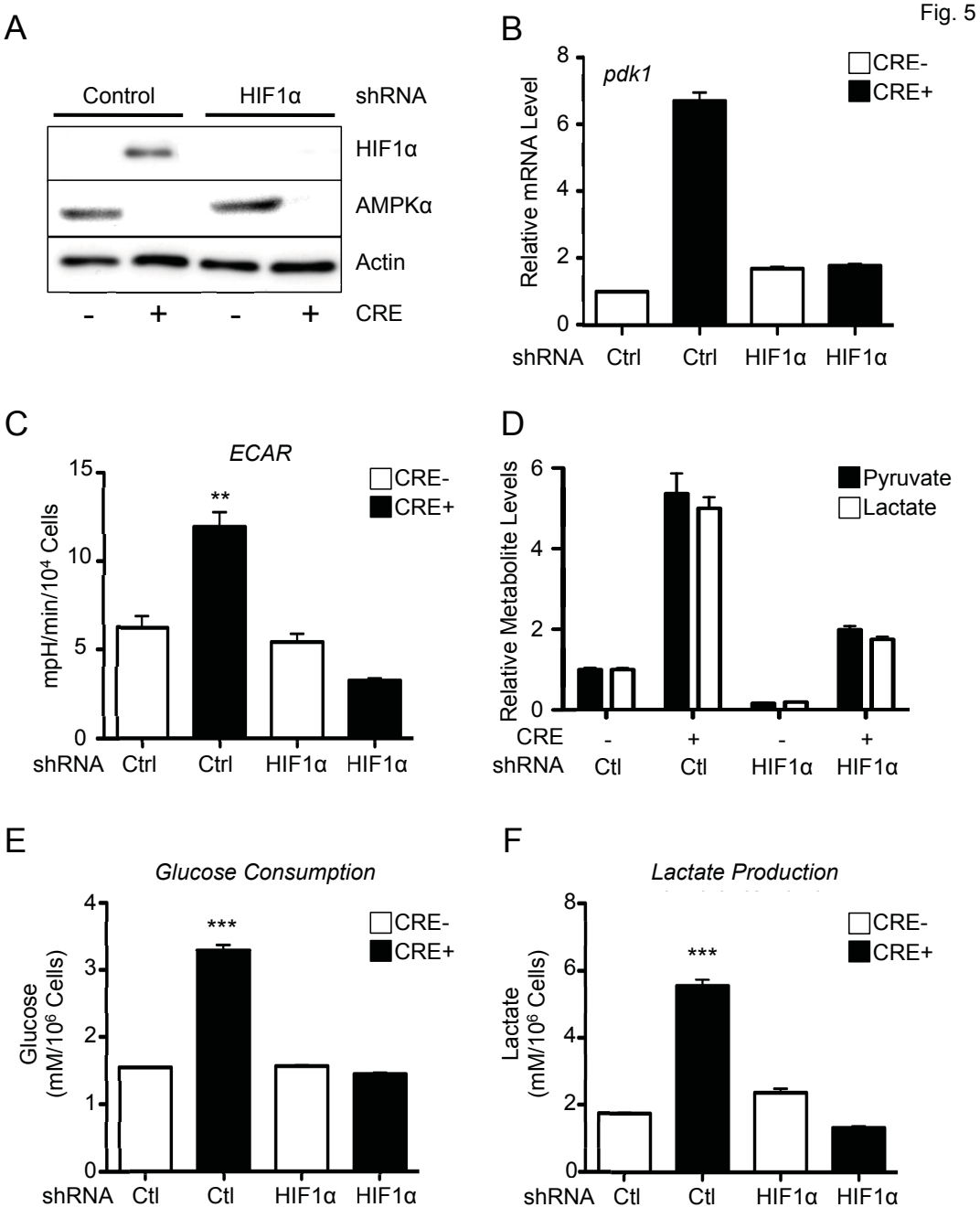
A
Control
HIF1α
shRNA
HIF1α
AMPKα
Actin
- + - +
CRE
B
pdk1
CRE-
CRE+
Relative mRNA Level
0 2 4 6 8
shRNA Ctrl Ctrl HIF1α HIF1α
C
ECAR
CRE-
CRE+
**
mpH/min/10⁴ Cells
0 5 10 15
shRNA Ctrl Ctrl HIF1α HIF1α
D
Pyruvate
Lactate
Relative Metabolite Levels
0 2 4 6
CRE - + - +
shRNA Ctl Ctl HIF1α HIF1α
E
Glucose Consumption
CRE-
CRE+
***
Glucose (mM/10⁶ Cells)
0 1 2 3 4
shRNA Ctl Ctl HIF1α HIF1α
F
Lactate Production
CRE-
CRE+
***
Lactate (mM/10⁶ Cells)
0 2 4 6 8
shRNA Ctl Ctl HIF1α HIF1α

Figure 5. HIF-1α mediates the effects of AMPK loss on aerobic glycolysis. A) HIF-1α protein expression in control (Cre-) or AMPKα-deficient (Cre+) MEFs also expressing control or HIF-1α-specific shRNAs. Cells were grown under normoxic conditions (20% O_2). AMPKα and actin protein levels are shown. B) Relative expression of *pdk1* mRNA in control (Cre-) or AMPKα-deficient (Cre+) MEFs expressing control (Ctrl) or HIF-1α-specific shRNAs. C-F) AMPK-dependent changes in the Warburg Effect are dependent on HIF-1α. C) ECAR of control (Cre-) or AMPKα-deficient (Cre+) MEFs expressing control (Ctrl) or HIF-1α-specific shRNAs grown under normoxic conditions (20% O_2). Relative intracellular pyruvate (closed bars) and lactate (open bars) levels (D), glucose consumption (E), and lactate production (F) for cells grown as in (C). **, $p<0.01$; ***, $p<0.001$.

Fig. 6

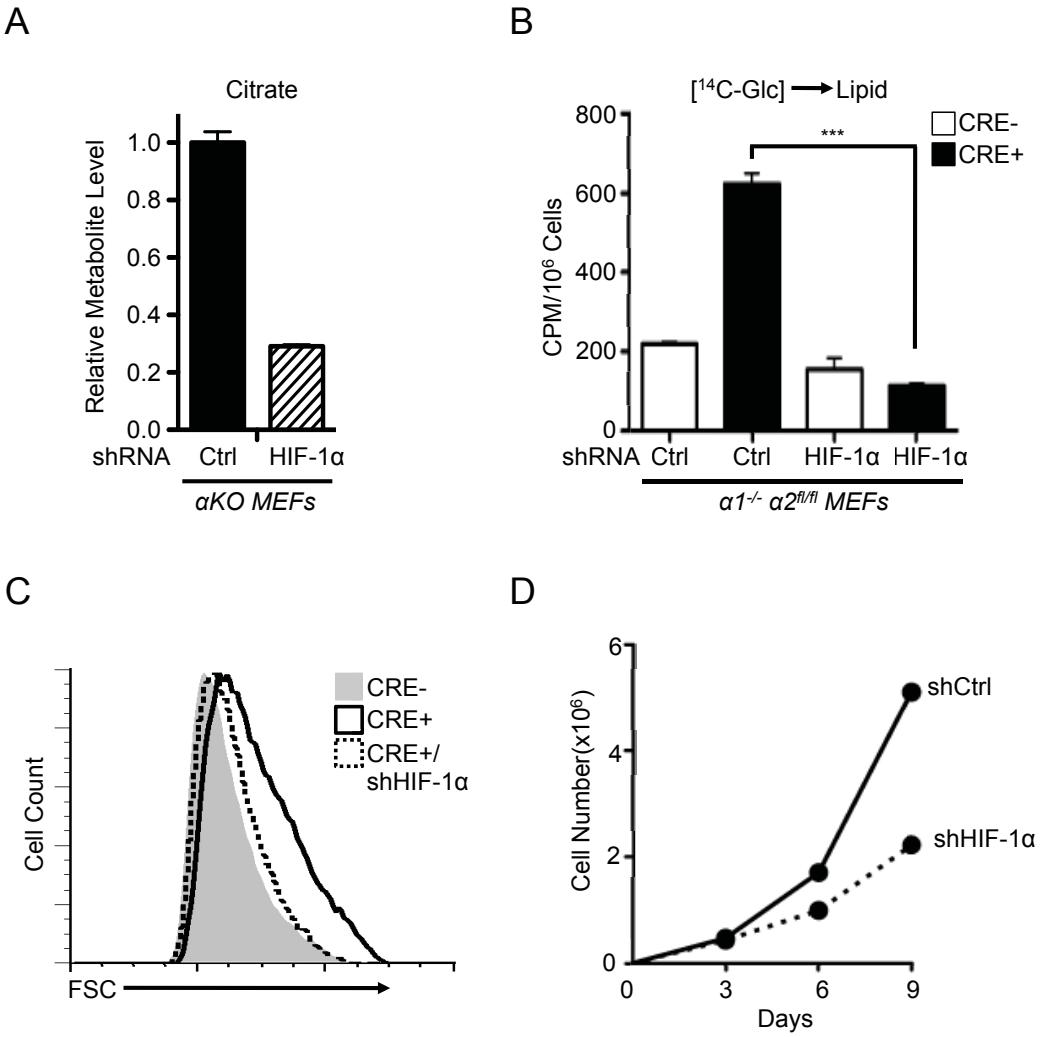
A
Citrate
Relative Metabolite Level
1.0
0.8
0.6
0.4
0.2
0.0
shRNA
Ctrl
HIF-1α
αKO MEFs
B
[14C-Glc] → Lipid
CPM/10^6 Cells
800
600
400
200
0
***
CRE-
CRE+
shRNA Ctrl
Ctrl
HIF-1α
HIF-1α
α1-/- α2fl/fl MEFs
C
Cell Count
CRE-
CRE+
CRE+/
shHIF-1α
FSC
D
Cell Number(x10^6)
6
4
2
0
shCtrl
shHIF-1α
0
3
6
9
Days

Figure 6. HIF-1α drives increased biosynthesis and proliferation of AMPKα-null cells. A) Relative citrate abundance in metabolite extracts from AMPKα-deficient (αKO) MEFs expressing control (Ctrl) or HIF-1α-specific shRNAs as determined by GC-MS. B) Lipid biosynthesis in AMPKα-deficient MEFs with HIF-1α knockdown. Control (Cre-) or AMPKα-deficient (Cre+) MEFs expressing control (Ctrl) or HIF-1α-specific shRNAs were incubated with uniformly labeled ^{14}C-glucose for 72 hours, and radioactive counts in extracted lipids were measured. C) Cell size of control (grey histogram), AMPKα-null (open histogram), and AMPKα-null MEFs expressing HIF-1α shRNA (dashed histogram) as measured by FSC intensity. D) Growth curves of AMPKα-null MEFs expressing control (shCtrl) or HIF-1α-specific (shHIF-1α) shRNAs grown under 20% O_2. Growth curves were determined using a 3T3 growth protocol and cell counts measured by trypan blue exclusion. ***, $p<0.001$.

Fig. 7

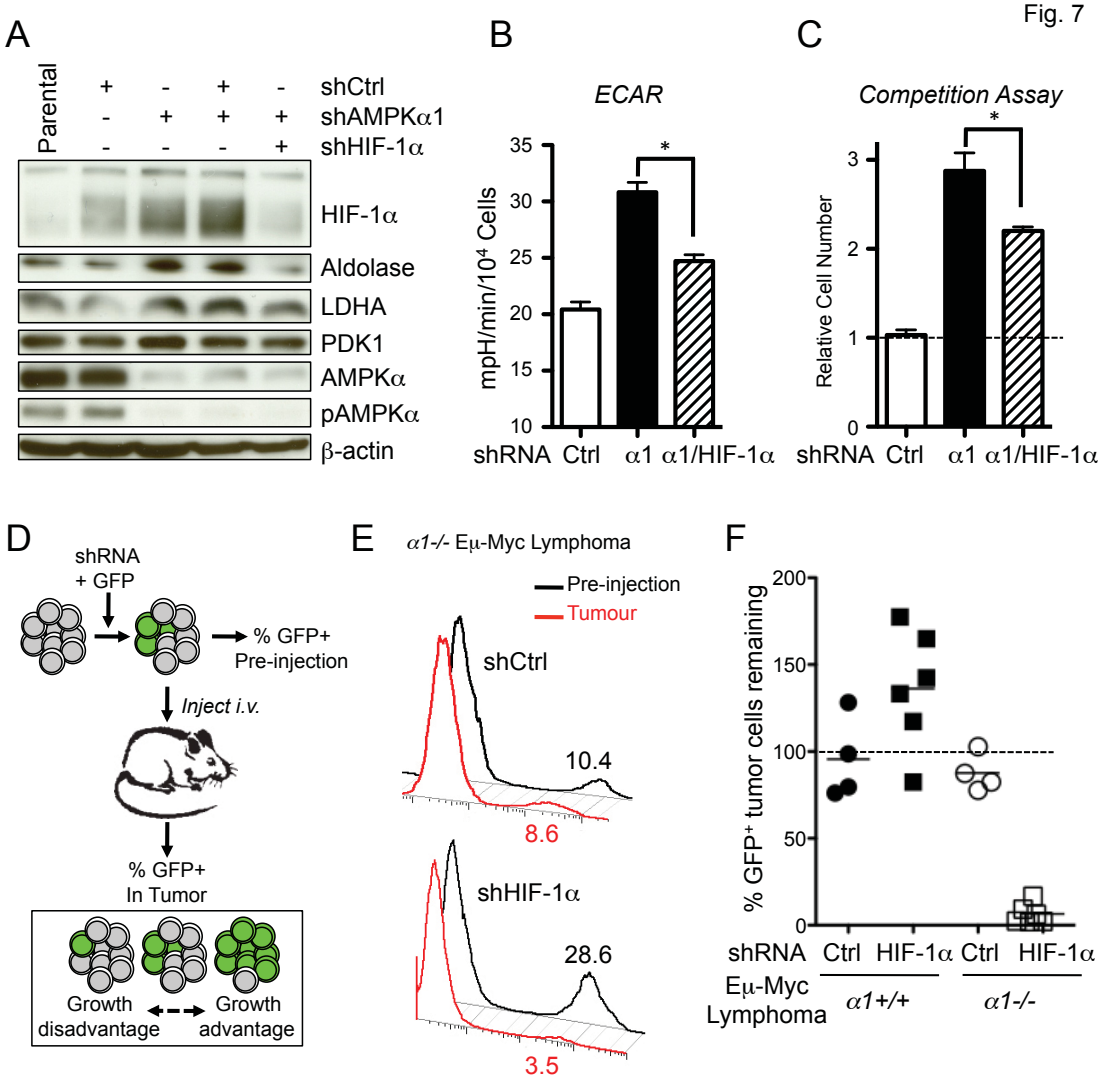
A
Parental
shCtrl
shAMPKα1
shHIF-1α
HIF-1α
Aldolase
LDHA
PDK1
AMPKα
pAMPKα
β-actin
B
ECAR
mpH/min/10⁴ Cells
shRNA Ctrl α1 α1/HIF-1α
C
Competition Assay
Relative Cell Number
shRNA Ctrl α1 α1/HIF-1α
D
shRNA
+ GFP
% GFP+
Pre-injection
Inject i.v.
% GFP+
In Tumor
Growth
disadvantage
Growth
advantage
E
α1-/- Eμ-Myc Lymphoma
Pre-injection
Tumour
shCtrl
10.4
8.6
shHIF-1α
28.6
3.5
F
% GFP⁺ tumor cells remaining
shRNA Ctrl HIF-1α Ctrl HIF-1α
Eμ-Myc
Lymphoma
α1+/+
α1-/-

Figure 7. HIF-1α mediates the metabolic and tumorigenic effects induced by AMPKα1 loss. A) Immunoblots of whole cell lysates from Eμ-Myc lymphoma cells expressing AMPKα1 and HIF-1α shRNAs. Cells were cultured under standard conditions (25 mM glucose, 20% O_2). Blots were probed with antibodies to the indicated proteins. B) ECAR of Eμ-Myc lymphoma cells expressing control (Ctrl), AMPKα1 (α1), or both AMPKα1 and HIF-1α (α1/HIF-1α) shRNAs and grown under standard conditions. C) Competition assay of Eμ-Myc lymphoma cells infected with retrovirus expressing GFP and control, AMPKα1 (α1), or both AMPKα1 and HIF-1α (α1/HIF-1α) shRNAs. The data are expressed as the relative increase in GFP^+ to GFP^- cells after 6 days of culture. D) Schematic of *in vivo* lymphoma competition assay. E) Representative histograms of GFP expression for *AMPKα1*$^{-/-}$ Eμ-Myc lymphoma cells prior to injection into recipient mice (Pre-injection, black) or isolated from lymph node tumors (Tumor, red). Numbers indicate the percentage of GFP^+ cells. F) Percent recovery of GFP^+ tumor cells from individual Eμ-Myc/*α1*$^{+/+}$ (black) or Eμ-Myc/*α1*$^{-/-}$ (white) tumors expressing the indicated shRNAs. *, $p<0.05$.

Supplemental Information for:

AMPK is a negative regulator of the Warburg Effect and suppresses tumor growth *in vivo*

Brandon Faubert, Gino Boily, Said Izreig, Takla Griss, Bozena Samborska, Zhifeng Dong, Fanny Dupuy, Christopher Chambers, Benjamin J. Fuerth, Benoit Viollet, Orval A. Mamer, Daina Avizonis, Ralph J. DeBerardinis, Peter M. Siegel, and Russell G. Jones.

Supplemental information Inventory

Figure S1 (Related to Figure 1): **Characterization of AMPKα1-deficient lymphomas.**

Figure S2 (Related to Figure 2): **Silencing AMPKα1 in Eμ-Myc lymphoma cells promotes increased glucose consumption and lactate production.**

Figure S3 (Related to Figure 3): **AMPKα-deficient cells display enhanced glycolytic metabolism and sustained mTORC1 activity.**

Figure S4 (Related to Figure 4): **Glycolytic gene expression and carbon flux analysis of AMPKα-deficient cells.**

Figure S5 (Related to Figure 5): **HIF-1α knockdown in AMPKα-deficient MEFs promotes increased aerobic glycolysis.**

Figure S6 (Related to Figure 6): **Rapamycin reduces cell size and *hif1a* mRNA levels in AMPKα-deficient MEFs.**

Table S1 (Related to Figure 3): **List of qPCR primers used in this study.**

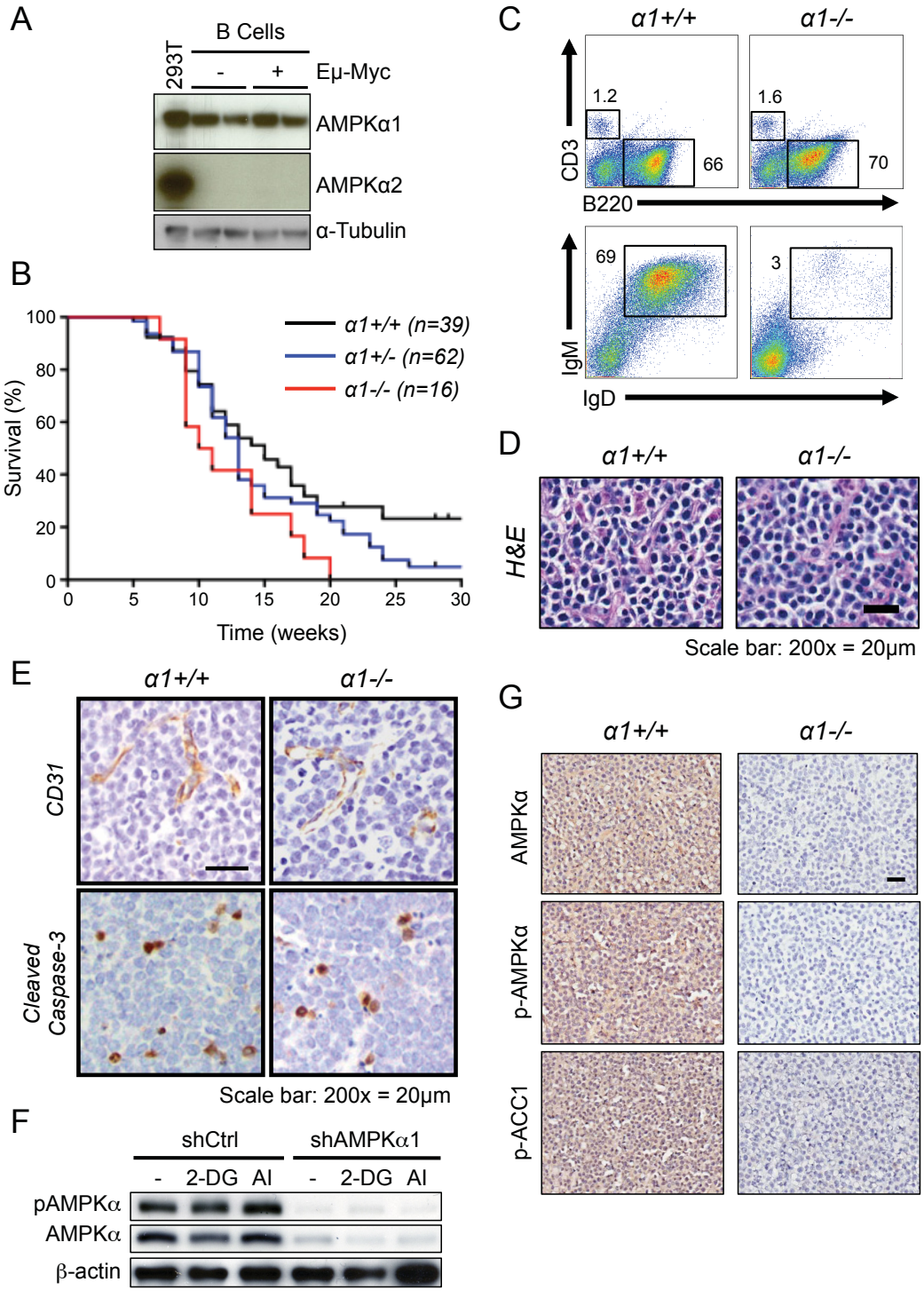
A
B Cells
293T
-
+
Eμ-Myc
AMPKα1
AMPKα2
α-Tubulin
B
Survival (%)
Time (weeks)
α1+/+ (n=39)
α1+/- (n=62)
α1-/- (n=16)
C
α1+/+
α1-/-
CD3
B220
1.2
66
1.6
70
IgM
IgD
69
3
D
α1+/+
α1-/-
H&E
Scale bar: 200x = 20μm
E
α1+/+
α1-/-
CD31
Cleaved Caspase-3
Scale bar: 200x = 20μm
F
shCtrl
shAMPKα1
-
2-DG
AI
pAMPKα
AMPKα
β-actin
G
α1+/+
α1-/-
AMPKα
p-AMPKα
p-ACC1

Figure S1. Characterization of AMPKα1-deficient Eμ-Myc lymphomas. A) Whole cell lysates from mouse B cells (+/- Eμ-Myc expression) and 293T cells were analyzed by immunoblot using antibodies against AMPKα1, AMPKα2 or actin. B) Kaplan-Meier curve showing overall survival of Eμ-Myc mice deficient ($\alpha 1^{-/-}$, red, n=16), heterozygous ($\alpha 1^{+/-}$, blue, n=62) or wild type ($\alpha 1^{+/+}$, black, n=39) for AMPKα1. C) Flow cytometry analysis of isolated lymph node tumors from Eμ-Myc/$\alpha^{+/+}$ and Eμ-Myc/$\alpha 1^{-/-}$ mice. (*Top*) Representative dot plots of CD3 versus B220 staining of lymph node cells isolated from Eμ-Myc/$\alpha^{+/+}$ and Eμ-Myc/$\alpha 1^{-/-}$ animals. (*Bottom*) Representative sIg^+ (IgM and IgD) surface staining on $B220^+$ cells. These data are representative of tumors from 4 Eμ-Myc/$\alpha^{+/+}$ and 5 Eμ-Myc/$\alpha 1^{-/-}$ mice. D) H&E staining of Eμ-Myc/$\alpha^{+/+}$ and Eμ-Myc/$\alpha 1^{-/-}$ lymphoma sections. E) Representative histological sections of Eμ-Myc/$\alpha^{+/+}$ and Eμ-Myc/$\alpha 1^{-/-}$ lymphomas stained for CD31 and cleaved Caspase-3. F) Eμ-Myc lymphoma cells expressing control (shCtrl) or AMPKα1-specific (shAMPKα1) shRNAs were treated with 2-deoxyglucose (2-DG, 10 mM) or AICAR (AI, 1 mM) for 1 hour, and whole cell lysates analyzed for total and phospho-T172-AMPKα by immunoblot. G) Histological analysis of cell signaling in Eμ-Myc/$\alpha 1^{-/-}$ lymphomas. Representative sections from Eμ-Myc/$\alpha^{+/+}$ and Eμ-Myc/$\alpha 1^{-/-}$ lymphomas were stained with antibodies detect AMPK activity (phosphorylated (pAMPKα, T172) and total AMPKα, and phospho-ACC1 (S79).

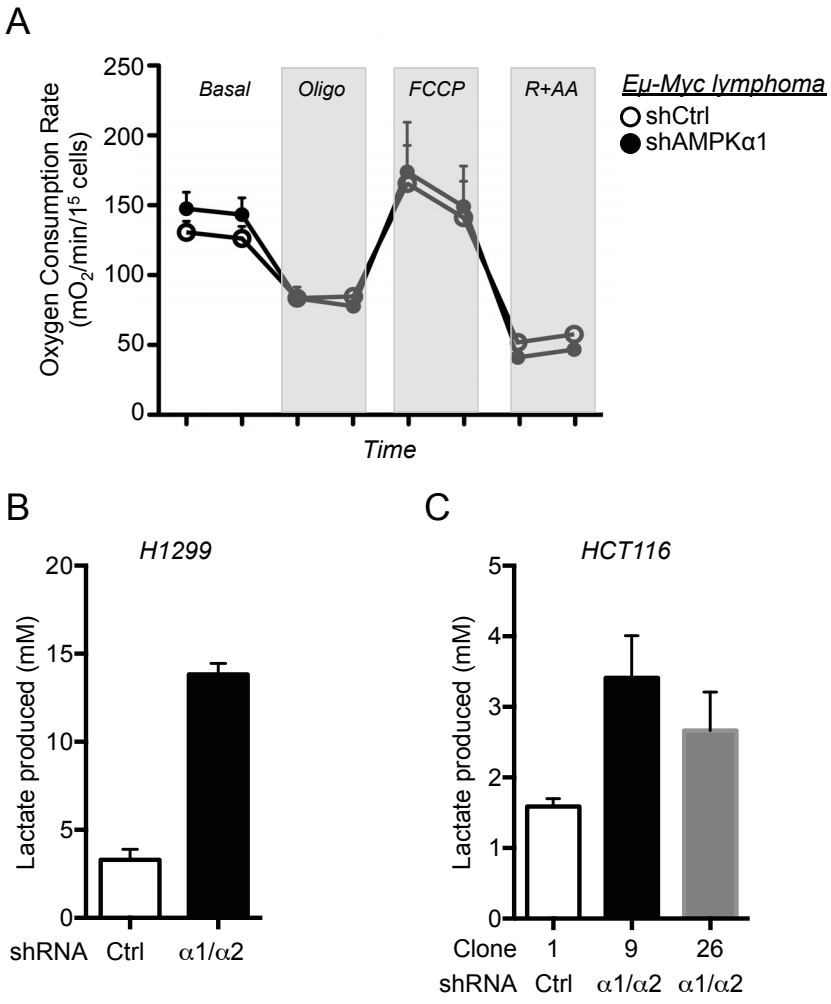
A
Basal
Oligo
FCCP
R+AA
Eμ-Myc lymphoma
shCtrl
shAMPKα1
Oxygen Consumption Rate
(mO2/min/15 cells)
250
200
150
100
50
0
Time
B
H1299
Lactate produced (mM)
20
15
10
5
0
shRNA Ctrl α1/α2
C
HCT116
Lactate produced (mM)
5
4
3
2
1
0
Clone 1 9 26
shRNA Ctrl α1/α2 α1/α2

Figure S2. Silencing AMPKα1 in Eμ-Myc lymphoma cells promotes increased glucose consumption and lactate production. A) Eμ-Myc lymphoma cells expressing control (Ctrl, open circle) or AMPKα1-specific (α1, closed circle) shRNAs were analyzed for oxygen consumption using the Seahorse XF-24 analyzer. A representative oxygen consumption trace is shown following treatment with oligomycin (ATP synthase inhibitor), FCCP (uncoupling agent), or Rotenone and Antimycin-A (Complex I and III inhibitors, respectively). B) H1299 cells expressing control (open bar) or AMPKα1/α2 (closed bar) shRNAs were cultured for 48 hours, and extracellular lactate produced was determined by enzymatic assay (n= 3 per sample). C) HCT116 cells expressing control (open bar) or AMPKα1/α2 (closed bar) shRNAs were cultured for 48 hours and extracellular lactate produced was determined by enzymatic assay (n= 3 per sample).

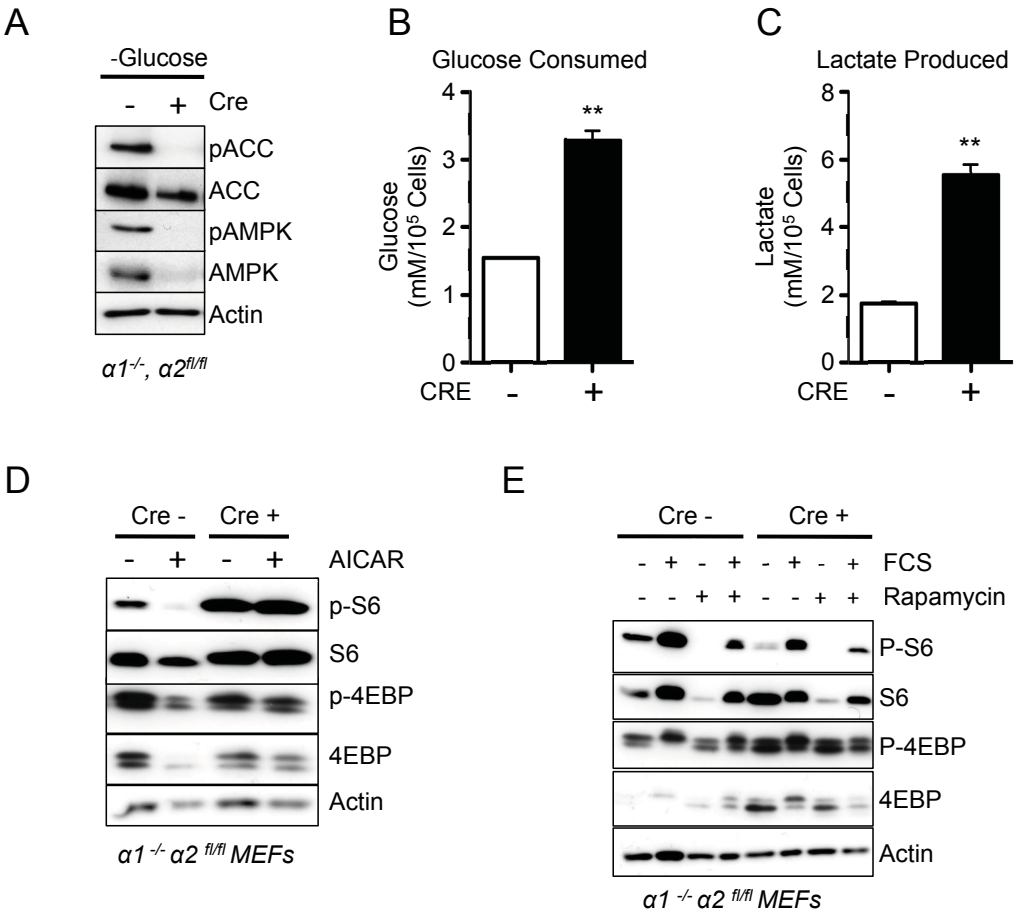
A
-Glucose
- + Cre
pACC
ACC
pAMPK
AMPK
Actin
α1-/-, α2fl/fl
B
Glucose Consumed
Glucose (mM/10^5 Cells)
4
3
2
1
0
**
CRE - +
C
Lactate Produced
Lactate (mM/10^5 Cells)
8
6
4
2
0
**
CRE - +
D
Cre - Cre +
- + - + AICAR
p-S6
S6
p-4EBP
4EBP
Actin
α1 -/- α2 fl/fl MEFs
E
Cre - Cre +
- + - + - + - + FCS
- - + + - - + + Rapamycin
P-S6
S6
P-4EBP
4EBP
Actin
α1 -/- α2 fl/fl MEFs

Figure S3. AMPKα-deficient cells display enhanced glycolytic metabolism and sustained mTORC1 activity. A) Immunoblot of whole cell lysates from control (Cre-) or AMPKα-deficient (Cre+) MEFs cultured in glucose-free medium for 24 hours using antibodies against phospho-T172 and total AMPKα, phospho-S79 and total ACC, and actin. B-C) Control (Cre-, open bar) or AMPKα-deficient (Cre+, closed bar) MEFs were analyzed for glucose consumption (B) and lactate production (C). Data are expressed as the mean ± SD (n=3 per sample). D) Control (Cre-) or AMPKα-deficient (Cre+) MEFs were treated with 1mM AICAR for 1 hour, and whole cell lysates analyzed by immunoblot using antibodies against total and phospho-ribosomal S6 (pS6, S240/244), total and phospho-4EBP1 (p4EBP1, S37/46), and actin. E) Serum-starved control (Cre-) or AMPKα-deficient (Cre+) MEFs were treated with 25nM rapamycin (25nM, 2hours), followed by re-addition of media containing 0% or 10% FCS for 15min. Immunoblot of whole cell lysates was conducted as in (a). **, $p<0.01$; ***, $p<0.001$.

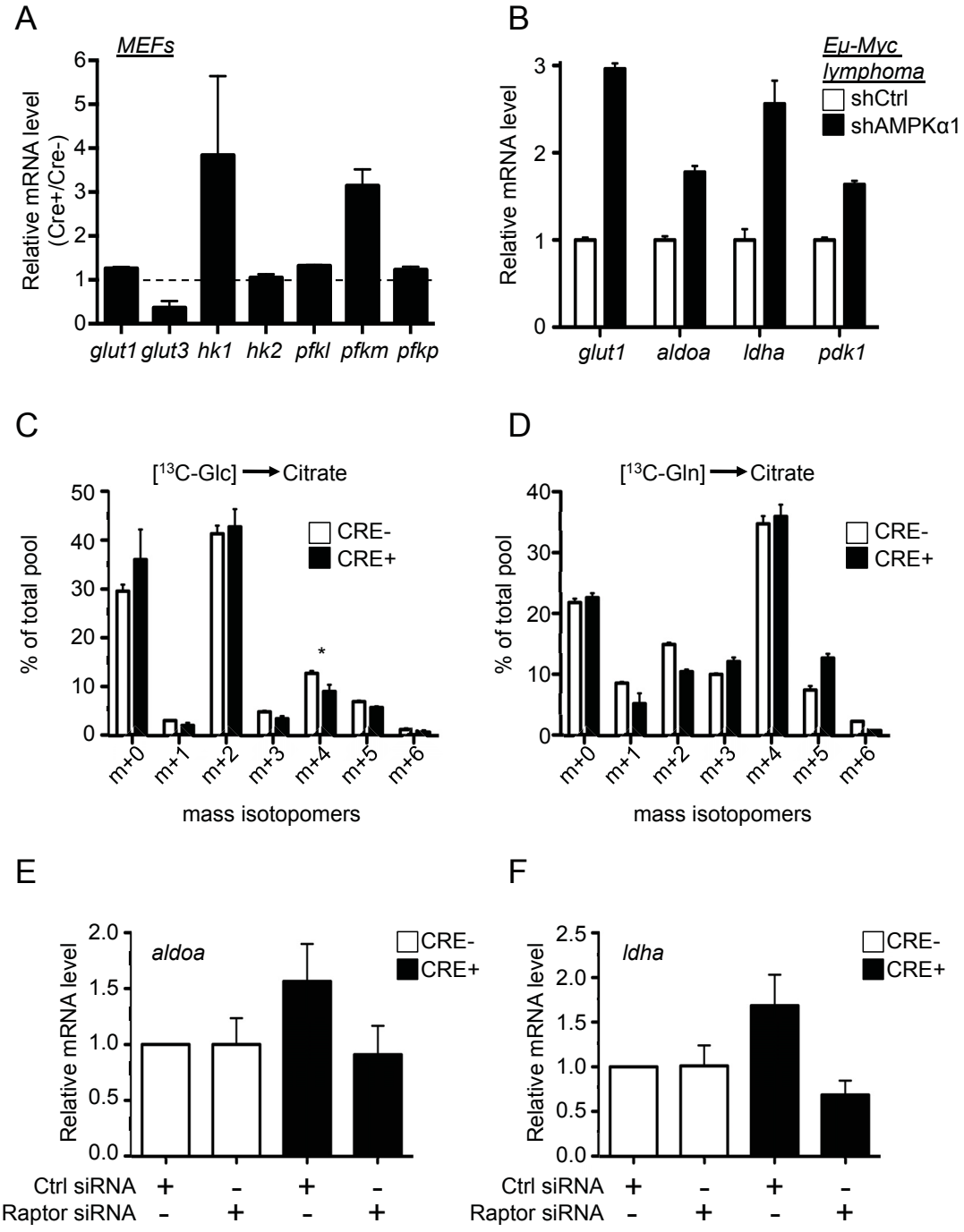
A
MEFs
Relative mRNA level (Cre+/Cre-)
glut1 glut3 hk1 hk2 pfkl pfkm pfkp
B
Eμ-Myc lymphoma
shCtrl
shAMPKα1
Relative mRNA level
glut1 aldoa ldha pdk1
C
[13C-Glc] → Citrate
CRE-
CRE+
% of total pool
mass isotopomers
D
[13C-Gln] → Citrate
E
aldoa
Ctrl siRNA
Raptor siRNA
F
ldha

Figure S4. Glycolytic gene expression and carbon flux analysis of AMPKα-deficient cells. A) Relative expression of *glut1, glut3, hk1, hk2, pfkl, pfkm* and *pfkp* mRNA by AMPKα-deficient MEFs. Expression of mRNA transcripts was determined relative to *actin* mRNA levels, and normalized relative to isogenic controls (Cre-). B) Relative expression of *glut1, aldoa*, *ldha*, and *pdk1* mRNA by Eμ-Myc lymphoma cells expressing control (shCtrl) or AMPKα1-specific (shRNA). Expression of mRNA transcripts was determined relative to *actin* mRNA levels, and normalized relative to parental lymphoma cells. C) Control (Cre-, open bars) or AMPKα-deficient (Cre+, closed bars) MEFs were cultured for 2 hours with medium containing uniformly labeled ^{13}C-glucose, metabolites extracted from cells, and enrichment of intracellular citrate was measured by GC-MS. Heavy-labeled mass isotopomers (m+) of citrate are indicated. D) Cells as in (C) were cultured for 2 hours with medium containing uniformly labeled ^{13}C-glutamine, and enrichment of glutamine-derived mass isotopomers in intracellular citrate was measured by GC-MS. E-F) Control (Cre-) or AMPKα-null (Cre+) MEFs were transfected with siRNA targeting Raptor (20 nM), and cells harvested for analysis 72 hours later. Relative expression of *aldoa* mRNA (E) and ldha mRNA (F) were determined by qPCR for triplicate samples. *, $p<0.05$.

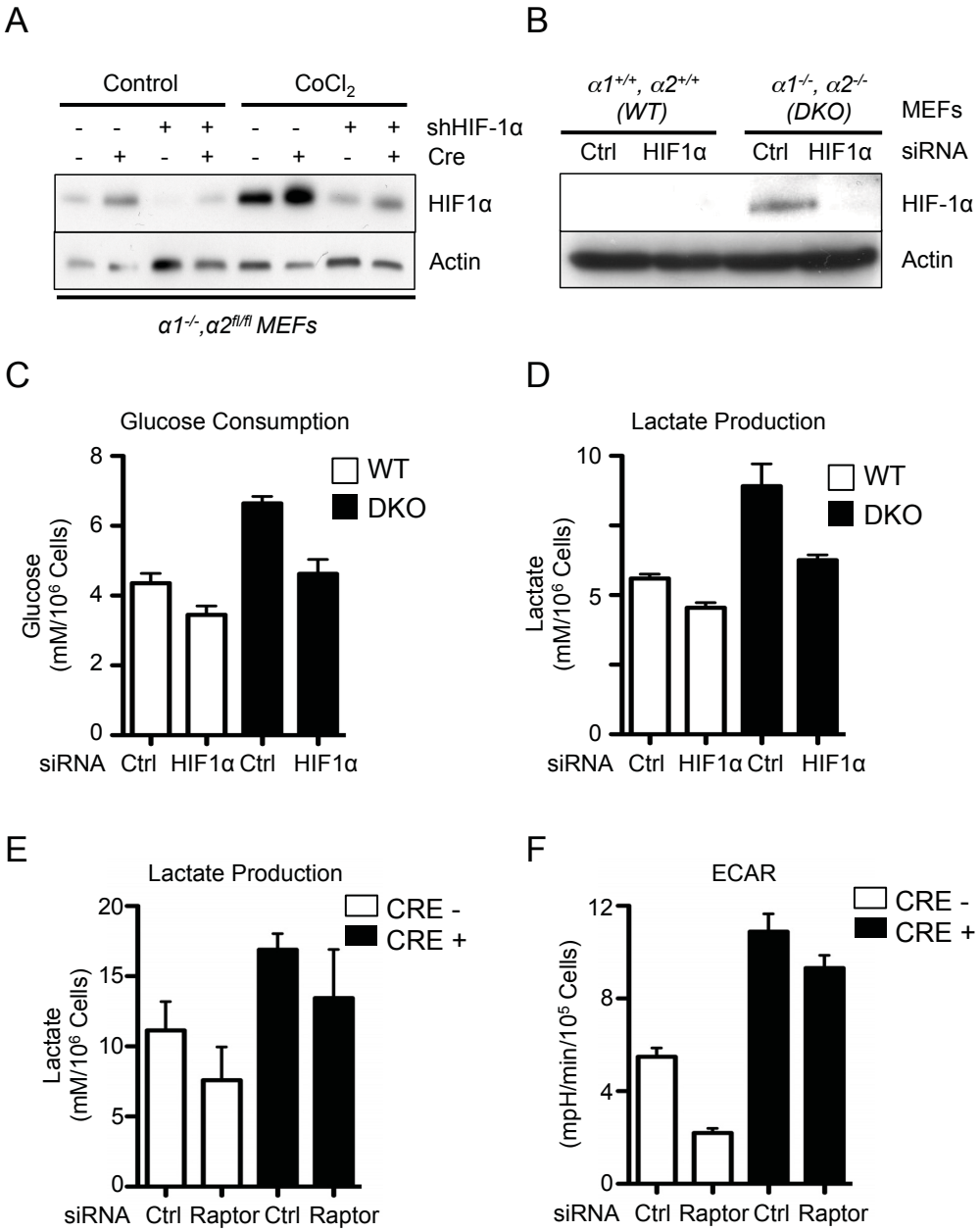
A
Control
CoCl2
shHIF-1α
Cre
HIF1α
Actin
α1-/-,α2fl/fl MEFs
B
α1+/+, α2+/+ (WT)
α1-/-, α2-/- (DKO)
MEFs
Ctrl
HIF1α
siRNA
HIF-1α
Actin
C
Glucose Consumption
Glucose (mM/10^6 Cells)
WT
DKO
siRNA Ctrl HIF1α Ctrl HIF1α
D
Lactate Production
Lactate (mM/10^6 Cells)
WT
DKO
siRNA Ctrl HIF1α Ctrl HIF1α
E
Lactate Production
Lactate (mM/10^6 Cells)
CRE -
CRE +
siRNA Ctrl Raptor Ctrl Raptor
F
ECAR
(mpH/min/10^5 Cells)
CRE -
CRE +
siRNA Ctrl Raptor Ctrl Raptor

.

Figure S5. HIF-1α knockdown in AMPKα-deficient MEFs promotes increased aerobic glycolysis. A) Cells were treated with $CoCl_2$ (150 μM, 30 min) and whole cell lysates analyzed by immunoblot using HIF-1α and actin antibodies. B) siRNA-mediated knockdown of HIF-1α in AMPK$\alpha^{-/-}$ MEFs. MEFs lacking AMPKα1 and α2 (DKO) were transfected with siRNA targeting HIF-1α (100nM), and cells harvested for analysis after 72 hours. Whole cell lysates were analyzed for HIF-1α and actin expression by immunoblot. C-D) AMPK$\alpha^{-/-}$ MEFs display enhanced aerobic glycolysis. Wild-type (WT, open bars) or AMPK$\alpha 1^{-/-}, \alpha 2^{-/-}$ (DKO, closed bar) MEFs were grown for 72 hours, and medium samples were analyzed for glucose (C) and lactate (D) levels by enzymatic assay. Data are expressed as the mean ± SD of total glucose consumed or lactate produced. E-F) siRNA-mediated knockdown of Raptor in AMPK$\alpha^{-/-}$ MEFs. MEFs lacking AMPKα1 and α2 were transfected with siRNA targeting HIF-1α (20nM), and medium samples were analyzed for lactate levels by enzymatic assay (E). F) ECAR was measured for cells treated as in E).

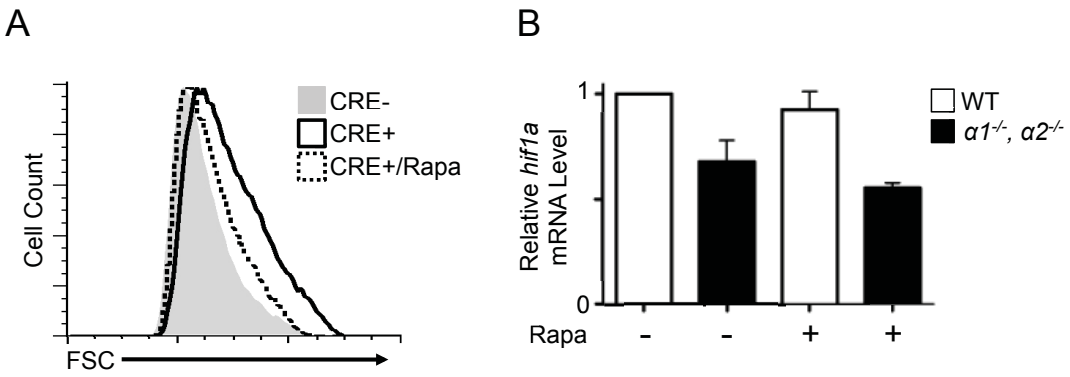
A
B
CRE-
CRE+
CRE+/Rapa
Cell Count
FSC
Relative hif1a mRNA Level
1
0
WT
α1-/-, α2-/-
Rapa
-
-
+
+

Figure S6. Rapamycin reduces cell size and *hif1a* mRNA levels in AMPKα-deficient MEFs. A) Representative forward scatter (FSC) of control (Cre-) or AMPKα-deficient (Cre+) MEFs cultured with or without 25nM rapamycin for 16 hours. B) Relative expression of *hif1a* mRNA by wild-type (WT) or AMPKα-deficient ($\alpha 1^{-/-}$, $\alpha 2^{-/-}$) MEFs cultured with or without 25nM rapamycin for 24 hours. Expression of mRNA transcripts was determined relative to *actin* mRNA levels, and normalized relative to wild type cells without rapamycin.

Table S1. List of qPCR primers used in this study.

Gene	Direction	Sequence
actb	Forward	atgctccccgggctgtat
	Reverse	cataggagtccttctgacccattc
Aldoa	Forward	gtgggaagaaggagaacctg
	Reverse	ctggagtgttgatggagcag
hif1a	Forward	accttcatcggaaactccaaag
	Reverse	ctgttaggctgggaaaagttagg
ldha	Forward	tgtctccagcaaagactactgt
	Reverse	gactgtacttgacaatgttggga
pdk1	Forward	acaaggagagcttcggggtggatc
	Reverse	ccacgtcgcagtttggatttatgc

Preface to Chapter 3

The deregulated growth and proliferation of tumor cells requires increased energy and biosynthetic intermediates. To meet these biosynthetic demands, cancer cells undergo fundamental changes in their pathways of energy metabolism and nutrient uptake. This altered metabolism, termed the Warburg effect, is characterized by enhanced aerobic glycolysis. However, our understanding of how oncogene and tumor suppressor networks regulate metabolism remains to be fully elucidated. LKB1 is a tumor suppressor that regulates several cellular processes, including cell proliferation, polarity, and apoptosis. In Chapter 2, we characterized the effects of AMPK loss on tumour growth and metabolism. However, AMPK can be activated by kinases other than LKB1, including CamKKβ and TAK1. Furthermore, AMPK is one of several proteins activated by LKB1. Despite being characterized as a tumour suppressor, and featuring various roles in mediating cellular metabolism, the role of LKB1 in the metabolic phenotype of cancer remains unknown.

Classification: Major: Biological Sciences; Minor: Cell Biology

Loss of the tumor suppressor LKB1 promotes metabolic reprogramming of cancer cells via HIF-1α

Brandon Faubert[1,2], Emma E. Vincent[1,2], Takla Griss[1,2], Bozena Samborska[1,2], Said Izreig[1,2], Robert Svensson[3], Orval A. Mamer[1,4], Daina Avizonis[1,4], David B. Shackelford[5], Reuben J. Shaw[3] and Russell G. Jones[1,2].

Author Affiliation: [1]Goodman Cancer Research Centre, McGill University, Montreal, QC, H3A 1A3, Canada; [2]Department of Physiology, McGill University, Montreal, QC, H3G 1Y6, Canada; [3]Howard Hughes Medical Institute, Molecular and Cell Biology Laboratory, The Salk Institute for Biological Studies, La Jolla CA, 92037, USA; [4]Metabolomics Core Facility, McGill University, Montreal, QC, H3A 1A3, Canada; [5]Departments of Molecular and Medical Pharmacology, Pulmonary and Critical Care Medicine, David Geffen UCLA School of Medicine, Los Angeles, CA 90095, USA

Corresponding author: Russell G. Jones, Goodman Cancer Research Centre, Department of Physiology, McGill University, 3655 Promenade Sir William Osler, Room 705, Montreal, Quebec, H3G 1Y6, CANADA. Email: russell.jones@mcgill.ca, Phone: (514) 398-3336, Fax: (514) 398-6769.

Keywords: LKB1, HIF-1α, cancer metabolism, biosynthesis, Warburg effect

Abstract

One of the major metabolic changes associated with cellular transformation is enhanced nutrient utilization, which supports tumor progression by fueling both energy production and providing biosynthetic intermediates for growth. The Liver kinase B1 (LKB1) is a serine/threonine kinase and tumor suppressor that couples bioenergetics to cell growth control through regulation of mTOR activity; however, the influence of LKB1 on tumor metabolism is not well defined. Here we show that loss of LKB1 induces a pro-growth metabolic program in proliferating cells. Cells lacking LKB1 display increased glucose and glutamine uptake and utilization, which support both cellular ATP levels and increased macromolecular biosynthesis. This LKB1-dependent reprogramming of cell metabolism is dependent on the hypoxia-inducible factor-1α (HIF-1α), which accumulates under normoxia in LKB1-deficient cells and is antagonized by inhibition of mTORC1 signaling. Silencing HIF-1α reverses the metabolic advantages conferred by reduced LKB1 signaling, and impairs the growth and survival of LKB1-deficient tumor cells under low nutrient conditions. Together our data implicate the tumor suppressor LKB1 as a central regulator of tumor metabolism and growth control through the regulation of HIF-1α-dependent metabolic reprogramming.

Significance Statement

LKB1 is a serine/threonine kinase often inactivated in human cancer. We demonstrate here that loss of LKB1 expression in cancer cells promotes a pro-growth metabolic profile that enables increased cell growth and proliferation. Loss of LKB1 promotes increased tumor cell metabolism through mTORC1- and ROS-dependent increases in HIF-1α. LKB1-null cells are dependent on HIF-1α to maintain cellular ATP and viability under poor nutrient conditions, raising the possibility of targeting HIF-1α for synthetic lethality in LKB1-deficient tumors. Together our data reveal that regulation of cellular metabolism is a key function of LKB1 that may contribute to its tumor suppressor function in human cancer.

Introduction

While unchecked cell proliferation and aberrant survival are hallmark features of cancer, tumor cells must also engage pathways of cellular metabolism to generate the energy and biosynthetic intermediates required to support increased cell division (DeBerardinis et al., 2008a). To meet increased energetic and biosynthetic demand, cancer cells often display fundamental changes in their cellular metabolism including a switch to aerobic glycolysis, a phenomenon known as the "Warburg effect" (Vander Heiden et al., 2009). Increased use of glutamine ("glutaminolysis") for mitochondrial-dependent ATP production and cellular biosynthesis is also a key feature of many tumor cells (Deberardinis et al., 2008b).

Many of the predominant driver mutations observed in cancer alter tumor cell metabolism as part of their mode of action (Jones and Thompson, 2009). For example, loss of the tumour suppressor PTEN can promote increased glucose uptake though elevated PI3K/Akt/mTOR signaling (Pan and Mak, 2007), while loss of the Von-Hippel-Lindau (VHL) tumor suppressor promotes a similar metabolic phenotype through stabilization of the hypoxia inducible factor (HIF)-1α (Semenza, 2011a). HIF-1α and HIF-2α are transcription factors whose activity is regulated by oxygen availability. HIF-1α and HIF-2α protein expression is normally stabilized only under hypoxic conditions; however, the HIFs are commonly expressed in human cancers even in the absence of hypoxia (Keith et al., 2012). Importantly, elevated expression of both HIF-1α and HIF-2α has been demonstrated in many cases of non-small cell lung cancer (NSCLC) (Giatromanolaki et al., 2001), and HIF-2α has been linked to poor prognosis in lung cancer patients (Roy et al., 2010).

The liver kinase B1 (LKB1) is a serine/threonine kinase encoded by *STK11*, the tumor suppressor gene responsible for Peutz-Jeghers Syndrome (PJS) (Avizienyte et al., 1999;

Hemminki et al., 1998). LKB1 is a unique serine-threonine kinase in that inactivation, rather than activation, of its kinase activity is associated with tumorigenesis. Somatic *STK11* mutations are associated with a number of human cancers including lung, breast, and cervical cancer (Contreras et al., 2008; Hearle et al., 2006a; Sanchez-Cespedes et al., 2002; Wingo et al., 2009), and genetic ablation of LKB1 in mice promotes tumorigenesis in a variety of tissues (Shackelford and Shaw, 2009). LKB1 is involved in a diverse array of cellular processes including cell polarity, apoptosis, and cell growth (Boudeau et al., 2003; Shaw, 2008). All these processes play a role in cancer initiation and progression, and as such their relative contribution to LKB1-mediated tumor suppression remains unclear.

While LKB1 is widely accepted as a regulator of cell growth control, the impact of LKB1 on tumor metabolism has remained unclear. Benign tumors haploinsufficient for LKB1 can be visualized using FDG-PET imaging (Shackelford et al., 2009), suggesting that loss of LKB1 can promote increased glucose uptake by tumor cells. LKB1 may also influence ATP consumption by limiting mTORC1-dependent mRNA translation (Corradetti et al., 2004; Shaw et al., 2004a). In this study we have characterized the impact of LKB1 loss on cellular metabolism in both transformed and non-transformed cells. We find that silencing LKB1 in tumor cells increases glucose and glutamine consumption and promotes a metabolic switch to aerobic glycolysis. We demonstrate that HIF-1α drives the metabolic shift induced by LKB1 loss, and that ablation of HIF-1α reverses the metabolic advantage of LKB1-deficient cells. Together our data implicate LKB1 loss as a key regulator of tumor cell metabolism and growth through regulation of HIF-1α-dependent metabolic reprogramming.

Results

Loss of LKB1 promotes enhanced glucose and glutamine metabolism. To examine the metabolic consequences of LKB1 loss, we manipulated LKB1 expression in mouse embryonic fibroblasts (MEFs) harboring a conditional mutation in the *stk11* gene (LKB1$^{fl/fl}$). We used Cre recombinase to generate isogenic MEFs expressing (Cre-) or lacking (Cre+) LKB1 expression (Fig. 1A), and then examined the effect of LKB1 loss on nutrient uptake. LKB1-deficient MEFs displayed increased glucose (Fig. 1B) and glutamine consumption (Fig. 1C) relative to control cells expressing LKB1. We next measured the basal extracellular acidification rate (ECAR) and oxygen consumption rate (OCR) for control or LKB1-deficient MEFs using a flux analyzer (Xu et al., 2011b). Cells lacking LKB1 displayed a 2-fold increase in ECAR (Fig. 1D), with no significant change in oxygen consumption (Fig. 1E). This change in ECAR displayed by LKB1-deficient MEFs correlated with increased lactate production by these cells (Fig. 1F).

We next cultured control or LKB1-null MEFs with uniformly labeled (U-^{13}C) glucose or glutamine, and examined the total ^{13}C contribution of these carbon sources to intracellular metabolite pools. Cells lacking LKB1 (closed bar) displayed a slight increase in intracellular lactate levels derived from glucose (Fig. 1G). The strong increase in ECAR (Fig. 1D) and extracellular lactate (Fig. 1F) associated with LKB1 loss suggests that intracellular lactate is rapidly exported once generated. Using ^{13}C-glutamine we observed increased glutamine conversion to glutamate and α-ketoglutarate (Fig. 1H), suggesting an increase in glutaminolysis in LKB1-deficient MEFs.

LKB1-deficient tumor cells display enhanced glycolytic and TCA cycle flux. To investigate the role of LKB1 loss on tumor cell metabolism we examined the metabolic activity of A549

NSCLC cells, which naturally lack LKB1 expression (Fig. 2A and S1A). Re-expression of LKB1 in A549 cells (A549/LKB1) promoted a ~20% decrease in ECAR relative to control cells lacking LKB1 expression (A549/Vec), while OCR was unaffected (Fig. 2B). A549 cells re-expressing LKB1 also displayed reduced production of glutamine-derived glutamate compared to control cells, consistent with a reduction in glutaminolysis in these cells (Fig. 2C). We observed similar effects of LKB1 expression on glycolysis using an independent LKB1-deficient NSCLC cell line (A427, (Shackelford et al., 2013)). A427/Vec cells lacking LKB1 displayed a ~2-fold higher ECAR relative to A427 cells re-expressing LKB1 (Fig. S1B).

We next examined the metabolic fate of glucose and glutamine in A549 cells using ^{13}C-labelled glucose and glutamine. A549/Vec cells lacking LKB1 displayed an increase in the total abundance of metabolites derived from both glycolysis (lactate) and the TCA cycle (citrate, alpha-ketoglutarate, fumarate, and malate) relative to A549 cells re-expressing LKB1 (A549/LKB1) (Fig. 2D). Moreover, the proportion of these metabolites containing ^{13}C label was also elevated in LKB1-null A549 cells. A549 cells displayed enrichment of ^{13}C-glucose carbon in lactate (Fig. 2D, black bars), consistent with the increased glycolytic activity of these cells. However, the relative proportion of ^{13}C-glucose-derived carbon in TCA metabolites downstream of citrate was low for both cell lines, despite the total metabolite levels remaining higher in A549 cells lacking LKB1. The decreased labeling from glucose in TCA cycle metabolites was compensated for by an increase in glutamine-derived carbons entering the TCA cycle at alpha-ketoglutarate, providing the majority of carbon pools for the TCA cycle (Fig. 2D, grey bars). Again, LKB1-deficient A549 cells displayed increased labeling from ^{13}C-glutamine in alpha-ketoglutarate, fumarate, malate, and citrate (Fig. 2D, grey bars).

While overall lactate and TCA cycle metabolite abundance, as well as flux into these pathways from glucose or glutamine, was elevated in LKB1-null cells, the relative distribution of mass isotopomers in the metabolite pools did not vary dramatically in A549 cells regardless of LKB1 status. One consistent difference was a small elevation in glutamine-dependent reductive carboxylation in A549 cells lacking LKB1, which was apparent by the slight increase in m+5 citrate production from ^{13}C-glutamine (Fig. S2A). Similar trends in metabolite abundance and labeling patterns from glucose and glutamine were observed in LKB1-deficient MEFs relative to controls (Fig. S1B). Thus, under normal growth conditions loss of LKB1 in tumor cells appears to enhance glucose and glutamine flux, but does not dramatically alter the metabolic fate of these carbon sources.

LKB1-null cells display enhanced growth and biosynthetic capacity. Given the observation of increased carbon flow of glucose and glutamine in LKB1-null cells, we examined the impact of LKB1 loss on proliferation and *de novo* lipid biosynthesis. LKB1-deficient MEFs displayed increased rates of proliferation (Fig. 3A) and displayed a 15% increase in cell size (Fig. 3B) relative to control cells. Given the enhanced carbon flow from glucose and glutamine observed in LKB1-null cells, we measured levels of glucose- and glutamine-derived lipid synthesis in these cells. MEFs were pulsed with radioactively labeled (^{14}C) glucose or glutamine, and ^{14}C-labeling in lipids was measured. LKB1-null cells displayed a twofold increase in glucose-dependent lipid biosynthesis relative to control cells (Fig. 3C), while no appreciable difference in ^{14}C-glutamine incorporation to fatty acids was observed between cell lines (Fig. 3D). We next used GC-MS to measure the total abundance of fatty acids in LKB1-deficient cells. The overall abundance of several fatty acid species was increased when LKB1 was absent in A549 cells (Fig. 3E).

Cumulatively these data indicate that loss of LKB1 enhances biosynthetic pathways that support cell growth and proliferation.

LKB1 deletion promotes HIF-1α protein expression in cancer cells under normoxia. It has previously been shown that LKB1-deficient MEFs display enhanced HIF-1α protein levels under normoxia (Shackelford et al., 2009). Acute deletion of LKB1 in MEFs also resulted in increased HIF-1α protein levels under normoxic conditions (Fig. 4A). HIF-1α mRNA levels were also elevated 5-fold in LKB1-deficient MEFs relative to isogenic controls (Fig. 4B). Similar to LKB1-null MEFs, A549 cells lacking LKB1 displayed elevated levels of HIF-1α protein expression under normoxia, which was reduced by re-expression of LKB1 (Fig. 4C). Similarly, HIF-1α protein was detectable in A427 cells under normoxic conditions, and was reduced upon ectopic expression of LKB1 in these cells (Fig. S3A). Furthermore, reducing LKB1 expression by siRNA treatment promoted an increase in HIF-1α protein levels in U20S cells (Fig. S2B) and HCT116 cells (Fig. S3C). We next examined the expression of several HIF-1α target genes involved in metabolic control, assessing both mRNA (Fig. 4D) and protein (Fig. 4E) levels. The expression levels of Aldolase A, pyruvate dehydrogenase kinase 1 (PDK1), and lactate dehydrogenase A (LDHA) were all specifically elevated in LKB1-null MEFs (Fig. 4E).

LKB1-dependent HIF-1α expression is regulated by mTORC1 and ROS. Aberrant mTOR signaling has been linked to deregulated HIF-1α protein expression under normoxic conditions (Brugarolas et al., 2003; Shackelford et al., 2009). Consistent with previous reports (Shaw et al., 2004a), acute deletion of LKB1 in MEFs promoted heightened activation of mTORC1 signaling marked by increased rS6 phosphorylation and hyperphosphorylation of 4E-BP1 (Fig. 5A). A549

cells lacking LKB1 also displayed increased rS6 phosphorylation (Fig. 5B). To test whether elevated HIF-1α protein levels in LKB1-null cells were supported by mTOR activity, we treated cells with the mTORC1 inhibitor rapamycin and measured HIF-1α protein levels in cell lysates. Rapamycin treatment reduced HIF-1α protein expression in LKB1-deficient A549 cells under normoxic conditions (Fig. 5B). Moreover, HIF-1α mRNA levels in LKB1-null cells were reduced in response to rapamycin treatment (Fig. 5C). Finally, we examined HIF-1α protein expression in LKB1-deficient MEFs with specific ablation of mTORC1 signaling by reducing expression of the mTORC1 complex component Raptor using RNAi. Similar to rapamycin, knockdown of Raptor ablated normoxic HIF-1α protein expression in LKB1-null MEFs (Fig. 5D).

Elevated levels of mitochondrial ROS have been shown to promote increased HIF-1α activity (Brunelle et al., 2005a; Guzy et al., 2005; Horak et al., 2010; Mansfield et al., 2005). Consistent with recent results in LKB1-null tumor cells (Shackelford et al., 2013), LKB1-deficient MEFs displayed a ~2-fold increase in ROS levels that could be reduced via addition of the ROS scavenger N-acetyl-cysteine (NAC) (Fig. 5E). The addition of NAC also reduced HIF-1α protein levels in LKB1-null MEFs back to levels observed in control MEFs (Fig. 5F). Together, these data suggest that both mTOR signaling and cellular ROS levels contribute to increased HIF-1α protein expression in cells lacking LKB1.

HIF-1α drives the metabolic phenotype induced by LKB1 loss. HIF-1α has well-established roles in redirecting metabolism in response to stress (Semenza, 2011b). To assess the contribution of HIF-1α to the metabolic phenotypes induced by LKB1 loss, we used siRNA to knockdown HIF-1α protein expression in LKB1-null MEFs (Fig. 6A). Knockdown of HIF-1α

had no effect on the level of lactate production by control cells, but specifically reduced the level of lactate produced by MEFs lacking LKB1 (Fig. 6B). Reductions in lactate production were also observed in LKB1-null MEFs (Fig. S4A) and A549 cells (Fig. S4B) treated with rapamycin. Reducing HIF-1α expression decreased the size of LKB1-deficient MEFs, restoring cell size to control levels (Fig. 6C). Next we reduced HIF-1α expression in A549 cells via stable expression of shRNA specific for HIF-1α (Fig. 6D). Knockdown of HIF-1α in A549 cells lacking LKB1 promoted a ~30% decrease in glutamine consumption by these cells (Fig. 6E). Glutaminolysis, as measured by ^{13}C-glutamine conversion to ^{13}C-glutamate, was similarly reduced in A549 cells when HIF-1α signaling was ablated (Fig. 6F).

HIF-1α promotes the growth and survival of LKB1-deficient cells under conditions of nutrient limitation. Data presented in Figures 1 through 3 indicate that loss of LKB1 promotes increased nutrient acquisition and processing, and ultimately increased cell growth. Given the importance of HIF-1α in directing metabolism and bioenergetics in the absence of LKB1, we next assessed the requirement of HIF-1α in regulating the growth and survival of LKB1-deficient tumor cells. A549 cells expressing control or HIF-1α shRNAs were grown under full (25 mM) or low (0.04 mM) glucose conditions, and cell counts measured over 72 hours. A549 cells lacking HIF-1α displayed a slight reduction in proliferative rate compared to control cells under full glucose conditions (Fig. 7A, left panel). However, under low glucose conditions, the proliferative capacity of A549 cells expressing HIF-1α shRNA was significantly impaired (Fig. 7A, right panel).

To further assess the dependence of A549 cells on HIF-1α for cell growth, we measured the proliferation of A549/Vec or A549/shHIF-1α cells under low glucose conditions along with

serum starvation and/or hypoxia (1% O_2). A549 cells cultured under low glucose displayed considerable blocks in cell growth when serum or oxygen were limiting (Fig. S5A). Interestingly, A549 cells lacking HIF-1α displayed increased sensitivity to combined glucose and serum starvation, but not glucose starvation combined with hypoxia (Fig. S5A). In addition, A549 cells expressing HIF-1α shRNA displayed reduced viability under glucose and glutamine withdrawal relative to A549 cells expressing control shRNA (Fig. 7B). A549 cells lacking HIF-1α displayed increased caspase-3 activation at low glucose concentrations (Fig. 7C), indicating the induction of apoptosis in these cells.

To investigate whether the increased apoptosis of A549 cells lacking HIF-1α was due to defects in cellular bioenergetics, we characterized the bioenergetic profile of LKB1-deficient tumor cells lacking HIF-1α. A549 cells with reduced HIF-1α displayed a modest increase in oxygen consumption under low glucose conditions (Fig. S5B). However, these cells also displayed a 50% reduction in spare respiratory capacity (SRC) (Fig. S5C), suggesting reduced mitochondrial fitness in these cells (Nicholls, 2009). We also measured the ATP content of A549 cells with or without HIF-1α expression (Fig 7D). Under basal growth conditions (25 mM glucose, 4 mM glutamine) silencing HIF-1α had little effect on cellular ATP levels. However, following overnight glucose withdrawal, A549 cells expressing HIF-1α shRNA displayed a significant drop in cellular ATP levels relative to control tumor cells. While glutamine starvation also stimulated a decrease in cellular ATP levels, this drop appeared to be HIF-1α-independent (Fig. 7D). Together these data suggest that LKB1-null tumor cells require HIF-1α to maintain mitochondrial respiratory capacity, ATP levels, and cell viability in response to nutrient limitation.

Discussion

In this study we provide evidence that the tumor suppressor LKB1 promotes a metabolic checkpoint that regulates carbon utilization in proliferating cells. To date, the main link between LKB1 and tumor metabolism has been the observation of increased FDG-PET signal *in vivo* in benign LKB1+/- tumors (Shackelford et al., 2009). Here we show that silencing LKB1 is sufficient to promote both aerobic glycolysis and glutaminolysis (Figs. 1, 2), and this increase in glucose and glutamine metabolism fuels cell growth and lipid biosynthesis in cells lacking LKB1 (Fig. 3). The pro-growth metabolic program induced by LKB1 loss is mediated by the transcription factor HIF-1α, which displays increased protein stabilization under normoxia when LKB1 is deleted (Fig. 4). We find that the metabolic and biosynthetic phenotypes of LKB1-null cells are dependent upon HIF-1α (Fig. 6), and that targeting HIF-1α impairs the growth and survival of LKB1-deficient tumor cells (Fig. 7). This work highlights the existence of a metabolic circuit regulated by HIF-1α that coordinates cellular bioenergetics when LKB1 activity is suppressed.

Our data suggest that LKB1 loss disrupts normal metabolic homeostasis in cells, which paradoxically has a net positive effect on cell growth and proliferation. Glucose-derived citrate is a key intermediate in lipid biosynthesis (Hatzivassiliou et al., 2005). Flux of glucose-derived pyruvate into citrate is enhanced by LKB1 loss, as is glucose-dependent lipid biosynthesis and overall lipid content. This occurs despite HIF-1α-dependent elevation of PDK1, which has been shown to negatively regulate pyruvate entry into the mitochondrion under hypoxic conditions (Kim et al., 2006; Papandreou et al., 2006). Interestingly, while glutaminolysis is increased in LKB1-deficient cells, LKB1 loss did not appear to promote increased glutamine-dependent lipid biosynthesis or the differential use of glutamine in pathways such as reductive carboxylation of

alpha-ketoglutarate (Metallo et al., 2012; Mullen et al., 2012; Wise et al., 2011). LKB1-null cells appear to use glutamine as an anaplerotic substrate to support mitochondrial metabolism.

Our work here identifies HIF-1α as a key mediator of the metabolic transformation triggered by LKB1 loss. Using multiple cell systems we demonstrate that acute downregulation of LKB1 is sufficient to increase HIF-1α protein levels under normoxic conditions. Reducing HIF-1α levels reverses the metabolic effects triggered by LKB1 loss in cells (Fig. 6). We show here that targeting the mTORC1 complex, either by using rapamycin or through Raptor knockdown, reduces HIF-1α protein expression in LKB1-null cells, suggesting that deregulated mTORC1 activity links LKB1 loss to elevated HIF-1α activity. However, we also demonstrate that elevated ROS levels may contribute to HIF-1α protein expression in LKB1-null cells. LKB1 loss has previously been reported to promote enhanced levels of intracellular ROS in A549 cells (Shackelford et al., 2013). Here we observe a similar trend in MEFs lacking LKB1. Reducing ROS levels with NAC abrogated the increase in HIF-1α levels in LKB1-null cells. It is unclear whether these two systems (mTORC1 and ROS) work separately or in concert to affect HIF-1α protein expression. One possibility is that increased metabolic activity of LKB1-deficient cells is driven by mTORC1, and that mitochondrial ROS generated as a consequence of this increased metabolic activity promotes HIF-1α expression, thus reinforcing the pro-growth metabolic program induced by LKB1 deletion.

Disruption of the downstream LKB1 effectors AMPK (Faubert et al., 2013) or TSC2 (Brugarolas et al., 2003) promotes elevated mTORC1 activity and increased HIF-1α protein levels under normoxia. We have recently demonstrated that loss of AMPK activity is sufficient to promote the Warburg effect in tumor cells (Faubert et al., 2013), suggesting that LKB1 may be linked to metabolic control through its upstream regulation of AMPK (Shackelford and Shaw,

2009). However, LKB1 and AMPK appear to influence HIF-1α protein expression through different mechanisms. Silencing LKB1 promotes both increased transcription and translation of HIF-1α, events which are sensitive to mTORC1 inhibition. In contrast, loss of AMPK results in increased HIF-1α protein levels with no discernable changes in mRNA levels (Faubert et al., 2013). Moreover, mTORC1 inhibition has little effect on HIF-1α protein levels when AMPK is silenced (Faubert et al., 2013). These data suggest the existence of both AMPK-dependent and -independent mechanisms linking LKB1 to HIF-1α and metabolic reprogramming.

Our observation that LKB1 loss promotes a pro-growth metabolic profile in tumor cells raises the prospect that there may be selective pressure for tumors to lose or silence LKB1-AMPK signaling (Hardie and Alessi, 2013), as suggested by the frequent inactivation of LKB1 in NSCLC (Sanchez-Cespedes et al., 2002). We speculate that the metabolic effects of LKB1 inactivating mutations may also synergize with other genetic lesions, ultimately favoring the selection of tumor cells with distinct metabolic advantage. For example, oncogenic K-ras mutations (G12D) in pancreatic ductal carcinoma have been shown to re-direct glucose metabolism to fuel increased pentose phosphate shunt activity and ribose biosynthesis (Ying et al., 2012). Interestingly, co-mutation of LKB1 and K-ras is frequently observed in NSCLC (Makowski and Hayes, 2008), and LKB1 inactivating mutations synergize with oncogenic K-ras to accelerate tumorigenesis in mouse models of lung cancer (Ji et al., 2007). Thus, LKB1 loss may augment the metabolic activities of other driver mutations in cancer by enhancing their ability to promote nutrient acquisition and utilization by tumor cells. However, while loss of LKB1 reprograms cancer cell metabolism, it also confers a dependence on HIF-1α, rendering LKB1-null tumor cells more susceptible to apoptosis under poor nutrient conditions. This raises the possibility of targeting HIF-1α for synthetic lethality in LKB1-deficient tumors. Given that

mTORC1 inhibition affects both aberrant mTORC1 signaling and HIF-1α expression in LKB1-deficient cancer cells, mTORC1-targeting compounds may be particularly effective for treating tumors with somatic LKB1 mutations or cancers associated with PJS.

Materials and Methods

Cell Lines, DNA Constructs, and Cell Culture

Primary mouse embryonic fibroblasts (MEFs) conditional for *stk11* (*LKB1-*$^{fl/fl}$) were generated by timed mating and immortalized with SV40 Large T Antigen as previously described (Jones et al., 2005). A549 cells have been previously described (Shackelford et al., 2013). DNA plasmids MigCD8t, pKD-HIF-1α hp, and LMP-based shRNAs against mouse and human LKB1 have been described previously (Bungard et al., 2010; Jones et al., 2005; Lum et al., 2007). Transduction of cell lines with high-titre retrovirus was conducted as previously described (Jones et al., 2005). Retrovirus-infected cells were cultured in 2 μg/ml puromycin and/or sorted 7 days post-infection by flow cytometry (for GFP or CD8t-expressing cells). *LKB1*$^{fl/fl}$ MEFs were transduced with either MiCD8t for control virus or MiCD8t-Cre to delete *stk11*-floxed alleles. *LKB1*$^{fl/fl}$ MEFs and A549 NSCLC cells were also transduced with pKD-HIF-1αhp or control retrovirus. For siRNA transfections, cells were subjected to two rounds of reverse transfection with pooled siRNAs against HIF-1α (Hatzivassiliou et al., 2005).

Determination of Cell Proliferation, Apoptosis Assays, and Cell Size

Growth curves for all cell lines was determined by cell counting using trypan blue exclusion, and a TC10 Automated Cell Counter (BioRad). Apoptosis assays were performed by washing cells twice with PBS and incubating in glucose- or glutamine- free media, containing 10% dialyzed FCS. Cells were incubated for times indicated, and apoptosis measurements were performed

using propidium iodide (PI) staining, and analyzed on FACS. Size of viable cells was measured by flow cytometry and quantified as the mean fluorescence intensity for FSC. Measurement of reactive oxygen species (ROS) was performed by incubating cells for 30 minutes with 2',7' – dichlorofluorescein diacetate (DCF-DA), followed by quantification using flow cytometry.. All flow cytometry was conducted using BD FACSCalibur (BD Biosciences, San Diego, CA) or Gallios (Beckman Coulter, Fullerton, CA) flow cytometers and analyzed with FlowJo software (Tree Star, Ashland, OR).

Western Blots

Cells were lysed in modified CHAPS buffer (10mM Tris-HCl, 1mM $MgCl_2$, 1mM EGTA, 0.5mM CHAPS, 10% glycerol, 5mM NaF) supplemented with the following protease additives: protease and phosphatase tablets (Roche), DTT (1 μg/ml), and benzamidine (1 μg/ml). Cleared lysates were resolved by SDS-PAGE, transferred to nitrocellulose, and incubated with primary antibodies. Primary antibodies to LKB1 (total), p70 S6-kinase (pT389-specific and total), S6 ribosomal protein (pS235/236-specific and total), 4E-BP1 (pT37/46-specific and total), LDHA, PDK1, Aldolase, and Actin, as well as HRP-conjugated anti-rabbit and anti-mouse secondary antibodies were obtained from Cell Signaling Technology (Danvers, MA). Anti-HIF-1α antibodies were from Cayman Chemical (Baton Rouge, LO). LKB1 antibodies were from Santa Cruz Biotechnologies (Santa Cruz, CA).

Quantitative Real-Time PCR

Total mRNA was isolated from cells using Trizol (Invitrogen), and cDNA was synthesized total RNA using the Superscript® VILO™ cDNA Synthesis Kit (Invitrogen). Quantitative PCR was

performed using SYBR Green qPCR SuperMix (Invitrogen) and an Mx3005 qPCR machine (Agilent) using primers against *hif1a*, *aldoA, ldha, pdk1* and *actin.* All samples were normalized to β-actin mRNA levels. Primer sequences have been previously described (Faubert et al., 2013).

Seahorse XF24 Respirometry

Respirometry (oxygen consumption rate, OCR) and the extracellular acidification rate (ECAR) of cells were measured using an XF24 Extracellular Flux Analyzer (Seahorse Bioscience, Billerica, MA) as previously described (Faubert et al., 2013). In brief, cells were plated at $5x10^5$/well in 625µl non-buffered DMEM containing 25mM glucose and 2mM glutamine. Cells were incubated in a CO_2-free incubator at 37°C for 1 hr to allow for temperature and pH equilibration prior to loading into the XF24 apparatus. XF assays consisted of sequential mix (3 min), pause (3 min), and measurement (5 min) cycles, allowing for determination of OCR/ECAR every 10 minutes.

Metabolic Assays

Glucose, lactate, and glutamine levels in culture medium were measured using a Flex Bioanalyzer (NOVA Biomedical, Waltham, MA). Glucose-derived lipid biosynthesis was determined by culturing cells in medium containing ^{14}C-glucose or ^{14}C-glutamine (Perkin Elmer, Waltham, MA) for 3 days, and extracted lipids using a 1:1:1 Water/Methanol/Chloroform extraction procedure (Folch et al., 1951) Following extraction, the organic layer was isolated, dried via N_2 stream, re-suspended in methanol, and incorporated radioactivity measured using a MicroBeta Liquid Scintillation Counter (Perkin Elmer, Waltham, MA).

GC-MS Analysis of ^{13}C Metabolites or Free Fatty Acids

For GC-MS analysis, protocols have been outlined previously (Faubert et al., 2013). Briefly, cells (2 – 5 x 10^6/10 cm dish) were cultured for three days and were lysed using ice-cold 80% methanol followed by sonication. For isotopomer labeling experiments, cells were treated with U-^{13}C-glucose or -glutamine (Cambridge Isotopes) (Mullen et al., 2012), and metabolites from tissue culture cells were extracted as described previously (Xu et al., 2011a).

For free fatty acid profiles, cells were grown for 72 hours under standard growth conditions. Triglycerides and other lipids were extracted using a modified Folch method (Folch et al., 1951) substituting methylene chloride for chloroform. Following extraction, the organic layer was isolated, dried in a warm N_2 stream and saponified in sodium hydroxide overnight at 60^oC. The free fatty acids were re-extracted and dried, derivatized as TBDMS esters and analyzed on GC-MS.

Growth assays

For analysis of adherent cell growth, cells were seeded (8000 cells/well) in a 96 well plate in DMEM containing 10% (v/v) FBS and penicillin/streptomycin. After 24h medium was replaced with fresh DMEM containing 25 mM or 0.04 mM glucose. Cells were fixed with 100µl 4% paraformaldehyde at 0, 24, 48 and 72h. Plates were incubated at 4˚C for 20 min. Cells were washed 2 x 5 min in 200 µl PBS and 100 µl of crystal violet solution (0.05% (w/v) crystal violet and 20% (v/v) 95% ethanol) was added to each well. Plates were incubated at room temperature for 30 min. Cells were washed 3 x 5 min in 200 µl PBS and solubilized on a plate shaker for 1 h in 100 µl of 1% SDS in PBS. The plates were analyzed at 595nm on a Molecular Devices Spectramax plate reader. Hypoxia experiments were conducted by incubating cells at 1% O_2, in a

Hera Cell 150 incubator (Mandel).

Statistical Analysis

Statistics were determined using paired Student's t test, ANOVA, or Log-rank (Mantel-Cox) test using Prism software (GraphPad). Data are calculated as the mean ± SEM unless otherwise indicated. Statistical significance is represented in figures by: *, $p<0.05$; **, $p<0.01$; ***, $p<0.001$

Acknowledgements

We acknowledge Ralph DeBerardinis, Arnim Pause, and members of the Jones Lab for critical reading of this manuscript. We acknowledge Marie-Claude Gingras, as well as Gäelle Bridon and Luc Choinière of the GCRC Metabolomics Core Facility (McGill University) for technical assistance. B.F. was funded by a fellowship from the Canadian Institutes of Health Research (CIHR). T.G. was funded by the McGill Integrated Cancer Research Training Program (MICRTP). This work was supported by grants to R.G.J. from the CIHR (MOP-93799), Canadian Cancer Society (2010-700586), and Terry Fox Research Foundation (TEF-116128).

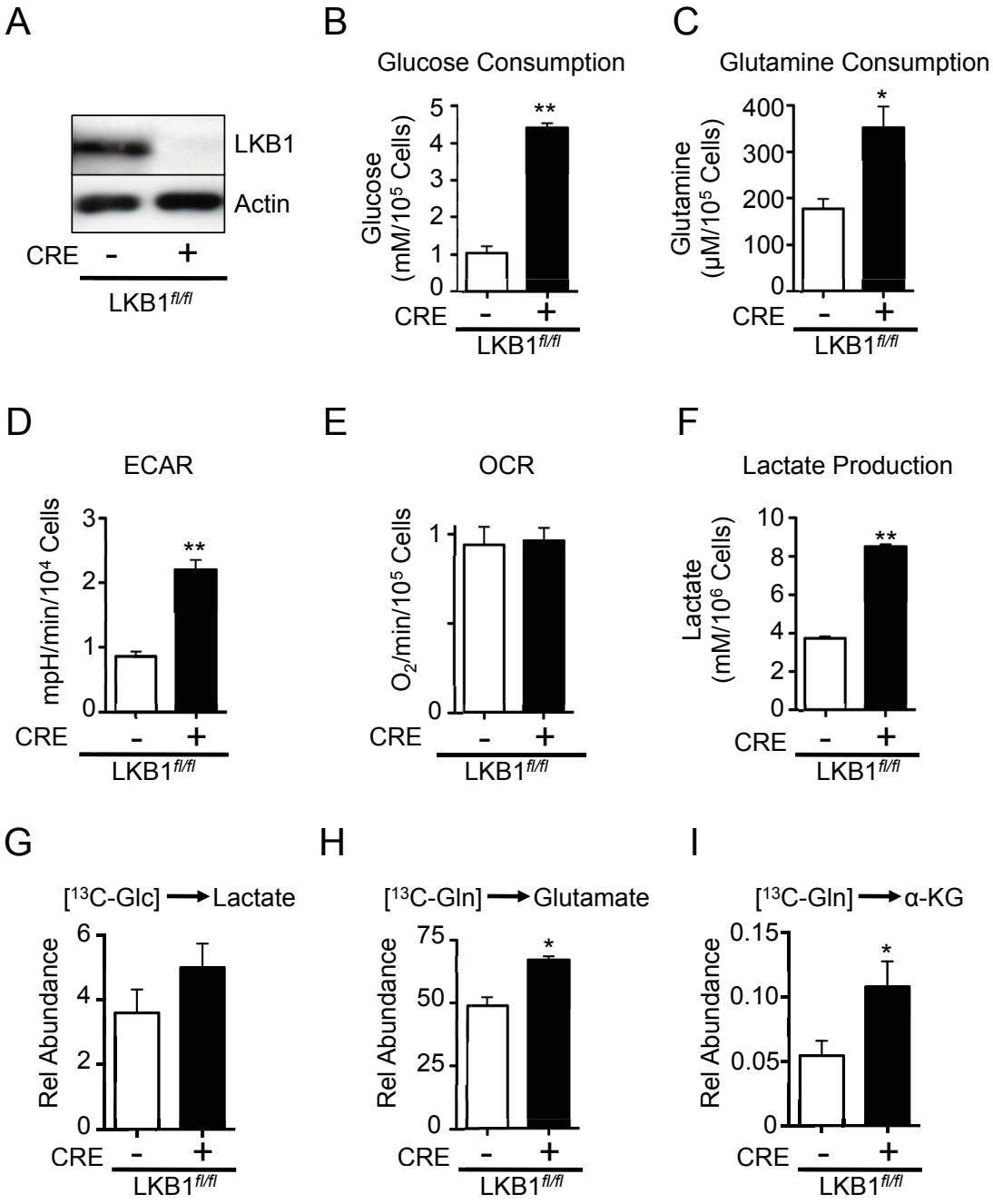
A
LKB1
Actin
CRE - +
LKB1fl/fl
B
Glucose Consumption
Glucose (mM/10^5 Cells)
**
CRE - +
LKB1fl/fl
C
Glutamine Consumption
Glutamine (μM/10^5 Cells)
*
CRE - +
LKB1fl/fl
D
ECAR
mpH/min/10^4 Cells
**
CRE - +
LKB1fl/fl
E
OCR
O2/min/10^5 Cells
CRE - +
LKB1fl/fl
F
Lactate Production
Lactate (mM/10^6 Cells)
**
CRE - +
LKB1fl/fl
G
[13C-Glc] → Lactate
Rel Abundance
CRE - +
LKB1fl/fl
H
[13C-Gln] → Glutamate
Rel Abundance
*
CRE - +
LKB1fl/fl
I
[13C-Gln] → α-KG
Rel Abundance
*
CRE - +
LKB1fl/fl

Fig. 1. Loss of LKB1 promotes enhanced glucose and glutamine metabolism. A) LKB1 immunoblot on lysates from LKB1$^{fl/fl}$ MEFs transduced with control retrovirus (Cre -) or a retrovirus expressing Cre recombinase (Cre +). (B-C) Glucose and glutamine consumption by LKB1-deficient MEFs. LKB1$^{fl/fl}$ MEFs expressing empty vector (open bar) or Cre recombinase (closed bar) were grown for 72 hours, and glucose consumption (B) and glutamine consumption (C) were determined by enzymatic assay. D-E) ECAR (D) and OCR (E) for LKB1$^{fl/fl}$ MEFs with (+) or without (-) Cre expression. F) Lactate production by LKB1-deficient MEFs. Cells were treated as in (B) and extracellular lactate in the culture medium was measured via enzymatic assay. G-I) Metabolic processing of glucose and glutamine by LKB1-null MEFs. LKB1-null (closed bar) or control (open bar) MEFs were pulsed with ^{13}C-glucose or ^{13}C-glutamine for 1 hour, and ^{13}C incorporation into lactate (G), glutamate (H), and α-ketoglutarate (I) was determined by GC-MS. *, $p<0.05$; **, $p<0.01$.

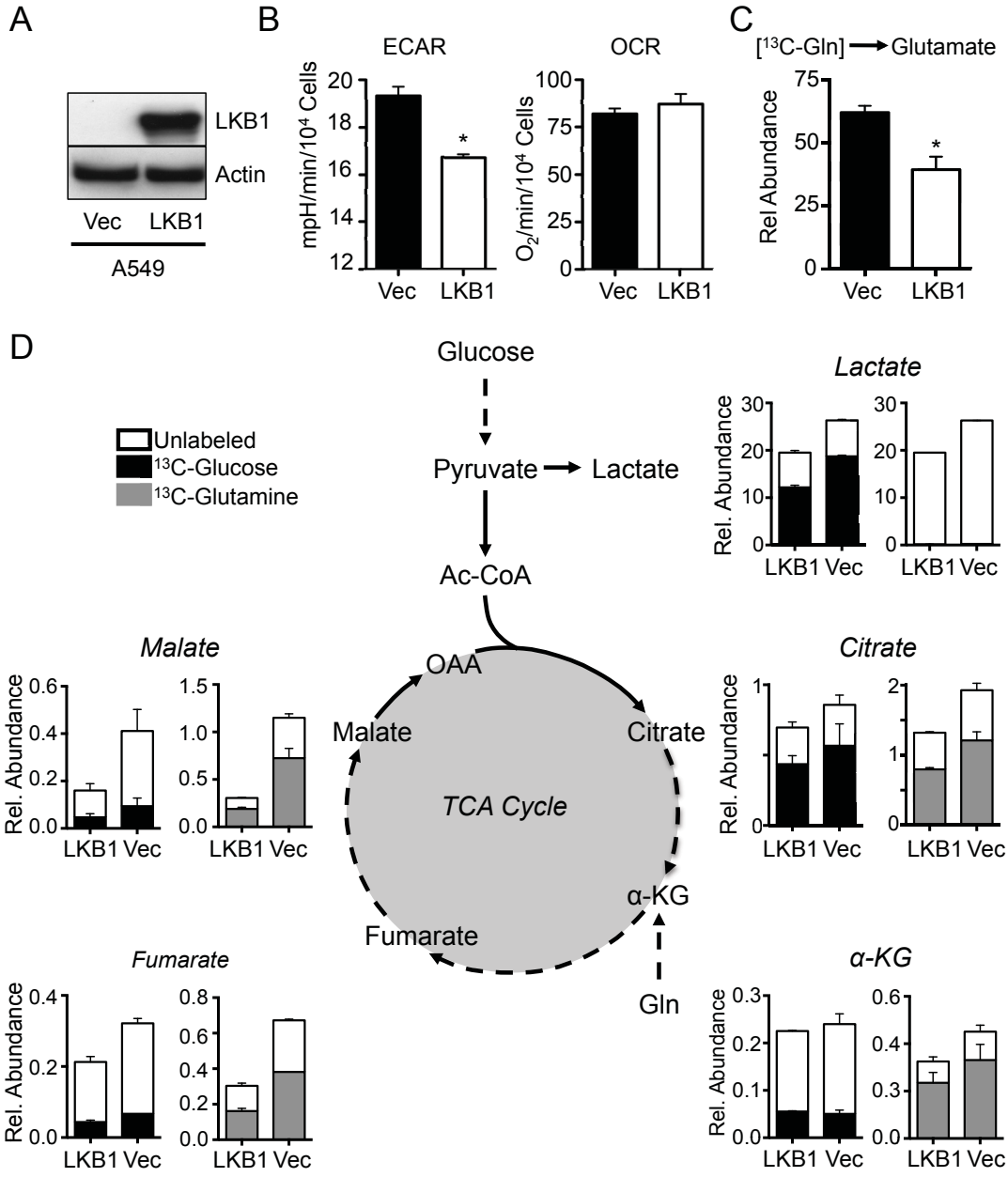
A
LKB1
Actin
Vec
LKB1
A549
B
ECAR
mpH/min/10^4 Cells
OCR
O2/min/10^4 Cells
Vec
LKB1
C
[13C-Gln] → Glutamate
Rel Abundance
D
Unlabeled
13C-Glucose
13C-Glutamine
Glucose
Pyruvate
Lactate
Ac-CoA
OAA
Citrate
α-KG
Fumarate
Malate
TCA Cycle
Gln
Lactate
Malate
Citrate
Fumarate
α-KG
Rel. Abundance
LKB1 Vec

Fig. 2. LKB1-deficient tumor cells display enhanced glycolytic and TCA cycle flux. A) LKB1 immunoblot on lysates from A549 cells transduced with empty vector (Ctl) or LKB1 cDNA. B) ECAR and OCR of A549 cells expressing empty vector (closed bar) or LKB1 cDNA (open bar). C) Intracellular glutamate levels derived from ^{13}C-glutamine in A549 cells expressing empty vector (Vec, closed bar) or LKB1 (LKB1, open bar) as measured by GC-MS. D) Metabolic flux analysis of LKB1-deficient A549 cells. A549 cells expressing empty vector (Vec) or LKB1 cDNA (LKB1) were pulsed with ^{13}C-glucose or ^{13}C-glutamine for 1 hour, and ^{13}C incorporation into lactate and TCA cycle metabolites were determined by GC-MS. Relative incorporation of ^{13}C into total metabolite pools are indicated by shaded bars for glucose (black) and glutamine (grey). Metabolite abundance is expressed relative to basal levels in A549/LKB1 cells. *, $p<0.05$.

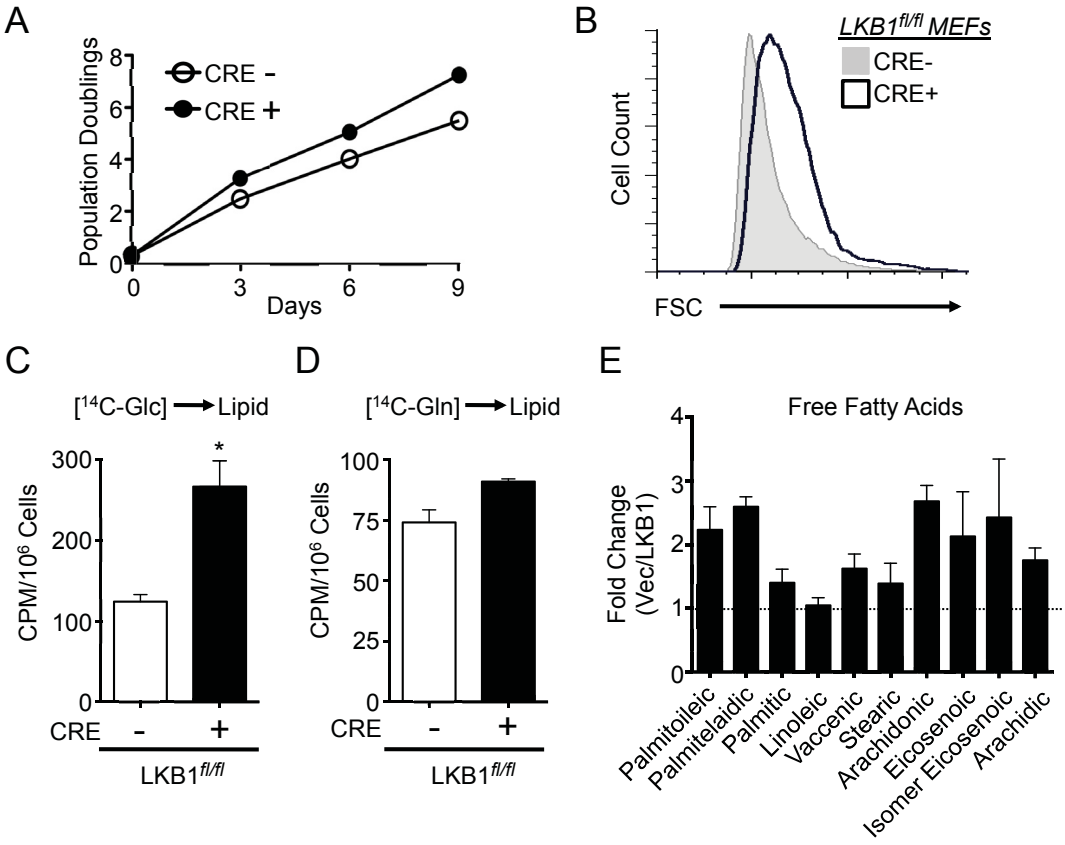
A
Population Doublings
CRE -
CRE +
Days
B
LKB1fl/fl MEFs
CRE-
CRE+
Cell Count
FSC
C
[14C-Glc] → Lipid
CPM/10^6 Cells
CRE
LKB1fl/fl
D
[14C-Gln] → Lipid
CPM/10^6 Cells
CRE
LKB1fl/fl
E
Free Fatty Acids
Fold Change (Vec/LKB1)
Palmitoileic
Palmitelaidic
Palmitic
Linoleic
Vaccenic
Stearic
Arachidonic
Eicosenoic
Isomer Eicosenoic
Arachidic

Fig. 3. LKB1-null cells display enhanced growth and biosynthetic capacity. A) Growth curve of LKB1$^{fl/fl}$ MEFs expressing empty vector (CRE-, open circle) or Cre recombinase (CRE+, closed circle) following a 3T3 passage protocol. B) Size of control (Cre-, grey histogram) or LKB1-deficient (Cre+, open histogram) MEFs as determined by forward scatter (FSC) of cells via flow cytometry. C-D) Glucose- and glutamine-dependent lipid biosynthesis by LKB-null MEFs. Control (Cre-, open bar) or LKB1-null (Cre+, closed bar) MEFs were incubated with uniformly labeled ^{14}C-glucose (C) or ^{14}C-glutamine (D) for 72 hours, and radioactive counts in extracted lipids measured. Data are expressed as CPM per 10^6 cells (mean ± SEM) for samples in triplicate. E) Free fatty acid (FFA) levels in LKB1-null cancer cells. FFAs in cell extracts from A549/Vec or A549/LKB1 cells were measured by GC-MS following 3 days of growth. Data are expressed as the ratio of FFA species in A549/Vec to A549/LKB1 cells. *, $p<0.05$.

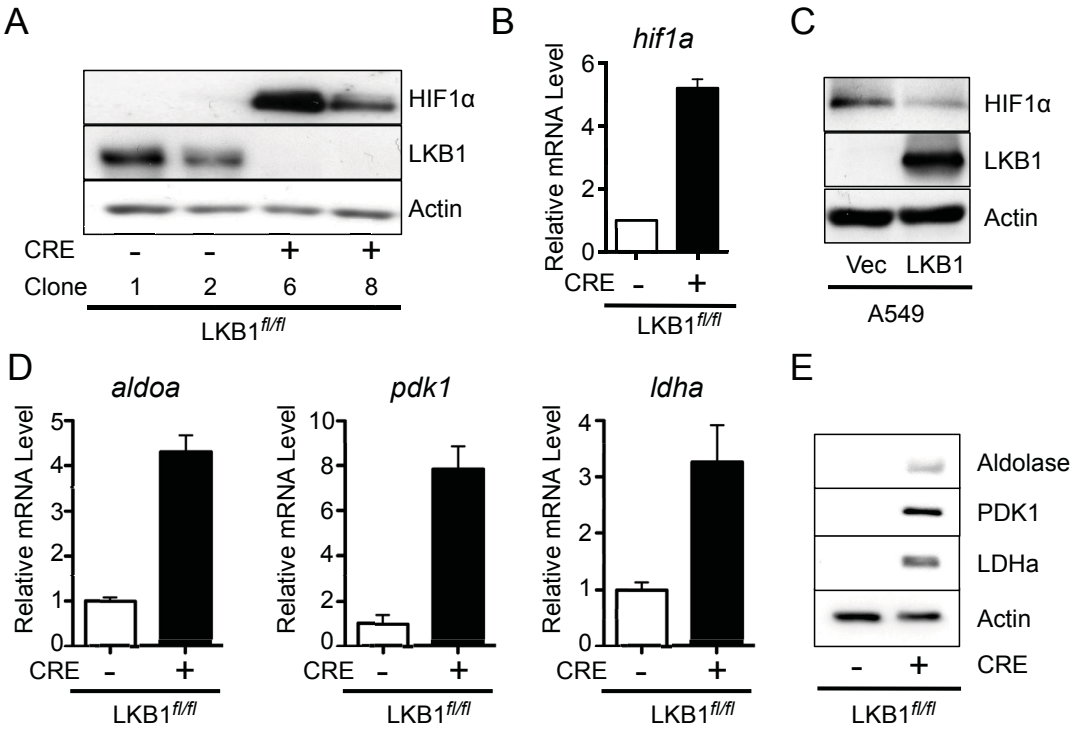
A
HIF1α
LKB1
Actin
CRE - - + +
Clone 1 2 6 8
LKB1fl/fl
B
hif1a
Relative mRNA Level
0 2 4 6
CRE - +
LKB1fl/fl
C
HIF1α
LKB1
Actin
Vec LKB1
A549
D
aldoa
pdk1
ldha
Relative mRNA Level
CRE - +
LKB1fl/fl
E
Aldolase
PDK1
LDHa
Actin
- + CRE
LKB1fl/fl

Fig. 4. LKB1 loss promotes HIF-1α protein expression under normoxic conditions. A) Immunoblot for HIF-1α protein expression in whole cell lysates from control (Cre-) or LKB1-null (Cre+) MEFs grown under 20% O_2. B) Relative expression of *hif1a* mRNA by control (Cre-, open bar) or LKB1-null (Cre+, closed bar) MEFs as determined by qPCR. Data were expressed relative to *actin* mRNA levels for triplicate samples and normalized relative to control (Cre-) cells. C) Immunoblot of HIF-1α protein in lysates from A549/Vec or A549/LKB1 cells grown under 20% O_2. D) Relative expression of *aldoa*, *ldha*, and *pdk1* mRNA levels in control (Cre-, open bar) or LKB1-null (Cre+, closed bar) MEFs as determined by qPCR. E) Immunoblot for Aldolase, PDK1, and LDHA expression in lysates from cells as in (D).

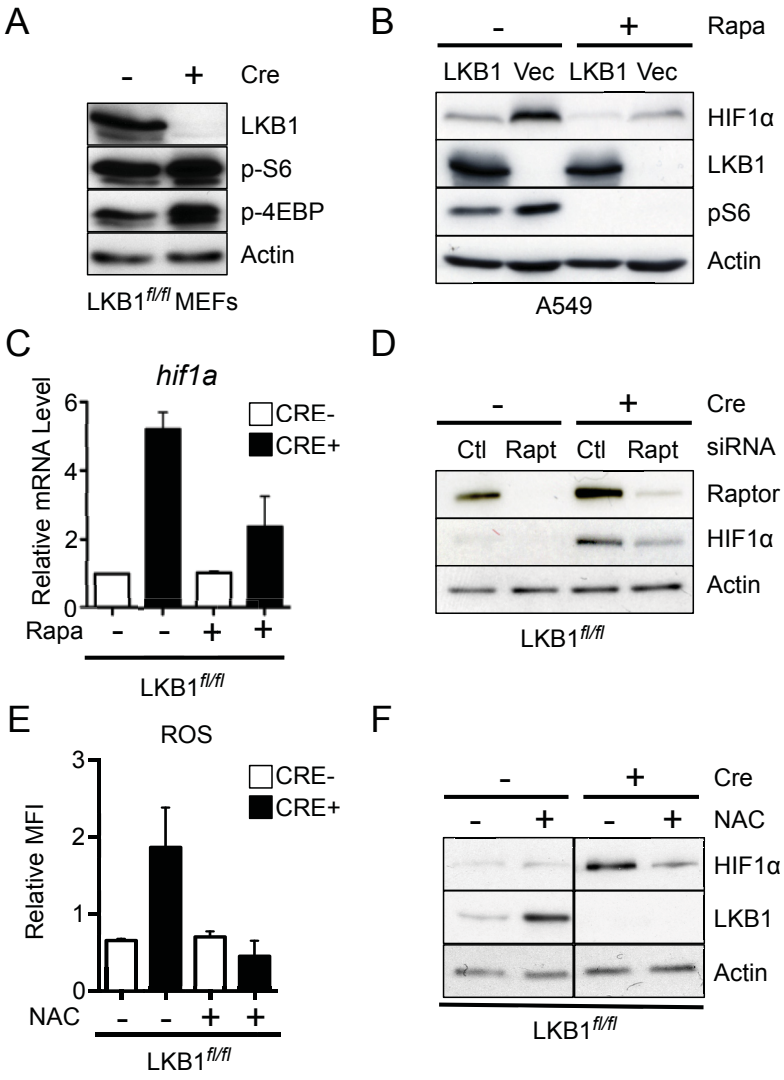
A
- + Cre
LKB1
p-S6
p-4EBP
Actin
LKB1fl/fl MEFs
B
- + Rapa
LKB1 Vec LKB1 Vec
HIF1α
LKB1
pS6
Actin
A549
C
hif1a
Relative mRNA Level
6
4
2
0
CRE-
CRE+
Rapa - - + +
LKB1fl/fl
D
- + Cre
Ctl Rapt Ctl Rapt siRNA
Raptor
HIF1α
Actin
LKB1fl/fl
E
ROS
Relative MFI
3
2
1
0
CRE-
CRE+
NAC - - + +
LKB1fl/fl
F
- + Cre
- + - + NAC
HIF1α
LKB1
Actin
LKB1fl/fl

Fig. 5. LKB1-dependent HIF-1α expression is regulated by mTORC1 and ROS. A) Immunoblot for LKB1, pS6, p4EBP, and actin protein levels in whole cell lysates from control (Cre-) or LKB1-null (Cre+) MEFs. B) Immunoblot for HIF-1α protein levels in A549/Vec or A549/LKB1 cells cultured with (+) or without (-) 25 nM rapamycin for 24 hours prior to cell lysis. Levels of LKB1, pS6, and actin are shown. (C) Relative HIF-1α mRNA expression in MEFs cells from control (Cre-) or LKB1-deficient (Cre+) MEFs treated with 25 nM rapamycin or vehicle control for 24 hours. D) Immunoblot for Raptor and HIF-1α protein levels in whole cell lysates from control (Cre-) and LKB1-null (Cre+) MEFs treated with control (Ctl) or Raptor-specific (Rapt) siRNA. E) Relative mean fluorescence intensity (MFI) of DFC-DA staining in $LKB1^{fl/fl}$ cells with (+) or without (-) Cre expression. Cells were treated with or without 10mM N-acetyl cysteine (NAC) for 1 hour prior to ROS measurements. F) Representative immunoblot of HIF-1α protein expression for cells treated as in (E).

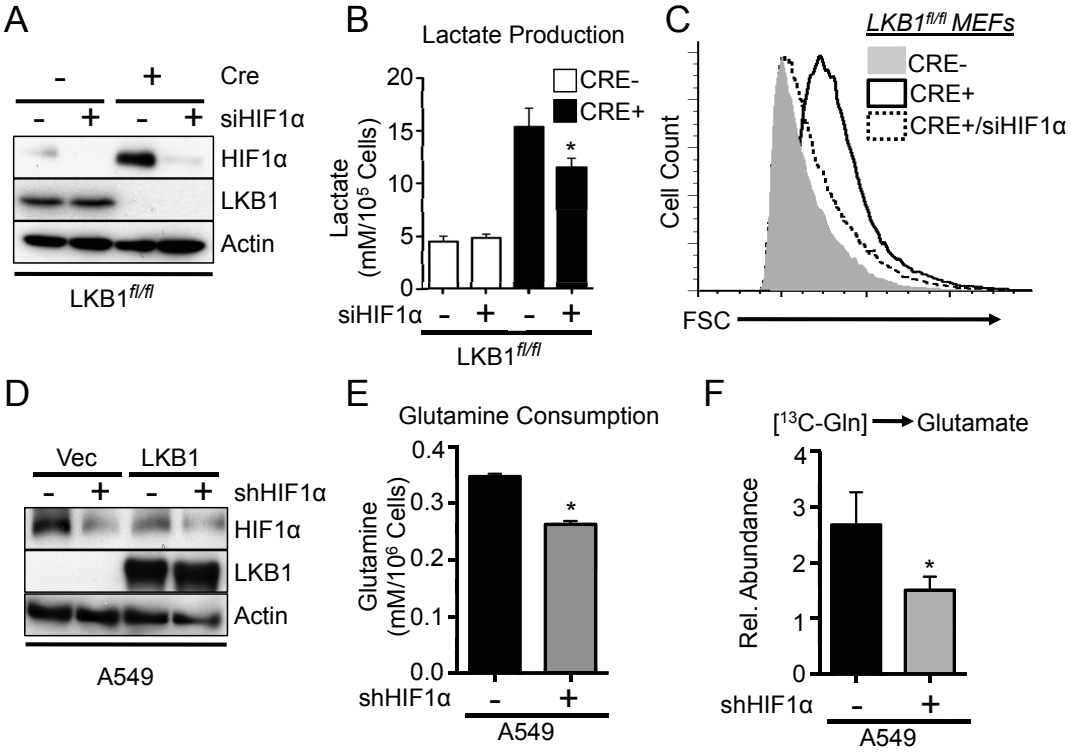
A
Cre
siHIF1α
HIF1α
LKB1
Actin
LKB1fl/fl
B
Lactate Production
CRE-
CRE+
Lactate (mM/10^5 Cells)
siHIF1α
LKB1fl/fl
C
LKB1fl/fl MEFs
CRE-
CRE+
CRE+/siHIF1α
Cell Count
FSC
D
Vec
LKB1
shHIF1α
HIF1α
LKB1
Actin
A549
E
Glutamine Consumption
Glutamine (mM/10^6 Cells)
shHIF1α
A549
F
[13C-Gln] → Glutamate
Rel. Abundance
shHIF1α
A549

Fig. 6. HIF-1α promotes the metabolic program induced by LKB1 loss. A) Immunoblot of HIF-1α protein expression in lysates from control (Cre-) or LKB1-deficient (Cre+) MEFs treated with control or HIF-1α siRNA. LKB1 and actin levels are shown. B) Lactate production by cells treated as in (A) after 72 hours of growth. C) Forward scatter (FSC) of control (grey histogram), LKB1-deficient (open histogram) or LKB1-deficient MEFs expressing HIF-1α siRNA (hatched histogram). D) Immunoblot of HIF-1α protein levels in lysates from A549/Vec or A549/LKB1 cells expressing control (-) or HIF-1α-specific (+) shRNAs. LKB1 and actin levels are shown. E) Glutamine consumption by A549 cells expressing control (black bar) or HIF-1α-specific (grey bar) shRNAs as determined by enzymatic assay. F) Glutamine-derived glutamate levels in A549 cells expressing control (-) or HIF-1α-specific (+) shRNA. ^{13}C incorporation into intracellular glutamate following 1h of culture with ^{13}C-glutamine was determined by GC-MS. *, $p<0.05$.

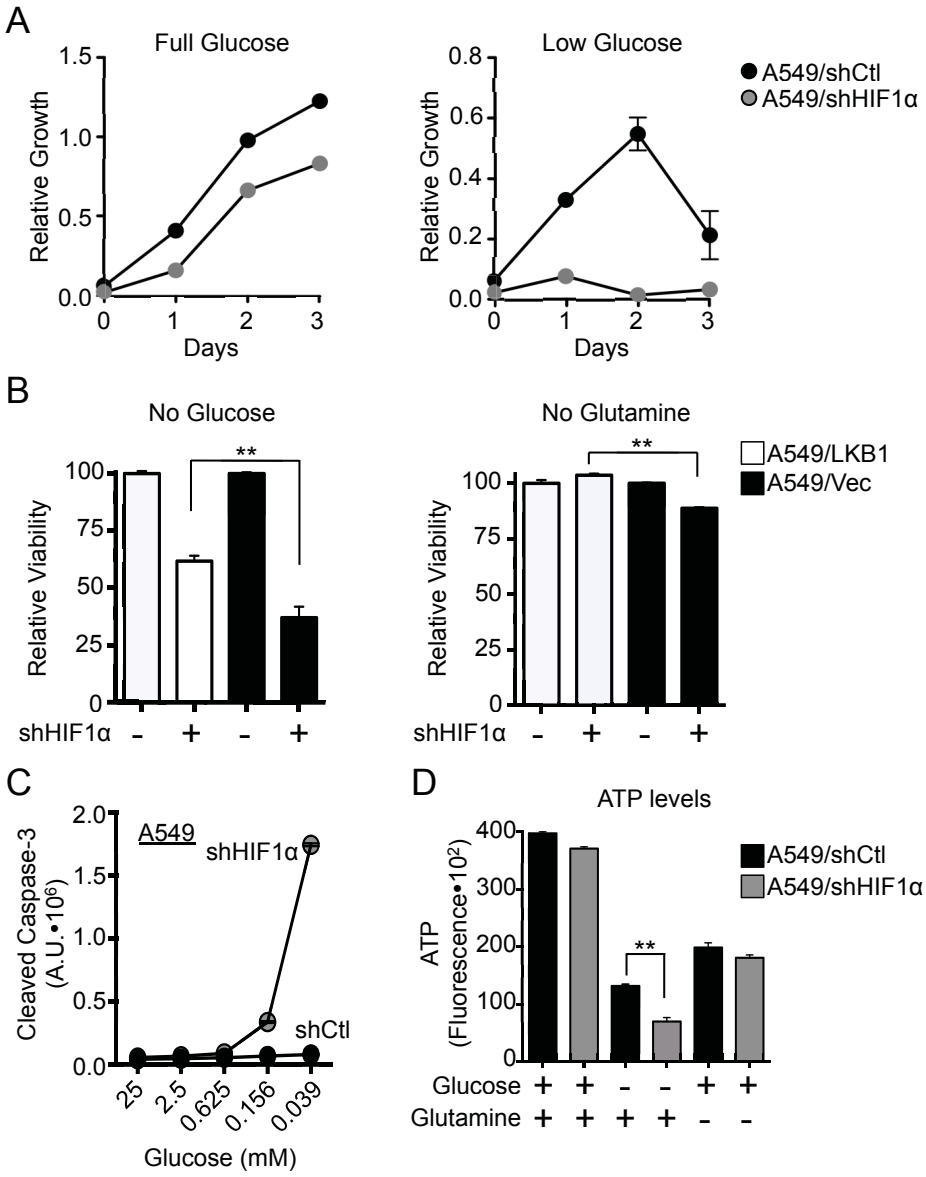
A
Full Glucose
Low Glucose
Relative Growth
Days
A549/shCtl
A549/shHIF1α
B
No Glucose
No Glutamine
Relative Viability
shHIF1α
A549/LKB1
A549/Vec
C
A549
shHIF1α
shCtl
Cleaved Caspase-3 (A.U.•10⁶)
Glucose (mM)
D
ATP levels
ATP (Fluorescence•10²)
Glucose
Glutamine

Fig. 7. HIF-1α is required for the growth and survival of LKB1-deficient cells in response to nutrient limitation. A) Growth curves of A549 cells expressing control (closed circle) or HIF-1α (grey circle) shRNA grown under full (25 mM) or low (0.4 mM) glucose conditions. B) Viability of A549/LKB1 (white bars) or A549/Vec (black bars) cells expressing control (-) or HIF-1α-specific (+) shRNA following culture in glucose- or glutamine-free media. Cell viability was measured after 48 hours by propidium iodide uptake. C) Caspase-3 activation in A549 cells expressing control (Vec, closed circles) or HIF-1α-specific (grey circles) shRNA following culture in decreasing concentrations of glucose. D) Relative ATP levels of A549 cells expressing control (black bars) or HIF-1α-specific (grey bars) shRNA following culture in glucose- or glutamine-free media. **, $p<0.01$.

Supplemental Information for:

Loss of the tumor suppressor LKB1 promotes metabolic reprogramming of cancer cells via HIF-1α

Brandon Faubert[1,2], Emma Vincent[1,2], Takla Griss[1,2], Bozena Samborska[1], Said Izreig[1,2], Rob Svensson[3], Orval A. Mamer[1,4], Daina Avizonis[1,4], David Shackelford[5], Reuben J. Shaw[3] and Russell G. Jones[1,2].

Supplemental Information Inventory

A

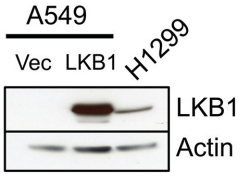
A549
Vec
LKB1
H1299
LKB1
Actin

B

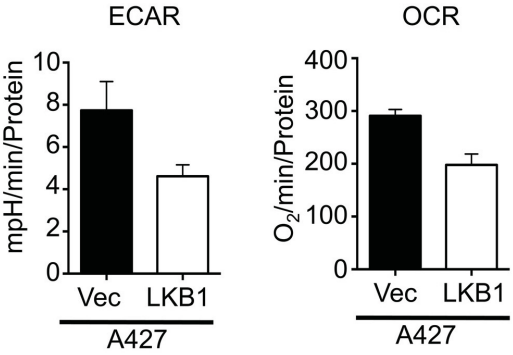
ECAR
mpH/min/Protein
10
8
6
4
2
0
Vec
LKB1
A427
OCR
O_2/min/Protein
400
300
200
100
0
Vec
LKB1
A427

Figure S1. Expression of LKB1 and metabolism of NSCLC cell lines.

A) LKB1 immunoblot on lysates from A549 cells transduced with empty vector (Vec) or LKB1 cDNA (LKB1), and H1299 cells. **B)** Basal extracellular acidification rate (ECAR) and oxygen consumption rate (OCR) for A427 cells expressing empty vector (Vec) or LKB1 cDNA (LKB1).

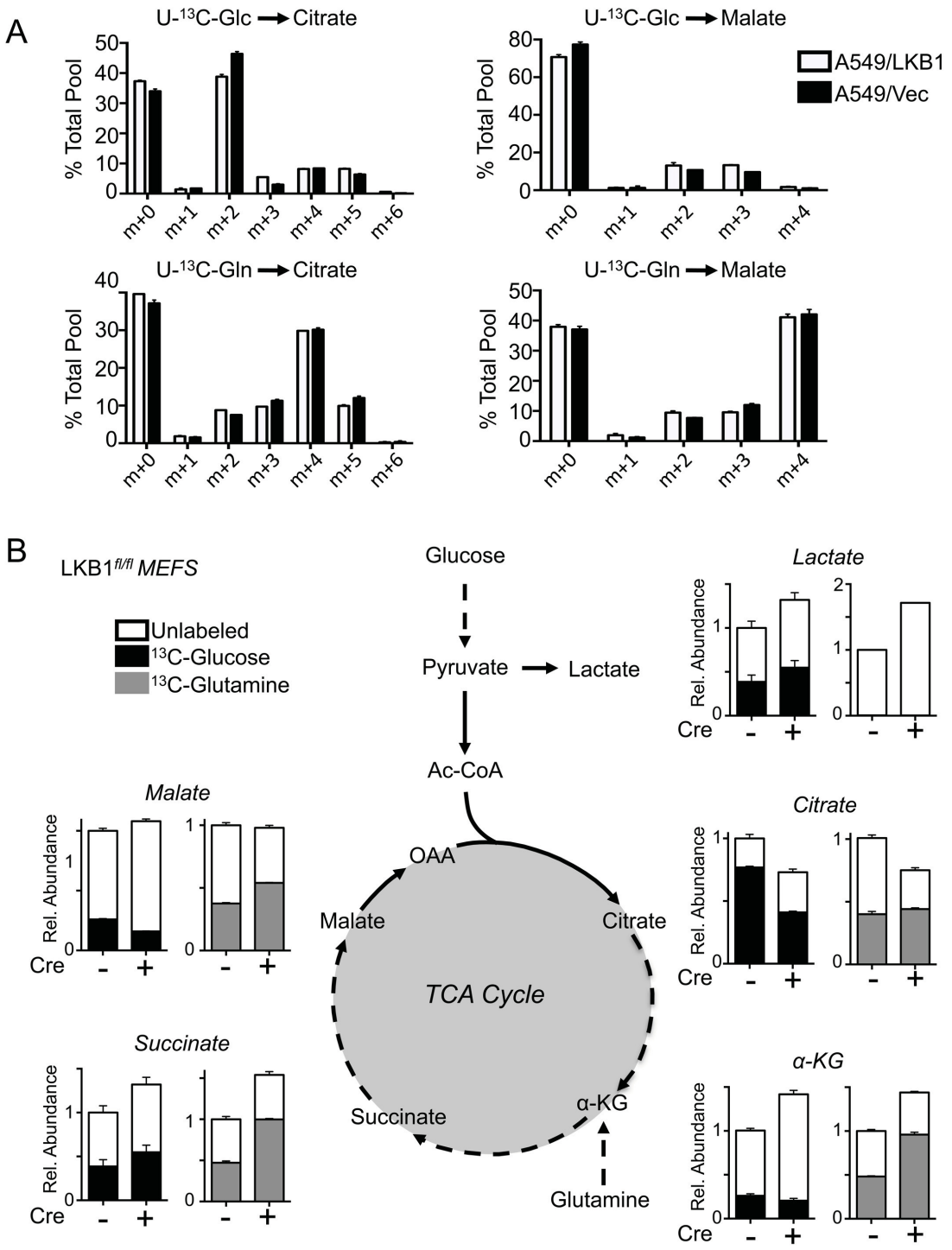
A
U-13C-Glc → Citrate
U-13C-Glc → Malate
U-13C-Gln → Citrate
U-13C-Gln → Malate
% Total Pool
m+0
m+1
m+2
m+3
m+4
m+5
m+6
A549/LKB1
A549/Vec
B
LKB1fl/fl MEFS
Unlabeled
13C-Glucose
13C-Glutamine
Glucose
Pyruvate
Lactate
Ac-CoA
OAA
Citrate
α-KG
Succinate
Malate
TCA Cycle
Glutamine
Lactate
Malate
Citrate
α-KG
Succinate
Rel. Abundance
Cre
-
+

Figure S2. LKB1-deficient cells display enhanced glycolytic and TCA cycle flux

A) Mass isotopomer profiles of A549 tumour cells with LKB1 re-expression (open bar) or lacking LKB1 (closed bar). Cells were pulsed with ^{13}C-labeled glucose (Glc) or glutamine (Gln) for one hour prior to metabolite extraction. Mass isotopes for citrate and malate are indicated. **B)** MEFs expressing LKB1 (Cre-) or deficient for LKB1 (Cre+) were pulsed with ^{13}C-glucose or ^{13}C-glutamine for 1 hour, and ^{13}C incorporation into lactate and TCA cycle metabolites was determined by GC-MS as in Figure 2. The relative incorporation of ^{13}C into total metabolite pools (lactate, citrate, α-ketoglutarate, succinate and malate) is indicated by shaded bars for glucose (black) and glutamine (grey). Metabolite abundance is expressed as the mean ± SD for triplicate samples, and expressed relative to basal levels in control (Cre-negative) cells.

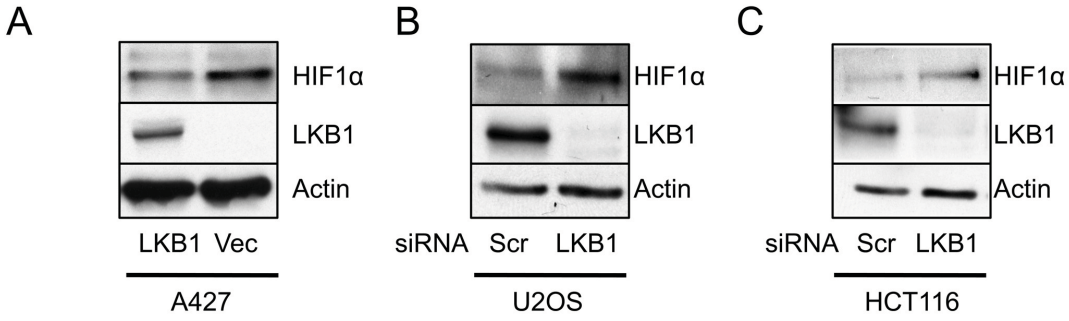
A
HIF1α
LKB1
Actin
LKB1 Vec
A427
B
HIF1α
LKB1
Actin
siRNA Scr LKB1
U2OS
C
HIF1α
LKB1
Actin
siRNA Scr LKB1
HCT116

Figure S3. Expression of HIF-1α protein levels in cell models of LKB1 deficiency.

A) Immunoblot for HIF-1α in A427 cells expressing empty vector (Vec) or LKB1 cDNA (LKB1). **B)** Immunoblot for HIF-1α in U20S cells transfected with 25nM scrambled (Scr) siRNA or siRNA targeting LKB1 (LKB1). A representative immunoblot is shown. **C)** Immunoblot for HIF-1α in HCT116 cells transfected with control (Scr) or LKB1-targeting (LKB1) siRNA.

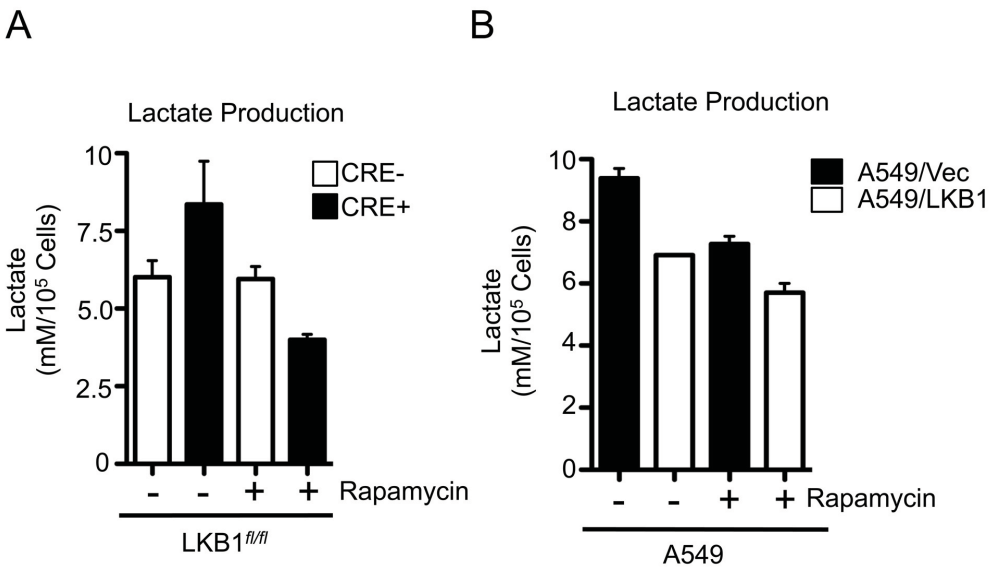
A
Lactate Production
Lactate (mM/10^5 Cells)
10
7.5
5.0
2.5
0
CRE-
CRE+
- - + + Rapamycin
LKB1fl/fl
B
Lactate Production
Lactate (mM/10^5 Cells)
10
8
6
4
2
0
A549/Vec
A549/LKB1
- - + + Rapamycin
A549

Figure S4. Rapamycin treatment of LKB1-null cells reduces lactate production.

MEFs expressing (Cre-) or lacking (Cre+) LKB1 expression **(A)** or A549 cells with (LKB1) or without (Vec) LKB1 re-expression **(B)** were treated for 24 hours with 25nM rapamycin, and lactate in the extracellular medium was measured via enzymatic assay. Lactate levels are expressed as the mean ± SD for triplicate samples.

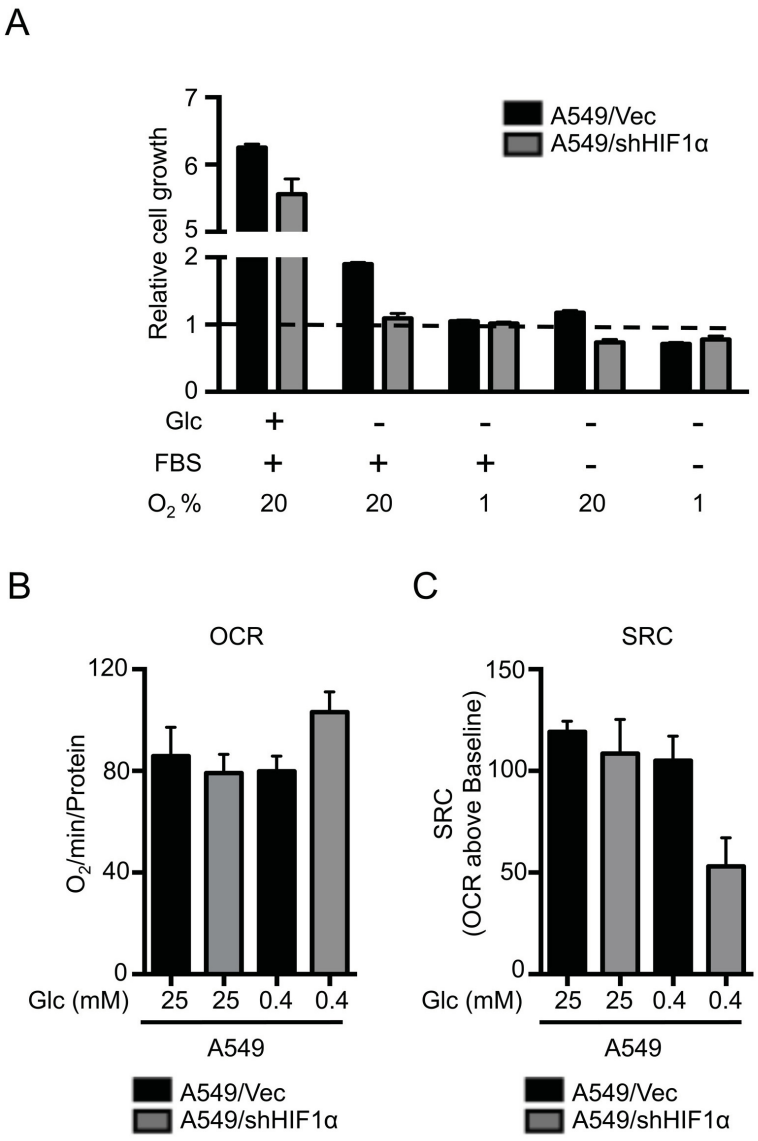
A
Relative cell growth
7
6
5
2
1
0
A549/Vec
A549/shHIF1α
Glc + - - - -
FBS + + + - -
O2 % 20 20 1 20 1
B
OCR
O2/min/Protein
120
80
40
0
Glc (mM) 25 25 0.4 0.4
A549
A549/Vec
A549/shHIF1α
C
SRC
SRC (OCR above Baseline)
150
100
50
0
Glc (mM) 25 25 0.4 0.4
A549
A549/Vec
A549/shHIF1α

Figure S5: A549 cells lacking HIF-1α expression display enhanced sensitivity to glucose and serum withdrawal. A) Growth curves of A549 cells expressing control (closed bar) or HIF-1α (grey bar) shRNAs, and grown under full (+, 25 mM) or no glucose (-, 0 mM) conditions. Cells were additionally cultured in the presence of absence of serum (FBS) or under normoxic (20% O_2) or hypoxic (1% O_2) conditions. **B)** Oxygen consumption rates of A549 cells expressing empty vector (Vec) or HIF-1α shRNA (shHIF-1α). Cells were grown under full glucose (25mM) or low glucose (0.4mM) conditions. **C)** Spare respiratory capacity (SRC) of cells treated as in (B).

Preface to Chapter 4

We and others (Shackelford et al., 2009) have demonstrated that cells lacking AMPK feature the normoxic stabilization of HIF-1α. However, the mechanism of stabilization had yet to be defined. The work in Chapter 2 showed no differences in transcription or translation of HIF-1α, and thus post-translational modifications were tested. Evidence first produced by Shackelford et al 2013 showed that HIF-1α stabilization in LKB1-null cells could occur due to increased levels of ROS. We were able to replicate this finding in Chapter 3 in LKB1-null cell lines. This prompted us to explore the possibility that AMPK may also be involved in the regulation of reactive oxygen species. Loss of AMPK would therefore result in aberrant levels of ROS, resulting in HIF-1α stabilization. In this work, we examined the role of mitochondrial ROS contributing to HIF-1a stabilization in the absence of AMPK.

Chapter 4

Regulation of mitochondrial ROS through an AMPK-dependent metabolic circuit

Brandon Faubert[1,2], Sylvia Andrzejewski[1,3], Eric Ma[1,2], Takla Griss[1,2], Julie St-Pierre[1,3], Russell G. Jones[1,2].

[1]Goodman Cancer Research Centre, McGill University, Montreal, QC, H3A 1A3, Canada; [2]Department of Physiology, McGill University, Montreal, QC, H3G 1Y6, Canada; [3]Department of Biochemistry, McGill University, Montreal, QC, H3G 1Y6,

Corresponding author: Russell G. Jones, Goodman Cancer Research Centre, Department of Physiology, McGill University, 3655 Promenade Sir William Osler, Room 708, Montreal, Quebec, H3G 1Y6, CANADA. Email: russell.jones@mcgill.ca, Phone: (514) 398-3336, Fax: (514) 398-6769.

Abstract

Reactive oxygen species (ROS) are continuously produced by mitochondria and eliminated via antioxidant systems. Proper maintenance of this redox balance supports proper cellular function and can facilitate adaptation to metabolic stress. The AMP-activated protein kinase (AMPK) is a central regulator of cellular metabolism. AMPK can be activated by ROS and has previously been linked to redox balance through control of ACC-dependent NADPH homeostasis. Here we show that AMPK functions in a feedback loop to limit mitochondrial ROS through regulation of mitochondrial metabolism. We demonstrate that the AMPK allosteric activator A-769662 promotes decreased mitochondrial membrane potential and suppression of State III (ADP-stimulated) respiration in cells, leading to ROS inhibition. Similarly, AMPK activation results in a PGC-1α-dependent increase of antioxidant genes. Conversely, loss of AMPKα in mouse embryonic fibroblasts promotes increased production of mitochondrial ROS, leading to HIF-1α stabilization and a metabolic shift to the Warburg effect.

Introduction

Reactive oxygen species (ROS) are the byproducts of aerobic metabolism. The incomplete reduction of molecular oxygen in the electron transport chain results in ROS production. 1-3% of O_2 consumed by cells is metabolized to ROS in the form of superoxides, hydrogen peroxide and hydroxyl radicals (Valko et al., 2007). The amount of ROS can correlate with increased metabolic activity (Wellen and Thompson, 2010), or under conditions of metabolic stress, such as hypoxia (Bell et al., 2007). The mitochondrial production of ROS can occur at various locations in the electron transport chain. However, only glycerol-3-phosphate dehydrogenase and Site IIIQo of complex III are capable of producing ROS into the intermembrane space. Of these, complex III has a higher capacity of ROS production (Brand, 2010; St-Pierre et al., 2002). Mitochondrial-derived ROS can act as secondary messengers for various signaling pathways, and play an important role in the physiological regulation of proliferation and differentiation (Gough and Cotter, 2011; Reczek and Chandel, 2014). Improper maintenance of ROS can lead to oxidative stress, resulting in damage to lipids, proteins, and mitochondrial DNA (Rubattu et al., 2014). Homeostatic levels of ROS must be therefore be balanced to prevent pathophysiological oxidative stress and allow for normal physiological function. In order to achieve this balance, cells must coordinate both responses to changes in ROS levels, and utilize antioxidant methods to scavenge potentially dangerous levels of ROS.

AMPK is an evolutionarily conserved serine/threonine kinase that acts as a guardian of energetic balance in the cell. Under conditions of energetic stress such as glucose withdrawal and hypoxia, AMPK is activated by changes in the AMP/ATP ratio, and initiates a number of biological pathways aimed at preserving energy (Hardie, 2011a). Several adaptive responses to oxidative stress are mediated by the AMP-activated protein kinase (AMPK) (Greer et al., 2007;

Jager et al., 2007; Wu et al., 2014). There is increasing evidence that AMPK can be activated under physiological and pathological conditions by increased levels of intracellular ROS, possibly independently of changes in AMP/ATP levels (Emerling et al., 2009; Zmijewski et al., 2010). AMPK activation has been observed in diseases associated with oxidative stress, including Huntington's disease (Fu et al., 2012) and diabetes (Mackenzie et al., 2013). In experimental systems, mitochondria-derived ROS play an important role in AMPK activation (Emerling et al., 2009), and pretreatment of the cells with the mitochondria-specific ROS scavenger Mito-tempol can attenuate AMPK activation (Han et al., 2010). It has also been demonstrated that ROS-induced activation of AMPK can induce an antioxidant cascade in skeletal muscle cells (Irrcher et al., 2009). An important downstream target of AMPK is PGC-1α, which acts to increase antioxidant enzymes such as superoxide dismutase (SOD) and catalase to attenuate ROS levels (Greer et al., 2007; Jager et al., 2007; St-Pierre et al., 2006).

PGC-1α is a master regulator of oxidative metabolism. As a transcriptional co-activator, PGC-1α controls both metabolic and mitochondrial gene expression (Meirhaeghe et al., 2003). PGC-1α acts to increase the oxidative capacity of cells through increased mitochondrial biogenesis. In response to oxidative stress, PGC-1α promotes the transcription of anti-ROS genes including superoxide dismutases (SODs), catalase, and uncoupling proteins (UCPs) (St-Pierre et al., 2006). SODs act to convert superoxide into hydrogen and oxygen, and H_2O_2 is reduced to water by catalase, glutathione peroxidases, and peroxiredoxins (Murphy, 2012). By balancing metabolic requirements and cytotoxic protection from ROS activation, PGC-1α serves as an adaptive set-point regulator of oxidative stress. PGC-1α activity can be increased through an increase of its expression as well as post-translational modification. AMPK phosphorylates PGC-

1α at T177 and S538, inducing processes such as mitochondrial biogenesis (Butow and Avadhani, 2004; Irrcher et al., 2009; Jager et al., 2007).

Cells with impaired OXPHOS activity often feature increased levels of glycolysis as an energetic compensation. This process is mediated by the hypoxia inducible factor 1α (HIF-1α). Under conditions of low oxygen or high ROS levels, HIF-1α transcriptionally increases several glycolytic intermediates such as *aldolase, glut1, LDHA and PDHK* (Papandreou et al., 2006; Semenza et al., 1994). The net result of this is to enhance glucose uptake and shift carbons away from entering the mitochondria so that they may be exported as lactate. Previous work by our lab and others has shown that loss of LKB1 or AMPK can result in enhanced HIF-1α activity in normoxic conditions (Faubert et al., 2013; Faubert et al., 2014; Shackelford et al., 2009). In the absence of LKB1, this HIF-1α activity was attributed to increased levels ROS, as ROS scavenging was able to ablate the HIF-1α-induced transcriptional and metabolic changes in LKB1-null cells (Faubert et al., 2014). HIF-1α is increased in the absence of AMPK, but the underlying mechanism has yet to be elucidated.

In this work we utilize isogenic cell lines to examine the importance of AMPK in the management of physiological ROS. We have found that the absence of AMPK leads to the deregulation of mitochondrial ROS, which results in the HIF-1α-driven Warburg effect. We have found that mitochondrial-derived ROS promote AMPK activation under stress conditions, and that, in a feedback-loop, AMPK activation limited the amount of mitochondrial ROS produced. These effects are attributed to PGC-1α signaling, specifically, transcriptional increases in the superoxide dismutases. We have found that de-regulated ROS management also occurs in the absence of PGC-1α, which confers a Warburg-like metabolism.

Results

Mitochondrial ROS is increased in the absence of AMPK

We and others have previously demonstrated that HIF-1α protein levels are increased in the absence of AMPK (Faubert et al., 2013; Shackelford et al., 2009). However, the mechanism responsible for this has yet to be elucidated. A putative mechanism for HIF-1α stabilization was found in the absence of LKB1, wherein high levels of reactive oxygen species contributed to HIF-1α levels and the Warburg Effect (Faubert et al., 2014; Shackelford et al., 2013). To test if deregulated ROS occurs in the context of AMPK, we generated mouse embryonic fibroblasts (MEFs) harboring conditional mutations for *prkaa1* and *prkaa2* (denoted hereafter as $\alpha 1^{fl/fl}$,$a2^{fl/fl}$). We generated paired isogenic cell lines that possess or completely lack AMPK catalytic activity depending on expression of Cre recombinase. Cells lacking AMPK (KO) featured higher levels of mitochondrial ROS, as measured by MitoSOX and FACS (Fig 1A, S1A). When these cells were stressed with glucose withdrawal, cells lacking AMPK (closed circles) feature an enhanced production of ROS, which is largely prevented in cells with AMPK (open circles) (Fig 1B). To identify the effects of AMPK activation on mitochondrial ROS levels, we treated cells with the AMPK activator A-769662. Here, A-769662 treatment resulted in decreased ROS levels under both basal (25mM glucose) and stressed (0mM glucose) conditions (Figure 1C, S1B). To elucidate the potential mechanisms by which AMPK activation could reduce ROS levels, we paneled known antioxidant genes. Overnight treatment of A-769662 increases several antioxidant transcripts in an AMPK-dependent manner, including catalase, cytochrome c, SOD1 and SOD2 (Figure 1D). Taken together these data indicate that AMPK activation plays a role in maintaining mitochondrial ROS in both basal and stress conditions.

AMPK activation decreases OXPHOS and mitochondrial membrane potential

We observed that activation of AMPK by A-769662 can reduce ROS levels in both basal and stressed conditions (Figure 1C). Mitochondrial ROS can be attenuated via increased transcription of antioxidant genes, as well as by decreasing mitochondrial potential. We first sought to explore the ability of A-769662 treatment to reduce mitochondrial potential. Acute treatment of A-769662 results in a 40% decrease in mitochondrial potential (Figure 2A). Cells were incubated with mitotracker green to quantify mitochondrial load, as well as mitotracker red to measure membrane potential. The ratio of these (potential/load) is decreased with A-769662 treatment in cells expressing AMPK. Mean fluorescence intensity of mitochondrial potential and load was measured using the Operetta microscope (Figure 2B). Recent work from out lab has shown that chronic treatment of A-769662 can decrease oxygen consumption (Vincent et al., 2014). To test if the decrease in mitochondrial potential could also decrease oxygen consumption, we treated cells as in (B), and utilized a Seahorse XF analyzer to measure oxygen consumption (Figure 2C). Here we observed a slight decrease in oxygen consumption in cells with AMPK (open bar) upon A-769662 stimulation, which did not occur in the absence of AMPK (closed bar).

AMPK activation decreases State 3 (ADP-stimulated) respiration

A potential consequence of decreased mitochondrial membrane potential is the inability to fully couple oxygen transport to ATP formation. To assess this possibility, wild-type MEFs were treated with vehicle control (open circle) or 25μM A-769662 (shaded circle) overnight. Mitochondria were isolated, and complex activity was tested as previously described (Andrzejewski et al., 2014). In complex I (Figure 3A) and complex II (Figure 3B) A-769662 treatment inhibited ADP-stimulated respiration, as well as decreased FCCP-stimulated proton release. The ability of complex I and II to functionally use pyruvate/malate, and succinate,

respectively is largely unaffected. Taken together, these results indicate that chronic treatment with A-769662 inhibits ADP-stimulated respiration in isolated mitochondria.

Mitochondrial ROS contributes to AMPK activity

Reactive oxygen species can be a potent activator of AMPK (Park et al., 2006; Shafique et al., 2013). The exact mechanism of this activation remains controversial (Shao et al., 2014; Zmijewski et al., 2010), and the physiological relevance of AMPK activation by ROS under endogenous conditions remains unexplored. Here, we show that pharmacological ROS scavenging via trolox, a vitamin E analogue and potent antioxidant (Figure 4A), is able to reduce AMPK activity under basal conditions (Figure 4B). To elucidate the effects of endogenous ROS on AMPK, we inhibited a component of Complex III of the electron transport chain, the Rieske Iron-Sulfur protein (RISP). Inhibition of RISP results in decreased production of ROS from the mitochondria (Tormos et al., 2011). Similar results were obtained with cells lacking RISP (Figure 4C, D). We next sought to explore this phenomenon under conditions of metabolic stress. Using Wild-type MEFs expressing either vector control or RISP shRNA, we tested AMPK phosphorylation under basal conditions, glucose withdrawal, and hypoxia. Here we observe both a decrease in total AMPK levels, as well as phosphorylated AMPK (Figure 4E). Under basal conditions, RISP shRNA cells have lower mitochondrial ROS levels (Figure 4F, G). When faced with a stress such as glucose withdrawal, mitochondrial ROS levels rose three fold in wild type cells with RISP expressed, and this increase is inhibited with cells expressing RISP shRNA (Figure 4F). Similarly, when exposed to hypoxia, cells feature an increase in mitochondrial ROS levels that is completely prevented when RISP is inhibited (Figure 4G). FACS plots of mitochondrial measurements are included in Supplemental Figure 2.

Mitochondrial ROS drives the Warburg effect in AMPK-deficient cells

We have previously shown that cells lacking AMPK feature enhanced glucose uptake and lactate production (Faubert et al., 2013). In AMPK-null cells featuring RISP shRNA, we see a complete abrogation of the glucose uptake and lactate production (Figure 5A,B). Similarly, there is a decrease of extracellular acidification (Figure 5C) and oxygen consumption (Figure 5D). To test if increased mitochondrial ROS in AMPK-null cells was responsible for the stabilization of HIF-1α, we utilized a series of reactive oxygen species scavengers. In AMPK-null cells treated with 1mM trolox, HIF-1α levels are completely abrogated (Figure 5E). MEFs lacking AMPK were treated with a series of antioxidants for 1 hour, including ascorbate (Asc) N-acetyl cysteine (NAC) and catalase (Cat). HIF-1α protein levels and its downstream target PDHK1 were assessed by immunoblotting (Fig. 5E). Using shRNA targeting RISP, we observed a decrease in mitochondrial ROS under basal and glucose-withdrawal conditions (Fig. S2), as well as a decrease in the stabilization HIF-1α (Figure 5F). Taken together, this data demonstrates that the HIF-1α protein stabilization and pro-glycolytic effects in AMPK-null cells is driven by ROS.

PGC-1α mediates the AMPK-dependent effects on ROS homeostasis

AMPK activation can induce an antioxidant response though various mechanisms, including phosphorylation the transcriptional co-activator PGC-1α (Jager et al., 2007). PGC-1α is a potent transcriptional co-activator in the antioxidant system (St-Pierre et al., 2006), and is a defined target of AMPK (Jager et al., 2007). Treatment of cells with A769662 caused an AMPK-dependent increase in PGC-1α mRNA (Figure 6A), but not PGC-1β (Figure 6B). To test ability of PGC-1α to mediate the effects of AMPK activation, we generated mouse embryonic

fibroblasts (MEFs) harboring a conditional mutation for *ppargc1a* (denoted hereafter as *PGC1α*$^{fl/fl}$). We generated paired isogenic cell lines that possess or completely lack AMPK catalytic activity depending on expression of Cre recombinase. We tested to see if the effects if AMPK activation were mediated by PGC-1α. We utilized PGC-1α MEFs featuring a conditional deletion of PCG-1α via Cre recombinase. When cells with or without PGC-1α were stimulated with A-769662 overnight, we observed that several of the AMPK-dependent increases of antioxidant transcript were also dependent upon PGC-1α including *catalase*, *cytochrome c*, and *SOD2* (Figure 6B). Similar to the AMPK-null phenotype, cells lacking PGC1α featured higher basal levels of mitochondrial ROS (Figure 6C). Cells lacking PGC-1α (Cre +) featured elevated HIF-1α protein levels, as well as increased protein of canonical HIF-1α targets LDHA and aldolase, as measured by immunoblotting (Figure 6D). Furthermore, PGC-1α-null cells display a Warburg-like metabolic phenotype, as they displayed increased glucose uptake and lactate excretion as compared to control cells (Figure 6F). Taken together, these data suggest that PGC-1α at least partially mediates the effects of AMPK on inhibiting mitochondrial ROS.

Discussion

AMPK responds to metabolic stress by engaging appropriate cellular responses to cope with metabolic stress. Stresses such as glucose withdrawal and hypoxia cause both energetic imbalances such as changes in the AMP/ATP ratio and increased production of mitochondrial reactive oxygen species. Here we provide evidence that the production of mitochondrial ROS is important for AMPK activity, and that AMPK is involved in a negative feedback loop to limit ROS production. AMPK-null cells feature increased amounts of mitochondrial ROS, under both basal and stressed conditions (Fig. 1). We find that these effects are mediated by mitochondrial

uncoupling, as AMPK activation leads to decreased membrane potential (Fig. 2), as well as decreased state 3 respiration (Fig 3.) These chronic levels of elevated ROS are responsible for HIF-1α protein stabilization and the Warburg effect in AMPK-null MEFs (Fig. 4). Limiting the production of mitochondrial ROS decreases AMPK activity both under basal and stress conditions (Fig. 5). Activation of AMPK by A-769662 increases transcript levels of PGC-1α, and PGC-1α-dependent antioxidant genes. Finally, we observed that PGC-1α-null cells display enhanced levels of mitochondrial ROS, increased HIF-1α and increased glycolytic metabolism (Fig. 6). Together our data suggest that mitochondrial ROS is a key component in AMPK activation, and initiates a cascade to reduce mitochondrial ROS via PGC-1α.

Oxidative stress can induce metabolic changes within cells, and increased ROS can be a marker of mitochondrial dysfunction. Cells can adapt to this by engaging in different forms of metabolism such as increasing glucose uptake. This is mediated by HIF-1α, which directs glucose-derived carbon away from the mitochondria, to be excreted as lactate. Similarly, cells can recycle damaged or dysfunctional mitochondria through mitophagy (Youle and Narendra, 2011) and create new mitochondria through PGC-1α-driven transcriptional programs. One consequence of chronically increased mitochondrial ROS is the stabilization of HIF-1α. As mitochondrial ROS are an indicator of stress within the mitochondria, ROS-induced stabilization of HIF-1α acts as a survival mechanism by re-directing energy production away from the mitochondria to glycolysis. When this occurs under normoxic conditions, due to AMPK loss, a Warburg metabolic phenotype is induced due to HIF-1α increasing glucose uptake and flux.

All cells must manage levels of reactive oxygen species to prevent oxidative damage. AMPK is regarded as an energy-sensitive kinase, though several recent studies have indicated that AMPK activity can also be regulated by oxidative stress (Choi et al., 2001; Emerling et al.,

2009; Zmijewski et al., 2010). The relationship of ROS and AMPK may be cell-type, or cysteine-residue dependent. Oxidation of AMPK Cys299 in HEK293 cells resulted in increased activity (Zmijewski et al., 2010), whereas in primary cardiomyocytes oxidation of Cys130 and Cys174 AMPK by ROS decreased its activity, by interfering with the AMPK/LKB1 interaction (Shao et al., 2014). The requirement of changes in the AMP:ATP ratio for oxidative stress-induced AMPK activation is still debated (Auciello et al., 2014; Emerling et al., 2009). Under metabolic stress conditions that increase mitochondrial ROS (glucose withdrawal, hypoxia), we observe an inhibition of the phosphorylation of AMPK and its canonical target ACC, when ROS is reduced either by trolox or the inhibition of the Rieske Iron Sulfur protein (Fig. 4). These data suggest that mitochondrial ROS are an integral part of the AMPK stress response.

In addition to the role of AMPK in restoring energy balance, AMPK also engages programs aimed at reducing ROS levels. Under conditions of oxidative stress, AMPK phosphorylates targets such as PGC-1α to promote the transcription of antioxidant genes, and proteins capable of reducing oxidative stress (Jager et al., 2007). PGC-1α plays a central role in regulating mitochondrial content and antioxidant response. PGC-1α can be regulated by addition of exogenous ROS and AMPK activators such as AICAR (St-Pierre et al., 2006; Suwa et al., 2003). Our findings are consistent with previous work demonstrating that AMPK-mediated phosphorylation of PGC-1α mediates an antioxidant response (Irrcher et al., 2009). Activation of AMPK by A-769662 resulted in increased mRNA of PGC-1α, and several antioxidant genes, including *catalase* and *superoxide dismutase 2* (Figure 6).

A recent study by (Hart et al., 2015) links increased SOD2-derived H_2O_2 with increased AMPK activity, resulting in an enhanced glycolytic phenotype. These results are complementary with the study by (Yan et al., 2014) wherein increased AMPK activation by FLCN loss drives a

ROS-induced Warburg phenotype. Taken together with the data presented in this paper, we highlight a role of AMPK of in the regulation of mitochondrial ROS. Diminished AMPK activity results in increased levels of ROS (due to chronic lack of antioxidant response), which stabilizes HIF-1α and promotes the Warburg effect. Chronic AMPK activation can both induce (Hart et al., 2015) and be caused by high levels of ROS (Yan et al., 2014), and result in the Warburg effect. At homeostatic and endogenous levels mitochondrial ROS lead to AMPK activation that concomitantly decreases ROS levels.

This work adds to the expanding role of AMPK in mitochondrial maintenance. Dysfunctional or stressed mitochondria display increased amounts of reactive oxygen species (Figure 4). AMPK responds to this in various ways, including decreasing membrane potential to decrease ROS levels (Figure 2). In addition, AMPK phosphorylates various transcription factors, including the transcriptional co-activator PGC-1α, to increase mitochondrial biogenesis and antioxidant systems. Furthermore, AMPK can help promote the degradation of unhealthy mitochondria by phosphorylating the mitochondrial fission factor (MFF) (Ducommun et al., 2015), which can act to separate damaged sections of mitochondria from healthy. AMPK continues this process by phosphorylation of ULK to increase mitophagy (Egan et al., 2011), thereby degrading the newly separated, damaged sections of mitochondria. Taken together, our work and others suggest that AMPK activity is a key regulator of maintaining functional mitochondria in cells.

Experimental Procedures

Cell Lines, DNA Constructs, and Cell Culture

Primary mouse embryonic fibroblasts (MEFs) conditional for *prkaa1* and *prkaa2* ($\alpha 1^{fl/fl}, \alpha 2^{fl/fl}$), and conditional for *ppargc1a* (PGC1$\alpha^{fl/fl}$) were generated by timed mating as previously described (Jones et al., 2005), and immortalized with SV40 Large T Antigen. Knockdown of UQCRFS1 was achieved using the lentiviral shRNA vectors from the TRC shRNA collection (Sigma-Aldritch, St. Louis MO). The ID number for UQCRFS1 shRNA vectors use in the study were TRCN0000070108-10. Lentiviral supernatants were generated as described (Huang et al., 2012). Transduction of cell lines with high-titre retrovirus was conducted as previously described (Jones et al., 2005). Retrovirus-infected cells were cultured in 2μg/ml puromycin or sorted 7 days post-infection by flow cytometry (for GFP or CD8t-expressing cells).

Western Blots

Cells were lysed in modified CHAPS buffer (10mM Tris-HCl, 1mM $MgCl_2$, 1mM EGTA, 0.5mM CHAPS, 10% glycerol, 5mM NaF), supplemented with the following protease additives: protease and phosphatase tablets (Roche), DTT (1 μg/ml), and benzamidine (1 μg/ml). Cleared lysates were resolved by SDS-PAGE, transferred to nitrocellulose, and incubated with primary antibodies. Primary antibodies to AMPK (pT172-specific and total), phospho-Acetyl-CoA-carboxylase (pS79), LDHA, PDK1, aldolase, and actin, as well as HRP-conjugated anti-rabbit and anti-mouse secondary antibodies were obtained from Cell Signaling Technology (Danvers, MA). Anti-HIF-1α antibodies were from Cayman Chemical (Baton Rouge, LO). Anti-RISP antibody was obtained from Abcam (Cambridge, UK).

Quantitative Real-Time PCR

Total mRNA was isolated from cells using Trizol (Invitrogen), and cDNA was synthesized from 100ng of total RNA using the Superscript® VILO™ cDNA Synthesis Kit (Invitrogen). Quantitative PCR was performed using SYBR Green qPCR SuperMix (Invitrogen) and an Mx3005 qPCR machine (Agilent) using primers against *ant, catalase, cytochrome c, gpx1, tbp, pgc1α, pgc1b, sod1, sod2, ucp2, ucp3*. All samples were normalized to β-actin mRNA levels. Primer sequences have been previously described (St-Pierre et al., 2006).

Determination of ROS and mitochondrial potential

Mitochondrial ROS was assessed by incubating cells with MitoSOX red for 15-30 minutes, followed by FACS analysis. The amount of mitochondrial ROS was measured by flow cytometry, and quantified as the mean florescence intensity for FL4. Mitochondrial load and potential were determined by staining with Mitotracker green, or Mitotracker red or TMRE. Cells were incubated with 50uM of the stain for 15-30 minutes, and analyzed on FACS. All flow cytometry was conducted using BD FACSCalibur (BD Biosciences, San Diego, CA) or Gallios (Beckman Coulter, Fullerton, CA) flow cytometers and analyzed with FlowJo software (Tree Star, Ashland, OR).

Metabolic Assays

Cells were grown in standard conditions for 2-3 days. Media was removed from cells and analyzed for glucose, lactate, and glutamine using a Flex Bioanalyzer (NOVA Biomedical, Waltham, MA).

SeahorseXF96 Respirometry

Respirometry (oxygen consumption rate, OCR) and the extracellular acidification rate (ECAR) of cells were measured using an XF96 Extracellular Flux Analyzer (Seahorse Bioscience, Billerica, MA) as previously described (Faubert et al., 2014). In brief, cells were plated at $3x10^4$/well in 100μl non-buffered DMEM containing 25mM glucose and 2mM glutamine. Cells were incubated in a CO_2-free incubator at 37°C for 1 hr to allow for temperature and pH equilibration prior to loading into the XF24 apparatus. XF assays consisted of sequential mix (3 min) measurement (5 min) cycles, allowing for determination of OCR/ECAR every 8 minutes.

Mitochondrial Isolation

Wild-type cells were incubated in the presence of A-769662 or vehicle control overnight. Isolation of mitochondria was conducted as previously described (Andrzejewski et al., 2014). Mitochondria were re-suspended in KHEB buffer (120 mM KCl, 5 mM KH_2PO_4, 3 mM Hepes, 1 mM EGTA, 0.2% (w/v) BSA) and spun at 10,000 *g* for 10 min. The resulting mitochondrial suspension was stored on ice and used for all further experiments. Mitochondrial protein content was determined using the Bradford assay (Bio-Rad, Mississauga, ON, Canada) in the presence of 0.2% sodium deoxycholate, using BSA as standard.

Mitochondrial Respiration

All respiration measurements were conducted using a Clarke-type electrode (Rank Brothers, Cambridge, UK). Mitochondria were incubated at a concentration of 0.25 mg mitochondrial protein ml^{-1} in KHEB buffer at 37 °C. The rate of oxygen consumption was determined by addition of substrates. State 2 respiration was determined by adding succinate (5 mM) in the

presence of rotenone (10 μM) or pyruvate (2.5 mM) and malate (2.5 mM). State 3 respiration was obtained by the addition of ADP (100 μM), and State 4 respiration was quantified by the addition of oligomycin (1 μg/mg mitochondrial protein).

Statistical Analysis

Statistics were determined using paired Student's t test, ANOVA, or Log-rank (Mantel-Cox) test using Prism software (GraphPad). Data are calculated as the mean ± SEM unless otherwise indicated. Statistical significance is represented in figures by: *, $p<0.05$; **, $p<0.01$; ***, $p<0.001$

Acknowledgements

We acknowledge the assistance of Dr. Sidon Huang who provided access to the shRNAs targeting RISP that were used in this study. We would like to thank members of the Jones lab for technical and administrative help and comments on this manuscript. B.F. was funded by a doctoral fellowship from the Canadian Institutes of Health Research (CIHR). This work was supported by grants to R.G.J. from the CIHR (MOP-93799).

Figure Legends

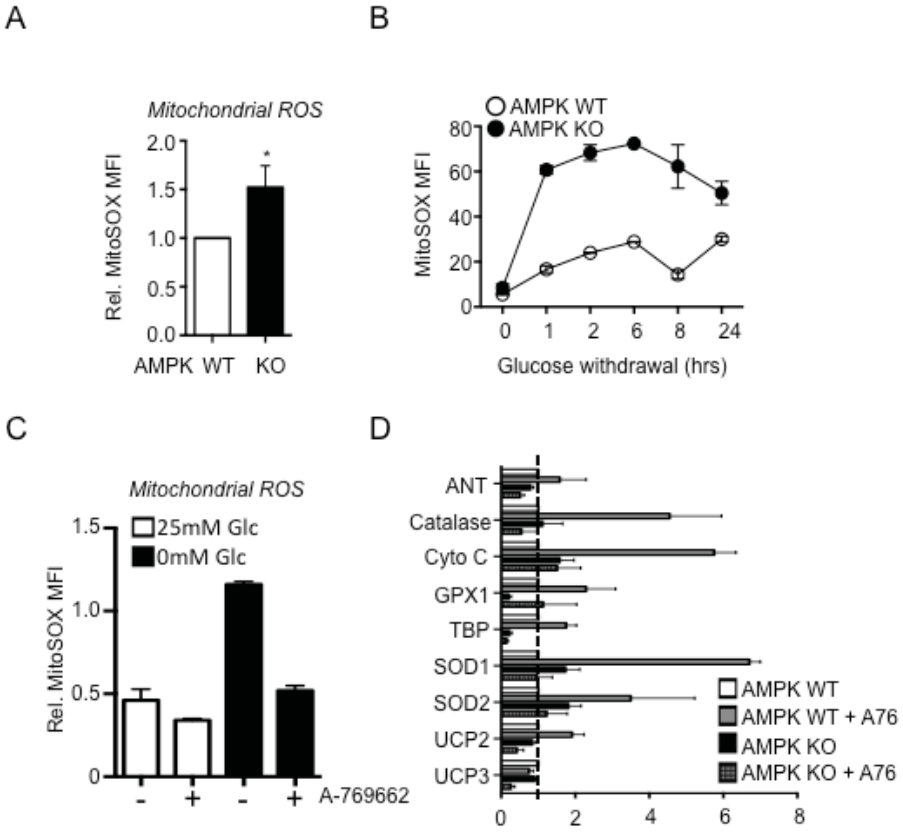

Figure 1. AMPK is involved in maintaining mitochondrial ROS levels under basal and stress conditions. A) Mitochondrial ROS levels were measured in wild type or AMPK-null MEFs in standard growth conditions. Data are expressed as mean fluorescence intensity relative to wild type cells of n= 5 experiments. B) Wild-type (open circle) and AMPK-null MEFs (closed circle) were subjected to glucose withdrawal. At the time indicated, mitochondrial ROS was measured. Data are expressed as mean fluorescence intensity relative to wild type cells of n= 2 experiments. A representative experiment is shown. C) Wild-type MEFs were pre-treated with 25uM A-769662 overnight. Cells were subjected to 6 hours of glucose withdrawal, and mitochondrial ROS levels were measured by FACS. Data are expressed as average mean fluorescence intensity ± SD, and are representative of 2-3 independent experiments. D) Wild type (WT) and AMPK-null (KO) MEFs were treated overnight with 25uM A-769662. Relative expression of indicated mRNA by control (WT) or AMPK-null (KO) MEFs as determined by qPCR. Data were expressed relative to *actin* mRNA levels for triplicate samples and normalized relative to control (WT) cells. *, $p<0.05$.

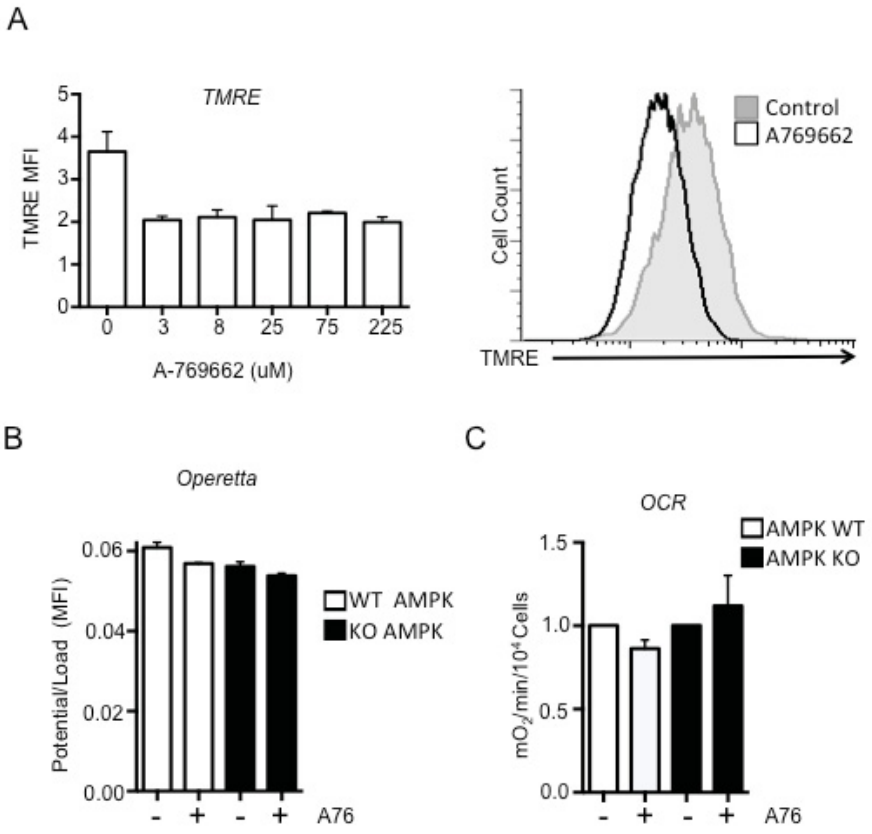
A
TMRE
TMRE MFI
5
4
3
2
1
0
0
3
8
25
75
225
A-769662 (uM)
Control
A769662
Cell Count
TMRE
B
Operetta
Potential/Load (MFI)
0.06
0.04
0.02
0.00
WT AMPK
KO AMPK
- + - +
A76
C
OCR
AMPK WT
AMPK KO
mO2/min/10^4 Cells
1.5
1.0
0.5
0.0
- + - +
A76

Figure 2. AMPK activation decreases mitochondrial potential. A) Treatment of wild-type cells with a dose curve of A-769662 decreases TMRE fluorescence by 50%. A representative FACS blot is shown on the right panel. B) Wild-type (open bar) or AMPK-null (closed bar) MEFs were treated with 25uM A-769662 overnight. The ratio of mitochondrial potential over mitochondrial load was measured by Operetta fluorescence microscopy. Data are expressed as the ratio of load/potential per condition. C) Wild-type (open bar) and AMPK-null (closed bar) cells were treated overnight with 25uM A-769662. Oxygen consumption rates were measured by Seahorse XF assay. Data represent Mean ± SD of a representative experiment (n=4).

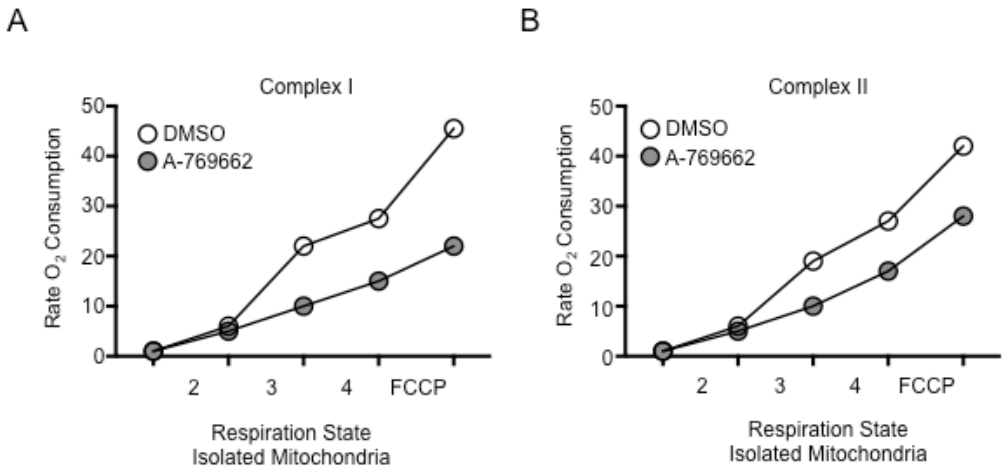
A
Complex I
DMSO
A-769662
Rate O_2 Consumption
50
40
30
20
10
0
2
3
4
FCCP
Respiration State
Isolated Mitochondria
B
Complex II
DMSO
A-769662
Rate O_2 Consumption
50
40
30
20
10
0
2
3
4
FCCP
Respiration State
Isolated Mitochondria

Figure 3. AMPK activation by A-769662 decreases state III respiration. A) Mitochondria were isolated form cells treated with vehicle control (open circle) or A-769662 (closed circle). Complex activity was measured by respirometry. Data are expressed as the rate of O2 consumption over time. State 2 respiration was determined by adding succinate (5 mM) in the presence of rotenone (10 μM) or pyruvate (2.5 mM) and malate (2.5 mM). State 3 respiration was obtained by the addition of ADP (100 μM), and State 4 respiration was quantified by the addition of oligomycin (1 μg/mg mitochondrial protein). FCCP respiration was determined by addition of FCCP (1 μg/mg mitochondrial protein).

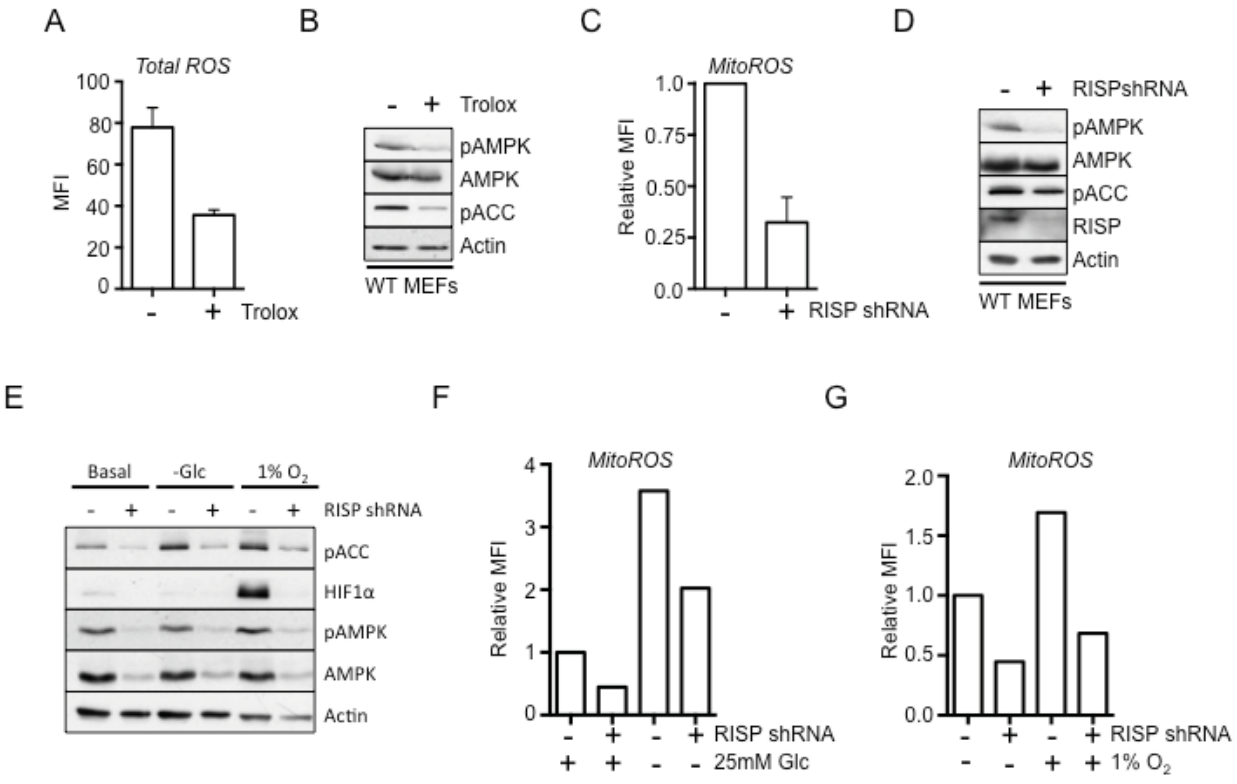
A
Total ROS
MFI
100
80
60
40
20
0
- + Trolox
B
- + Trolox
pAMPK
AMPK
pACC
Actin
WT MEFs
C
MitoROS
Relative MFI
1.0
0.75
0.50
0.25
0.0
- + RISP shRNA
D
- + RISPshRNA
pAMPK
AMPK
pACC
RISP
Actin
WT MEFs
E
Basal
-Glc
1% O2
- + - + - + RISP shRNA
pACC
HIF1α
pAMPK
AMPK
Actin
F
MitoROS
Relative MFI
4
3
2
1
0
- + - + RISP shRNA
+ + - - 25mM Glc
G
MitoROS
Relative MFI
2.0
1.5
1.0
0.5
0.0
- + - + RISP shRNA
- - + + 1% O2

Figure 4. Mitochondrial ROS contributes to AMPK activity. A) ROS levels were measured in wild-type MEFs with vehicle (-) or 1mM Trolox (+). Values are expressed as mean fluorescent intensity ± SD. B) Cells treated as in (A) were immunoblotted for pAMPK, AMPK, pACC and Actin. A representative immunoblot is shown. C) Mitochondrial ROS was measured in wild type MEFs featuring control (-) or vectors expressing RISP shRNA (+). Data are expressed as mean fluorescence intensity ± SD relative to control. D) Wild-type MEFs featuring control (-) or RISP shRNA (+) expressing vectors were immunoblotted for the proteins indicated. A representative immunoblot is shown. E) Wild-type MEFs expressing control (-) or RISP shRNA (+) vectors were grown in basal conditions, 0mM glucose (2 hours), 1% O2 (2 hours) or treated with 500uM phenformin (30 minutes). Immunoblot analysis of pACC, HIF-1α, pAMPK, AMPK and Actin from whole cell lysates of treated cells. F-G) Mitochondrial ROS was analyzed from cells treated as in (A). Cells were incubated with MitoSOX, and mitochondrial ROS was measured on FACS. Data are expressed as mean fluorescent intensity relative to control.

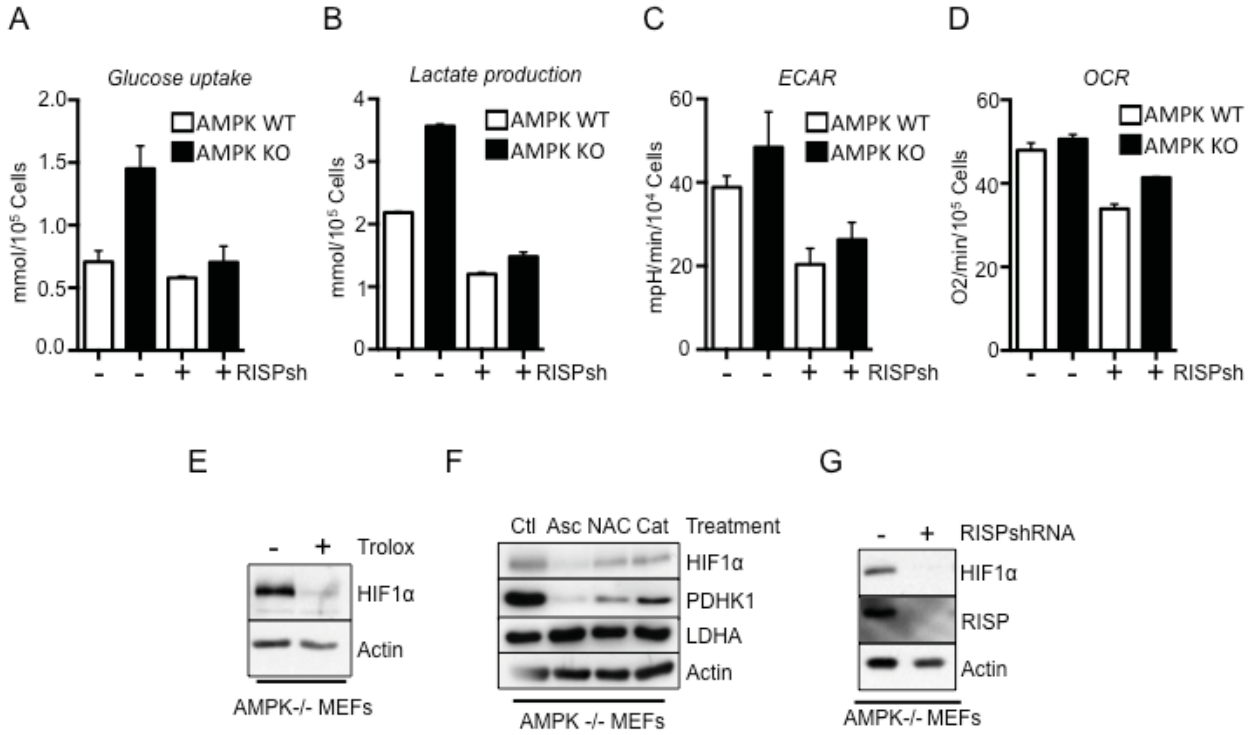
A
Glucose uptake
mmol/10^5 Cells
2.0
1.5
1.0
0.5
0.0
AMPK WT
AMPK KO
- - + + RISPsh
B
Lactate production
mmol/10^5 Cells
4
3
2
1
0
AMPK WT
AMPK KO
- - + + RISPsh
C
ECAR
mpH/min/10^4 Cells
60
40
20
0
AMPK WT
AMPK KO
- - + + RISPsh
D
OCR
O2/min/10^5 Cells
60
40
20
0
AMPK WT
AMPK KO
- - + + RISPsh
E
- + Trolox
HIF1α
Actin
AMPK-/- MEFs
F
Ctl Asc NAC Cat Treatment
HIF1α
PDHK1
LDHA
Actin
AMPK -/- MEFs
G
- + RISPshRNA
HIF1α
RISP
Actin
AMPK-/- MEFs

Figure 5. Inhibition of ROS reverses the HIF-1α-induced Warburg effect in cells lacking AMPK. A-B) Wild type (open bar) and AMPK-null (closed bars) MEFs with and without vectors expression RISP shRNA were analyzed for glucose uptake (A), lactate production (B). Data are expressed as Avg ± SD of a representative experiment (n=2). C-D) Cells were seeded in normal growth conditions, and basal extracellular acidification (C) and oxygen consumption rates (D) were recorded. Data represent the mean ± SD for quadruplicate samples, and are representative of two independent runs. E) Inhibition of ROS decreases HIF-1a levels. Immunoblot analysis of cells treated with 1mM Trolox for 1 hour. HIF-1α, AMPK, and actin protein levels in whole cell lysates from control (WT) and AMPKα-null (KO) MEFs. F) Multiple ROS scavengers decrease HIF-1α protein levels in AMPK-null MEFs. Cells were treated with 100uM ascorbate (Asc), 1mM N-acetyl cysteine (NAC) or 1000units catalase (Cat). Immunoblot analysis of HIF-1α, PDHK1, LDHA and Actin levels. G) AMPK wild type and AMPK-null cells featuring expression of Control (-) or vectors expression RISP shRNA (+). Immunoblot analysis of HIF-1α, pAMPK, AMPK, pACC, RISP and Actin are represented.

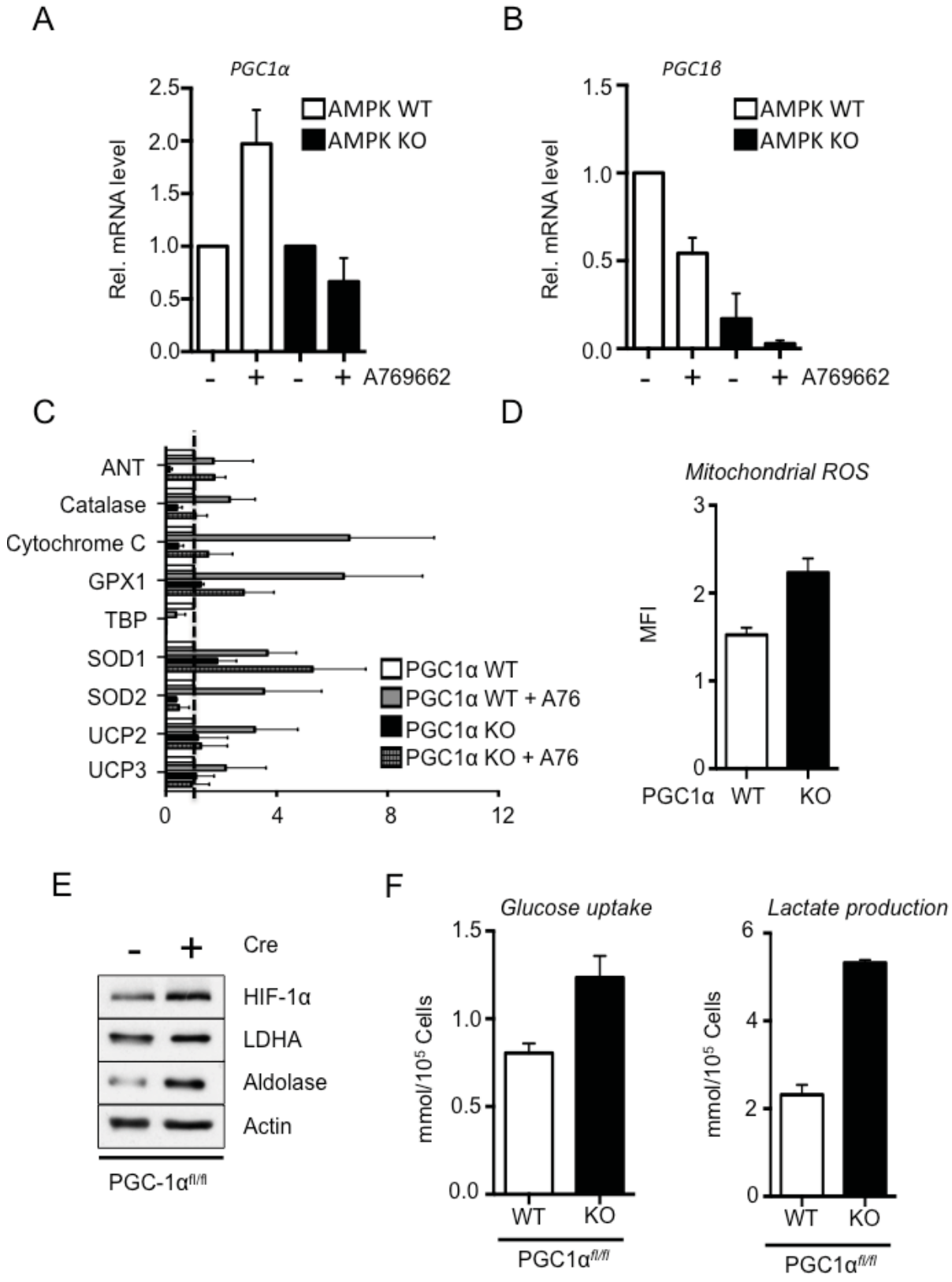
A
PGC1α
Rel. mRNA level
AMPK WT
AMPK KO
- + - + A769662
B
PGC1β
Rel. mRNA level
AMPK WT
AMPK KO
- + - + A769662
C
ANT
Catalase
Cytochrome C
GPX1
TBP
SOD1
SOD2
UCP2
UCP3
PGC1α WT
PGC1α WT + A76
PGC1α KO
PGC1α KO + A76
D
Mitochondrial ROS
MFI
PGC1α WT KO
E
- + Cre
HIF-1α
LDHA
Aldolase
Actin
PGC-1α fl/fl
F
Glucose uptake
mmol/10⁵ Cells
WT KO
PGC1α fl/fl
Lactate production
mmol/10⁵ Cells
WT KO
PGC1α fl/fl

G

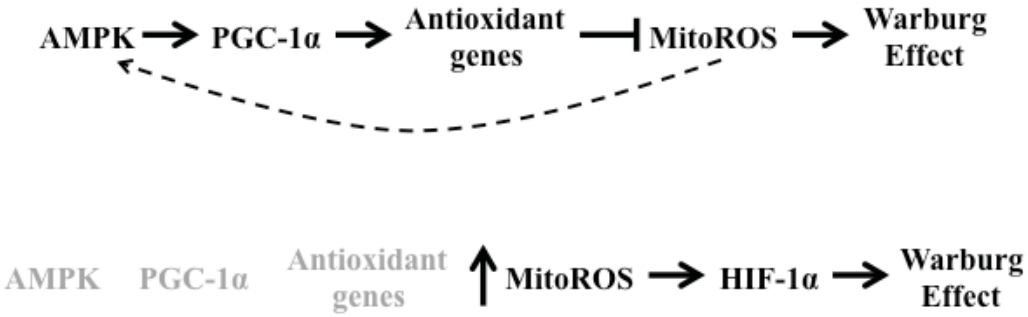
AMPK
PGC-1α
Antioxidant genes
MitoROS
Warburg Effect
AMPK
PGC-1α
Antioxidant genes
MitoROS
HIF-1α
Warburg Effect

Figure 6. AMPK activation induces an antioxidant transcriptional program.

A-B) Wild type (WT) and AMPK-null (KO) MEFs were treated with A-769662 overnight. Relative expression *pgc1α* or *pgc1ß* by control (WT) or AMPK-null (KO) MEFs as determined by qPCR. Data were expressed relative to *actin* mRNA levels for duplicate samples and normalized relative to control (WT) cells. C) Wild type (WT) and PGC-1α-null (KO) MEFs were treated with 25uM A-769662. Relative expression of indicated mRNA by control (WT) or PGC-1α-null (KO) MEFs as determined by qPCR. Data were expressed relative to *actin* mRNA levels for duplicate samples and normalized relative to control (WT) cells. D) PGC-1α-null MEFs show increased levels of mitochondrial ROS. Mitochondrial ROS was measured in wild-type (WT) and PGC-1α-null (KO) MEFs. Data are expressed as mean fluorescence intensity ± SD. E) Immunoblot analysis of HIF-1α, LDHA, Aldolase and Actin from whole cell lysates of cells. F) Glucose uptake and lactate production were assessed in wild type (open bar) and PGC-1α-null MEFs (closed bar) MEFs. Data are expressed as mean ± SD, and a representative of 2-3 independent experiments. G) A representative schematic of the relationship between mitochondrial ROS and AMPK activity.

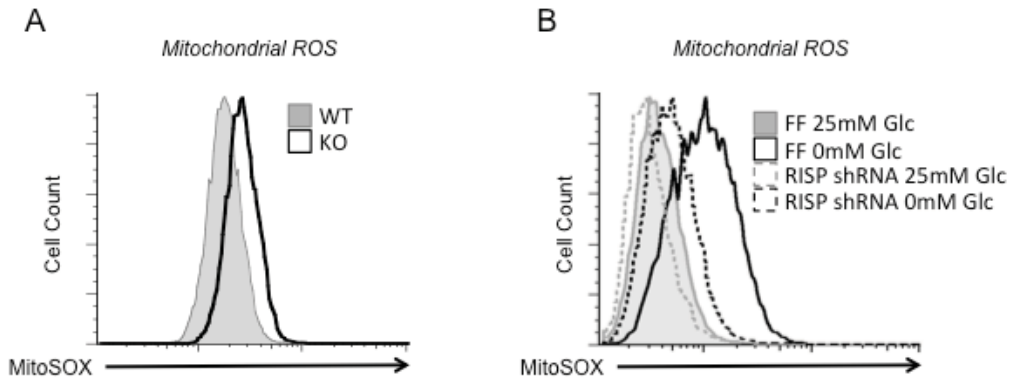
A
Mitochondrial ROS
WT
KO
Cell Count
MitoSOX
B
Mitochondrial ROS
FF 25mM Glc
FF 0mM Glc
RISP shRNA 25mM Glc
RISP shRNA 0mM Glc
Cell Count
MitoSOX

Supplementary Figure 1. AMPK is involved in maintaining mitochondrial ROS levels. A) Wild type (WT) and AMPK-null (KO) MEFs were incubated with MitoSox. A representative FACS plot is shown. B) MEFs featuring control shRNA (FF) solid lines, or RISP shRNA (RISP) dotted lines, were incubated in 25mM glucose (blank lines) or 0mM glucose (grey lines) for 6 hours. A representative FACS plot is shown.

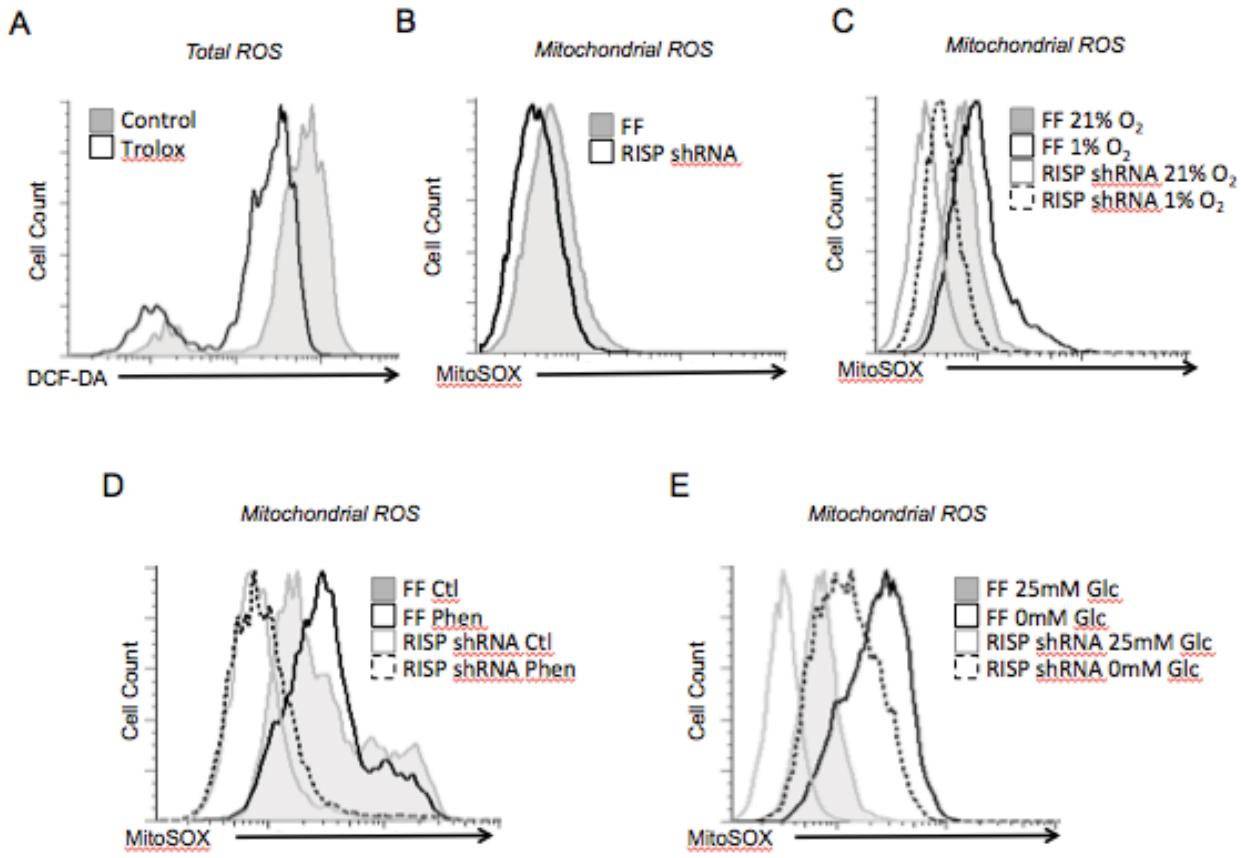
A
Total ROS
Control
Trolox
Cell Count
DCF-DA
B
Mitochondrial ROS
FF
RISP shRNA
Cell Count
MitoSOX
C
Mitochondrial ROS
FF 21% O2
FF 1% O2
RISP shRNA 21% O2
RISP shRNA 1% O2
Cell Count
MitoSOX
D
Mitochondrial ROS
FF Ctl
FF Phen
RISP shRNA Ctl
RISP shRNA Phen
Cell Count
MitoSOX
E
Mitochondrial ROS
FF 25mM Glc
FF 0mM Glc
RISP shRNA 25mM Glc
RISP shRNA 0mM Glc
Cell Count
MitoSOX

Supplementary Figure 2. Mitochondrial ROS contribute to AMPK activity.

A) Wild type MEFs were incubated with (open) and without (shaded) 1mM Trolox for 1 hour, and DCF-DA for 15 minutes. Mean fluorescence intensity was measured via FACS. A representative FACS plot is shown. B) Wild type MEFs expressing control (FF) or RISP shRNA (RISP) were incubated with MitoSOX for 20 minutes. Mean fluorescence intensity was measured via FACS. C-E) Wild type MEFs expressing control (FF) (solid line) or RISP shRNA (RISP) (broken line) were grown under basal conditions (black line) or metabolically stressed (grey line) with hypoxia (C) glucose withdrawal (D) or phenformin (E). Cells were incubated with MitoSOX, and MFI was measured via FACS.

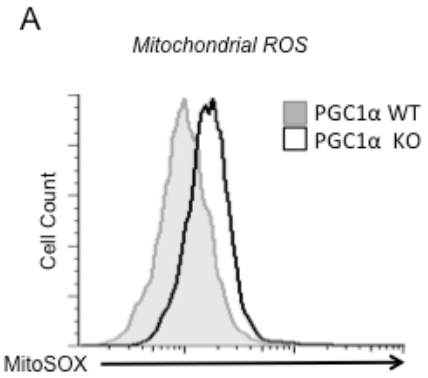
A
Mitochondrial ROS
PGC1α WT
PGC1α KO
Cell Count
MitoSOX

Supplementary Figure 3. PGC-1α-null MEFs feature higher levels of mitochondrial ROS. A) Wild type (WT) and PGC-1α-null (KO) MEFs were incubated with MitoSox, and mean fluorescence intensity was recorded. A representative FACS plot is shown.

Chapter 5

LKB1 and AMPK negatively regulate the Warburg effect in cancer: Discussion

5.1 Novel Contributions to Literature

The LKB1-AMPK pathway has been established as a highly conserved energy-sensing axis (Hardie, 2007). At the outset of this thesis, little had been established regarding the role of AMPK in cancer. The metabolic role of LKB1 loss in cancer was also largely unexplored, and the mechanism of HIF-1α stabilization in AMPK or LKB1 knockout cell lines was unknown.

In this thesis several novel aspects of the role of AMPK in cancer are described. In Chapter 2, we observed that the loss of AMPKα1 cooperates with the MYC oncogene to accelerate lymphomagenesis. In addition to the work published by other labs, we helped establish the paradigm of AMPK being a contextual oncogene or tumour suppressor, dependent upon cell type specificity and context. We demonstrated that AMPKα dysfunction enhances aerobic glycolysis, which was driven by HIF-1α. We observe that inhibiting HIF-1α reverses the metabolic effects of AMPKα loss, and importantly, that HIF-1α mediates the growth advantage of tumors with reduced AMPK signaling.

In Chapter 3, we show that loss of LKB1 expression in cancer cells promotes a pro-growth metabolic phenotype, driven by enhanced glycolysis and glutaminolysis. Loss of LKB1 promotes increased tumor cell metabolism through mTORC1- and ROS-dependent increases in HIF-1α. LKB1-null cells are dependent on HIF-1α to maintain cellular ATP and viability under poor nutrient conditions, raising the possibility of targeting HIF-1α for synthetic lethality in LKB1-deficient tumors. Together our data reveal that regulation of cellular metabolism is a key function of LKB1 that may contribute to its tumor suppressor function in human cancer.

In Chapter 4 we explored the mechanism of HIF-1α stabilization in the absence of AMPK. We also discovered the requirement of AMPK in the regulation of mitochondrial ROS homeostasis and characterized the role of mitochondrial ROS in both basal and stress-induced AMPK activity. We speculate the mechanism of this ROS control to be the decrease in mitochondrial membrane potential and the PGC-1α-dependent induction of antioxidant enzymes. Taken together, this thesis provides evidence for the contextual role of AMPK as a metabolic tumour suppressor.

5.1 AMPK in cancer

5.2.1 AMPK function in Cancer: Is it all about context?

Given the tumour-suppressing and tumour-promoting capabilities of AMPK, assessing the role of AMPK in tumourigenesis depends on context. A positive or negative role for AMPK in tumour growth will depend on the degree and/or mechanism of AMPK activation, the specific expression of AMPK isoforms, AMPK subcellular localization, the activity of other signalling networks in the cell, and extracellular environmental conditions.

AMPK loss in cancer. Loss of LKB1-AMPK signalling can drive a proliferative and metabolic phenotype favourable for tumour cells when resources are plentiful. In this light, loss of LKB1-AMPK signalling can promote a pro-growth metabolic program in tumour cells (Figure 5.1). Tumour cells lacking LKB1 or AMPK can gain enhanced mTOR activity, increase HIF-1α-driven glucose and glutamine metabolism, and bypass metabolic checkpoints that normally restrict cell growth under low nutrient conditions (Faubert et al., 2013; Faubert et al., 2014; Shackelford et al., 2009). Though genetic deletion in cancer is not observed with AMPK, recent work has suggested that AMPK may be inhibited by oncogenic activation of the MAGE-A3/6-

TRIM28E3 ligase complex. This complex can cause ubiquitination of AMPKα1, targeting it for proteasomal degradation. The activation of MAGE-A3/6 expression in several cancer types may signify an alternative mechanism for inhibiting AMPK signalling (Pineda et al., 2015). Furthermore, gain of function p53 mutations have been shown to bind to AMPKα. This binding results in preventing AMPK activation, thereby promoting anabolic processes (Zhou et al., 2014). In this context, silencing AMPK signaling via post-translational modifications and protein-protein interactions may provide tumor cells with a selective metabolic growth advantage, without subjecting cells to the deleterious effects of AMPK loss.

Conversely, tumor cells lacking LKB1 or AMPK undergo apoptosis at higher rates when subjected to energetic stress (Bungard et al., 2010; Dupuy et al., 2013; Faubert et al., 2013; Shaw et al., 2004b). Shackelford *et al.* recently demonstrated that phenformin can act as a single agent to promote tumour cell apoptosis *in vivo* using a Kras-driven lung cancer mouse model, but only in tumours lacking LKB1 expression (Shackelford et al., 2013). These data support the idea that upon application of a metabolic stress, LKB1-null cells cannot activate AMPK and have a reduced ability to survive disruption of mitochondrial function. In AMPK-null cells, we find that compounds that cause metabolic stress (phenformin, AICAR, salicylate, and 2DG) are considerably more effective at inducing cell death in tumor cells (Vincent et al., 2014). Thus, the use of biguanides such as phenformin may be most effective when used in combination with agents that inhibit, rather than activate, AMPK.

Activation of AMPK in cancer. Activation of AMPK displays conflicting roles in cancer. Pharmacological activation of AMPK by metformin or AICAR was shown to inhibit tumour growth in HCT116 xenografts (Buzzai et al., 2007). Furthermore, energetic stress causes an AMPK-dependent phosphorylation of the yes-associated protein (YAP) to inhibit its

transcriptional activity. This decreases the oncogenic activity of YAP, and promotes the tumour suppressive activity of the HIPPO pathway (Mo et al., 2015).

In certain tumour types AMPK activity can be instrumental for tumour survival. The various stresses that occur in the tumour microenvironment, including energetic stress (Hardie et al., 2012), hypoxia (Emerling et al., 2009), oxidative stress (Jeon et al., 2012), matrix detachment (Fung et al., 2008), are all potent activators of AMPK. This is best demonstrated by Jeon et al, where AMPK-dependent regulation of NADPH levels was necessary for cells to survive oxidative stress. The AMPK-dependent increase of CPT1c was also shown to be necessary for tumour survival. Elevated CPT1c levels caused enhanced β-oxidation, allowing for tumour cell survival against metabolic stress (Sanchez-Macedo et al., 2013; Zaugg et al., 2011). Similarly, loss of FLCN promotes constitutive AMPK activation. This chronic AMPK activation promotes glycolytic metabolism and oxidative phosphorylation and enhances cell growth (Yan et al., 2014).

Ultimately, for AMPK to be considered a viable target for cancer treatment in a clinical setting, understanding the roles of AMPK in cancer development and progression is essential. Data highlighting roles for AMPK in cancer cell survival raise the concern that AMPK activation may not be beneficial, and in some cases could be pro-tumorigenic. Given these results, we argue that, in addition to AMPK agonists, AMPK inhibitors may have a place as anti-cancer therapeutics. The use of AMPK inhibitors, used alone or in conjunction with compounds that activate metabolic stress, may be effective in exploiting the altered metabolic demand of tumour cells.

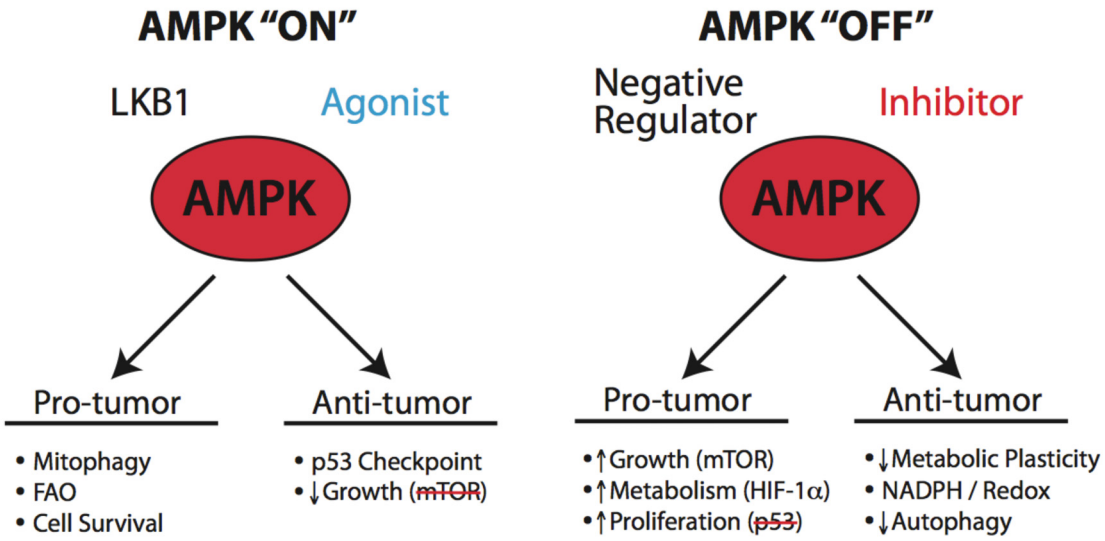

Figure 5.1 Summary of the context-dependent nature of AMPK in cancer.

5.2.2 Pharmacologic Targeting of AMPK in Cancer

Interest in activating AMPK in tumours has flourished as more evidence has emerged supporting an anti-tumorigenic role for the kinase. Much work has been proposed using agonists of AMPK for cancer treatment, and the number of patents describing AMPK activators has rapidly increased (Giordanetto and Karis, 2012). The most convincing data to support the use of AMPK-activating compounds as anti-cancer agents has been through the use of the therapeutic biguanides: metformin and phenformin. The growing interest in the LKB1-AMPK pathway in cancer prompted retrospective analysis of cancer incidence in patients with Type II diabetes. Several studies found that metformin treatment was associated with a significantly lower cancer incidence in patients relative to those using other medications to manage their diabetes (Decensi et al., 2010; Evans et al., 2005). Experimental evidence has also supported an anti-neoplastic effect for metformin. Treatment of animals harboring tumor xenografts with metformin or

phenformin has been shown to delay tumor progression (Appleyard et al., 2012; Buzzai et al., 2007; Kuznetsov et al., 2011; Wu et al., 2011). Other AMPK agonists, such as AICAR, salicylate and 2-Deoxyglucose have also been shown to inhibit tumour cell proliferation *in vitro* (Din et al., 2012; Dong et al., 2013; El-Masry et al., 2012; Elder et al., 1996; Petti et al., 2012; Rosilio et al., 2013; Vakana et al., 2011), providing further rationale for use of these agents in cancer therapy.

Many AMPK agonists, including the biguanides, activate AMPK through indirect mechanisms. Thus, to truly assess the benefit of AMPK activation as a therapeutic option, direct AMPK activators are necessary. The direct activator A-769662 is emerging as a valuable tool to study AMPK-dependent cellular effects *in vitro* and *in vivo*. A-769662 has been shown to delay tumour onset in PTEN+/- mice (Huang et al., 2008), suggesting that A-769662 can exert anti-tumour effects *in vivo* within the context of PTEN loss (and the resultant increase in Akt and mTORC1 signalling). Similarly, another AMPK agonist, the PPARγ active derivative OSU-53, has been shown to inhibit the growth of triple negative breast cancer *in vitro* and tumour xenografts (Lee et al., 2011).

The majority of evidence supporting the use of AMPK agonists as anti-cancer agents has been derived using compounds that do not directly activate AMPK, but do so indirectly through application of a metabolic stress. It stands to reason that these compounds will also elicit AMPK-independent cellular effects. AMPK-independent effects of metformin on cell growth have already been documented (Kalender et al., 2010). A recent studied has shown that the efficacy of many of these agonists may be due to the fact that they induce metabolic stress in tumors, rather than any effect on AMPK activation (Vincent et al., 2014).

5.2.3 Evidence for Targeting the LKB1-AMPK pathway.

Understanding the important metabolic differences between differentiated and cancer cells have become the key to the development of potential new therapeutic applications. Research focused on identifying the unique energy metabolism, or the unique weaknesses of altered metabolism has allowed for a rational design of single or combinatorial-targeted therapies. Of distinct relation to this thesis is work performed by Shackelford et al. It was previously identified that a significant percentage of NSCLC feature LKB1 loss (Ding et al., 2008). Phenformin is a potent activator of AMPK, but requires LKB1 (Dykens et al., 2008; El-Mir et al., 2000; Owen et al., 2000). In the study by Shackelford et al., administration of phenformin to tumours lacking LKB1 resulted in a significant therapeutic benefit. This benefit correlated with the inability of AMPK to trigger the ULK1 signalling pathway, preventing mitophagy in response to mitochondrial stress. Similarly in Chapter 2, we observe that cancer cells lacking AMPK activity are susceptible to metabolic stresses, despite their metabolic advantages. In Chapter 3, we observe that HIF-1α stabilization in LKB1-null cells was critical for the maintenance of the enhanced glycolytic and glutaminolytic phenotype. We also observed that cancer cells expressing HIF-1α shRNA in the absence of LKB1 were unable to adequately form tumours in a xenograft model (Data not shown). Taken together, these results provide rationale for inhibiting LKB1-AMPK signalling in cancer cells. While loss of this pathway may provide a metabolic growth advantage under basal (non-stressed) conditions, it may confer susceptibility to metabolic drugs such as phenformin.

While AMPK lies directly downstream of LKB1, it is important to note that the metabolic effects of LKB1 deficiency do not directly mirror those induced by AMPK loss. LKB1 and AMPK influence HIF-1α protein expression through slightly different mechanisms. Silencing

LKB1 promotes both increased transcription and translation of HIF-1α, events which are sensitive to mTORC1 inhibition (Faubert et al., 2014; Shackelford et al., 2009). In contrast, loss of AMPK results in increased HIF-1α protein levels with no discernable changes in HIF-1α mRNA levels, while inhibiting mTORC1 has little effect on HIF-1α protein levels when AMPK is silenced (Faubert et al., 2013). These data indicate that LKB1 exerts both AMPK-dependent and -independent mechanisms of metabolic regulation in tumor cells, and may impact mTOR signaling through other AMPK-related kinases such as MARK4 (Li and Guan, 2013). Exploration of the specific roles of the various AMPK-related kinases is an ongoing project in the AMPK field.

5.3 Regulation of AMPK by mitochondrial ROS.

The ability of ROS to increase AMPK activity has been well documented (Choi et al., 2001; Emerling et al., 2009; Wu et al., 2014). The work presented in Chapter 4 uses endogenously produced ROS, as well as pharmacologic and genetic inhibition of ROS production to identify the ability of mitochondrial ROS to activate AMPK. This work adds to the current controversy of the AMPK/ROS dynamic. This debate occurs on two topics: the ability of ROS to activate AMPK, and if ROS-induced activation of AMPK requires changes in AMP:ATP ratios.

ROS-induced activation of AMPK may be cell-type or cysteine-residue dependent. In HEK 293 cells the oxidation of AMPK Cys299 increased AMPK activity (Zmijewski et al., 2010), whereas in primary cardiomyocytes, oxidation of AMPK Cys130 and Cys174 interfered with the AMPK/LKB1 interaction causing a decrease in AMPK activity (Shao et al., 2014). The differences between these two studies highlights the importance of elucidating cell type specificity and cysteine oxidation sites will be important to fully elucidate these effects.

There is current controversy of the ROS-induced activation of AMPK requiring a change in AMP:ATP ratio. In mouse embryonic fibroblasts hypoxia-induced ROS caused AMPK activation occurred independently of changes in the AMP:ATP ratio (Emerling et al., 2009). However, changes in the AMP:ATP ratio were observed when glucose oxidase (a ROS-producing enzyme) was exogenously added to HEK 293 cells. Utilization of an AMP-independent mutant also prevented the ROS-induced activation of AMPK. (Auciello et al., 2014; Emerling et al., 2009). The work presented in Chapter 4 supports the evidence that ROS activates AMPK, and does so independently of changes in the AMP:ATP ratio. Conditions of metabolic stress (glucose withdrawal, hypoxia) increase mitochondrial ROS as well as increase phosphorylation of AMPK and its canonical target ACC. When this stress-induced ROS is reduced either by antioxidant scavengers or inhibition of the Rieske iron-sulfur protein, the activation of AMPK and its downstream targets is severely attenuated. These data suggest that mitochondrial ROS are an integral part of the AMPK stress response.

5.3.1 The role of AMPK in mitochondrial dynamics.

AMPK has been classically described as a regulator of cellular energy. In this work we propose the ability of AMPK to act as a rheostat to oxidative stress. AMPK has previously been shown to play a diverse role in mitochondrial maintenance, including AMPK-dependent phosphorylation and activation of ULK to induce mitophagy (Egan et al., 2011) and PGC-1α to induce mitogenesis (Handschin and Spiegelman, 2006; Jager et al., 2007; Wu et al., 1999). Recent work has identified the ability of AMPK to phosphorylate the mitochondrial fission factor (MFF) (Ducommun et al., 2015), which can act to separate damaged and healthy sections of mitochondria. Our work helps establish another connection between these processes and

solidifies a role for AMPK in mitochondrial dynamics. Under conditions of oxidative stress or stimulation by A-769662, AMPK can decrease the mitochondrial membrane potential, thereby decreasing ROS production. Similarly, through phosphorylation of the transcription factor PGC-1α AMPK acts to promote an antioxidant cascade to manage ROS levels. Taken together, we propose an overarching hypothetical model. Energetic stress results in increased ROS production from the mitochondria. This increased mitochondrial ROS activates AMPK which in turn can concomitantly decrease ROS levels by decreasing mitochondrial membrane potential and causing PGC-1α-dependent increases in antioxidants, as shown in Chapter 4. Continued energetic stress and mitochondrial dysfunction can result in AMPK-dependent phosphorylation of MFF, which separates functional and dysfunctional sections of mitochondria. AMPK can then commit damaged mitochondria to mitophagy by phosphorylation of ULK, and replenish lost mitochondria through PGC-1α-dependent mitogenesis.

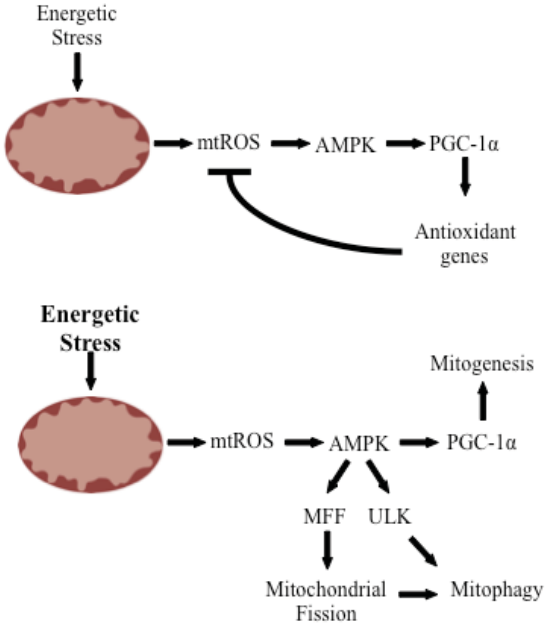

Figure 5.2 Various roles of AMPK in mitochondrial regulation in response to energetic

stress. In response to energetic stress, AMPK signaling causes a series of mitochondria responses, including induction of antioxidant genes, promoting mitochondrial fission, mitophagy, and mitogenesis.

5.3.2 High and low AMPK activity lead to a ROS-induced Warburg effect

Increased AMPK activity promotes the Warburg effect. Recent work by Yan et al. demonstrated that loss of the tumour suppressor folliculin results in constitutive activation of AMPK. This AMPK hyper-activation promoted increased mitochondrial biogenesis, glycolysis, and resulted in ROS-dependent HIF-1α stabilization. Similarly, a recent paper by Hart et al. has shown that overexpression of SOD2 causes increased H_2O_2, which enhances AMPK activity and promotes a shift from oxidative phosphorylation to glycolysis. Constant over-activation of AMPK can lead to increased numbers of mitochondria and increased oxygen consumption. These changes can in turn increase intracellular ROS levels (Yan et al., 2014). Similarly, constant ROS production by SOD2 overexpression can chronically activate AMPK. It would be pertinent to see if HIF-1α levels were changed in this study, as the high levels of ROS, decrease in oxygen consumption and increased glycolysis point to canonical HIF-1α activity. Taken together, these studies show that highly active AMPK promotes the Warburg effect.

Decreased AMPK activity promotes the Warburg effect. How then can these results be reconciled with data displayed in Chapters 2 and 4, wherein the absence of AMPK promotes the same glycolytic metabolism through aberrant mitochondrial ROS levels? In these chapters we propose that AMPK acts as an oxidative stress rheostat. Activation of AMPK acts to reduce ROS levels through various mechanisms. In the absence of AMPK, this checkpoint on ROS levels is lost, causing consistently elevated ROS levels, which promote a HIF-1α-driven Warburg effect.

These studies show opposite ends of the spectrum of AMPK activity and ROS management. Taken together, these results suggest then when AMPK activity is pushed to either extreme, the aberrant levels of mitochondrial ROS result in the stabilization of HIF-1α, which in turn promotes the Warburg effect. This concept is summarized in Figure 5.2.

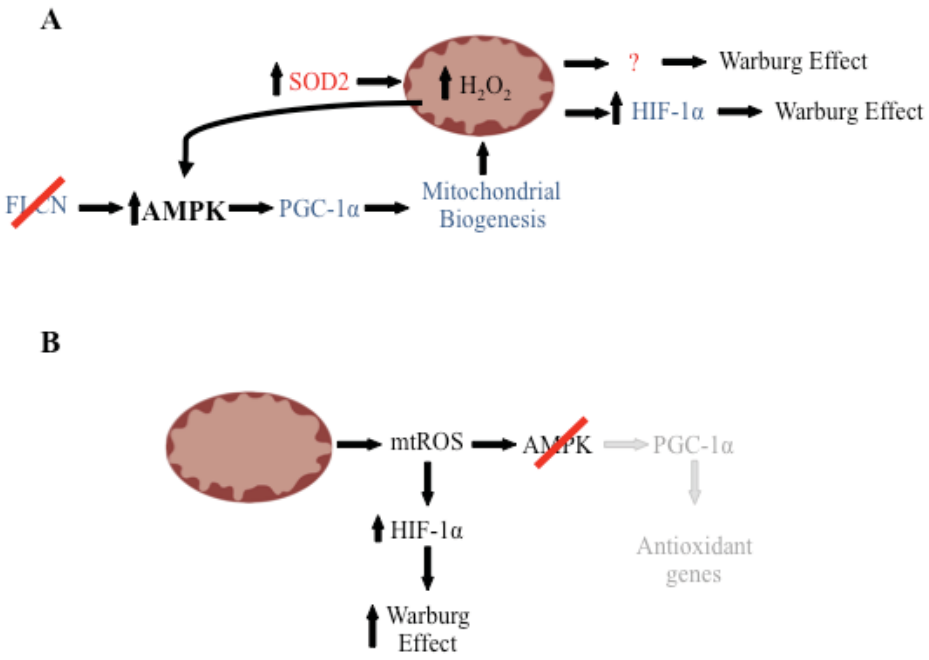

Figure 5.3 Both hyperactive and AMPK-null cells lead to the Warburg effect. A) Chronically active AMPK leads to the Warburg effect. Observations unique from Hart et al are shown in red. Observations unique to Yan et al. are shown in blue. Shared traits are in black. **B)** Loss of AMPK results in elevated mitochondrial ROS that promotes the Warburg effect through HIF-1α.

5.4 Future Directions.

In our initial evaluation of the effects of AMPK loss on cancer metabolism we panelled a wide array of intra- and extra-cellular metabolites via numerous methods, including nuclear

magnetic resonance (NMR), GC-MS, Seahorse, and metabolic assays. This panel of analyses provided interesting data sets that were beyond the scope of the questions examined in Chapters 2-4. Similarly, several phenotypes were observed in both the cellular and mouse models that have either spawned new projects in the lab or remained unexplored. Several of the unexplored observations are as follows.

5.4.1 Inhibited AMPK activity: A putative role in cachexia?

Cachexia is defined by a loss of weight and muscle atrophy that cannot be corrected by nutritional intervention. Though the underlying mechanisms remain unknown, much of the focus of cancer cachexia has examined impaired functionality of mTOR in these models, due to inflammation or AMPK signaling (Manne et al., 2013; White et al., 2013). An early observation in our work hinted at the potential of the role of AMPK in cachexia. Cells lacking AMPK display a large intracellular decrease of a variety of amino acids (i.e., aspartate, proline), and mild increases of extracellular amino acids. This result could putatively be correlated to a lack of AMPK-mediated regulation on mTOR. In the absence of the negative regulation of mTOR by AMPK there is increased mRNA translation, and a concomitant decrease of available amino acids. A far more significant observation was reached in the AMPK-null mouse model. Mice featuring Eμ-MYC-$\alpha1^{-/-}$ lymphoma exhibited an extreme cachexia phenotype compared to Eμ-MYC $\alpha1^{+/+}$ mice. Mice bearing Eμ-MYC-$\alpha1^{-/-}$ tumours developed cachexia regardless of the genetic background of the mouse itself. Taken together, these data suggest that AMPK may feature a regulatory role of amino acids (putatively through mTOR) in non-transformed cells. This regulation may also be driving observed cachexia in the Eμ-MYC-$\alpha1^{-/-}$ model.

5.4.2 New potential metabolic pathways regulated by AMPK.

While the work presented in this thesis has been focused on the Warburg effect, there has been an increasing appreciation for alternative metabolic fuels in cancer. Many studies show that cancer cells can utilize a variety of fuels in culture, which argues that *in vivo* cancer cell metabolism can be heavily influenced by nutrient availability of the local microenvironment (Mashimo et al., 2014). In our early screens of metabolic changes induced by AMPK loss, metabolites such as acetate and choline were vastly changed in cells lacking AMPK. To date, there exists little to no evidence for a role of AMPK in the management of these metabolites. However, given the ability of AMPK to engage different metabolic pathways in order to ensure cell survival, exploration of this potential may be warranted. These metabolites are of particular interest, as they have recently been demonstrated to have significant roles in tumours. For instance, both glioblastomas and brain metastases from different tissues of origin showed a dependence on acetate when in the brain in both humans and mice (Comerford et al., 2014; Mashimo et al., 2014). Similarly, prostate cancers have shown to increase choline uptake, which is utilized both as a diagnostic marker and for PET-CT visualization. The metabolic consequences of this uptake remain unexplored, but may be related to the creation of phospholipids.

5.4.3 Evaluating the role of AMPK-dependent effects on metabolism in vivo.

Extensive research has focused on a better understanding of the energy metabolism of cancer cells. It is clear that rapidly dividing cells require various metabolites that extend beyond the need of ATP to generate the necessary macromolecules for growth and proliferation (Vander Heiden et al., 2009). The molecular mechanisms driving these effects continue to be elucidated,

and certain therapeutic vulnerabilities are being exploited. For the field of cancer metabolism to progress, this same rigour of molecular and mechanistic evaluation must be utilized in *in vivo* systems.

Given the central role of AMPK in the management of metabolic stress in the tumour microenvironment, analyzing *in vivo* metabolism of tumours with and without AMPK expression would be instrumental in advancing this work. One of the more diverse methods of *in vivo* analysis is magnetic resonance spectroscopy (MRS). MRS is an analytical technique complimentary to magnetic resonance imaging that can be used to determine the relative quantitation of metabolites *in vivo*. Due to the complexity of metabolic systems, tracer molecules of stable isotopes are often employed, such as ^{1}H and ^{13}C. MRS can visualize metabolites by specific chemical shifts, and they are identified by their unique set of peaks. The goal of this work would be to examine the same metabolic profile of cells with and without AMPK in an *in vivo* system. If AMPK activity correlates with the observed metabolic changes from our initial screens, expanding upon this work with AMPK activators in vivo and tumour outcome would be of great interest.

5.4.4 Therapeutic advances by targeting AMPK.

The work presented here can serve as the basis for multiple new branches of study, including technologically and therapeutically. AMPK remains an attractive therapeutic target in cancer, including drugs inducing activation and testing drugs capable of AMPK inhibition. To date, the inhibitor Compound C was the only pharmacological inhibitor of AMPK. However the drug is very promiscuous, inhibiting a wide variety of kinases. Sunitinib was recently identified as being able to inhibit AMPK activity (Kerkela et al., 2009; Laderoute et al., 2010) and may be

of use experimentally, though selective inhibitors of AMPK are still in development. Inhibition of AMPK activity, as shown in our work, promotes growth and metabolism of tumours. However, the inhibition of AMPK also removes the metabolic flexibility of tumours when faced with energetic stress. By inhibiting this key adaptive pathway, tumours may be forced into energetic crisis. Further understanding of the state of tumour growth and level of AMPK activity will be instrumental in advancing these pharmacologic possibilities.

5.4.5 AMPK and metabolic adaptation.

AMPK can cause metabolic adaptation on several time intervals. Short-term adaptation via phosphorylation and regulation of a variety of cell processes can occur on the order of hours. Inducing transcriptional changes, whether through activation of transcription factors such as PGC-1α, FOXO, and direct histone phosphorylation via H2B can affect long-term changes (hours-days), such as protein levels, mitochondrial biogenesis, etc. It may be of interest to examine the ability of AMPK to affect changes on an epigenetic level. There is increasing appreciation between the dynamic regulation of cellular metabolism on epigenetics, including how metabolic intermediates can influence histone modifications such as acetylation, as the production of acetyl-coA from citrate provides a large pool of resources to be used in acetylation marks on histones (Wellen et al., 2009).

Preliminary data from our lab indicates that AMPK may play a role in the regulation of trimethylation marks on histones. Cells lacking AMPK featured higher levels of trimethylation marks on histone resides associated with increased transcription. Under conditions of repeated nutrient stress (glucose withdrawal), cells lacking AMPK were unable to decrease these trimethylation marks. Examining these effects in a cancer model, where tumours undergo cycles

of starvation and nutrient replete conditions, may elucidate unique levels of AMPK-dependent regulation to metabolic stress.

5.5 Summary.

This thesis explores the role of AMPK in cancer metabolism. Here it is established that AMPK loss promotes tumour formation and growth in MYC-driven lymphoma, and does so through HIF-1α-driven Warburg metabolism. It is observed the LKB1 loss largely recapitulates the phenotype of AMPK loss, with few key differences. Importantly, the metabolic phenotype induced by LKB1 loss was also driven by HIF-1α. The mechanism of HIF-1α stabilization appears to be driven by mitochondrial ROS, which hints at an under-appreciated role of AMPK activation by physiological levels of ROS. This work adds to the growing body of evidence that AMPK plays a key, context-dependent role in cancer metabolism.

References

Adams, J.M., Harris, A.W., Pinkert, C.A., Corcoran, L.M., Alexander, W.S., Cory, S., Palmiter, R.D., and Brinster, R.L. (1985). The c-myc oncogene driven by immunoglobulin enhancers induces lymphoid malignancy in transgenic mice. Nature *318*, 533-538.

Alessi, D.R., Sakamoto, K., and Bayascas, J.R. (2006). LKB1-dependent signaling pathways. Annu Rev Biochem *75*, 137-163.

Andrzejewski, S., Gravel, S.P., Pollak, M., and St-Pierre, J. (2014). Metformin directly acts on mitochondria to alter cellular bioenergetics. Cancer & metabolism *2*, 12.

Antico Arciuch, V.G., Russo, M.A., Kang, K.S., and Di Cristofano, A. (2013). Inhibition of AMPK and Krebs cycle gene expression drives metabolic remodeling of Pten-deficient preneoplastic thyroid cells. Cancer Res *73*, 5459-5472.

Aon, M.A., Cortassa, S., and O'Rourke, B. (2010). Redox-optimized ROS balance: a unifying hypothesis. Biochim Biophys Acta *1797*, 865-877.

Apfeld, J., O'Connor, G., McDonagh, T., DiStefano, P.S., and Curtis, R. (2004). The AMP-activated protein kinase AAK-2 links energy levels and insulin-like signals to lifespan in C. elegans. Genes Dev *18*, 3004-3009.

Appleyard, M.V., Murray, K.E., Coates, P.J., Wullschleger, S., Bray, S.E., Kernohan, N.M., Fleming, S., Alessi, D.R., and Thompson, A.M. (2012). Phenformin as prophylaxis and therapy in breast cancer xenografts. Br J Cancer *106*, 1117-1122.

Ashrafian, H., O'Flaherty, L., Adam, J., Steeples, V., Chung, Y.L., East, P., Vanharanta, S., Lehtonen, H., Nye, E., Hatipoglu, E., et al. (2010). Expression profiling in progressive stages of fumarate-hydratase deficiency: the contribution of metabolic changes to tumorigenesis. Cancer Res *70*, 9153-9165.

Auciello, F.R., Ross, F.A., Ikematsu, N., and Hardie, D.G. (2014). Oxidative stress activates AMPK in cultured cells primarily by increasing cellular AMP and/or ADP. FEBS Lett *588*, 3361-3366.

Avizienyte, E., Loukola, A., Roth, S., Hemminki, A., Tarkkanen, M., Salovaara, R., Arola, J., Butzow, R., Husgafvel-Pursiainen, K., Kokkola, A., et al. (1999). LKB1 somatic mutations in sporadic tumors. Am J Pathol *154*, 677-681.

Baba, M., Hong, S.B., Sharma, N., Warren, M.B., Nickerson, M.L., Iwamatsu, A., Esposito, D., Gillette, W.K., Hopkins, R.F., 3rd, Hartley, J.L., et al. (2006). Folliculin encoded by the BHD gene interacts with a binding protein, FNIP1, and AMPK, and is involved in AMPK and mTOR signaling. Proc Natl Acad Sci U S A *103*, 15552-15557.

Bateman, A. (1997). The structure of a domain common to archaebacteria and the homocystinuria disease protein. Trends Biochem Sci *22*, 12-13.

Baysal, B.E., Ferrell, R.E., Willett-Brozick, J.E., Lawrence, E.C., Myssiorek, D., Bosch, A., van der Mey, A., Taschner, P.E., Rubinstein, W.S., Myers, E.N., et al. (2000). Mutations in SDHD, a mitochondrial complex II gene, in hereditary paraganglioma. Science *287*, 848-851.

Beale, E.G. (2008). 5'-AMP-activated protein kinase signaling in Caenorhabditis elegans. Experimental biology and medicine *233*, 12-20.

Beg, Z.H., Allmann, D.W., and Gibson, D.M. (1973). Modulation of 3-hydroxy-3-methylglutaryl coenzyme A reductase activity with cAMP and wth protein fractions of rat liver cytosol. Biochem Biophys Res Commun *54*, 1362-1369.

Bell, E.L., Klimova, T.A., Eisenbart, J., Moraes, C.T., Murphy, M.P., Budinger, G.R., and Chandel, N.S. (2007). The Qo site of the mitochondrial complex III is required for the

transduction of hypoxic signaling via reactive oxygen species production. The Journal of cell biology *177*, 1029-1036.

Berg, J.T., JL. Stryer, L. (2012). Biochemistry. (New York: W.H. Freeman).

Bergstrom, J., Furst, P., Noree, L.O., and Vinnars, E. (1974). Intracellular free amino acid concentration in human muscle tissue. J Appl Physiol *36*, 693-697.

Blodgett, T.M., Meltzer, C.C., and Townsend, D.W. (2007). PET/CT: form and function. Radiology *242*, 360-385.

Bordo, D., Djinovic, K., and Bolognesi, M. (1994). Conserved patterns in the Cu,Zn superoxide dismutase family. Journal of molecular biology *238*, 366-386.

Boudeau, J., Sapkota, G., and Alessi, D.R. (2003). LKB1, a protein kinase regulating cell proliferation and polarity. FEBS Lett *546*, 159-165.

Brand, M.D. (2010). The sites and topology of mitochondrial superoxide production. Experimental gerontology *45*, 466-472.

Brugarolas, J.B., Vazquez, F., Reddy, A., Sellers, W.R., and Kaelin, W.G., Jr. (2003). TSC2 regulates VEGF through mTOR-dependent and -independent pathways. Cancer Cell *4*, 147-158.

Brunelle, J.K., Bell, E.L., Quesada, N.M., Vercauteren, K., Tiranti, V., Zeviani, M., Scarpulla, R.C., and Chandel, N.S. (2005a). Oxygen sensing requires mitochondrial ROS but not oxidative phosphorylation. Cell Metab *1*, 409-414.

Brunelle, J.K., Bell, E.L., Quesada, N.M., Vercauteren, K., Tiranti, V., Zeviani, M., Scarpulla, R.C., and Chandel, N.S. (2005b). Oxygen sensing requires mitochondrial ROS but not oxidative phosphorylation. Cell Metab *1*, 409-414.

Bungard, D., Fuerth, B.J., Zeng, P.Y., Faubert, B., Maas, N.L., Viollet, B., Carling, D., Thompson, C.B., Jones, R.G., and Berger, S.L. (2010). Signaling kinase AMPK activates stress-promoted transcription via histone H2B phosphorylation. Science *329*, 1201-1205.

Butow, R.A., and Avadhani, N.G. (2004). Mitochondrial signaling: the retrograde response. Mol Cell *14*, 1-15.

Buzzai, M., Jones, R.G., Amaravadi, R.K., Lum, J.J., DeBerardinis, R.J., Zhao, F., Viollet, B., and Thompson, C.B. (2007). Systemic treatment with the antidiabetic drug metformin selectively impairs p53-deficient tumor cell growth. Cancer Res *67*, 6745-6752.

Caino, M.C., Chae, Y.C., Vaira, V., Ferrero, S., Nosotti, M., Martin, N.M., Weeraratna, A., O'Connell, M., Jernigan, D., Fatatis, A., et al. (2013). Metabolic stress regulates cytoskeletal dynamics and metastasis of cancer cells. J Clin Invest *123*, 2907-2920.

Cairns, R.A., Harris, I.S., and Mak, T.W. (2011). Regulation of cancer cell metabolism. Nat Rev Cancer *11*, 85-95.

Cancer Genome Atlas, N. (2012a). Comprehensive molecular characterization of human colon and rectal cancer. Nature *487*, 330-337.

Cancer Genome Atlas, N. (2012b). Comprehensive molecular portraits of human breast tumours. Nature *490*, 61-70.

Cancer Genome Atlas Research, N. (2012). Comprehensive genomic characterization of squamous cell lung cancers. Nature *489*, 519-525.

Carlson, C.A., and Kim, K.H. (1973). Regulation of hepatic acetyl coenzyme A carboxylase by phosphorylation and dephosphorylation. J Biol Chem *248*, 378-380.

Carlson, M., Osmond, B.C., and Botstein, D. (1981). Mutants of yeast defective in sucrose utilization. Genetics *98*, 25-40.

Celenza, J.L., and Carlson, M. (1986). A yeast gene that is essential for release from glucose repression encodes a protein kinase. Science *233*, 1175-1180.

Chan, K.T., Asokan, S.B., King, S.J., Bo, T., Dubose, E.S., Liu, W., Berginski, M.E., Simon, J.M., Davis, I.J., Gomez, S.M., et al. (2014). LKB1 loss in melanoma disrupts directional migration toward extracellular matrix cues. The Journal of cell biology *207*, 299-315.

Chang, C.H., Curtis, J.D., Maggi, L.B., Jr., Faubert, B., Villarino, A.V., O'Sullivan, D., Huang, S.C., van der Windt, G.J., Blagih, J., Qiu, J., et al. (2013). Posttranscriptional control of T cell effector function by aerobic glycolysis. Cell *153*, 1239-1251.

Chatterjee, A., Mambo, E., and Sidransky, D. (2006). Mitochondrial DNA mutations in human cancer. Oncogene *25*, 4663-4674.

Cheng, H., Liu, P., Wang, Z.C., Zou, L., Santiago, S., Garbitt, V., Gjoerup, O.V., Iglehart, J.D., Miron, A., Richardson, A.L., et al. (2009). SIK1 couples LKB1 to p53-dependent anoikis and suppresses metastasis. Sci Signal *2*, ra35.

Choi, S.L., Kim, S.J., Lee, K.T., Kim, J., Mu, J., Birnbaum, M.J., Soo Kim, S., and Ha, J. (2001). The regulation of AMP-activated protein kinase by H(2)O(2). Biochem Biophys Res Commun *287*, 92-97.

Choo, A.Y., Yoon, S.O., Kim, S.G., Roux, P.P., and Blenis, J. (2008). Rapamycin differentially inhibits S6Ks and 4E-BP1 to mediate cell-type-specific repression of mRNA translation. Proc Natl Acad Sci U S A *105*, 17414-17419.

Cockman, M.E., Masson, N., Mole, D.R., Jaakkola, P., Chang, G.W., Clifford, S.C., Maher, E.R., Pugh, C.W., Ratcliffe, P.J., and Maxwell, P.H. (2000). Hypoxia inducible factor-alpha binding and ubiquitylation by the von Hippel-Lindau tumor suppressor protein. J Biol Chem *275*, 25733-25741.

Comerford, S.A., Huang, Z., Du, X., Wang, Y., Cai, L., Witkiewicz, A.K., Walters, H., Tantawy, M.N., Fu, A., Manning, H.C., et al. (2014). Acetate dependence of tumors. Cell *159*, 1591-1602.

Contreras, C.M., Gurumurthy, S., Haynie, J.M., Shirley, L.J., Akbay, E.A., Wingo, S.N., Schorge, J.O., Broaddus, R.R., Wong, K.K., Bardeesy, N., et al. (2008). Loss of Lkb1 provokes highly invasive endometrial adenocarcinomas. Cancer Res *68*, 759-766.

Cool, B., Zinker, B., Chiou, W., Kifle, L., Cao, N., Perham, M., Dickinson, R., Adler, A., Gagne, G., Iyengar, R., et al. (2006). Identification and characterization of a small molecule AMPK activator that treats key components of type 2 diabetes and the metabolic syndrome. Cell Metab *3*, 403-416.

Corradetti, M.N., Inoki, K., Bardeesy, N., DePinho, R.A., and Guan, K.L. (2004). Regulation of the TSC pathway by LKB1: evidence of a molecular link between tuberous sclerosis complex and Peutz-Jeghers syndrome. Genes Dev *18*, 1533-1538.

Cortassa, S., O'Rourke, B., and Aon, M.A. (2014). Redox-optimized ROS balance and the relationship between mitochondrial respiration and ROS. Biochim Biophys Acta *1837*, 287-295.

Corton, J.M., Gillespie, J.G., Hawley, S.A., and Hardie, D.G. (1995). 5-aminoimidazole-4-carboxamide ribonucleoside. A specific method for activating AMP-activated protein kinase in intact cells? Eur J Biochem *229*, 558-565.

Cox, A.G., Winterbourn, C.C., and Hampton, M.B. (2010). Mitochondrial peroxiredoxin involvement in antioxidant defence and redox signalling. Biochem J *425*, 313-325.

Crighton, D., Wilkinson, S., O'Prey, J., Syed, N., Smith, P., Harrison, P.R., Gasco, M., Garrone, O., Crook, T., and Ryan, K.M. (2006). DRAM, a p53-induced modulator of autophagy, is critical for apoptosis. Cell *126*, 121-134.

Cross, C.E., Halliwell, B., Borish, E.T., Pryor, W.A., Ames, B.N., Saul, R.L., McCord, J.M., and Harman, D. (1987). Oxygen radicals and human disease. Annals of internal medicine *107*, 526-545.

Curtis, R., O'Connor, G., and DiStefano, P.S. (2006). Aging networks in Caenorhabditis elegans: AMP-activated protein kinase (aak-2) links multiple aging and metabolism pathways. Aging Cell *5*, 119-126.

Dagon, Y., Hur, E., Zheng, B., Wellenstein, K., Cantley, L.C., and Kahn, B.B. (2012). p70S6 kinase phosphorylates AMPK on serine 491 to mediate leptin's effect on food intake. Cell Metab *16*, 104-112.

Dang, C.V. (1999). c-Myc target genes involved in cell growth, apoptosis, and metabolism. Mol Cell Biol *19*, 1-11.

Dang, C.V. (2010). Glutaminolysis: supplying carbon or nitrogen or both for cancer cells? Cell Cycle *9*, 3884-3886.

Dang, L., White, D.W., Gross, S., Bennett, B.D., Bittinger, M.A., Driggers, E.M., Fantin, V.R., Jang, H.G., Jin, S., Keenan, M.C., et al. (2009). Cancer-associated IDH1 mutations produce 2-hydroxyglutarate. Nature *462*, 739-744.

Davies, S.P., Sim, A.T., and Hardie, D.G. (1990). Location and function of three sites phosphorylated on rat acetyl-CoA carboxylase by the AMP-activated protein kinase. Eur J Biochem *187*, 183-190.

DeBerardinis, R.J., Lum, J.J., Hatzivassiliou, G., and Thompson, C.B. (2008a). The biology of cancer: metabolic reprogramming fuels cell growth and proliferation. Cell Metab *7*, 11-20.

DeBerardinis, R.J., Mancuso, A., Daikhin, E., Nissim, I., Yudkoff, M., Wehrli, S., and Thompson, C.B. (2007). Beyond aerobic glycolysis: transformed cells can engage in glutamine

metabolism that exceeds the requirement for protein and nucleotide synthesis. Proc Natl Acad Sci U S A *104*, 19345-19350.

Deberardinis, R.J., Sayed, N., Ditsworth, D., and Thompson, C.B. (2008b). Brick by brick: metabolism and tumor cell growth. Curr Opin Genet Dev *18*, 54-61.

Decensi, A., Puntoni, M., Goodwin, P., Cazzaniga, M., Gennari, A., Bonanni, B., and Gandini, S. (2010). Metformin and cancer risk in diabetic patients: a systematic review and meta-analysis. Cancer Prev Res (Phila) *3*, 1451-1461.

Din, F.V., Valanciute, A., Houde, V.P., Zibrova, D., Green, K.A., Sakamoto, K., Alessi, D.R., and Dunlop, M.G. (2012). Aspirin inhibits mTOR signaling, activates AMP-activated protein kinase, and induces autophagy in colorectal cancer cells. Gastroenterology *142*, 1504-1515 e1503.

Ding, L., Getz, G., Wheeler, D.A., Mardis, E.R., McLellan, M.D., Cibulskis, K., Sougnez, C., Greulich, H., Muzny, D.M., Morgan, M.B., et al. (2008). Somatic mutations affect key pathways in lung adenocarcinoma. Nature *455*, 1069-1075.

Dizdaroglu, M., and Jaruga, P. (2012). Mechanisms of free radical-induced damage to DNA. Free radical research *46*, 382-419.

Dong, L.X., Sun, L.L., Zhang, X., Pan, L., Lian, L.J., Chen, Z., and Zhong, D.S. (2013). Negative regulation of mTOR activity by LKB1-AMPK signaling in non-small cell lung cancer cells. Acta pharmacologica Sinica *34*, 314-318.

Ducommun, S., Deak, M., Sumpton, D., Ford, R.J., Nunez Galindo, A., Kussmann, M., Viollet, B., Steinberg, G.R., Foretz, M., Dayon, L., et al. (2015). Motif affinity and mass spectrometry proteomic approach for the discovery of cellular AMPK targets: Identification of mitochondrial fission factor as a new AMPK substrate. Cell Signal.

Dupuy, F., Griss, T., Blagih, J., Bridon, G., Avizonis, D., Ling, C., Dong, Z., Siwak, D.R., Annis, M.G., Mills, G.B., et al. (2013). LKB1 is a central regulator of tumor initiation and pro-growth metabolism in ErbB2-mediated breast cancer. Cancer & metabolism *1*, 18.

Duvel, K., Yecies, J.L., Menon, S., Raman, P., Lipovsky, A.I., Souza, A.L., Triantafellow, E., Ma, Q., Gorski, R., Cleaver, S., et al. (2010). Activation of a metabolic gene regulatory network downstream of mTOR complex 1. Mol Cell *39*, 171-183.

Dykens, J.A., Jamieson, J., Marroquin, L., Nadanaciva, S., Billis, P.A., and Will, Y. (2008). Biguanide-induced mitochondrial dysfunction yields increased lactate production and cytotoxicity of aerobically-poised HepG2 cells and human hepatocytes in vitro. Toxicology and applied pharmacology *233*, 203-210.

Egan, D.F., Shackelford, D.B., Mihaylova, M.M., Gelino, S., Kohnz, R.A., Mair, W., Vasquez, D.S., Joshi, A., Gwinn, D.M., Taylor, R., et al. (2011). Phosphorylation of ULK1 (hATG1) by AMP-activated protein kinase connects energy sensing to mitophagy. Science *331*, 456-461.

El-Masry, O.S., Brown, B.L., and Dobson, P.R. (2012). Effects of activation of AMPK on human breast cancer cell lines with different genetic backgrounds. Oncol Lett *3*, 224-228.

El-Mir, M.Y., Nogueira, V., Fontaine, E., Averet, N., Rigoulet, M., and Leverve, X. (2000). Dimethylbiguanide inhibits cell respiration via an indirect effect targeted on the respiratory chain complex I. J Biol Chem *275*, 223-228.

Elder, D.J., Hague, A., Hicks, D.J., and Paraskeva, C. (1996). Differential growth inhibition by the aspirin metabolite salicylate in human colorectal tumor cell lines: enhanced apoptosis in carcinoma and in vitro-transformed adenoma relative to adenoma relative to adenoma cell lines. Cancer Res *56*, 2273-2276.

Elstrom, R.L., Bauer, D.E., Buzzai, M., Karnauskas, R., Harris, M.H., Plas, D.R., Zhuang, H., Cinalli, R.M., Alavi, A., Rudin, C.M., et al. (2004). Akt stimulates aerobic glycolysis in cancer cells. Cancer Res *64*, 3892-3899.

Emerling, B.M., Weinberg, F., Snyder, C., Burgess, Z., Mutlu, G.M., Viollet, B., Budinger, G.R., and Chandel, N.S. (2009). Hypoxic activation of AMPK is dependent on mitochondrial ROS but independent of an increase in AMP/ATP ratio. Free radical biology & medicine *46*, 1386-1391.

Engelman, J.A., Luo, J., and Cantley, L.C. (2006). The evolution of phosphatidylinositol 3-kinases as regulators of growth and metabolism. Nature reviews. Genetics *7*, 606-619.

Evans, J.M., Donnelly, L.A., Emslie-Smith, A.M., Alessi, D.R., and Morris, A.D. (2005). Metformin and reduced risk of cancer in diabetic patients. BMJ *330*, 1304-1305.

Faubert, B., Boily, G., Izreig, S., Griss, T., Samborska, B., Dong, Z., Dupuy, F., Chambers, C., Fuerth, B.J., Viollet, B., et al. (2013). AMPK is a negative regulator of the Warburg effect and suppresses tumor growth in vivo. Cell Metab *17*, 113-124.

Faubert, B., Vincent, E.E., Griss, T., Samborska, B., Izreig, S., Svensson, R.U., Mamer, O.A., Avizonis, D., Shackelford, D.B., Shaw, R.J., et al. (2014). Loss of the tumor suppressor LKB1 promotes metabolic reprogramming of cancer cells via HIF-1alpha. Proc Natl Acad Sci U S A *111*, 2554-2559.

Ferrannini, E. (2014). The target of metformin in type 2 diabetes. N Engl J Med *371*, 1547-1548.

Ferrer, A., Caelles, C., Massot, N., and Hegardt, F.G. (1985). Activation of rat liver cytosolic 3-hydroxy-3-methylglutaryl coenzyme A reductase kinase by adenosine 5'-monophosphate. Biochem Biophys Res Commun *132*, 497-504.

Ferrer, C.M., Lynch, T.P., Sodi, V.L., Falcone, J.N., Schwab, L.P., Peacock, D.L., Vocadlo, D.J., Seagroves, T.N., and Reginato, M.J. (2014). O-GlcNAcylation regulates cancer metabolism and survival stress signaling via regulation of the HIF-1 pathway. Mol Cell *54*, 820-831.

Folch, J., Ascoli, I., Lees, M., Meath, J.A., and Le, B.N. (1951). Preparation of lipide extracts from brain tissue. J Biol Chem *191*, 833-841.

Fox, M.M., Phoenix, K.N., Kopsiaftis, S.G., and Claffey, K.P. (2013). AMP-Activated Protein Kinase alpha 2 Isoform Suppression in Primary Breast Cancer Alters AMPK Growth Control and Apoptotic Signaling. Genes & cancer *4*, 3-14.

Frigo, D.E., Howe, M.K., Wittmann, B.M., Brunner, A.M., Cushman, I., Wang, Q., Brown, M., Means, A.R., and McDonnell, D.P. (2011). CaM kinase kinase beta-mediated activation of the growth regulatory kinase AMPK is required for androgen-dependent migration of prostate cancer cells. Cancer Res *71*, 528-537.

Fu, J., Jin, J., Cichewicz, R.H., Hageman, S.A., Ellis, T.K., Xiang, L., Peng, Q., Jiang, M., Arbez, N., Hotaling, K., et al. (2012). trans-(-)-epsilon-Viniferin increases mitochondrial sirtuin 3 (SIRT3), activates AMP-activated protein kinase (AMPK), and protects cells in models of Huntington Disease. J Biol Chem *287*, 24460-24472.

Fung, C., Lock, R., Gao, S., Salas, E., and Debnath, J. (2008). Induction of autophagy during extracellular matrix detachment promotes cell survival. Mol Biol Cell *19*, 797-806.

Garami, A., Zwartkruis, F.J., Nobukuni, T., Joaquin, M., Roccio, M., Stocker, H., Kozma, S.C., Hafen, E., Bos, J.L., and Thomas, G. (2003). Insulin activation of Rheb, a mediator of mTOR/S6K/4E-BP signaling, is inhibited by TSC1 and 2. Mol Cell *11*, 1457-1466.

Gatenby, R.A., and Gillies, R.J. (2008). A microenvironmental model of carcinogenesis. Nat Rev Cancer *8*, 56-61.

Gaude, E., and Frezza, C. (2014). Defects in mitochondrial metabolism and cancer. Cancer & metabolism *2*, 10.

Gerencser, A.A., Neilson, A., Choi, S.W., Edman, U., Yadava, N., Oh, R.J., Ferrick, D.A., Nicholls, D.G., and Brand, M.D. (2009). Quantitative microplate-based respirometry with correction for oxygen diffusion. Analytical chemistry *81*, 6868-6878.

Giardiello, F.M., Welsh, S.B., Hamilton, S.R., Offerhaus, G.J., Gittelsohn, A.M., Booker, S.V., Krush, A.J., Yardley, J.H., and Luk, G.D. (1987). Increased risk of cancer in the Peutz-Jeghers syndrome. N Engl J Med *316*, 1511-1514.

Giatromanolaki, A., Koukourakis, M.I., Sivridis, E., Turley, H., Talks, K., Pezzella, F., Gatter, K.C., and Harris, A.L. (2001). Relation of hypoxia inducible factor 1 alpha and 2 alpha in operable non-small cell lung cancer to angiogenic/molecular profile of tumours and survival. Br J Cancer *85*, 881-890.

Gimm, O., Armanios, M., Dziema, H., Neumann, H.P., and Eng, C. (2000). Somatic and occult germ-line mutations in SDHD, a mitochondrial complex II gene, in nonfamilial pheochromocytoma. Cancer Res *60*, 6822-6825.

Giordanetto, F., and Karis, D. (2012). Direct AMP-activated protein kinase activators: a review of evidence from the patent literature. Expert Opin Ther Pat *22*, 1467-1477.

Godlewski, J., Nowicki, M.O., Bronisz, A., Nuovo, G., Palatini, J., De Lay, M., Van Brocklyn, J., Ostrowski, M.C., Chiocca, E.A., and Lawler, S.E. (2010). MicroRNA-451 regulates LKB1/AMPK signaling and allows adaptation to metabolic stress in glioma cells. Mol Cell *37*, 620-632.

Gordan, J.D., and Simon, M.C. (2007). Hypoxia-inducible factors: central regulators of the tumor phenotype. Curr Opin Genet Dev *17*, 71-77.

Gordon, A.E., and Frigerio, A. (1972). Mass fragmentography as an application of gas-liquid chromatography-mass spectrometry in biological research. Journal of chromatography *73*, 401-417.

Gough, D.R., and Cotter, T.G. (2011). Hydrogen peroxide: a Jekyll and Hyde signalling molecule. Cell death & disease *2*, e213.

Greer, E.L., Oskoui, P.R., Banko, M.R., Maniar, J.M., Gygi, M.P., Gygi, S.P., and Brunet, A. (2007). The energy sensor AMP-activated protein kinase directly regulates the mammalian FOXO3 transcription factor. J Biol Chem *282*, 30107-30119.

Guertin, D.A., and Sabatini, D.M. (2007). Defining the role of mTOR in cancer. Cancer Cell *12*, 9-22.

Guo, C., Pirozzi, C.J., Lopez, G.Y., and Yan, H. (2011). Isocitrate dehydrogenase mutations in gliomas: mechanisms, biomarkers and therapeutic target. Current opinion in neurology *24*, 648-652.

Guo, S., and Kemphues, K.J. (1995). par-1, a gene required for establishing polarity in C. elegans embryos, encodes a putative Ser/Thr kinase that is asymmetrically distributed. Cell *81*, 611-620.

Guzy, R.D., Hoyos, B., Robin, E., Chen, H., Liu, L., Mansfield, K.D., Simon, M.C., Hammerling, U., and Schumacker, P.T. (2005). Mitochondrial complex III is required for hypoxia-induced ROS production and cellular oxygen sensing. Cell Metab *1*, 401-408.

Gwinn, D.M., Shackelford, D.B., Egan, D.F., Mihaylova, M.M., Mery, A., Vasquez, D.S., Turk, B.E., and Shaw, R.J. (2008). AMPK phosphorylation of raptor mediates a metabolic checkpoint. Mol Cell *30*, 214-226.

Hadad, S.M., Baker, L., Quinlan, P.R., Robertson, K.E., Bray, S.E., Thomson, G., Kellock, D., Jordan, L.B., Purdie, C.A., Hardie, D.G., et al. (2009). Histological evaluation of AMPK signalling in primary breast cancer. BMC cancer *9*, 307.

Halestrap, A.P., and Price, N.T. (1999). The proton-linked monocarboxylate transporter (MCT) family: structure, function and regulation. Biochem J *343 Pt 2*, 281-299.

Hallstrom, T.C., Mori, S., and Nevins, J.R. (2008). An E2F1-dependent gene expression program that determines the balance between proliferation and cell death. Cancer Cell *13*, 11-22.

Han, Y., Wang, Q., Song, P., Zhu, Y., and Zou, M.H. (2010). Redox regulation of the AMP-activated protein kinase. PLoS One *5*, e15420.

Hanahan, D., and Weinberg, R.A. (2011). Hallmarks of cancer: the next generation. Cell *144*, 646-674.

Hanahan, D.a.W., R.A. (2000). The hallmarks of cancer. Cell *100*, 57-70.

Handschin, C., and Spiegelman, B.M. (2006). Peroxisome proliferator-activated receptor gamma coactivator 1 coactivators, energy homeostasis, and metabolism. Endocrine reviews *27*, 728-735.

Hardie, D.G. (2003). Minireview: the AMP-activated protein kinase cascade: the key sensor of cellular energy status. Endocrinology *144*, 5179-5183.

Hardie, D.G. (2007). AMP-activated/SNF1 protein kinases: conserved guardians of cellular energy. Nat Rev Mol Cell Biol *8*, 774-785.

Hardie, D.G. (2011a). AMP-activated protein kinase: an energy sensor that regulates all aspects of cell function. Genes Dev *25*, 1895-1908.

Hardie, D.G. (2011b). Sensing of energy and nutrients by AMP-activated protein kinase. Am J Clin Nutr *93*, 891S-896.

Hardie, D.G., and Alessi, D.R. (2013). LKB1 and AMPK and the cancer-metabolism link - ten years after. BMC biology *11*, 36.

Hardie, D.G., Carling, D., and Carlson, M. (1998). The AMP-activated/SNF1 protein kinase subfamily: metabolic sensors of the eukaryotic cell? Annu Rev Biochem *67*, 821-855.

Hardie, D.G., Carling, D., and Gamblin, S.J. (2011). AMP-activated protein kinase: also regulated by ADP? Trends Biochem Sci *36*, 470-477.

Hardie, D.G., Ross, F.A., and Hawley, S.A. (2012). AMPK: a nutrient and energy sensor that maintains energy homeostasis. Nat Rev Mol Cell Biol *13*, 251-262.

Hart, P.C., Mao, M., de Abreu, A.L., Ansenberger-Fricano, K., Ekoue, D.N., Ganini, D., Kajdacsy-Balla, A., Diamond, A.M., Minshall, R.D., Consolaro, M.E., et al. (2015). MnSOD upregulation sustains the Warburg effect via mitochondrial ROS and AMPK-dependent signalling in cancer. Nature communications *6*, 6053.

Hateboer, G., Timmers, H.T., Rustgi, A.K., Billaud, M., van 't Veer, L.J., and Bernards, R. (1993). TATA-binding protein and the retinoblastoma gene product bind to overlapping epitopes on c-Myc and adenovirus E1A protein. Proc Natl Acad Sci U S A *90*, 8489-8493.

Hatzivassiliou, G., Zhao, F., Bauer, D.E., Andreadis, C., Shaw, A.N., Dhanak, D., Hingorani, S.R., Tuveson, D.A., and Thompson, C.B. (2005). ATP citrate lyase inhibition can suppress tumor cell growth. Cancer Cell *8*, 311-321.

Hawley, S.A., Boudeau, J., Reid, J.L., Mustard, K.J., Udd, L., Makela, T.P., Alessi, D.R., and Hardie, D.G. (2003). Complexes between the LKB1 tumor suppressor, STRADalpha/beta and MO25alpha/beta are upstream kinases in the AMP-activated protein kinase cascade. J Biol *2*, 28.

Hearle, N., Schumacher, V., Menko, F.H., Olschwang, S., Boardman, L.A., Gille, J.J., Keller, J.J., Westerman, A.M., Scott, R.J., Lim, W., et al. (2006a). Frequency and spectrum of cancers in the Peutz-Jeghers syndrome. Clin Cancer Res *12*, 3209-3215.

Hearle, N., Schumacher, V., Menko, F.H., Olschwang, S., Boardman, L.A., Gille, J.J., Keller, J.J., Westerman, A.M., Scott, R.J., Lim, W., et al. (2006b). Frequency and spectrum of cancers in the Peutz-Jeghers syndrome. Clin Cancer Res *12*, 3209-3215.

Hemminki, A., Markie, D., Tomlinson, I., Avizienyte, E., Roth, S., Loukola, A., Bignell, G., Warren, W., Aminoff, M., Hoglund, P., et al. (1998). A serine/threonine kinase gene defective in Peutz-Jeghers syndrome. Nature *391*, 184-187.

Holmstrom, K.M., and Finkel, T. (2014). Cellular mechanisms and physiological consequences of redox-dependent signalling. Nat Rev Mol Cell Biol *15*, 411-421.

Hon, W.C., Wilson, M.I., Harlos, K., Claridge, T.D., Schofield, C.J., Pugh, C.W., Maxwell, P.H., Ratcliffe, P.J., Stuart, D.I., and Jones, E.Y. (2002). Structural basis for the recognition of hydroxyproline in HIF-1 alpha by pVHL. Nature *417*, 975-978.

Horak, P., Crawford, A.R., Vadysirisack, D.D., Nash, Z.M., DeYoung, M.P., Sgroi, D., and Ellisen, L.W. (2010). Negative feedback control of HIF-1 through REDD1-regulated ROS suppresses tumorigenesis. Proc Natl Acad Sci U S A *107*, 4675-4680.

Huang, S., Holzel, M., Knijnenburg, T., Schlicker, A., Roepman, P., McDermott, U., Garnett, M., Grernrum, W., Sun, C., Prahallad, A., et al. (2012). MED12 controls the response to multiple cancer drugs through regulation of TGF-beta receptor signaling. Cell *151*, 937-950.

Huang, X., Wullschleger, S., Shpiro, N., McGuire, V.A., Sakamoto, K., Woods, Y.L., McBurnie, W., Fleming, S., and Alessi, D.R. (2008). Important role of the LKB1-AMPK pathway in suppressing tumorigenesis in PTEN-deficient mice. Biochem J *412*, 211-221.

Imamura, K., Ogura, T., Kishimoto, A., Kaminishi, M., and Esumi, H. (2001). Cell cycle regulation via p53 phosphorylation by a 5'-AMP activated protein kinase activator, 5-aminoimidazole- 4-carboxamide-1-beta-D-ribofuranoside, in a human hepatocellular carcinoma cell line. Biochem Biophys Res Commun *287*, 562-567.

Inbar, L., and Lapidot, A. (1987). 13C-NMR, 1H-NMR and gas-chromatography mass-spectrometry studies of the biosynthesis of 13C-enriched L-lysine by Brevibacterium flavum. Eur J Biochem *162*, 621-633.

Inoki, K., Li, Y., Zhu, T., Wu, J., and Guan, K.L. (2002). TSC2 is phosphorylated and inhibited by Akt and suppresses mTOR signalling. Nat Cell Biol *4*, 648-657.

Inoki, K., Zhu, T., and Guan, K.L. (2003). TSC2 mediates cellular energy response to control cell growth and survival. Cell *115*, 577-590.

Iommarini, L., Kurelac, I., Capristo, M., Calvaruso, M.A., Giorgio, V., Bergamini, C., Ghelli, A., Nanni, P., De Giovanni, C., Carelli, V., et al. (2014). Different mtDNA mutations modify tumor progression in dependence of the degree of respiratory complex I impairment. Human molecular genetics *23*, 1453-1466.

Irrcher, I., Ljubicic, V., and Hood, D.A. (2009). Interactions between ROS and AMP kinase activity in the regulation of PGC-1alpha transcription in skeletal muscle cells. Am J Physiol Cell Physiol *296*, C116-123.

Isaacs, J.S., Jung, Y.J., Mole, D.R., Lee, S., Torres-Cabala, C., Chung, Y.L., Merino, M., Trepel, J., Zbar, B., Toro, J., et al. (2005). HIF overexpression correlates with biallelic loss of fumarate hydratase in renal cancer: novel role of fumarate in regulation of HIF stability. Cancer Cell *8*, 143-153.

Ishikawa, K., Takenaga, K., Akimoto, M., Koshikawa, N., Yamaguchi, A., Imanishi, H., Nakada, K., Honma, Y., and Hayashi, J. (2008). ROS-generating mitochondrial DNA mutations can regulate tumor cell metastasis. Science *320*, 661-664.

Itkonen, H.M., Minner, S., Guldvik, I.J., Sandmann, M.J., Tsourlakis, M.C., Berge, V., Svindland, A., Schlomm, T., and Mills, I.G. (2013). O-GlcNAc transferase integrates metabolic pathways to regulate the stability of c-MYC in human prostate cancer cells. Cancer Res *73*, 5277-5287.

Ivan, M., Kondo, K., Yang, H., Kim, W., Valiando, J., Ohh, M., Salic, A., Asara, J.M., Lane, W.S., and Kaelin, W.G., Jr. (2001). HIFalpha targeted for VHL-mediated destruction by proline hydroxylation: implications for O2 sensing. Science *292*, 464-468.

Izyumov, D.S., Avetisyan, A.V., Pletjushkina, O.Y., Sakharov, D.V., Wirtz, K.W., Chernyak, B.V., and Skulachev, V.P. (2004). "Wages of fear": transient threefold decrease in intracellular ATP level imposes apoptosis. Biochim Biophys Acta *1658*, 141-147.

Jager, S., Handschin, C., St-Pierre, J., and Spiegelman, B.M. (2007). AMP-activated protein kinase (AMPK) action in skeletal muscle via direct phosphorylation of PGC-1alpha. Proc Natl Acad Sci U S A *104*, 12017-12022.

Jain, M., Nilsson, R., Sharma, S., Madhusudhan, N., Kitami, T., Souza, A.L., Kafri, R., Kirschner, M.W., Clish, C.B., and Mootha, V.K. (2012). Metabolite profiling identifies a key role for glycine in rapid cancer cell proliferation. Science *336*, 1040-1044.

Jeon, S.M., Chandel, N.S., and Hay, N. (2012). AMPK regulates NADPH homeostasis to promote tumour cell survival during energy stress. Nature *485*, 661-665.

Ji, H., Ramsey, M.R., Hayes, D.N., Fan, C., McNamara, K., Kozlowski, P., Torrice, C., Wu, M.C., Shimamura, T., Perera, S.A., et al. (2007). LKB1 modulates lung cancer differentiation and metastasis. Nature *448*, 807-810.

Jiang, P., Du, W., Wang, X., Mancuso, A., Gao, X., Wu, M., and Yang, X. (2011). p53 regulates biosynthesis through direct inactivation of glucose-6-phosphate dehydrogenase. Nat Cell Biol *13*, 310-316.

Jin, L., Li, D., Alesi, G.N., Fan, J., Kang, H.B., Lu, Z., Boggon, T.J., Jin, P., Yi, H., Wright, E.R., et al. (2015). Glutamate Dehydrogenase 1 Signals through Antioxidant Glutathione Peroxidase 1 to Regulate Redox Homeostasis and Tumor Growth. Cancer Cell *27*, 257-270.

Jones, R.G., Plas, D.R., Kubek, S., Buzzai, M., Mu, J., Xu, Y., Birnbaum, M.J., and Thompson, C.B. (2005). AMP-activated protein kinase induces a p53-dependent metabolic checkpoint. Mol Cell *18*, 283-293.

Jones, R.G., and Thompson, C.B. (2009). Tumor suppressors and cell metabolism: a recipe for cancer growth. Genes Dev *23*, 537-548.

Jorgensen, S.B., Viollet, B., Andreelli, F., Frosig, C., Birk, J.B., Schjerling, P., Vaulont, S., Richter, E.A., and Wojtaszewski, J.F. (2004). Knockout of the alpha2 but not alpha1 5'-AMP-activated protein kinase isoform abolishes 5-aminoimidazole-4-carboxamide-1-beta-4-ribofuranosidebut not contraction-induced glucose uptake in skeletal muscle. J Biol Chem *279*, 1070-1079.

Kalderon, B., Lapidot, A., Korman, S.H., and Gutman, A. (1988). Glucose recycling and production in children with glycogen storage disease type I, studied by gas chromatography/mass spectrometry and (U-13C)glucose. Biomedical & environmental mass spectrometry *16*, 305-308.

Kalender, A., Selvaraj, A., Kim, S.Y., Gulati, P., Brule, S., Viollet, B., Kemp, B.E., Bardeesy, N., Dennis, P., Schlager, J.J., et al. (2010). Metformin, independent of AMPK, inhibits mTORC1 in a rag GTPase-dependent manner. Cell Metab *11*, 390-401.

Kato, K., Ogura, T., Kishimoto, A., Minegishi, Y., Nakajima, N., Miyazaki, M., and Esumi, H. (2002). Critical roles of AMP-activated protein kinase in constitutive tolerance of cancer cells to nutrient deprivation and tumor formation. Oncogene *21*, 6082-6090.

Keith, B., Johnson, R.S., and Simon, M.C. (2012). HIF1alpha and HIF2alpha: sibling rivalry in hypoxic tumour growth and progression. Nat Rev Cancer *12*, 9-22.

Kerkela, R., Woulfe, K.C., Durand, J.B., Vagnozzi, R., Kramer, D., Chu, T.F., Beahm, C., Chen, M.H., and Force, T. (2009). Sunitinib-induced cardiotoxicity is mediated by off-target inhibition of AMP-activated protein kinase. Clinical and translational science *2*, 15-25.

Kil, I.S., Kim, S.Y., Lee, S.J., and Park, J.W. (2007). Small interfering RNA-mediated silencing of mitochondrial NADP+-dependent isocitrate dehydrogenase enhances the sensitivity of HeLa cells toward tumor necrosis factor-alpha and anticancer drugs. Free radical biology & medicine *43*, 1197-1207.

Kim, J., Kundu, M., Viollet, B., and Guan, K.L. (2011). AMPK and mTOR regulate autophagy through direct phosphorylation of Ulk1. Nat Cell Biol *13*, 132-141.

Kim, J.W., Gao, P., Liu, Y.C., Semenza, G.L., and Dang, C.V. (2007). Hypoxia-inducible factor 1 and dysregulated c-Myc cooperatively induce vascular endothelial growth factor and metabolic switches hexokinase 2 and pyruvate dehydrogenase kinase 1. Mol Cell Biol *27*, 7381-7393.

Kim, J.W., Tchernyshyov, I., Semenza, G.L., and Dang, C.V. (2006). HIF-1-mediated expression of pyruvate dehydrogenase kinase: a metabolic switch required for cellular adaptation to hypoxia. Cell Metab *3*, 177-185.

Kim, S., Kim do, H., Jung, W.H., and Koo, J.S. (2013). Succinate dehydrogenase expression in breast cancer. SpringerPlus *2*, 299.

Kim, Y.H., Liang, H., Liu, X., Lee, J.S., Cho, J.Y., Cheong, J.H., Kim, H., Li, M., Downey, T., Dyer, M.D., et al. (2012). AMPKalpha modulation in cancer progression: multilayer integrative transcriptome analysis in Asian gastric cancer. Cancer Res.

Knox, W.E., Horowitz, M.L., and Friedell, G.H. (1969). The proportionality of glutaminase content to growth rate and morphology of rat neoplasms. Cancer Res *29*, 669-680.

Krebs, H.A., and Johnson, W.A. (1937). Metabolism of ketonic acids in animal tissues. Biochem J *31*, 645-660.

Kuznetsov, J.N., Leclerc, G.J., Leclerc, G.M., and Barredo, J.C. (2011). AMPK and Akt determine apoptotic cell death following perturbations of one-carbon metabolism by regulating ER stress in acute lymphoblastic leukemia. Mol Cancer Ther *10*, 437-447.

Laderoute, K.R., Amin, K., Calaoagan, J.M., Knapp, M., Le, T., Orduna, J., Foretz, M., and Viollet, B. (2006). 5'-AMP-activated protein kinase (AMPK) is induced by low-oxygen and glucose deprivation conditions found in solid-tumor microenvironments. Mol Cell Biol *26*, 5336-5347.

Laderoute, K.R., Calaoagan, J.M., Madrid, P.B., Klon, A.E., and Ehrlich, P.J. (2010). SU11248 (sunitinib) directly inhibits the activity of mammalian 5'-AMP-activated protein kinase (AMPK). Cancer biology & therapy *10*, 68-76.

Laplante, M., and Sabatini, D.M. (2009). mTOR signaling at a glance. J Cell Sci *122*, 3589-3594.

Lee, K.H., Hsu, E.C., Guh, J.H., Yang, H.C., Wang, D., Kulp, S.K., Shapiro, C.L., and Chen, C.S. (2011). Targeting energy metabolic and oncogenic signaling pathways in triple-negative

breast cancer by a novel adenosine monophosphate-activated protein kinase (AMPK) activator. J Biol Chem *286*, 39247-39258.

Lee, S.H., Jo, S.H., Lee, S.M., Koh, H.J., Song, H., Park, J.W., Lee, W.H., and Huh, T.L. (2004). Role of NADP+-dependent isocitrate dehydrogenase (NADP+-ICDH) on cellular defence against oxidative injury by gamma-rays. International journal of radiation biology *80*, 635-642.

Leprivier, G., Remke, M., Rotblat, B., Dubuc, A., Mateo, A.R., Kool, M., Agnihotri, S., El-Naggar, A., Yu, B., Somasekharan, S.P., et al. (2013). The eEF2 kinase confers resistance to nutrient deprivation by blocking translation elongation. Cell *153*, 1064-1079.

Levine, A.J., and Puzio-Kuter, A.M. (2010). The control of the metabolic switch in cancers by oncogenes and tumor suppressor genes. Science *330*, 1340-1344.

Li, J., Jiang, P., Robinson, M., Lawrence, T.S., and Sun, Y. (2003). AMPK-beta1 subunit is a p53-independent stress responsive protein that inhibits tumor cell growth upon forced expression. Carcinogenesis *24*, 827-834.

Li, L., and Guan, K.L. (2013). Microtubule-associated protein/microtubule affinity-regulating kinase 4 (MARK4) is a negative regulator of the mammalian target of rapamycin complex 1 (mTORC1). J Biol Chem *288*, 703-708.

Li, Y., Xu, S., Mihaylova, M.M., Zheng, B., Hou, X., Jiang, B., Park, O., Luo, Z., Lefai, E., Shyy, J.Y., et al. (2011). AMPK phosphorylates and inhibits SREBP activity to attenuate hepatic steatosis and atherosclerosis in diet-induced insulin-resistant mice. Cell Metab *13*, 376-388.

Liang, J., and Mills, G. (2013). AMPK: a contextual oncogene or tumor suppressor? Cancer Res *73*, 2929-2935.

Liang, J., Shao, S.H., Xu, Z.X., Hennessy, B., Ding, Z., Larrea, M., Kondo, S., Dumont, D.J., Gutterman, J.U., Walker, C.L., et al. (2007). The energy sensing LKB1-AMPK pathway

regulates p27(kip1) phosphorylation mediating the decision to enter autophagy or apoptosis. Nat Cell Biol *9*, 218-224.

Liu, L., Cash, T.P., Jones, R.G., Keith, B., Thompson, C.B., and Simon, M.C. (2006). Hypoxia-induced energy stress regulates mRNA translation and cell growth. Mol Cell *21*, 521-531.

Liu, L., Ulbrich, J., Muller, J., Wustefeld, T., Aeberhard, L., Kress, T.R., Muthalagu, N., Rycak, L., Rudalska, R., Moll, R., et al. (2012). Deregulated MYC expression induces dependence upon AMPK-related kinase 5. Nature *483*, 608-612.

Lizcano, J.M., Goransson, O., Toth, R., Deak, M., Morrice, N.A., Boudeau, J., Hawley, S.A., Udd, L., Makela, T.P., Hardie, D.G., et al. (2004). LKB1 is a master kinase that activates 13 kinases of the AMPK subfamily, including MARK/PAR-1. The EMBO journal *23*, 833-843.

Lobo, C., Ruiz-Bellido, M.A., Aledo, J.C., Marquez, J., Nunez De Castro, I., and Alonso, F.J. (2000). Inhibition of glutaminase expression by antisense mRNA decreases growth and tumourigenicity of tumour cells. Biochem J *348 Pt 2*, 257-261.

Locasale, J.W., Grassian, A.R., Melman, T., Lyssiotis, C.A., Mattaini, K.R., Bass, A.J., Heffron, G., Metallo, C.M., Muranen, T., Sharfi, H., et al. (2011). Phosphoglycerate dehydrogenase diverts glycolytic flux and contributes to oncogenesis. Nature genetics *43*, 869-874.

Loeb, L.A., Loeb, K.R., and Anderson, J.P. (2003). Multiple mutations and cancer. Proc Natl Acad Sci U S A *100*, 776-781.

Loffler, A.S., Alers, S., Dieterle, A.M., Keppeler, H., Franz-Wachtel, M., Kundu, M., Campbell, D.G., Wesselborg, S., Alessi, D.R., and Stork, B. (2011). Ulk1-mediated phosphorylation of AMPK constitutes a negative regulatory feedback loop. Autophagy *7*, 696-706.

Lu, C., Ward, P.S., Kapoor, G.S., Rohle, D., Turcan, S., Abdel-Wahab, O., Edwards, C.R., Khanin, R., Figueroa, M.E., Melnick, A., et al. (2012). IDH mutation impairs histone demethylation and results in a block to cell differentiation. Nature *483*, 474-478.

Lum, J.J., Bauer, D.E., Kong, M., Harris, M.H., Li, C., Lindsten, T., and Thompson, C.B. (2005). Growth factor regulation of autophagy and cell survival in the absence of apoptosis. Cell *120*, 237-248.

Lum, J.J., Bui, T., Gruber, M., Gordan, J.D., DeBerardinis, R.J., Covello, K.L., Simon, M.C., and Thompson, C.B. (2007). The transcription factor HIF-1alpha plays a critical role in the growth factor-dependent regulation of both aerobic and anaerobic glycolysis. Genes Dev *21*, 1037-1049.

Lunt, S.Y., and Vander Heiden, M.G. (2011). Aerobic glycolysis: meeting the metabolic requirements of cell proliferation. Annual review of cell and developmental biology *27*, 441-464.

MacIver, N.J., Blagih, J., Saucillo, D.C., Tonelli, L., Griss, T., Rathmell, J.C., and Jones, R.G. (2011). The liver kinase B1 is a central regulator of T cell development, activation, and metabolism. J Immunol *187*, 4187-4198.

Mackenzie, R.M., Salt, I.P., Miller, W.H., Logan, A., Ibrahim, H.A., Degasperi, A., Dymott, J.A., Hamilton, C.A., Murphy, M.P., Delles, C., et al. (2013). Mitochondrial reactive oxygen species enhance AMP-activated protein kinase activation in the endothelium of patients with coronary artery disease and diabetes. Clinical science *124*, 403-411.

Madiraju, A.K., Erion, D.M., Rahimi, Y., Zhang, X.M., Braddock, D.T., Albright, R.A., Prigaro, B.J., Wood, J.L., Bhanot, S., MacDonald, M.J., et al. (2014). Metformin suppresses gluconeogenesis by inhibiting mitochondrial glycerophosphate dehydrogenase. Nature *510*, 542-546.

Mahon, P.C., Hirota, K., and Semenza, G.L. (2001). FIH-1: a novel protein that interacts with HIF-1alpha and VHL to mediate repression of HIF-1 transcriptional activity. Genes Dev *15*, 2675-2686.

Makowski, L., and Hayes, D.N. (2008). Role of LKB1 in lung cancer development. Br J Cancer *99*, 683-688.

Manne, N.D., Lima, M., Enos, R.T., Wehner, P., Carson, J.A., and Blough, E. (2013). Altered cardiac muscle mTOR regulation during the progression of cancer cachexia in the ApcMin/+ mouse. International journal of oncology *42*, 2134-2140.

Mansfield, K.D., Guzy, R.D., Pan, Y., Young, R.M., Cash, T.P., Schumacker, P.T., and Simon, M.C. (2005). Mitochondrial dysfunction resulting from loss of cytochrome c impairs cellular oxygen sensing and hypoxic HIF-alpha activation. Cell Metab *1*, 393-399.

Martin, S.G., and St Johnston, D. (2003). A role for Drosophila LKB1 in anterior-posterior axis formation and epithelial polarity. Nature *421*, 379-384.

Mashimo, T., Pichumani, K., Vemireddy, V., Hatanpaa, K.J., Singh, D.K., Sirasanagandla, S., Nannepaga, S., Piccirillo, S.G., Kovacs, Z., Foong, C., et al. (2014). Acetate is a bioenergetic substrate for human glioblastoma and brain metastases. Cell *159*, 1603-1614.

Matoba, S., Kang, J.G., Patino, W.D., Wragg, A., Boehm, M., Gavrilova, O., Hurley, P.J., Bunz, F., and Hwang, P.M. (2006). p53 regulates mitochondrial respiration. Science *312*, 1650-1653.

Maxwell, P.H., Wiesener, M.S., Chang, G.W., Clifford, S.C., Vaux, E.C., Cockman, M.E., Wykoff, C.C., Pugh, C.W., Maher, E.R., and Ratcliffe, P.J. (1999). The tumour suppressor protein VHL targets hypoxia-inducible factors for oxygen-dependent proteolysis. Nature *399*, 271-275.

Mayer, A., Denanglaire, S., Viollet, B., Leo, O., and Andris, F. (2008). AMP-activated protein kinase regulates lymphocyte responses to metabolic stress but is largely dispensable for immune cell development and function. Eur J Immunol *38*, 948-956.

Meirhaeghe, A., Crowley, V., Lenaghan, C., Lelliott, C., Green, K., Stewart, A., Hart, K., Schinner, S., Sethi, J.K., Yeo, G., et al. (2003). Characterization of the human, mouse and rat PGC1 beta (peroxisome-proliferator-activated receptor-gamma co-activator 1 beta) gene in vitro and in vivo. Biochem J *373*, 155-165.

Merrill, G.F., Kurth, E.J., Hardie, D.G., and Winder, W.W. (1997). AICA riboside increases AMP-activated protein kinase, fatty acid oxidation, and glucose uptake in rat muscle. The American journal of physiology *273*, E1107-1112.

Metallo, C.M., Gameiro, P.A., Bell, E.L., Mattaini, K.R., Yang, J., Hiller, K., Jewell, C.M., Johnson, Z.R., Irvine, D.J., Guarente, L., et al. (2012). Reductive glutamine metabolism by IDH1 mediates lipogenesis under hypoxia. Nature *481*, 380-384.

Mitchelhill, K.I., Stapleton, D., Gao, G., House, C., Michell, B., Katsis, F., Witters, L.A., and Kemp, B.E. (1994). Mammalian AMP-activated protein kinase shares structural and functional homology with the catalytic domain of yeast Snf1 protein kinase. J Biol Chem *269*, 2361-2364.

Mitchell, P. (1961). Coupling of phosphorylation to electron and hydrogen transfer by a chemi-osmotic type of mechanism. Nature *191*, 144-148.

Mo, J.S., Meng, Z., Kim, Y.C., Park, H.W., Hansen, C.G., Kim, S., Lim, D.S., and Guan, K.L. (2015). Cellular energy stress induces AMPK-mediated regulation of YAP and the Hippo pathway. Nat Cell Biol.

Moeller, B.J., Dreher, M.R., Rabbani, Z.N., Schroeder, T., Cao, Y., Li, C.Y., and Dewhirst, M.W. (2005). Pleiotropic effects of HIF-1 blockade on tumor radiosensitivity. Cancer Cell *8*, 99-110.

Mullen, A.R., Wheaton, W.W., Jin, E.S., Chen, P.H., Sullivan, L.B., Cheng, T., Yang, Y., Linehan, W.M., Chandel, N.S., and DeBerardinis, R.J. (2012). Reductive carboxylation supports growth in tumour cells with defective mitochondria. Nature *481*, 385-388.

Mungai, P.T., Waypa, G.B., Jairaman, A., Prakriya, M., Dokic, D., Ball, M.K., and Schumacker, P.T. (2011). Hypoxia triggers AMPK activation through reactive oxygen species-mediated activation of calcium release-activated calcium channels. Mol Cell Biol *31*, 3531-3545.

Murphy, M.P. (2009). How mitochondria produce reactive oxygen species. Biochem J *417*, 1-13.

Murphy, M.P. (2012). Mitochondrial thiols in antioxidant protection and redox signaling: distinct roles for glutathionylation and other thiol modifications. Antioxidants & redox signaling *16*, 476-495.

Narbonne, P., and Roy, R. (2009). Caenorhabditis elegans dauers need LKB1/AMPK to ration lipid reserves and ensure long-term survival. Nature *457*, 210-214.

Nicholls, D.G. (2009). Spare respiratory capacity, oxidative stress and excitotoxicity. Biochem Soc Trans *37*, 1385-1388.

Oakhill, J.S., Chen, Z.P., Scott, J.W., Steel, R., Castelli, L.A., Ling, N., Macaulay, S.L., and Kemp, B.E. (2010). beta-Subunit myristoylation is the gatekeeper for initiating metabolic stress sensing by AMP-activated protein kinase (AMPK). Proc Natl Acad Sci U S A *107*, 19237-19241.

Oberley, L.W., and Oberley, T.D. (1988). Role of antioxidant enzymes in cell immortalization and transformation. Molecular and cellular biochemistry *84*, 147-153.

Oligschlaeger, Y., Miglianico, M., Chanda, D., Scholz, R., Thali, R.F., Tuerk, R., Stapleton, D.I., Gooley, P.R., and Neumann, D. (2015). The Recruitment of AMP-activated Protein Kinase to Glycogen Is Regulated by Autophosphorylation. J Biol Chem *290*, 11715-11728.

Owen, M.R., Doran, E., and Halestrap, A.P. (2000). Evidence that metformin exerts its anti-diabetic effects through inhibition of complex 1 of the mitochondrial respiratory chain. Biochem J *348 Pt 3*, 607-614.

Pan, J.G., and Mak, T.W. (2007). Metabolic targeting as an anticancer strategy: dawn of a new era? Sci STKE *2007*, pe14.

Papandreou, I., Cairns, R.A., Fontana, L., Lim, A.L., and Denko, N.C. (2006). HIF-1 mediates adaptation to hypoxia by actively downregulating mitochondrial oxygen consumption. Cell Metab *3*, 187-197.

Park, H.U., Suy, S., Danner, M., Dailey, V., Zhang, Y., Li, H., Hyduke, D.R., Collins, B.T., Gagnon, G., Kallakury, B., et al. (2009). AMP-activated protein kinase promotes human prostate cancer cell growth and survival. Mol Cancer Ther *8*, 733-741.

Park, I.J., Hwang, J.T., Kim, Y.M., Ha, J., and Park, O.J. (2006). Differential modulation of AMPK signaling pathways by low or high levels of exogenous reactive oxygen species in colon cancer cells. Ann N Y Acad Sci *1091*, 102-109.

Parks, S.K., Chiche, J., and Pouyssegur, J. (2011). pH control mechanisms of tumor survival and growth. J Cell Physiol *226*, 299-308.

Pernicova, I., and Korbonits, M. (2014). Metformin--mode of action and clinical implications for diabetes and cancer. Nature reviews. Endocrinology *10*, 143-156.

Petti, C., Vegetti, C., Molla, A., Bersani, I., Cleris, L., Mustard, K.J., Formelli, F., Hardie, G.D., Sensi, M., and Anichini, A. (2012). AMPK activators inhibit the proliferation of human melanomas bearing the activated MAPK pathway. Melanoma research *22*, 341-350.

Phoenix, K.N., Devarakonda, C.V., Fox, M.M., Stevens, L.E., and Claffey, K.P. (2012). AMPKalpha2 Suppresses Murine Embryonic Fibroblast Transformation and Tumorigenesis. Genes & cancer *3*, 51-62.

Pineda, C.T., Ramanathan, S., Fon Tacer, K., Weon, J.L., Potts, M.B., Ou, Y.H., White, M.A., and Potts, P.R. (2015). Degradation of AMPK by a Cancer-Specific Ubiquitin Ligase. Cell *160*, 715-728.

Plas, D.R., and Thompson, C.B. (2005). Akt-dependent transformation: there is more to growth than just surviving. Oncogene *24*, 7435-7442.

Pope, W.B., Prins, R.M., Albert Thomas, M., Nagarajan, R., Yen, K.E., Bittinger, M.A., Salamon, N., Chou, A.P., Yong, W.H., Soto, H., et al. (2012). Non-invasive detection of 2-hydroxyglutarate and other metabolites in IDH1 mutant glioma patients using magnetic resonance spectroscopy. Journal of neuro-oncology *107*, 197-205.

Preston, R.S., Philp, A., Claessens, T., Gijezen, L., Dydensborg, A.B., Dunlop, E.A., Harper, K.T., Brinkhuizen, T., Menko, F.H., Davies, D.M., et al. (2011). Absence of the Birt-Hogg-Dube gene product is associated with increased hypoxia-inducible factor transcriptional activity and a loss of metabolic flexibility. Oncogene *30*, 1159-1173.

Reczek, C.R., and Chandel, N.S. (2014). ROS-dependent signal transduction. Current opinion in cell biology *33C*, 8-13.

Rich, P.R., and Marechal, A. (2010). The mitochondrial respiratory chain. Essays in biochemistry *47*, 1-23.

Ricketts, C., Woodward, E.R., Killick, P., Morris, M.R., Astuti, D., Latif, F., and Maher, E.R. (2008). Germline SDHB mutations and familial renal cell carcinoma. Journal of the National Cancer Institute *100*, 1260-1262.

Robert, F., Carrier, M., Rawe, S., Chen, S., Lowe, S., and Pelletier, J. (2009). Altering chemosensitivity by modulating translation elongation. PLoS One *4*, e5428.

Rosilio, C., Lounnas, N., Nebout, M., Imbert, V., Hagenbeek, T., Spits, H., Asnafi, V., Pontier-Bres, R., Reverso, J., Michiels, J.F., et al. (2013). The metabolic perturbators metformin, phenformin and AICAR interfere with the growth and survival of murine PTEN-deficient T cell lymphomas and human T-ALL/T-LL cancer cells. Cancer letters *336*, 114-126.

Roy, B.C., Kohno, T., Iwakawa, R., Moriguchi, T., Kiyono, T., Morishita, K., Sanchez-Cespedes, M., Akiyama, T., and Yokota, J. (2010). Involvement of LKB1 in epithelial-mesenchymal transition (EMT) of human lung cancer cells. Lung Cancer *70*, 136-145.

Rubattu, S., Pagliaro, B., Pierelli, G., Santolamazza, C., Castro, S.D., Mennuni, S., and Volpe, M. (2014). Pathogenesis of Target Organ Damage in Hypertension: Role of Mitochondrial Oxidative Stress. Int J Mol Sci *16*, 823-839.

Sanchez-Cespedes, M., Parrella, P., Esteller, M., Nomoto, S., Trink, B., Engles, J.M., Westra, W.H., Herman, J.G., and Sidransky, D. (2002). Inactivation of LKB1/STK11 is a common event in adenocarcinomas of the lung. Cancer Res *62*, 3659-3662.

Sanchez-Macedo, N., Feng, J., Faubert, B., Chang, N., Elia, A., Rushing, E.J., Tsuchihara, K., Bungard, D., Berger, S.L., Jones, R.G., et al. (2013). Depletion of the novel p53-target gene carnitine palmitoyltransferase 1C delays tumor growth in the neurofibromatosis type I tumor model. Cell death and differentiation *20*, 659-668.

Sanders, M.J., Ali, Z.S., Hegarty, B.D., Heath, R., Snowden, M.A., and Carling, D. (2007). Defining the mechanism of activation of AMP-activated protein kinase by the small molecule A-769662, a member of the thienopyridone family. J Biol Chem *282*, 32539-32548.

Scott, J.W., Ling, N., Issa, S.M., Dite, T.A., O'Brien, M.T., Chen, Z.P., Galic, S., Langendorf, C.G., Steinberg, G.R., Kemp, B.E., et al. (2014). Small molecule drug A-769662 and AMP synergistically activate naive AMPK independent of upstream kinase signaling. Chemistry & biology *21*, 619-627.

Selak, M.A., Armour, S.M., MacKenzie, E.D., Boulahbel, H., Watson, D.G., Mansfield, K.D., Pan, Y., Simon, M.C., Thompson, C.B., and Gottlieb, E. (2005). Succinate links TCA cycle dysfunction to oncogenesis by inhibiting HIF-alpha prolyl hydroxylase. Cancer Cell *7*, 77-85.

Semenza, G.L. (2004). Hydroxylation of HIF-1: oxygen sensing at the molecular level. Physiology *19*, 176-182.

Semenza, G.L. (2007). Hypoxia-inducible factor 1 (HIF-1) pathway. Sci STKE *2007*, cm8.

Semenza, G.L. (2011a). Oxygen sensing, homeostasis, and disease. N Engl J Med *365*, 537-547.

Semenza, G.L. (2011b). Regulation of Metabolism by Hypoxia-Inducible Factor 1. Cold Spring Harb Symp Quant Biol.

Semenza, G.L., Roth, P.H., Fang, H.M., and Wang, G.L. (1994). Transcriptional regulation of genes encoding glycolytic enzymes by hypoxia-inducible factor 1. J Biol Chem *269*, 23757-23763.

Shackelford, D.B., Abt, E., Gerken, L., Vasquez, D.S., Seki, A., Leblanc, M., Wei, L., Fishbein, M.C., Czernin, J., Mischel, P.S., et al. (2013). LKB1 Inactivation Dictates Therapeutic Response of Non-Small Cell Lung Cancer to the Metabolism Drug Phenformin. Cancer Cell *23*, 143-158.

Shackelford, D.B., and Shaw, R.J. (2009). The LKB1-AMPK pathway: metabolism and growth control in tumour suppression. Nat Rev Cancer *9*, 563-575.

Shackelford, D.B., Vasquez, D.S., Corbeil, J., Wu, S., Leblanc, M., Wu, C.L., Vera, D.R., and Shaw, R.J. (2009). mTOR and HIF-1alpha-mediated tumor metabolism in an LKB1 mouse model of Peutz-Jeghers syndrome. Proc Natl Acad Sci U S A *106*, 11137-11142.

Shafique, E., Choy, W.C., Liu, Y., Feng, J., Cordeiro, B., Lyra, A., Arafah, M., Yassin-Kassab, A., Zanetti, A.V., Clements, R.T., et al. (2013). Oxidative stress improves coronary endothelial function through activation of the pro-survival kinase AMPK. Aging *5*, 515-530.

Shao, D., Oka, S., Liu, T., Zhai, P., Ago, T., Sciarretta, S., Li, H., and Sadoshima, J. (2014). A redox-dependent mechanism for regulation of AMPK activation by Thioredoxin1 during energy starvation. Cell Metab *19*, 232-245.

Shaw, R.J. (2008). LKB1: cancer, polarity, metabolism, and now fertility. Biochem J *416*, e1-3.

Shaw, R.J., Bardeesy, N., Manning, B.D., Lopez, L., Kosmatka, M., DePinho, R.A., and Cantley, L.C. (2004a). The LKB1 tumor suppressor negatively regulates mTOR signaling. Cancer Cell *6*, 91-99.

Shaw, R.J., Kosmatka, M., Bardeesy, N., Hurley, R.L., Witters, L.A., DePinho, R.A., and Cantley, L.C. (2004b). The tumor suppressor LKB1 kinase directly activates AMP-activated kinase and regulates apoptosis in response to energy stress. Proc Natl Acad Sci U S A *101*, 3329-3335.

Shen, C.H., Yuan, P., Perez-Lorenzo, R., Zhang, Y., Lee, S.X., Ou, Y., Asara, J.M., Cantley, L.C., and Zheng, B. (2013). Phosphorylation of BRAF by AMPK Impairs BRAF-KSR1 Association and Cell Proliferation. Mol Cell *52*, 161-172.

Shim, H., Dolde, C., Lewis, B.C., Wu, C.S., Dang, G., Jungmann, R.A., Dalla-Favera, R., and Dang, C.V. (1997). c-Myc transactivation of LDH-A: implications for tumor metabolism and growth. Proc Natl Acad Sci U S A *94*, 6658-6663.

Simon, M., Binder, M., Adam, G., Hartig, A., and Ruis, H. (1992). Control of peroxisome proliferation in Saccharomyces cerevisiae by ADR1, SNF1 (CAT1, CCR1) and SNF4 (CAT3). Yeast *8*, 303-309.

Simon, M.C. (2006). Mitochondrial reactive oxygen species are required for hypoxic HIF alpha stabilization. Adv Exp Med Biol *588*, 165-170.

Sonveaux, P., Vegran, F., Schroeder, T., Wergin, M.C., Verrax, J., Rabbani, Z.N., De Saedeleer, C.J., Kennedy, K.M., Diepart, C., Jordan, B.F., et al. (2008). Targeting lactate-fueled respiration selectively kills hypoxic tumor cells in mice. J Clin Invest *118*, 3930-3942.

St-Pierre, J., Buckingham, J.A., Roebuck, S.J., and Brand, M.D. (2002). Topology of superoxide production from different sites in the mitochondrial electron transport chain. J Biol Chem *277*, 44784-44790.

St-Pierre, J., Drori, S., Uldry, M., Silvaggi, J.M., Rhee, J., Jager, S., Handschin, C., Zheng, K., Lin, J., Yang, W., et al. (2006). Suppression of reactive oxygen species and neurodegeneration by the PGC-1 transcriptional coactivators. Cell *127*, 397-408.

Sullivan, L.B., and Chandel, N.S. (2014). Mitochondrial metabolism in TCA cycle mutant cancer cells. Cell Cycle *13*, 347-348.

Suwa, M., Nakano, H., and Kumagai, S. (2003). Effects of chronic AICAR treatment on fiber composition, enzyme activity, UCP3, and PGC-1 in rat muscles. J Appl Physiol (1985) *95*, 960-968.

Svensson, R.U., and Shaw, R.J. (2012). Cancer Metabolism: Tumour friend or foe. Nature *485*, 1.

Thomas, G.V., Tran, C., Mellinghoff, I.K., Welsbie, D.S., Chan, E., Fueger, B., Czernin, J., and Sawyers, C.L. (2006). Hypoxia-inducible factor determines sensitivity to inhibitors of mTOR in kidney cancer. Nature medicine *12*, 122-127.

Thompson-Jaeger, S., Francois, J., Gaughran, J.P., and Tatchell, K. (1991). Deletion of SNF1 affects the nutrient response of yeast and resembles mutations which activate the adenylate cyclase pathway. Genetics *129*, 697-706.

Thorpe, L.M., Yuzugullu, H., and Zhao, J.J. (2015). PI3K in cancer: divergent roles of isoforms, modes of activation and therapeutic targeting. Nat Rev Cancer *15*, 7-24.

Tormos, K.V., Anso, E., Hamanaka, R.B., Eisenbart, J., Joseph, J., Kalyanaraman, B., and Chandel, N.S. (2011). Mitochondrial complex III ROS regulate adipocyte differentiation. Cell Metab *14*, 537-544.

Torres, C.R., and Hart, G.W. (1984). Topography and polypeptide distribution of terminal N-acetylglucosamine residues on the surfaces of intact lymphocytes. Evidence for O-linked GlcNAc. J Biol Chem *259*, 3308-3317.

Vakana, E., Altman, J.K., Glaser, H., Donato, N.J., and Platanias, L.C. (2011). Antileukemic effects of AMPK activators on BCR-ABL-expressing cells. Blood *118*, 6399-6402.

Valentine, R.J., Coughlan, K.A., Ruderman, N.B., and Saha, A.K. (2014). Insulin inhibits AMPK activity and phosphorylates AMPK Ser(4)(8)(5)/(4)(9)(1) through Akt in hepatocytes, myotubes and incubated rat skeletal muscle. Archives of biochemistry and biophysics *562*, 62-69.

Valko, M., Leibfritz, D., Moncol, J., Cronin, M.T., Mazur, M., and Telser, J. (2007). Free radicals and antioxidants in normal physiological functions and human disease. The international journal of biochemistry & cell biology *39*, 44-84.

Vander Heiden, M.G., Cantley, L.C., and Thompson, C.B. (2009). Understanding the Warburg effect: the metabolic requirements of cell proliferation. Science *324*, 1029-1033.

Vincent, E.E., Coelho, P.P., Blagih, J., Griss, T., Viollet, B., and Jones, R.G. (2014). Differential effects of AMPK agonists on cell growth and metabolism. Oncogene.

Voet, D.a.V., J, G. (2011). Biochemistry. (Hoboken, NJ.: J. Wiley & Sons. Inc.

).

Vogelstein, B., and Kinzler, K.W. (2004). Cancer genes and the pathways they control. Nature medicine *10*, 789-799.

Wang, L., and Brautigan, D.L. (2013). alpha-SNAP inhibits AMPK signaling to reduce mitochondrial biogenesis and dephosphorylates Thr172 in AMPKalpha in vitro. Nature communications *4*, 1559.

Warburg, O. (1956). On the origin of cancer cells. Science *123*, 309-314.

Weiner, I.D., and Hamm, L.L. (2007). Molecular mechanisms of renal ammonia transport. Annual review of physiology *69*, 317-340.

Wellen, K.E., Hatzivassiliou, G., Sachdeva, U.M., Bui, T.V., Cross, J.R., and Thompson, C.B. (2009). ATP-citrate lyase links cellular metabolism to histone acetylation. Science *324*, 1076-1080.

Wellen, K.E., and Thompson, C.B. (2010). Cellular metabolic stress: considering how cells respond to nutrient excess. Mol Cell *40*, 323-332.

White, J.P., Puppa, M.J., Gao, S., Sato, S., Welle, S.L., and Carson, J.A. (2013). Muscle mTORC1 suppression by IL-6 during cancer cachexia: a role for AMPK. American journal of physiology. Endocrinology and metabolism *304*, E1042-1052.

Wick, A.N., Drury, D.R., Nakada, H.I., and Wolfe, J.B. (1957). Localization of the primary metabolic block produced by 2-deoxyglucose. J Biol Chem *224*, 963-969.

Wingo, S.N., Gallardo, T.D., Akbay, E.A., Liang, M.C., Contreras, C.M., Boren, T., Shimamura, T., Miller, D.S., Sharpless, N.E., Bardeesy, N., et al. (2009). Somatic LKB1 mutations promote cervical cancer progression. PLoS One *4*, e5137.

Winkler, B.S., DeSantis, N., and Solomon, F. (1986). Multiple NADPH-producing pathways control glutathione (GSH) content in retina. Experimental eye research *43*, 829-847.

Wise, D.R., DeBerardinis, R.J., Mancuso, A., Sayed, N., Zhang, X.-Y., Pfeiffer, H.K., Nissims, I., Daikhin, E., Yudkoff, M., McMahon, S.B., et al. (2008a). Myc Regulates a Transcriptional Program that Stimulates Mitochondrial Glutaminolysis and Leads to Glutamine Addiction Proc Natl Acad Sci U S A *In Press*.

Wise, D.R., DeBerardinis, R.J., Mancuso, A., Sayed, N., Zhang, X.Y., Pfeiffer, H.K., Nissim, I., Daikhin, E., Yudkoff, M., McMahon, S.B., et al. (2008b). Myc regulates a transcriptional program that stimulates mitochondrial glutaminolysis and leads to glutamine addiction. Proc Natl Acad Sci U S A *105*, 18782-18787.

Wise, D.R., Ward, P.S., Shay, J.E., Cross, J.R., Gruber, J.J., Sachdeva, U.M., Platt, J.M., DeMatteo, R.G., Simon, M.C., and Thompson, C.B. (2011). Hypoxia promotes isocitrate dehydrogenase-dependent carboxylation of alpha-ketoglutarate to citrate to support cell growth and viability. Proc Natl Acad Sci U S A *108*, 19611-19616.

Wood, Z.A., Schroder, E., Robin Harris, J., and Poole, L.B. (2003). Structure, mechanism and regulation of peroxiredoxins. Trends Biochem Sci *28*, 32-40.

Woods, A., Munday, M.R., Scott, J., Yang, X., Carlson, M., and Carling, D. (1994). Yeast SNF1 is functionally related to mammalian AMP-activated protein kinase and regulates acetyl-CoA carboxylase in vivo. J Biol Chem *269*, 19509-19515.

Wu, M., Neilson, A., Swift, A.L., Moran, R., Tamagnine, J., Parslow, D., Armistead, S., Lemire, K., Orrell, J., Teich, J., et al. (2007). Multiparameter metabolic analysis reveals a close link between attenuated mitochondrial bioenergetic function and enhanced glycolysis dependency in human tumor cells. Am J Physiol Cell Physiol *292*, C125-136.

Wu, N., Gu, C., Gu, H., Hu, H., Han, Y., and Li, Q. (2011). Metformin induces apoptosis of lung cancer cells through activating JNK/p38 MAPK pathway and GADD153. Neoplasma *58*, 482-490.

Wu, S.B., Wu, Y.T., Wu, T.P., and Wei, Y.H. (2014). Role of AMPK-mediated adaptive responses in human cells with mitochondrial dysfunction to oxidative stress. Biochim Biophys Acta *1840*, 1331-1344.

Wu, Z., Puigserver, P., Andersson, U., Zhang, C., Adelmant, G., Mootha, V., Troy, A., Cinti, S., Lowell, B., Scarpulla, R.C., et al. (1999). Mechanisms controlling mitochondrial biogenesis and respiration through the thermogenic coactivator PGC-1. Cell *98*, 115-124.

Xiao, B., Heath, R., Saiu, P., Leiper, F.C., Leone, P., Jing, C., Walker, P.A., Haire, L., Eccleston, J.F., Davis, C.T., et al. (2007). Structural basis for AMP binding to mammalian AMP-activated protein kinase. Nature *449*, 496-500.

Xiao, B., Sanders, M.J., Carmena, D., Bright, N.J., Haire, L.F., Underwood, E., Patel, B.R., Heath, R.B., Walker, P.A., Hallen, S., et al. (2013). Structural basis of AMPK regulation by small molecule activators. Nature communications *4*, 3017.

Xiao, B., Sanders, M.J., Underwood, E., Heath, R., Mayer, F.V., Carmena, D., Jing, C., Walker, P.A., Eccleston, J.F., Haire, L.F., et al. (2011). Structure of mammalian AMPK and its regulation by ADP. Nature *472*, 230-233.

Xu, Q., Vu, H., Liu, L., Wang, T.C., and Schaefer, W.H. (2011a). Metabolic profiles show specific mitochondrial toxicities in vitro in myotube cells. J Biomol NMR.

Xu, Q., Vu, H., Liu, L., Wang, T.C., and Schaefer, W.H. (2011b). Metabolic profiles show specific mitochondrial toxicities in vitro in myotube cells. J Biomol NMR *49*, 207-219.

Yan, H., Parsons, D.W., Jin, G., McLendon, R., Rasheed, B.A., Yuan, W., Kos, I., Batinic-Haberle, I., Jones, S., Riggins, G.J., et al. (2009). IDH1 and IDH2 mutations in gliomas. N Engl J Med *360*, 765-773.

Yan, M., Gingras, M.C., Dunlop, E.A., Nouet, Y., Dupuy, F., Jalali, Z., Possik, E., Coull, B.J., Kharitidi, D., Dydensborg, A.B., et al. (2014). The tumor suppressor folliculin regulates AMPK-dependent metabolic transformation. J Clin Invest *124*, 2640-2650.

Yang, M., Haase, A.D., Huang, F.K., Coulis, G., Rivera, K.D., Dickinson, B.C., Chang, C.J., Pappin, D.J., Neubert, T.A., Hannon, G.J., et al. (2014). Dephosphorylation of tyrosine 393 in argonaute 2 by protein tyrosine phosphatase 1B regulates gene silencing in oncogenic RAS-induced senescence. Mol Cell *55*, 782-790.

Ye, D., Ma, S., Xiong, Y., and Guan, K.L. (2013). R-2-hydroxyglutarate as the key effector of IDH mutations promoting oncogenesis. Cancer Cell *23*, 274-276.

Yeh, L.A., Lee, K.H., and Kim, K.H. (1980). Regulation of rat liver acetyl-CoA carboxylase. Regulation of phosphorylation and inactivation of acetyl-CoA carboxylase by the adenylate energy charge. J Biol Chem *255*, 2308-2314.

Ying, H., Kimmelman, A.C., Lyssiotis, C.A., Hua, S., Chu, G.C., Fletcher-Sananikone, E., Locasale, J.W., Son, J., Zhang, H., Coloff, J.L., et al. (2012). Oncogenic Kras maintains pancreatic tumors through regulation of anabolic glucose metabolism. Cell *149*, 656-670.

Youle, R.J., and Narendra, D.P. (2011). Mechanisms of mitophagy. Nat Rev Mol Cell Biol *12*, 9-14.

Yuneva, M., Zamboni, N., Oefner, P., Sachidanandam, R., and Lazebnik, Y. (2007). Deficiency in glutamine but not glucose induces MYC-dependent apoptosis in human cells. The Journal of cell biology *178*, 93-105.

Zaugg, K., Yao, Y., Reilly, P.T., Kannan, K., Kiarash, R., Mason, J., Huang, P., Sawyer, S.K., Fuerth, B., Faubert, B., et al. (2011). Carnitine palmitoyltransferase 1C promotes cell survival and tumor growth under conditions of metabolic stress. Genes Dev *25*, 1041-1051.

Zhang, Y.L., Guo, H., Zhang, C.S., Lin, S.Y., Yin, Z., Peng, Y., Luo, H., Shi, Y., Lian, G., Zhang, C., et al. (2013). AMP as a low-energy charge signal autonomously initiates assembly of AXIN-AMPK-LKB1 complex for AMPK activation. Cell Metab *18*, 546-555.

Zhao, G., Zhang, J.G., Liu, Y., Qin, Q., Wang, B., Tian, K., Liu, L., Li, X., Niu, Y., Deng, S.C., et al. (2013). miR-148b functions as a tumor suppressor in pancreatic cancer by targeting AMPKalpha1. Mol Cancer Ther *12*, 83-93.

Zheng, B., Jeong, J.H., Asara, J.M., Yuan, Y.Y., Granter, S.R., Chin, L., and Cantley, L.C. (2009). Oncogenic B-RAF negatively regulates the tumor suppressor LKB1 to promote melanoma cell proliferation. Mol Cell *33*, 237-247.

Zhou, G., Myers, R., Li, Y., Chen, Y., Shen, X., Fenyk-Melody, J., Wu, M., Ventre, J., Doebber, T., Fujii, N., et al. (2001). Role of AMP-activated protein kinase in mechanism of metformin action. J Clin Invest *108*, 1167-1174.

Zhou, G., Wang, J., Zhao, M., Xie, T.X., Tanaka, N., Sano, D., Patel, A.A., Ward, A.M., Sandulache, V.C., Jasser, S.A., et al. (2014). Gain-of-function mutant p53 promotes cell growth and cancer cell metabolism via inhibition of AMPK activation. Mol Cell *54*, 960-974.

Zilfou, J.T., and Lowe, S.W. (2009). Tumor suppressive functions of p53. Cold Spring Harbor perspectives in biology *1*, a001883.

Zmijewski, J.W., Banerjee, S., Bae, H., Friggeri, A., Lazarowski, E.R., and Abraham, E. (2010). Exposure to hydrogen peroxide induces oxidation and activation of AMP-activated protein kinase. J Biol Chem *285*, 33154-33164.